Stem Cell Antigen 1 Positive Resident Vascular Stem Cells and their Contribution to Vascular Disease

Thesis presented for the degree of

Doctor of Philosophy

by

Emma Fitzpatrick, B.Sc.

under the primary supervision of

Professor Paul A. Cahill, B.Sc., Ph.D.

and secondary supervision of

Dermot Walls, B.Sc., Ph.D.

School of Biotechnology

Dublin City University

Ireland

June 2017

Declaration

I hereby certify that this material, which I now submit for assessment on the programme of study leading to the award of Degree of Doctor of Philosophy is entirely my own work, and that I have exercised reasonable care to ensure that the work is original, and does not to the best of my knowledge breach any law of copyright, and has not been taken from the work of others save and to the extent that such work has been cited and acknowledged within the text of my work.

Signed:_____ ID No.: _____

Date:_____

Chapter 1

Chapter 2

Table of Figures

List of Tables

Publications

Embryonic rat vascular smooth muscle cells revisited - a model for neonatal, neointimal SMC or differentiated vascular stem cells?

Eimear Kennedy, Roya Hakimjavadi, Chris Greene, Ciaran J Mooney, **Emma Fitzpatrick**, Laura E Collins, Christine E Loscher, Shaunta Guha, David Morrow, Eileen M Redmond, and Paul A Cahill

Journal: Vascular Cell 2014, 6(1):6

Adult vascular smooth muscle cells in culture express neural stem cell markers typical of resident multipotent vascular stem cells.

Eimear Kennedy, Ciaran J Mooney, Roya Hakimjavadi, **Emma Fitzpatrick**, Shaunta Guha, Laura E Collins, Christine E Loscher, David Morrow, Eileen M Redmond, and Paul A Cahill

Journal: Cell tissue Research 2014, 358(1):203-16

Hedgehog and Resident Vascular Stem Cells Fate

Ciaran Mooney, Roya Hakimjavadi, **Emma Fitzpatrick**, Eimear Kennedy, Dermot Walls, David Morrow, Eileen M. Redmond and Paul A. Cahill

Stem Cells International 2015, DOI 10.1155/2015/468428

Oral Presentations

"Isolation and characterization of adventitial Sca1⁺ vascular stem cells –role of Hedgehog", Science Foundation Ireland Audit, DCU, Ireland, November 2014.

"Adventitial Progenitor Stem Cells – Role in In-Stent Restenosis", Research Day, DCU, Ireland, January 2015.

"Hedgehog-Responsive Stem Cell Antigen 1 Positive Cells Contribute To Vascular Smooth Muscle Cell Accumulation Following Vascular Injury", Atherosclerosis, Thrombosis and Vascular Biology (ATVB) Conference, Nashville, U.S.A, May 2016.

Poster Presentations

"Adventitial Progenitor Stem Cells – Role in In-Stent Restenosis", Research Day, DCU, Ireland, January 2015.

"Adventitial Stem Cell Progenitors Express Neural Stem Cell Markers", Atherosclerosis, Thrombosis and Vascular Biology (ATVB) Conference, San Francisco, U.S.A, May 2015.

"Hedgehog Responsive Cells Contribute to vSMC Accumulation following Vascular Injury", European Atherosclerosis Society Conference, Innsbruck, Austria, June 2016.

Acknowledgements

Firstly I would like to thank my legs for supporting me, my arms for always being by my side, and my fingers…I could always count on them (Should I start referencing now?!...Some random Internet meme that made me laugh 2016).

Foreword: I am not going to lie, after writing this section I realize it has become ridiculously lengthy; however there is no way around the fact that this Ph.D. was not fuelled solely by my perseverance (stubbornness), self-reserve and "intellect". There are in fact numerous more people I wish to thank but in view of this not becoming an autobiography, or on paper the point where the Oscars begin playing the music, I will mention those whom bared the brunt of me during this Ph.D.

I would like to thank my primary supervisor Professor Paul Cahill. I feel honored to have spent so much time in your presence; your unwavering guidance, patience and faith in my abilities were my lifejacket throughout the choppy sea of Sca1 expression work. You taught me more about myself than you may ever realize and for that I am eternally grateful. To my secondary supervisor Dr. Dermot Walls, you left me to my own devices but were always there for me when I needed you; you let me away with murder (months and months of no contact) and always gave me the best labs to demonstrate, for all those and much, much more, you have my absolute thanks.

To Professor Eileen Redmond, you welcomed me with open arms into your lab and your life. I will always treasure my memories from my time in your lab and under your supervision. You once told me that Professor Cahill is a genius, he is not alone. Diana, Paivi and Linda, there is no way I would have gotten half the work done without you, you are absolute legends! To Joe and Jay, you showed me all the wonders of Raaachester and made my time there unforgettably hilarious, maybe some day I can return the favor.

To all my students/test subjects, you stressed me beyond my wits end but if it were not for you, I would not have spawned my beloved dark sense of humor and a bank of ridiculous and funny memories/anecdotes.

To all the DCU technical staff and Damian and Carolyn of the BRU, you saved my butt on more than one occasion and never once looked for anything in return. You are all the unsung heroes of research life in DCU.

To all the postgrads and postdocs of the School of Biotechnology 2012 - 2016, for every time I annoyed you for "just one second" and every time you saved my experiments (by borrowing me something that vanished from our lab), I will never forget what you individually did for me.

To the girls in the lab, my partners in crime, Claire (in particular), Abi, Gill, Mariana, Maryam and Roa… and not forgetting Joe, remember to watch out for each other and more importantly have a laugh. I need to also mention Richard the "engineer",

you bring truth to the saying: “arguing with an engineer is a lot like wrestling in the mud with a pig, after a couple of hours you realize the pig likes it”. I can’t wait to see you all the far side of this roller coaster we jumped on together.

To my Irish Red Cross friends and mentors, Ciara Jean, Eoghan, Niall, Cyril, John Shanley, Sarah-Jane. Thank you for all your patience over the last year in particular, you truly inspire me with your endless acts of selflessness. I always treasure our time together.

To my dearest friends Claire and Shane Fitzpatrick, Rachel Brophy and Liam Hughes, Conor McErlean, Clare and Dash Triton Selvaratnam, Orla and Graham Barker, Eimear and Shaunta Guha, you always met me with open arms, listened to me vent, “vinoed” (definition: the act of sharing liquor of the gods) and never let me forget how to laugh, even when I was the most neglectful friend, your unrelenting acts of love and pure kindness towards me will never be forgotten or forgiven.

To my families (in no particular order): the Fitzers, Behans, Jones, Kilcullens, Whites, Carters and McCarthys. Thank you for all the love, laughs (which were to be honest at, not with me) and unreciprocated presents… which I promise to reciprocate when I get a “real” job.

To my most beloved Colm, words can do you no justice. You are the non-coding strand to my coding self…this sounded better in my head; anyway, you are my backbone, my compliment, and bringer of clarity and purpose when I lose my way. You are my role model, on call technical advisor, sciencey-stuff proof reader, temper-beast tamer, bringer of belly aching joy and laughter, and most importantly, my best friend and the love of my life, and there is certainly no way I would have made it to this point without you so, cheers big ears (couldn’t end on a soppy note).

To all of Colms family, for welcoming me into your lives and homes, for all your love and kindness, and letting me release my inner 7-year-old self while playing silly games with your precious and beautiful children/grandchildren.

To my cherished parents Ursula and Larry, without you none of this would have been possible. I don’t claim to be an easy daughter to have, from the hours and hours of incomprehension of fractions using sweets as a kid, to being, honestly, a nightmare teenager/20-something. Your unconditional love and limitless patience and solid advice are the foundation of all my achievements.

And last but certainly not least, my twin of this world and my heart, my brother Larry (aka Lala). You have always been a far superior best friend and sibling to me than I ever have to you. You have always been the more intelligent twin, even if you are clueless about biology.

P.s.

xx

This Ph.D. should in reality have 4 more authors, Colm, my parents and my brother, for without them I would have had no one to talk at (yes I meant at) while I internally tried to figure out the numerous roadblocks I hit throughout the last number of years. However, sadly, since they are not technically associated with this thesis, I will just have to take all the glory myself…it is a hard cross to bear, but I will do my best, and that's all that matters…right?

Abbreviations

- APC – Adventitial Progenitor Cell
- APS – Ammonium Per Sulfate
- BCA - Bicinchoninic Acid
- BMS – Bare Metal Stents
- BSA – Bovine Serum Albumin
- CNN – Calponin
- CVD – Cardiovascular Disease
- DAPI - 4',6-diamidino-2-phenylindole
- DEPC – Diethylpyrocarbonate
- DES – Drug Eluting Stents
- DMEM – Dulbecco's Modified Essential Medium
- DMSO - Dimethyl Sulfoxide
- DNA – Deoxyribose Nucleic Acid
- EC – Endothelial Cell
- ECM – Extra Cellular Matrix
- EMEM – Eagle's Minimum Essential Medium
- EndMT - Endothelial-Mesenchymal Transition
- FC – Flow Cytometry
- FBS – Fetal Bovine Serum
- Fu - Serine/ Threonine Kinase Fused
- GFP – Green Fluorescent Protein
- GSK3β - Glycogen Synthase Kinase 3β
- HES - Hairy and Enhancer Split
- HERP - HES-related Repressor Protein
- HB-EGF - Heparin-Binding Epidermal Growth-like Factor
- HPF – High Power Field
- hhip 1 - hedgehog interacting protein 1
- IMT – Intimal Medial Thickening
- ISR – In-stent Restenosis
- Kif7 - Kinesin Family Member 7
- LTBP - Latent TGFβ Binding Protein

- LAP - Latency-Associated Peptide
- LIF – Leukemia Inhibitory Factor
- αMEM – Alpha Minimal Essential Medium
- MSC – Mesenchymal Stem Cell
- MVSC – Multipotent Vascular Stem Cell
- NICD - Notch Intracellular Domain
- OCT - Optimal Cutting Temperature
- P/S – Penicillin-Streptomycin
- PBS – Phosphate Buffer Saline
- PCR – Polymerase Chain Reaction
- PDGF – Platelet Derived Growth Factor
- PTA- Percutaneous Transluminal Angioplasty
- RIPA - Radioimmunoprecipitation Assay
- RNA – Ribo-nucleic Acid
- rMSC – rat Mesenchymal Stem Cell
- RT – Room Temperature
- Sca1 – Stem Cell Antigen 1
- SDS-PAGE - Sodium Dodecyl Sulfate Polyacrylamide Gel Electrophoresis
- SRF - Serum Response Factor
- SMA – Smooth Muscle Actin
- SmαA - Smooth Muscle alpha A
- SM22α - Smooth Muscle 22 alpha
- SMC – Smooth Muscle Cell
- vSMC – Vascular Smooth Muscle Cell
- SMSC – Skeletal Muscle Stem Cell
- SMMHC – Smooth Muscle Myosin Heavy Chain
- SMMHC II – Smooth Muscle Myosin Heavy Chain II
- Shh – Sonic Hedgehog
- Sufu - Suppressor of Fused
- Sox (2/10/17) - SRY (sex determining region Y)-box (2/10/17)
- TA – Transplant Arteriosclerosis

- TEMED- Tetramethylethylenediamine
- TGFβ – Transforming Growth Factor Beta
- TNFα - Transforming Growth Factor-α
- TMB - 3,3',5,5' Tetramethylbenzidine

Units

- cm - centimetres
- cm^2 – centimetres squared
- °C – degrees celsius
- g - grams
- h - hours
- kDa – kilo daltons
- L - litre
- M - mole
- min - minutes
- mL – millilitres
- mm - millimetres
- mM - millimole
- ng - nanogram
- Sec - seconds
- µg - microgram
- µl - microlitre
- µm - micrometer
- µM - micromolar
- V/v – volume per volume
- V – volts
- *x* g – gravity

Thesis Abstract

Stem Cell Antigen 1 Positive Resident Vascular Stem Cells and their Contribution to Vascular Disease

Emma Fitzpatrick

Vascular remodelling occurs during many forms of cardiovascular disease (CVD). This vascular remodelling can be either symmetrical as observed in arteriosclerotic conditions (e.g. natural vascular aging, transplant arteriosclerosis and in-stent restenosis (ISR)), or asymmetrical as observed in atherosclerosis. An integral part of the pathology of symmetrical vascular remodelling is the formation of a "neointimal layer", also known as "intimal medial thickening" (IMT), whereby cells (widely considered to be vascular smooth muscle cells (vSMC)) accumulate within the vessel and obstruct circulatory blood flow. Currently, there are two predominant and contrasting fields of thought as to the origin of these neointimal cells: 1. resident vSMCs and 2. resident vascular stem cells. While this thesis discusses both theories in detail; it focuses on the role of a stem cell antigen 1 positive ($Sca1^+$) resident vascular stem cell, and shows evidence of its contribution to vascular remodelling both *in vitro* and *in vivo*. Previously, a $Sca1^+$ adventitial cell has been shown to co-localise at the adventitial medial boundary with the hedgehog (Hh) signalling activation morphogen Shh and its receptor Patched 1. Moreover, Patched 1^+ cells are present in the medial and intimal layers following vascular injury and remodelling. Therefore, the aim of this thesis was to investigate the role of $Sca1^+$ adventitial progenitor cells (APC) during vascular remodelling, with a focus on exploring the role of Hh-responsive $Sca1^+$ APC contribution to IMT. Characterisation of two widely used model cell lines ($Sca1^+$ ESC and $Sca1^+$ C3H) and APC highlighted variable expression profiles. Additionally, *in vitro* exposure of $Sca1^+$ APC and $Sca1^+$ C3H to Shh demonstrated contrasting maintenance of "stemness" responses (with Shh inducing significant maintenance of "stemness" in $Sca1^+$ C3H but not in $Sca1^+$ APC). Importantly, *in vitro* exposure of $Sca1^+$ APC to Shh activated Hh signalling, and induced cellular proliferation and SMC differentiation, a process that was attenuated using the Hh specific inhibitor

cyclopamine. Crucially, *in vivo* analysis demonstrated that Sca1$^+$ APC proliferate/expand following injury-induced vascular remodelling, and Sca1$^+$ Hh responsive cells were found in the neointima of remodelling vessels. *In vivo* analysis also demonstrated that the recapitulation of Hh signalling during vascular remodelling is essential to pathological IMT (as confirmed by significant attenuation of vascular remodelling following treatment with the cyclopamine). To conclude, Hh responsive Sca1$^+$ resident vascular stem cells are key to the progression of pathological vascular remodelling and ultimately cardiovascular disease.

Chapter 1

Introduction

1.1 Introduction

Cardiovascular disease (CVD) remains the leading cause of global morbidity (World Health Organisation 2014) and is responsible for 33% of deaths/annum in Ireland (Irish Hearth Foundation 2014). CVD typically presents as a blockage in blood vessels leading to an obstruction to blood flow caused by a localised pathological change in vascular tissue. The most successful treatment to date involves percutaneous transluminal angioplasty (PTA) to remove the obstruction, followed by stent implantation to prevent re-occlusion (Kereiakes et al. 2005). However, in stent restenosis (ISR) is a major limitation of PTA and presents as a formation of a new/thickened layer of cells known as a neointima and is characterised by vascular smooth muscle cells (vSMC) accumulating within the stented domain (Simard et al. 2014 and Orlandi and Bennett 2010). Using various animal models, numerous studies have investigated but not elucidated the origin of the vSMC that accumulate to result in the neointima (Majesky et al. 2011; Bautch 2011 and Orlandi and Bennett 2010) with strong evidence indicating a role for an adventitial progenitor stem cells that are $Sca1^+$ $CD34^+$ and Lin^- (Passman et al. 2008 and Majesky et al. 2011). Currently stents are coated with anti-proliferative drugs in an attempt to prevent ISR but these come with serious pro-thrombogenic side effects due to the impairment of endothelial function (Nickenig and Sinning 2009 and Lüscher et al. 2007). Hence new therapies are being investigated to specifically target the progenitors and their differentiated progeny responsible for neointimal formation (Simard et al. 2014 and Redmond et al. 2011).

1.2 The Vasculature

The vasculature is composed of an intricate network of arteries, veins and capillaries that extend to all tissues in vertebrates (Larrivee et al. 2009). The highly organised branching pattern that leads to the development of major and minor branching at specific sites is developmentally conserved and the factors that control vascular patterning have yet to be elucidated (Larrivee et al. 2009). Nonetheless, the formation of a complete and intact vascular system is key to embryonic and postnatal survival. Arteries' primary role is to

carry oxygenated blood to the tissues of the body; veins carry deoxygenated blood away from the tissue in the body, and capillaries are the site of gas exchange (National Institutes of Health 2011).

1.2.1 Vessel Structure

Arteries and veins have three distinct layers, the following paragraphs will describe these layers starting from the outermost and working into the lumen:

1. The Tunica Adventitia

The tunica adventitia is the outermost layer of a vessel and is surrounded by adipose tissue. The tunica adventitia is a collagen matrix that is noted for being less rigid than the other vascular layers, and is rich with stem cells, perivascular nerves, adventitial macrophages, mast cells, T cells, microvascular endothelial cells and adipocytes. This dynamic layer is the primary focus of this thesis and therefore will be discussed at greater length in the coming pages; however it is important to note that the adventitia has been implicated in numerous vascular pathologies due to its complex network of interacting cells and biological factors (Majesky et al. 2011 and Potter et al. 2014) (Figure 1.1).

2. The Tunica Media

The tunica media or "middle" layer is primarily comprised of smooth muscle cells, however a minority population of stem cells have been identified within the medial layer. Smooth muscle cells within this layer are compartmentalised into further layers separated by elastic lamina which provides a fibrous structure that lends rigid support to the media (Tang et al. 2012; Potter et al. 2014 and Ramamurthi and Kotthapalli 2016) (Figure 1.1).

3. The Tunica Intima/Endothelium

This innermost layer is the thinnest of the three; the tunica intima/endothelium is comprised of an intimal layer of smooth muscle cells (which humans, pigs and primates have but rodents lack) and a single layer of endothelial cells responsible for the maintenance of vessel homeostasis.

The endothelial cells are tightly connected to the basal elastic lamina of the tunica media which has additional collagen, proteoglycans and glycans essential for endothelial support and function. The endothelial cells are a critical component of the vasculature as they are in direct contact with the lumen, and therefore are subjected to blood flow forces and interactions with blood components. Therefore endothelial cells have unique characteristics to deal with their dynamic environment such as promote anti-thrombotic and anti-inflammatory events, and are phenotypically flat in order to prevent friction and reduce resistance to blood flow (Schwartz et al. 1995; Kockx 1995 and Catravas et al. 1999) (Figure 1.1).

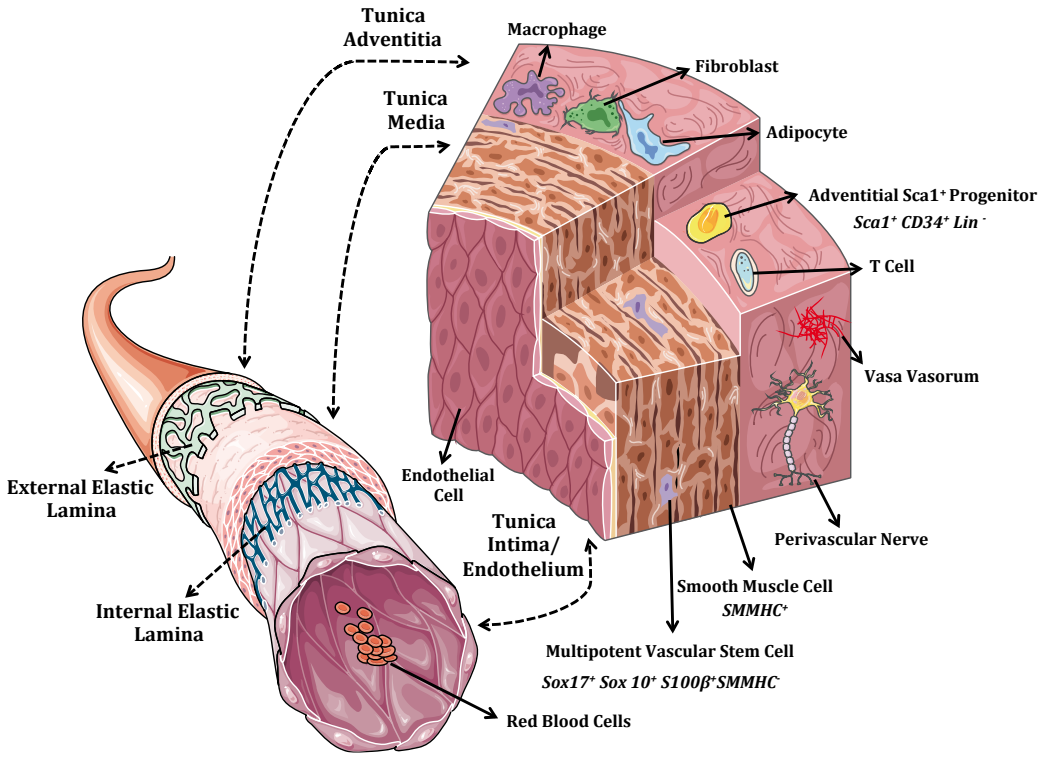

Figure 1.1: Rodent Vessel Structure and Cellular Content. Vessels are compartmentalised into three layers: Tunica Adventitia, Tunica Media and Tunica Intima/Endothelium. The Tunica Adventitia and Tunica Media are separated by the External Elastic Lamina, and the Tunica Media and Tunica Intima/Endothelium are separated by the Internal Elastic Lamina. The Tunica Adventitia is composed of a plethora of cell types including macrophages, fibroblasts, adipocytes, Adventitial Sca1+ Progenitors, T cells, Perivascular Nerves and Vasa Vasorum. The Tunica Media is primarily composed of Smooth Muscle Cells, however a small subpopulation of Multipotent Vascular Stem Cells also exists in this layer. The Tunica Intima/Endothelium is made up of an intimal layer of SMC and a single layer of endothelial cells.

1.3 Cardiovascular Disease – Vascular Remodelling

The classic hallmarks of CVD are hypertension, atherosclerosis and arteriosclerosis; the problematic aspect of each disease state is the resulting accumulation of vascular smooth muscle cells (vSMCs). It has been long established that hypertension accelerates the development of atherosclerosis (Matova and Vihert 1976) and arteriosclerosis (Sasamura and Itoh 2011). Arteriosclerosis by definition is a generalised term for the symmetrical thickening and hardening of arteries. In contrast, atherosclerosis (asymmetrical thickening) is a type of arteriosclerosis caused by lipid accumulation and plaque formation (American Heart Association 2014).

Ultrasound has emerged as a useful tool in CVD prediction and prevention (Adams et al. 2002 and Benetos et al. 2015). The detection of increased intima-media thickness (IMT) by ultrasound is considered state of the art in risk stratification regardless of the ultrasound frequency used (Ray et al. 2010 and Bhagirath et al. 2012). Prior to carotid IMT, clinicians depended on risk score algorithms such as the Framingham Risk Score method, however these approaches have limitations such as underestimating atherosclerosis risk in asymptomatic women (Michos et al. 2006; Schlendorf et al. 2009 and Stern 2014). Carotid IMT measurement by appropriately trained clinicians on the other hand is sensitive, non-invasive and reproducible, and advances are currently being made to completely automate the technique (Ray et al. 2010; Molinari et al. 2010 and Molinari et al. 2012).

Vascular remodelling (both arteriosclerosis and atherosclerosis) is initiated by endothelial dysfunction (Davignon and Ganz 2004 and Vanhoutte 2009) however despite the identical origin, there are several dissimilarities worth mentioning.

1.3.1 Atherosclerosis – Asymmetric Vascular Remodelling

Atherosclerosis almost exclusively disturbs conduit function, and the characteristics of an arterial atherosclerotic lesion are vastly different to non-atherosclerotic conditions (Drüeke and London 1997). Atherosclerosis is a chronic inflammatory disease whereby arterial lumen diameter is reduced

(stenosed) by the asymmetrical accumulation of lipids, inflammatory cells, dead cells and fibrous tissue, as opposed to arteriosclerosis which is defined as symmetrical intimal medial thickening and calcification (Figure 1.2) (Andersson et al. 2010; Drüeke and London 1997 and Adams et al. 2002). Atherosclerosis is accelerated by hypertension and myocardial infarction events (Matova and Vihert 1976 and Dutta et al. 2012). Cerebrovascular and cardiovascular events are triggered when granulocytes and monocytes destabilise plaques in the arterial walls causing them to rupture (Dutta et al. 2012).

Due to atherosclerosis affecting conduit function, the most effective treatment is balloon angioplasty and stent implantation where PTA impacts the plaque against the vessel wall, reducing the luminal restriction, and the stent provides structural support for the vessel and attempts to prevent re-occlusion (Kereiakes et al. 2005 and Simard et al. 2014). The use of the word attempts is not an oversight as in-stent restenosis is a common post-treatment complication which in effect makes the treatment procedure redundant ~10 % of the time despite current advances (Sciahbasi et al. 2009; Orlandi and Bennett 2010; Marx et al. 2011 and Simard et al. 2014). The next section will discuss in-stent restenosis in greater detail.

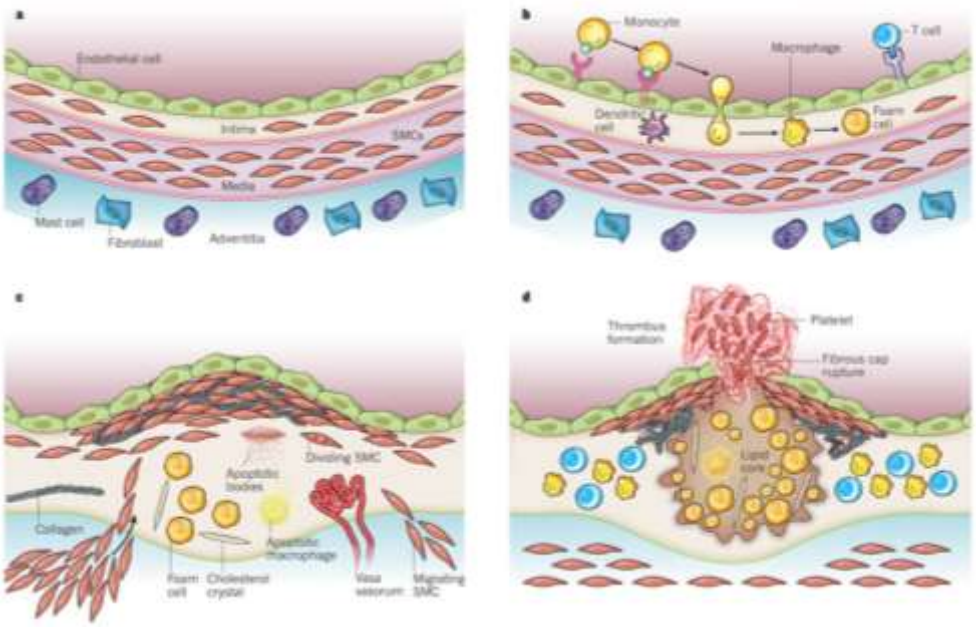

Figure 1.2: Development of an atherosclerotic lesion. A: Healthy human vessel with inactivated endothelium. B: Immune system activation is an initial stage of atherosclerotic lesion development. C: Following immune system activation, the asymmetrical accumulation of lipids, inflammatory cells, dead cells and fibrous tissue occurs and vascular stenosis occurs. D: If atherosclerosis continues to go undiagnosed, the atherosclerotic lesion will continue to grow until complete vascular occlusion, or the formed lipid core ruptures and thrombus formation occurs. Image taken from Libby et al. 2011.

1.3.2 Arteriosclerosis – Symmetric Vascular Remodelling

Primarily a degenerative condition of the tunica media throughout the thoracic and central arteries; arteriosclerosis results in dilation, diffuse hypertrophy and arterial hardening. Arteriosclerosis is considered to be a "physiological" aging phenomenon advanced by hypertension, it involves symmetrical intimal medial thickening and calcification that does not disturb conduit function. Arteriosclerosis and atherosclerosis frequently coexist, and distinguishing between the two is often challenging due to several shared pathogenic mechanisms (Drüeke and London 1997 and Adams et al. 2002).

Non-aging associated arteriosclerosis also occurs in transplant patients (transplant arteriosclerosis) and atherosclerotic PTA/Stented patients (in-stent restenosis (ISR)). The following paragraphs will describe these arteriosclerotic phenotypes in greater detail.

Transplant Arteriosclerosis (TA)

The development of immunosuppressive strategies overcame the initial and crucial limitation of allograft and autograft procedures – transplant rejection. Since then, TA has proved to be a critical limitation to the long-term survival of transplant procedures, with severe TA occurring in 50 % of transplant patients within five years and 90 % of patients after ten years. Unfortunately, the current therapy is re-transplantation due to the diffuse nature of the TA in the grafts vascular bed. TA is characterised as the development of severe intimal hyperplasia lesions that ultimately compromise luminal blood flow and result in ischemic graft failure. Vascular remodelling in TA is initiated by EC dysfunction and apoptosis, and results in adventitial fibrosis, increased medial volume and intimal hyperplasia formation (accumulation of SMC-like and immune cells). Therefore TA shares pathological similarities to other vasculopathies such as atherosclerosis and in-stent restenosis (Hruban et al. 1990; Mitchell and Libby 2007; Vanhoutte 2009; Li et al. 2015 and Yang et al. 2015).

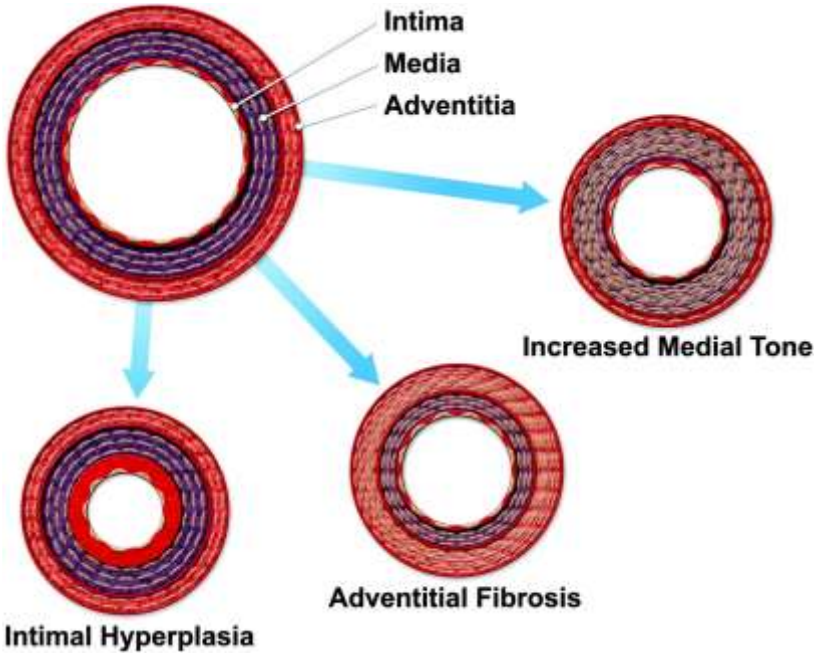

Figure 1.3: Vascular Remodelling in Transplant Arteriosclerosis. Vascular remodelling in all three vessel layers reduces luminal volume during transplant arteriosclerosis. Adventitial fibrosis limits positive remodelling of the perivascular extracellular matrix and indirectly leads to luminal compromise, and medial-intimal thickening directly results in luminal compromise. Image taken from Mitchell and Libby 2007.

In-stent Restenosis (ISR)

As described previously, the most effective treatment for atherosclerosis is percutaneous transluminal angioplasty (PTA), where an obstructing atherosclerotic mass (an asymmetrical accumulation of lipids, inflammatory cells, dead cells and fibrous tissue) is compacted against the vascular wall resulting in a re-opening of the lumen and restored blood flow, and PTA is combined with stent implantation for structural support (Andersson et al. 2010; Drüeke and London 1997; Kereiakes et al. 2005; Simard et al. 2014 and Adams et al. 2002). Unfortunately a gradual re-narrowing/re-blocking (restenosis) of the stented area (ISR) occurs between 3 and 12 months after placement, and complete re-blocking/restenosis requiring re-intervention occurs in approximately 20 % of cases utilising bare metal stents, and in roughly 10 % of cases using the most advanced drug-eluting stents (DES) (Sciahbasi et al. 2009 and Marx et al. 2011). While DES are currently coated with anti-proliferative (chemotoxic) drugs in an attempt to prevent ISR, DES have been unsuccessful in eradicating it, and unfortunately drug-related endothelial dysfunction results in life-threatening thrombogenesis (Nickenig and Sinning 2009 and Lüscher et al. 2007). Therefore there is a demand to move away from systemic unspecific approaches, and focus on elucidating the specific cells and mechanisms involved in ISR in order to specifically target them and prevent ISR without additional complications (Simard et al. 2014 and Redmond et al. 2011).

The underlying atherosclerotic microenvironment makes ISR a complex pathology; ISR is primarily considered a cellular proliferative disease. While scientists agree that ISR and other forms of arteriosclerotic disease that are defined by the presence of neointimal formation is caused by the accumulation of primarily smooth muscle and some inflammatory cells, there are currently two primary schools of thought on the theory of which particular cell type are the root of the problem.

1. Stem Cells
2. Resident Smooth Muscle Cells

The following sections (1.4 and 1.5) will introduce these cell types and discuss their potential role in ISR (vascular remodelling) in greater detail.

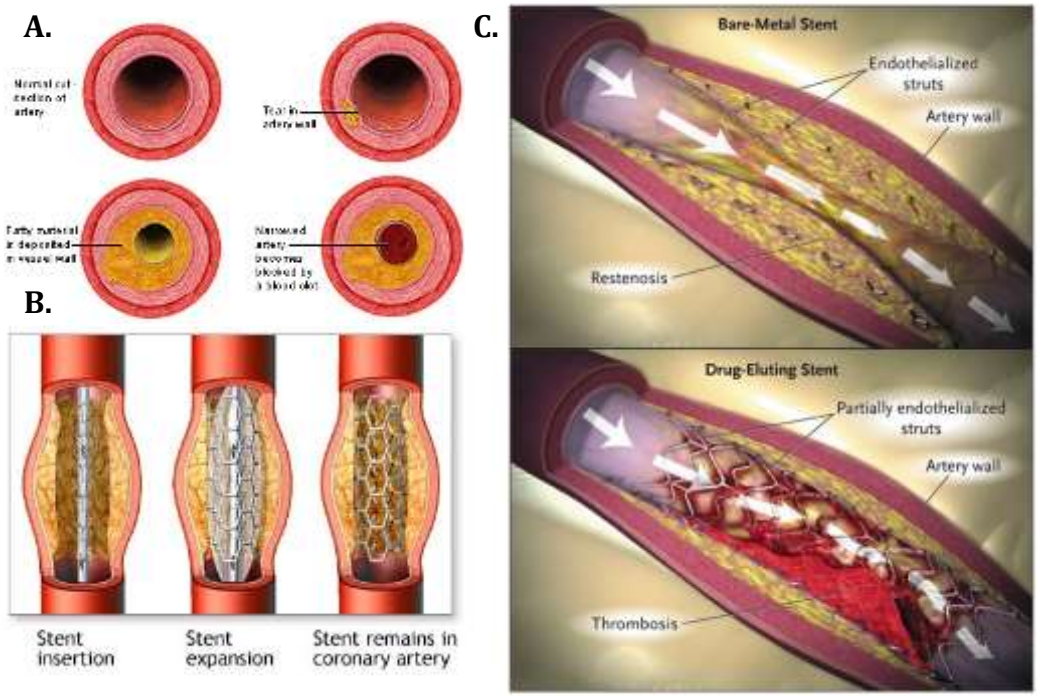

Figure 1.4: General overall schematic of atherosclerotic treatment (PTA and Stent Implantation) and ISR. A: Overview of the development of atherosclerosis, B: PTA and stent implantation. C: bare metal stent complications (ISR) vs. drug eluting stent complications (ISR and thrombosis). Image adapted from A.D.A.M® 2015.

In vivo Models of Symmetric Vascular Remodelling

There are three primary experimental injury methods that elicit reproducible symmetric arterial vascular remodelling: wire-induced, balloon-induced and ligation-induced. Despite each injury being different in nature, they all establish time-dependent stenotic neointimal formation. The following section will briefly discuss each of these injury models.

Wire-Induced Injury

This technique, originally developed in 1993, utilises an angiocatheter guide wire that is inserted into the arterial system in the absence of medial distension, and removes (denudes) the endothelial layer. The vascular remodelling response initially involves medial damage (resulting in SMC apoptosis) and rapid platelet adherence, followed by adventitial and medial

thickening, endothelial regeneration and neointimal formation (Linder et al. 1993; Xu 2004 and Holt et al. 2013).

Balloon-Induced Injury (Angioplasty)

This technique, originally developed in 1983, utilises a balloon catheter that is inserted into the arterial system and deployed, typically in the common carotid artery, which results in medial distension and endothelial denudation (removal). The vascular remodelling response involves SMC apoptosis, adventitial and medial thickening, partial endothelial regeneration and neointimal formation (Clowes et al. 1983a; Clowes et al. 1983b and Holt and Tulis 2013).

Ligation-Induced Injury

This technique, originally used in 1793 to stop a patient from haemorrhagic shock, is typically conduced on the common carotid artery (or branches of). Sutures are used to ligate (tie off) the artery to result in either a partial or full obstruction to blood flow. This injury does not result in endothelial compromise and additionally mimics the hemodynamic perturbation associated with a vascular pathology. The vascular remodelling response involves adventitial and medial thickening and neointimal formation (Friedman 2005 and Holt and Tulis 2013).

1.4 Vascular Smooth Muscle Cells (vSMC)

1.4.1 Introduction to vSMC

As mentioned previously, the tunica media is composed of smooth muscle cells that are compartmentalised into layers that are separated by elastic lamina (Tang et al. 2012; Potter et al. 2014 and Ramamurthi and Kotthapalli 2016) (Figure 1.1). During development, vSMC produce the extracellular matrix (ECM) which provides support to vSMC so that they can be constantly subjected to mechanical signals and regulate blood pressure (Lacolley et al. 2012). These mechanical signals (e.g. vasoactive peptides for example angiotensin II) produce a contractile tone in vSMC; an absence of arterial vSMC tone leads to imminent death, whereas excessive vSMC tone results in

pathological high blood pressure (Wynne et al. 2009 and Lacolley et al. 2012). The following sections will discuss the embryonic origin of aortic vSMC and introduce the concept of vSMC contribution to vascular remodelling.

1.4.2 The Embryonic Origin of vSMC

There is estimated to be a minimum of 5 different progenitor sources that produce vSMC during embryonic development. These include the proepicardium, serosal mesothelium, secondary heart field, somites and neural crest. An interesting discovery from the analysis of the highly mosaic cell types within the vasculature is that vSMC and their progenitors arise from distinct embryonic origins. Most relevantly, aortic root vSMC are derived from the mesoderm, the ascending aortic arch (proximal aorta) vSMC are neural crest derived, and the descending aortic vSMC are mesoderm derived (Figure 1.5). The latter phenomenon is maintained from development through adulthood (Douarin and Nantes 1975; Jiang et al. 2000; Wasteson et al. 2008; Cheung et al. 2012; Wang et al. 2015 and Pfaltzgraff et al. 2015). This is relevant as vascular disease studies including analysis of aortic homograft transplantations (of atherosclerotic-prone vessel regions into atherosclerotic-resistant vessel regions), show that a contributing factor to disease susceptibility is cell lineage and its' position (i.e. the cells' origin can dictate disease progression rather than its' location) (Woyda et al. 1960; Haimovici and Maier 1964; Haimovici and Maier 1971; Topouzis and Majesky 1996; Debakey 2000; Tanous et al. 2009; Leroux-Berger et al. 2011; Majesky, Dong and Hoglund 2011). The latter, combined with the fact that SMC of different embryonic origins respond in a lineage-specific manner to common stimuli, means that identifying the embryonic origin of vSMC and their progenitors as well as their juxtaposition is critical to informed studies and treatment development for human vascular disease conditions. Specific examples of lineage-specific cells responding in contrasting ways to common stimuli include studies conducted on chick embryo aortic arch neural crest derived vSMC and chick embryo abdominal aortic mesodermal derived SMC. In these cases, both cell types were treated with transforming growth factor β1 (TGF-β1) with an increase in DNA synthesis and cell proliferation

documented for the neural crest derived vSMC, whereas growth inhibition was observed in the mesodermal derived SMC from the same vessel (Topouzis and Majesky 1996 and Nakamura et al. 2006). In addition, TGF-β1 has been documented as producing a greater contractile response in mesodermal-derived SMC when compared with neural crest-derived SMC (Gadson et al. 1997).

To summarize, the risk of vascular disease may depend in part on the embryological origin of vSMC progenitors, with vSMCs of neuroectodermal origin exhibiting a higher risk compared to their paraxial mesodermal counterparts, a consideration which should be taken into account when conducting investigation of resident vascular stem cells' potential contribution to vessel remodeling.

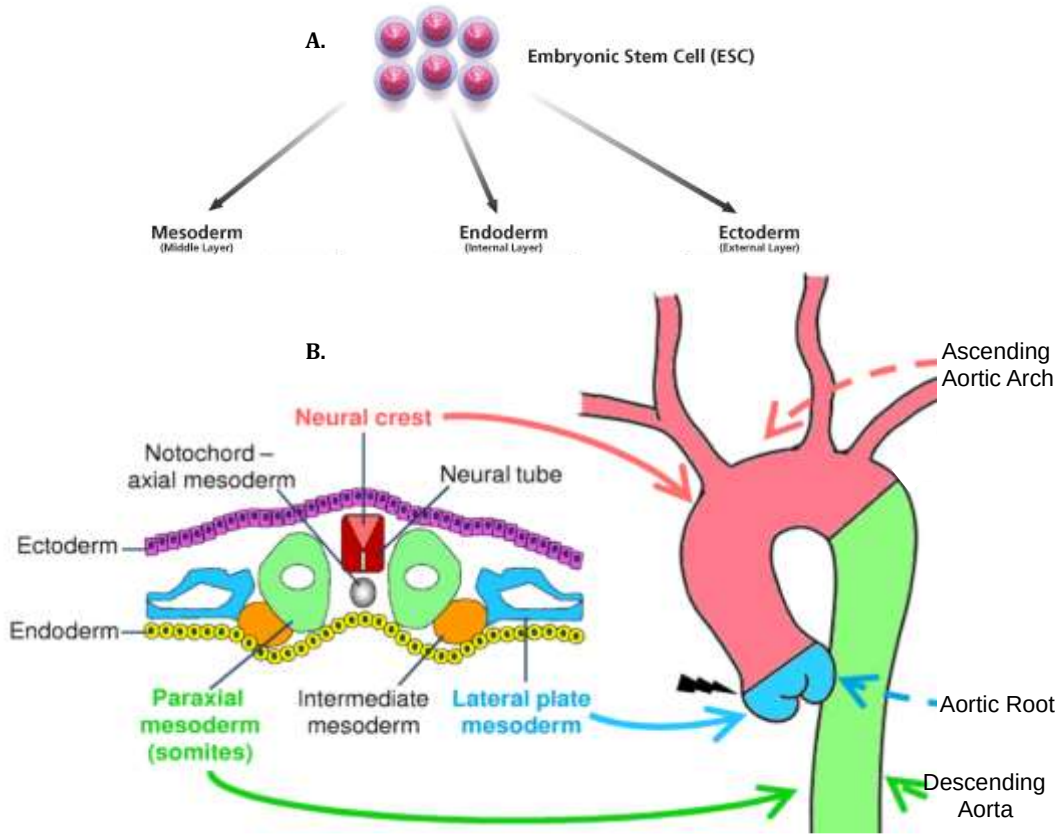

Figure 1.5: Embryonic Origin of Aortic vSMC. A: ESC differentiate into three primary germ layers: Mesoderm, Endoderm and Ectoderm. B: Aortic root vSMC derive from the mesoderm (lateral plate), the ascending aortic arch vSMC derive from the neural crest (ectoderm) and the descending aorta vSMC derive from the mesoderm (paraxial). Images edited from Cheung et al. 2012 and Sigma 2014.

1.4.3 vSMC in Vascular Remodelling

Vascular SMC (vSMC) are defined by phenotypic cell expression of α-Actin, Calponin 1 and Smooth Muscle Myosin Heavy Chain. While α-Actin and Calponin 1 are early and middle stage vSMC markers respectively, they are also observed in non-vSMC cells therefore are not definitive markers of vSMC (Hinz et al. 2001; Lu et al. 2004; Garcia et la. 2008; Tang et al. 2012; Liu et al. 2013 and Desai et al. 2014). Smooth Muscle Myosin Heavy Chain (SMMHC) on the other hand is considered a late stage vSMC marker and the most significant indicator of vSMC status (Owens 1995 and Owens et al. 2004). Therefore SMMHC has been utilised in numerous animal model investigations into the determination of vSMC contribution to vascular remodelling (Nemenoff et al. 2011; Tang et al. 2012; Herring et al. 2014 and Yang et al. 2015).

In normal physiological circumstances, the medial layer is considered poorly accessible (even to immune-privileged cells such as leucocytes), however this inaccessibility does not extend to circulating soluble plasma components (Plissonnier et al. 1995; Plissonnier et al. 2000 and Michel et al. 2007). However during vascular remodelling, cellular migration through the medial layers appears to be dependent on cell specific traits (adherence, migration and proliferation) and responses to transmural gradients of growth factors (Lacolley et al. 2012). Also during vascular remodelling, vSMC of the medial layer undergo functional changes; currently there are two theories of vSMC response to vascular remodelling:

1. vSMC exist in intermediary forms of proliferative synthetic and quiescent contractile vSMC, and the proliferative synthetic vSMC are responsible for medial thickening and neointimal lesion formation

2. quiescent contractile vSMC de-differentiate in response to stimuli to produce a proliferative synthetic vSMC that is responsible for medial thickening and neointimal lesion formation

(Owens et al. 2004; Rensen et al. 2007; Lacolley et al. 2012; Alexander and Owens 2012 and Wang et al. 2015)

Environmental cues such as growth factors and mechanical forces induce proliferation of synthetic vSMC during vascular remodelling. Additionally pathways such as the Notch and TGFβ/Smad signalling pathways (detailed in section 1.6.5) play prominent roles in modulating vSMC differentiation and proliferation (Tang et al. 2011 and Lacolley et al. 2012).

1.5 Vascular Stem Cells

1.5.1 An Introduction to Stem Cells

Stem cells are unique to other cells types in that they are unspecialised cells capable of self-renewal (sometimes after long periods of inactivity) and can be induced to proliferate and differentiate into specialised cell types following exposure to particular physiologic or experimental conditions (National Institutes of Health 2015).

All mammals derive from a single totipotent zygote (a female ova fertilised by a male sperm), which differentiates and proliferates into more than 200 cell types during embryogenesis, prenatal and postnatal development, to result in a fully developed adult mammalian body. Pluripotent embryonic stem cells are derived from a blastocysts (early embryo) inner cell mass, and give rise to the three primary germ layers: mesoderm, endoderm and ectoderm (Gilbert 2000 and Medvedev 2010) (Figure 1.6).

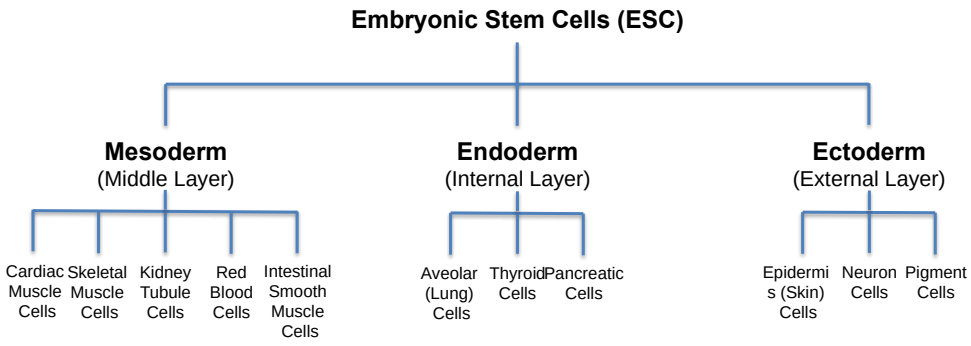

Figure 1.6: Embryonic Stem Cell (ESC) Differentiation Pathway. ESC differentiates into three primary germ layers: 1. Mesoderm, 2. Endoderm, 3. Ectoderm. These three primary germ layers give rise to derivatives with specific lineages. 1. Mesoderm – gives rise to the "middle layer", i.e. cardiac muscles and heart; skeletal muscles, connective tissue, bone and cartilage; the kidneys, spleen, gonads, genital ducts and suprarenal cortices; haematopoietic lineages (blood and immune cells); gut smooth muscle and serous membranes that line the body cavities. 2. Endoderm – gives rise to the "internal layer", i.e. the epithelial lining of the GI and respiratory tracts; the thyroid, parathyroid, the thymus and tonsil parenchyma; the

pancreas, epithelial lining of urinary tract (including bladder and urethra) and tympanic cavity (including the tympanic antrum and auditory tube). 3. Ectoderm – gives rise to the "external layer", i.e. the epidermis (skin); neuronal cells (the central and peripheral nervous system); subcutaneous and mammary glands (Pansky 1982 and Sigma 2014).

Due to this unique pluripotent capability, ESC integrity is critical and ESC are highly sensitive and rapid responders to stimuli, including heightened sensitivity to DNA damage and subsequent ability to rapidly activate apoptosis (Dumitru et al. 2012). Numerous mechanisms are involved in gene regulation and expression of ESC, epigenetically, post-transcriptionally and posttranslationally (Tay et al. 2008; Lunyak and Rosenfeld 2008; Atkinson and Armstrong 2008; Martinez and Gregory 2010; Medvedev 2010; Buckley et al. 2012; Prasad et al. 2012; Zhang et al. 2012; Zhao et al. 2012 and Boland et al. 2014).

As the embryo develops, the expanding cell populations lose their totipotency and a discrete population of resident cells maintain a level of multipotency (referred to as resident stem cells), however the majority of cells become specialised in order to fulfil their final intended purpose. High-level cell turnover tissues including the intestinal tract and bone marrow require regular resident stem cell proliferation and differentiation in order to repair or replace compromised tissues. However, other resident stem cell populations only actively proliferate and differentiate under specific conditions, for example, skeletal muscle stem cells can completely regenerate skeletal muscle following intense exercise or injury and resident cardiac stem cells can also regenerate the heart following cardiac injury (Shi and Garry 2006; Angert et al. 2012; Leite et al. 2015 and National Institutes of Health 2015). The following paragraphs will briefly discuss both active stem cell populations required for homeostasis (typically active throughout the organisms' life span) and inactive stem cell populations involved in injury response (typically inactive until condition-induced activation).

Stem Cells Involved in Homeostasis: Intestinal Crypt Stem Cells

In the gastrointestinal tract, maintenance of normal homeostasis requires rapid epithelial cell turnover in intestinal villi every 2 – 7 days, therefore

resident stem cells are critical to intestinal regeneration and continued function (Brittan and Wright 2002; Yen and Wright 2006; Clevers 2013 and Barker 2013) (Figure 1.7). Intestinal stem cells are located in the base of the intestinal crypt (paneth compartment) and generate more than 300 million new epithelial cells daily to compensate for villi shedding during the digestive process (Brittan and Wright 2002 and Barker et al. 2008). Intestinal crypt stem cells (ICSC) express high levels of Notch signalling components (pathway involved in cell fate determination), which is one of the signalling mechanisms ICSC use to regulate proliferation (self-renewal) and differentiation (to endothelia) (Brittan and Wright 2002 and Barker 2013).

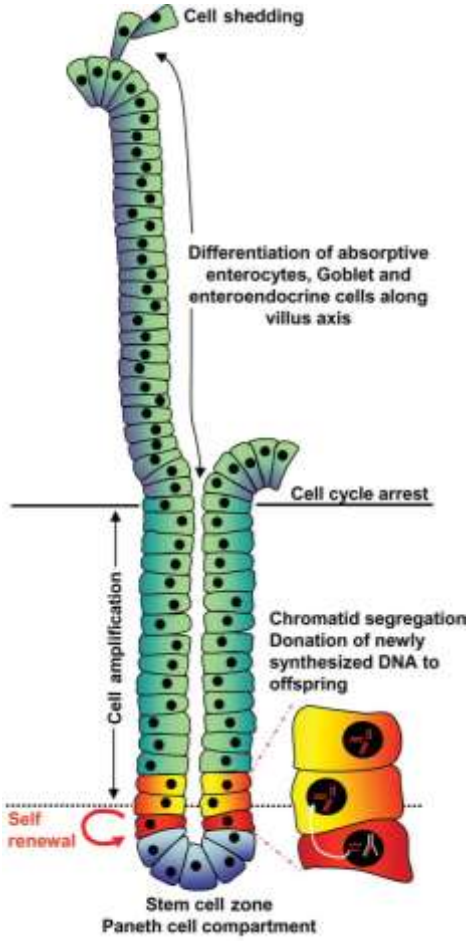

Figure 1.7: Cells of the Intestinal Crypt and Villi. Intestinal stem cells (ISC) originate from the paneth cell compartment of intestinal crypts. ISC undergo either self-renewal or begin differentiation and enter the crypts amplification zone. When ISC reach the top of the crypt and the bottom of the villus, they undergo cell cycle arrest and begin differentiating into absorptive enterocytes, Goblet and enteroendocrine cell lineages. This process is constantly occurring as differentiated GI cells are continuously shed by the digestive process hence these cells need to be constantly replaced. Image taken from Burke et al. 2007.

Stem Cells Involved in Homeostasis: Bone Marrow Stem Cells

A wide array of stem cells also reside in bone marrow, including a myeloid progenitor cell type that is required to continuously proliferate and differentiate into circulating red blood cells (erythrocytes – approximate lifespan of 115 days), platelets (maximum 7 day circulation life before destruction by liver and spleen macrophages) and immune cells such as monocytes and resident tissue macrophages and dendritic cells (Shemin and Rittenberg 1946; Handin et al. 2003 and Franco 2012) (Figure 1.8). The life span of immune cells is complicated by the nature of their purpose i.e. depends on the cell type and conditions (whether infection is present or not), however an example of an immune cells' life span is that lymph and memory T cells have been estimated to exist between 10 days and 10 years, depending on the immune systems condition (Romanyukha and Yashin 2003).

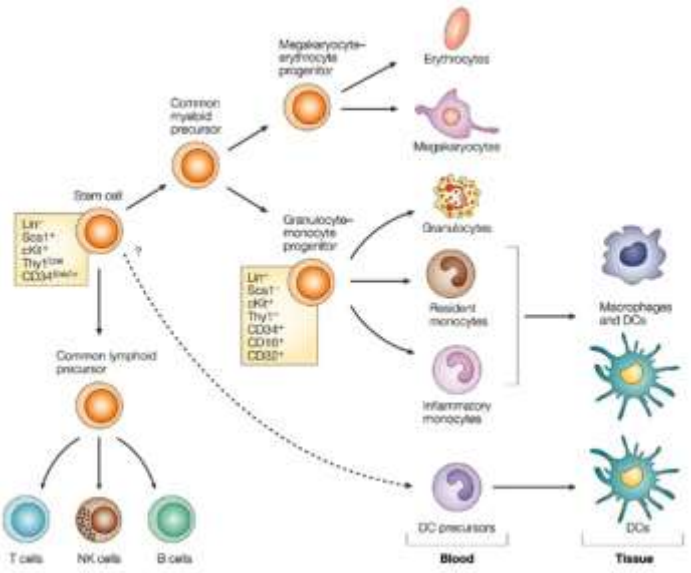

Figure 1.8: Haematopoietic Stem Cells Found in Bone Marrow. Haematopoietic stem cells originating from the bone marrow differentiate into either lymphoid or myeloid lineage stem cells. Lymphoid stem cells differentiate to produce T, B and natural killer (NK) immune cells. Myeloid stem cells can further differentiate into two stem cell sub-populations, megakaryocyte-erythrocyte stem cells which produce erythrocytes (red blood cells) or megakaryocyte (platelet producing cells) or, granulocytes-monocyte stem cells which produce granulocytes, resident blood and inflammatory monocytes (which become dendritic cells and macrophages in resident tissue) and dendritic stem cells (which become dendritic cells in resident tissue). Image taken from Imhof and Auraand-Lions 2004.

Stem Cells Involved in Injury Response: Skeletal Muscle Stem Cells

Resident skeletal muscle stem cells (SMSC) are the main contributors to postnatal muscle fibre growth, as well as regeneration following injuries such as strains and trauma (Saverio-Tedesco et al. 2010). SMSC also play a key role in muscle regeneration during degenerative muscular diseases such as muscular dystrophy, which results in progressive muscle wasting. However, their regenerative capacity is eventually exhausted in severe cases such as Duchenne Muscular Dystrophy and leads to anything from wheelchair confinement to heart and/or respiratory failure (Shi and Garry 2006 and Saverio-Tedesco et al. 2010). SMSC are located in a specialised niche under the basal lamina of muscle fibres and above the muscle sarcolemma (myofibers outer membrane), and while SMSC originate from mesodermal stem cells, the exact parent stem cell they derive from has yet to be elucidated (Saverio-Tedesco et al. 2010 and Almada and Wagers 2016). Skeletal muscle accounts for 30 – 50 % of human body mass and SMSC represent ~ 2 – 7 % of healthy adult skeletal muscle. Within days of injury, these ~ 2 – 7 % SMSC both self-renew (in preparation for subsequent injury response) and generate a large number of new myofibers to repair damage (Saverio-Tedesco et al. 2010; Fu et al. 2015 and Almada and Wagers 2016). Physiological cues regulate SMSC activation through a number of pathways including but not limited to the Notch and Wnt signalling pathways (Fu et al. 2015 and Almada and Wagers 2016). Both the Notch and Wnt pathways control cell fate, with Notch being key to myogenic cell fate commitment and SMSC maintenance, and Wnt being key to stem cell population maintenance as well as cell polarity and morphology (Fu et al. 2015 and Almada and Wagers 2016). Some of these physiological cues include the following signalling molecules and epigenetic factors:

<u>Signalling molecules</u>

- Vascular circulatory factors such as Vascular Endothelial Growth Factor (VEGF) and Platelet Derived Growth Factor (PDGF) (Fu et al. 2015)

- Immune cell released cytokines and chemokines such as Interleukin-6 (IL-6) and Interferon gamma (IFNγ) (Fu et al. 2015)
- SMSC microRNA such as miR-29a and miR-1 (Fu et al. 2015 and Galimove et al. 2016)

Epigenetic factors

- Release of epigenetic regulators such as the Polycomb and Ttrithorax groups (Fu et al. 2015)

SMSC activation results in proliferation (SMSC population maintenance) and differentiation (to replace damaged tissue) (Saverio-Tedesco et al. 2010; Fu et al. 2015 and Almada and Wagers 2016) (Figure 1.9).

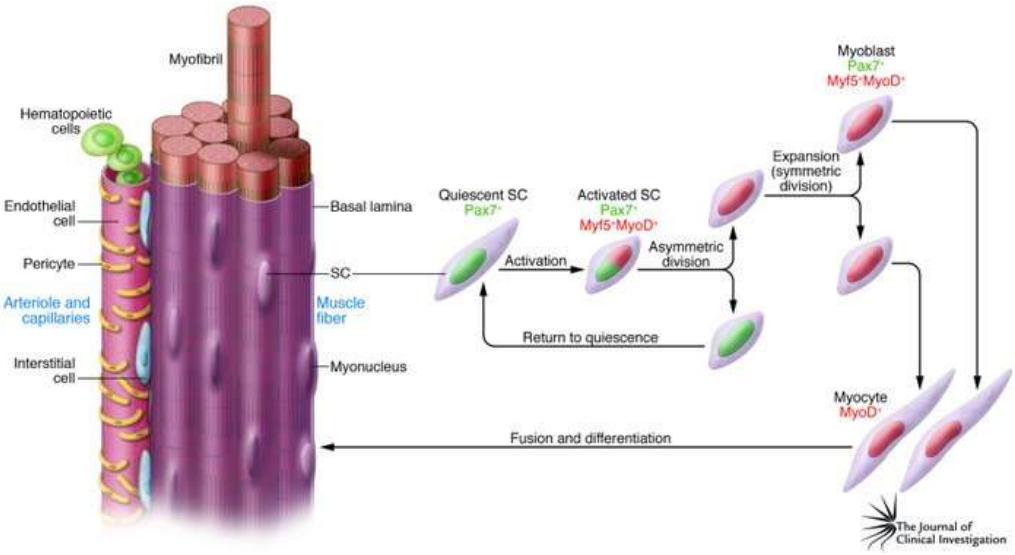

Figure 1.9: Activation of Skeletal Muscle Stem Cells (SMSC). Representative schematic of a skeletal muscle fibre and associated blood vessel. Injury induced SMSC activation results in asymmetric cell division where self-renewal SMSC populations are Pax7⁺ (maintenance of stem cell population) and differentiating cells destined to replace damaged cells are Pax7⁺, MyoD⁺ and Myf5⁺. Image taken from Saverio-Tedesco et al. 2010.

Stem Cells Involved in Injury Response: Cardiac Stem Cells

Unlike SMSC of the skeletal muscular system, cardiac stem cells are a relatively recent phenomenon. Historically, the hearts' cardiac population was deemed to contain terminally differentiated cardiac cells exclusively, however irrefutable evidence over the last decade has subsequently muted the theory (Beltrami et al. 2003; Torella et al. 2005; Barile et al. 2007; Angert et al. 2012; Ellison et al. 2013; Leri et la. 2014; Nadal-Ginard et al. 2014 and Leite et al. 2015). Cardiac stem cells (CSC) regenerate the hearts terminally differentiated cardiac cell population in response to pathological stress such as myocardial infarction (which results in cardiac cell death and deterioration of cardiac performance) (Angert et al. 2011 and Nadal-Ginard et al. 2014). A variety of CSC have been identified, however their contribution to normal heart physiology and specific capacity for cardiac regeneration has yet be elucidated as a large number of post-infarct survivors do not recover sufficiently and ultimately succumb to pre-mature cardiac failure (Beltrami et al. 2003; Torella et al. 2005; Barile et al. 2007; Ballard and Edelbery 2008 and Angert et al. 2012). Nonetheless, a multipotent adult resident CSC known as c-kit^{+} CSC can regenerate most cardiac cells (including associated microvascular cells) lost in an severe infarct injury (Beltrami et al. 2003; Barile et al. 2007; Ballard and Edelbery 2008 and Ellison et al. 2013) (Figure 1.10). Importantly, components of the previously mentioned Notch signalling pathway (which controls cell fate), are found in the cardiac niche of the myocardial interstitium, and have been shown to regulate CSC-cardiac cell transition (Leri et al. 2014).

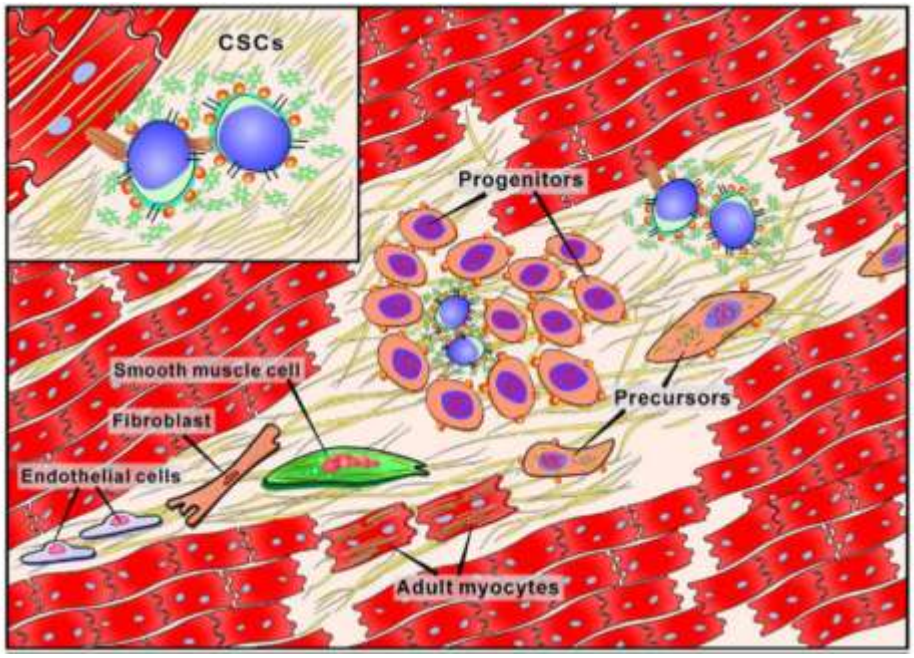

Figure 1.10: The Cardiac Stem Cell (CSC) Niche. Representative schematic of the CSC niche. When activated, CSC proliferate (maintain the CSC population) and into differentiate into a cardiac stem/differentiated intermediate (progenitor). The progenitor cell will continue down the differentiation pathway through precursors to specific terminally differentiated cardiac cell type such as adult myocytes, smooth muscle cells and endothelial cells. Image taken from Leri et al. 2014.

1.5.2 Stem Cell-Associated Pathologies

The balance between stem and differentiated cell population composition is a critical phenomenon throughout prenatal development and postnatal existence. Starting at the developmental stage, the balance between proliferation and differentiation must be strictly controlled in order to establish appropriate quantities of lineage-specific precursors and functional differentiated cells in their desired spatial and temporal sequences (Blanpain and Simons 2013 and Dahmann et al. 2011). Dysregulation of such at the developmental stage causes havoc ranging from embryonic lethality to severe birth defects. Classic examples of such are mutations to key components of the Notch and Hedgehog signalling systems. Mutations in the Notch signalling system produce severe birth defects, and mutations in the Hedgehog signalling system, for example knockout of Sonic Hedgehog (Shh), is associated with holoprosencephaly and increased Shh signalling is linked to spina bifida and exencephaly (Murdoch and Copp 2010; Roessler and Muenke 2003; High et al. 2008; Fischer et al. 2004; Wang et al. 2003 and Iso

et al. 2003). In adult systems, this phenomenon continues in the form of tissue homeostasis and again dysregulation can have serious consequences, a classic example are *Notch 3* mutations resulting in Cerebral Autosomal Dominant Arteriopathy with Subcortical Infarcts and Leukoencephalopathy (Joutel et al. 1996). The latter affects young or middle aged adults and presents as frequent migraine attacks, recurrent strokes and vascular dementia (Ayata 2010). Also, mutations to Hedgehog signalling components such as Gli1, result in a variety of adult cancers such as Glioblastoma, Rhabdomyosarcoma, Osteosarcoma and B cell carcinoma to name but a few (Villavicencio et al. 2000).

1.6 Pathways and Factors Involved in Vascular Remodelling

1.6.1 Introduction to the Hedgehog (Hh) Signalling Pathway

The evoluntarily conserved Hh pathway is one of a limited number of signalling pathways that can direct stem cells as well as regulate differentiation and regeneration. The Hh signalling pathway is initially activated in embryonic development as an embryonic patterning regulator and is maintained in postnatal physiology for the purposes of adult tissue maintenance, renewal and regeneration (Liu 2006 and Wilson and Chuang 2010). Inadequate regulation or mutation of key Hh signalling components are embryonic lethal or result in congenital birth defects such holoprosencephaly; or manifest as cancer such as rhabdomyosarcoma in adults (Haines and Heuvel 2000; Johnson et al. 1996; Hahn et al. 1996; Kappler et al. 2004 and Hammond and Schulte-Merker 2009). Interestingly, core signalling genes in the mammalian Hh pathway have not undergone extensive gene duplication, making it unique compared to other major signalling pathways like Fgf, Notch and Wnt (Pires-daSilva and Sommer 2003). The significance of the Hh signalling pathway is highlighted by the large number of reviews published over the last decade alone (Bijlsma et al. 2006; Varjosalo and Taipale 2008; Marasani et al. 2010; Cohen 2010; Wilson and Chuang 2010; Hui and Angers 2011; Briscoe and Thérond 2013; Choudhry et al. 2014 and Falkenstein and Vokes 2014).

1.6.2 Key Components of the Hh Signalling Pathway

The following table lists the key components of the Hh signalling pathway and briefly describes their function:

Signalling Ligands*	Membrane Bound Receptors	Cytoplasmic Proteins	Target Genes
Desert Hedgehog (Dhh)	Dispatched 1, 2 - are involved in Hh ligand release	Kinesin Family Member 7 (Kif7) - is an intraflagellar transport protein which acts as a scaffold for Gli processing by regulating signalling from Smoothened, has both positive and negative roles	*patched 1, 2*
Indian Hedgehog (Ihh)	Smoothened - is a positive membrane transducer	Gli 1, 2, 3 - Gli1 appears to be a constitutive activator and has a function not shared with Gli2. It can also antagonize Gli3, and rescue Gli2s function *in vivo* Gli2 is known to act as both a transcriptional activator and repressor, with defect studies suggesting its primary function as an activator *in vivo* Gli3 is considered to be a transcriptional repressor	*hedgehog interacting protein 1 (hhip 1)* - is a Hh signalling repressor
Sonic Hedgehog (Shh)	Patched 1, 2 - are inhibitors of Smoothened	Serine/ Threonine Kinase Fused (Fu) - is a positive transducer and is necessary for Sufu phosphorylation	*gli 1, 2, 3* - The target genes *gli1, gli2 and gli3* are considered to have derived from the duplication of a single ancestral gene

	CDON and BOC – are Patched co-receptors and play a positive role in Hh signalling	Suppressor of Fused (Sufu) - is a negative regulator by protecting Gli proteins from Spop-induced degradation	
References: (Echelard et al. 1993; Briscoe and Thérond 2013; Cohen 2010 and Choudhry et al. 2014).	References: (Wilson and Chuang 2010 and Beachy et al. 2012)	References: (Bai and Joyner 2001; Huangfu et al. 2003; Ocbinaac 2009; Wilson and Chuang 2010; Ishikawa and Marshall 2011 and Briscoe and Thérond 2013)	References: (Cohen 2010; Hui and Angers 2011 and Holtz et al. 2013)

Table 1.1: Key Components of the Hh signalling pathway. * Hedgehog signalling ligands act both locally and distantly.

1.6.3 Hh Signalling

Hh signalling regulates Gli activation and repression; it is a complex process with numerous publications detailing the mechanisms hence the following is a brief summary of the signalling process using information gathered from Varjosalo and Taipale 2008, Wilson and Chuang 2010, Cohen 2010, Beachy et al. 2012, Briscoe and Thérond 2013, Teperino et al. 2014 and Choudhry et al. 2014. See table 1.1 for further details on each Hh signalling component.

Gli Repression (See figure 1.11 "Off State")

In the absence of a signal, the Gli proteins are converted into transcriptional repressors. This is done by the sequential phosphorylation of the Sufu-Gli protein complex by glycogen synthase kinase 3β (GSK3β), a process which is assisted by Kif7; this phosphorylation promotes Gli ubiquitylation and partial proteolytic processing to become a truncated protein denoted Gli-R. Gli-R then translocates to the nucleus to repress gene expression due to the preservation of the DNA-binding domain (Briscoe and Thérond 2013; Cohen 2010 and Choudhry et al. 2014).

Gli Activation (See figure 1.11 "On State")

Target cells are activated when Hh signalling ligands are released from the Hh secreting cell through Dispatched. The Hh signalling ligands then bind to

Patched and Patched co-receptors CDON and BOC. This binding inactivates Patched which de-represses Smoothened by accumulation and phosphorylation in the presence of Hh proteins and β-arrestin. Smoothened then mediates the disassembly of the Sufu-Gli complex which releases activated Gli which then translocates to the nucleus to activate target gene transcription (Briscoe and Thérond 2013; Cohen 2010 and Choudhry et al. 2014).

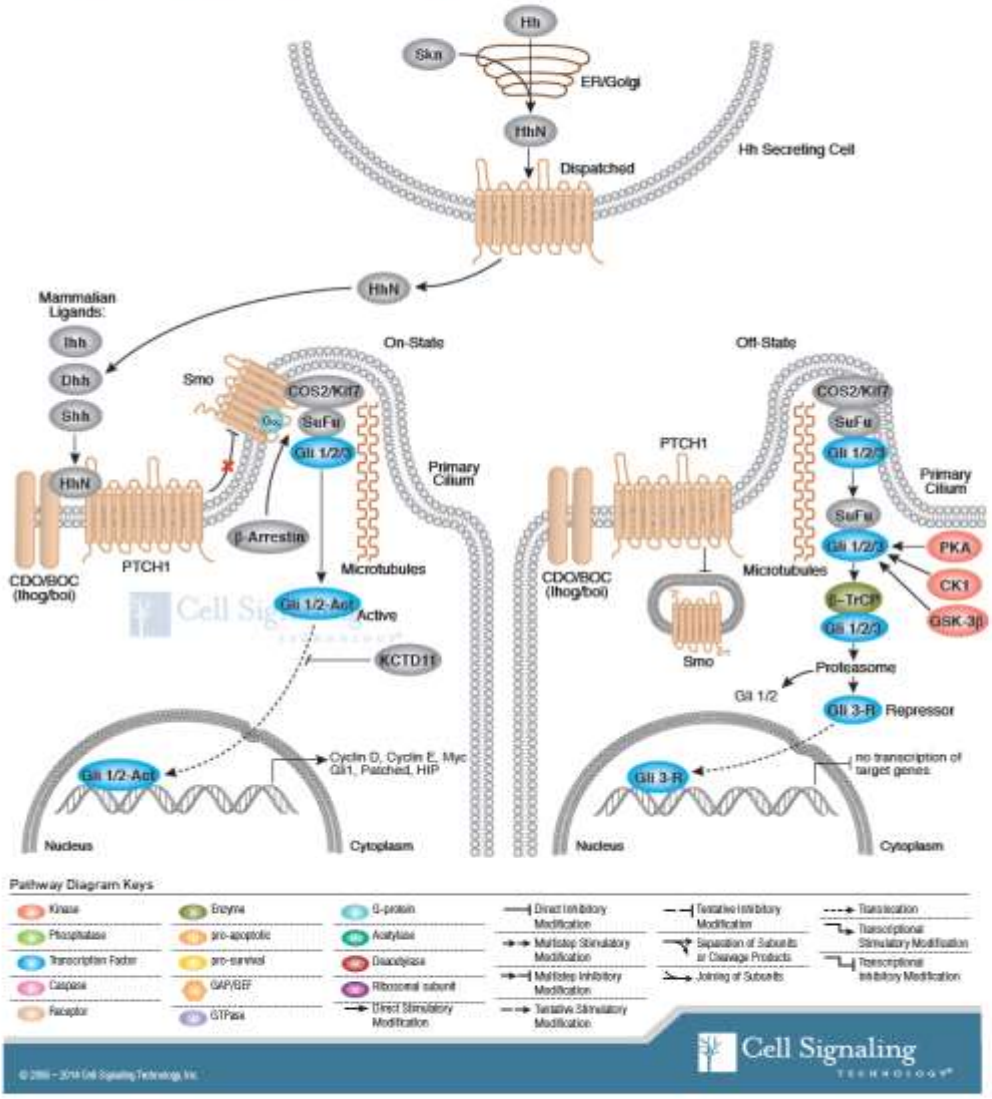

Figure 1.11: Hh signalling. Off state: in the absence of Hh signalling molecules cytoplasmic Sufu-Gli protein complexes are phosphorylated by GSK3β which results in partial proteolytic cleave of Gli to become a repressor protein Gli3-R with the ability to translocate to the nucleus for subsequent system repression. On state: Hh signalling ligands are secreted from Hh secreting cells by Dispatched and subsequently bind to Patched and Patched co-receptors to activate Smoothened. Activated Smoothened is accumulated and disassembles Sufu-Gli

complexes to release Gli, Gli then translocates to the nucleus to initiate target gene transcription. Image taken from Cell Signalling Technologies 2014.

1.6.4 Hh Signalling in Vascular Biology and Remodelling

The development of the cardiovascular system specifically also requires appropriate Hh signalling which has been shown to be recapitulated during vascular injury and remodelling which will be discussed at length in the next section (Bijlsma et al. 2006; Passman et al. 2008;Morrow et al. 2008; Morrow et al. 2009; Redmond et al. 2013 and Holtz et al. 2013). However briefly, Passman et al. 2008 published a ground breaking paper that showed resident adventitial vascular stem cells have a Shh signalling domain which co-localises with the Shh receptor Patched 1. They theorised that the Hh signalling molecules may support resident Stem Cell Antigen 1 positive ($Sca1^{+}$) vascular stem cells. Our lab group have also shown the presence of Patched 1 in healthy vessels, as well as Hh signalling recapitulation following injury, and the attenuation of vascular remodelling using Hh specific knockdown techniques (Morrow et al. 2008; Morrow et al. 2009 and Redmond et al. 2013).

1.6.5 Other Pathways and Factors Involved in Vascular Remodelling

Vascular remodelling is a complex pathology due to the interaction of injury-induced apoptotic and non-apoptotic cells (stem, non-stem and immune (both circulatory and resident)) at the site of injury. Therefore a range of chemokines, cytokines and signalling pathways other than the aforementioned Hh pathway feature in vascular remodelling (Baker et al. 2001; Weyrich et al. 2002; Morrow et al. 2009; Sprague et al. 2010; Qi et al. 2011; Suwanabol et al. 2011 and Redmond et al. 2013). The following will give a brief introduction to two of the other key signalling systems observed during vascular remodelling: the Notch and TGFβ/Smad signaling pathways.

Introduction to Pathways Involved In Vascular Development

The Notch signalling pathway is highly conserved in metazoans and regulates cell fate determination and vascular development. Notch receptor (Notch 1 – 4) interaction with specific ligands (Delta like 1, Delta like 3, Delta like 4, Jagged 1, Jagged 2) results in the cleavage of the Notch intracellular domain

(NICD). The NICD then translocates to the nucleus where it associates with a transcription factor (RBP-Jk) to form a NICD-RBP-Jk complex. The NICD-RBP-Jk complex upregulates Notch primary target gene expression (hairy and enhancer split (HES) and HES-related repressor protein (HERP, also known as HEY and HRT)). HES and HERP expression negatively regulate downstream Notch target genes to influence angiogenesis and arterial–venous differentiation and cellular proliferation, differentiation (especially SMC) and migration. Notch signalling can also influence SMC survival through modulation of apoptosis mediator expression such as Bax. This regulation can be through direct transcriptional regulation, post-transcriptional regulation and post translation regulation. The Notch receptors 1, 3 and 4 and ligands Delta like 4 and Jagged 1, 2 are primarily expressed in arteries, and activated Notch signalling has been shown to promote SMC differentiation whereas expression of Notch target genes *hrt1* and *hrt2* suppresses SMC differentiation (Iso et al. 2003a; Iso et al. 2003b; Fischer et al. 2004; Morrow et al. 2009 and Tang et al. 2010). Interestingly, extracellular processing of the Notch receptor following ligand activation is thought to be conducted by a transforming growth factor-α (TNFα) converting enzyme (Hartmann et al. 2001). Notch 3 mutations result in the vessel homeostasis pathology cerebral autosomal arteriopathy with subcortical infarcts and leukoencephalopathy (CADASIL) (Iso et al. 2003a).

The TGFβ/Smad pathway is heavily involved in cell proliferation, differentiation, survival and apoptosis, and the TGFβ protein family are potent cytokines with multifunctional capabilites (Wang et al. 2015). TGFβ is a member of a highly evolutionarily conserved growth factor superfamily and exists in three isoforms: TGF-β1, 2 and 3, and TGF-β1 is expressed in fibroblasts, hematopoietic cells, SMCs and epithelial cells. Cells synthesize TGFβ ligands as dimeric pro-hormones which associate with a latent TGFβ binding protein (LTBP) and latency-associated peptide (LAP) before secretion into the extracellular matrix as a latent dimeric complex. The active signalling molecule is produced when the latent dimeric complex is cleaved by convertases. TGFβ signalling activation occurs following TGFβ ligand-

receptor binding. TGFβ binds to a constitutively phosphorylated bi-dimeric receptor system (two pairs of transmembrane serine-threonine kinaseses) and results in a complex formation that starts a signalling cascade that recruits Smad signalling proteins (cytoplasmic signal transducers) which are essential for TGFβ target gene activation and regulation (Smad regulates TGFβ receptor degradation) (Suwanabol et al. 2011). An example of TGFβs' influence on SMC differentiation is Serum Response Factor (SRF)-myocardin activation following TGFβ1-initiated NADPH oxidase 4 induction and H_2O_2 production (Clempus et al. 2007 and Xiao et al. 2009). The SRF-myocardin complex is key for SMC differentiation, with SRF deficiency resulting in inactive SmαA (Smooth Muscle alpha A) and SM22α (Smooth Muscle 22 alpha) promoters and impaired SMC differentiation (Wang et al. 2015).

Pathway Interactions

Notch and TGFβ pathway interaction is also critical during vascular development and vascular pathologies. Notch and TGFβ use parrallel signalling axes to cooperatively activate SMC differentiation (co-regulation of SMC promoter Smad activity), and Notch signalling antagonists such as HRT proteins also suppress multiple stimuli induced SMC differentiation, such as Notch, TGFβ and myocardin-induced SMC differentiation (Tang et al. 2010).

Interestingly the Notch and Hh pathways also interact, with Shh inducing SMC expression of Notch target genes through vascular endothelial growth factor A (VEGF-A) activation, a process which can be attenuated following Notch inhibiton (Morrow et al. 2009).

1.6.6. Stem Cells Involved in Injury Response: Vascular Remodelling

Experimental data has shown that the adventitia responds rapidly and dramatically to vascular injury and stress (Sartore et al. 2001; Korshunov and Berk 2004; Torsney et al. 2005 and Tigges et al. 2012). Adventitial cell proliferation (neoadventitia formation and adventitial fibrosis) has been documented in hypertension, pulmonary hypoxia, ligation injury and haemodynamic stress (low shear stress and high heart rate), arterial flow

reduction and balloon injury (overstretching) respectively (McGrath et al. 2005; Stenmark et al. 2006; Korshunov and Berk 2004; Korshunov and Berk 2003 and Faggin et al. 1999).

One of the first papers to show adventitial progenitor cell's (APC) potential for migration to the neointima used a β-galactosidase reporter to track APCs (Li et al. 2000). The data suggested that β-gal$^+$ cells were not the most abundant neointimal cell yet the experimental design limited the exact quantitation of APCs involvement in neointimal formation (Li et al. 2000). A similar study was later published by another group and came to the same conclusion (Siow et al. 2003). More recently, others have reported an adventitial CD44$^+$ multipotent stem cell that contributes to new vessel maturation (Klein et al. 2011).

In 2004, Hu et al., published a ground-breaking paper that characterised the aortic root adventitia and revealed that it harbours a large number of stem cell marker positive cells, including 21 % population expression of the stem cell marker stem cell antigen 1 (Sca1) (Hu et al. 2004). They also showed that adventitial Sca1$^+$ cells have the potential to become SMC *in vitro* and *in vivo*. The *in vitro* study involved culturing explanted adventitial cells and showed that isolated Sca1$^+$ cells have the potential for differentiating into SMCs and endothelial cells (ECs). The *in vivo* study used ApoE-deficient mice with lethally irradiated veins seeded with adventitial Sca1$^+$ cells' from SM-LacZ mice and demonstrated adventitial Sca1$^+$ cells contribution to neointimal formation.

Since then there have been numerous studies published on the role of Sca1$^+$ stem cells in promoting myocardial and vessel regeneration (Wang et al. 2006; Passman et al. 2008; Orlandi and Bennett 2010; Majesky et al. 2011; Hu and Xu 2011; Liang et al. 2011; Bautch 2011; Uchida et al. 2013 and Tigges et al. 2013). Passman et al., reported that the Hedgehog signalling pathway receptor, Patched 1 is present in the adventitial boundary, and colocalises with Sca1 and Shh in healthy vessels (Passman et al., 2008, Figure

1.12). The authors concluded that adventitial Hh signalling is crucial for the maintenance of resident $Sca1^+$ cells in vivo. Interestingly, the co-localisation of $Sca1^+$ cells with Shh was made in young healthy vessels. Similar findings were reported *in vivo* by our lab group in older healthy carotid arteries (Morrow et al. 2009). In this study, healthy carotid arteries express Patched 1 predominantly within in the adventitia, and the relative absence of Gli 2 (a hedgehog target gene) suggests that Hh signalling is primarily inactive in healthy vessels despite the presence of the Patched 1 Hh receptor (Morrow et al. 2009) and Shh ligand (Passman et al. 2008). The authors also present compelling evidence of Patched 1 and Gli 2 expression following ligation-induced injury in both adventitial and neointimal cells (Figures 1.13 and 1.14). Additionally *patched 1* and *gli 2* genes (transcriptional targets of the Hh signalling pathway) are upregulated in response to Hh signalling, and the injury-induced activation of Hh target genes occurs within the adventitia and intimal layers (Holmes and Stanford 2007). Hence these study suggest that Hh activation occurs in both the adventitia and neointimal cells following injury, and the significance of Hh signalling in vascular remodelling is further reinforced by follow-up studies whereby perivascular knock down of Patched 1 using siRNA attenuates vessel remodelling (Figure 1.14).

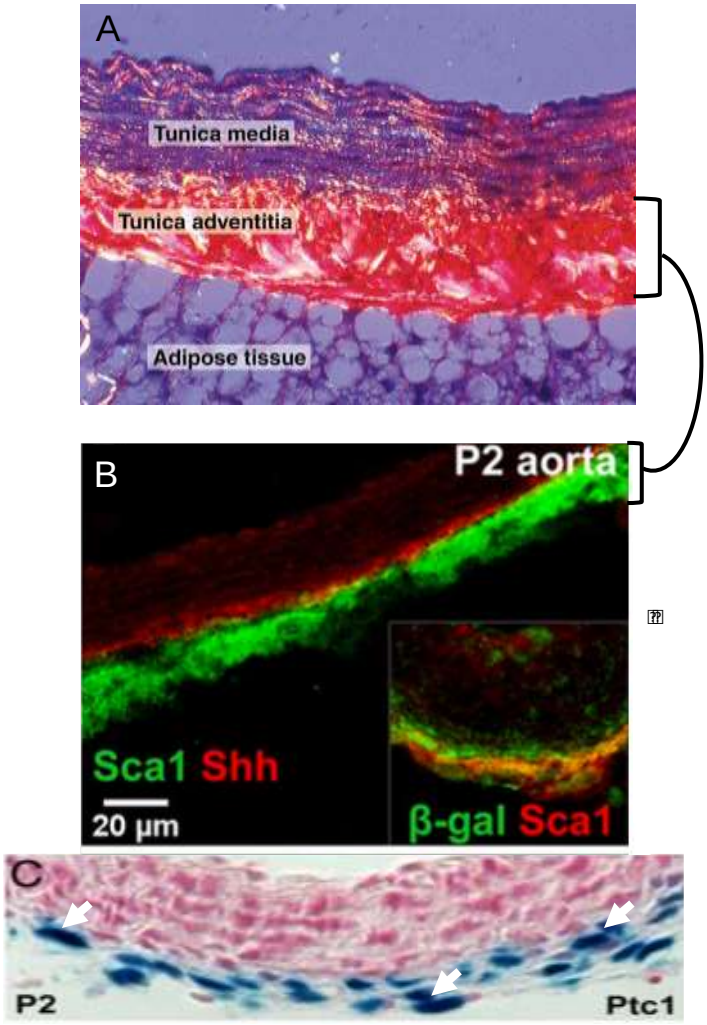

Figure 1.12: Localisation of Sca1⁺ cells and Hh signalling components. A: Cross-section of vessel explant showing the tunica adventitia is located between the tunica media and adipose tissue. B: Cross-section of the tunica adventitia; Sca1 (green) is found in close proximity to Shh (red). C: Cross-section of the tunica media and tunica adventitia; showing *Ptc1lacZ staining*. Images taken from Passman et al. 2008.

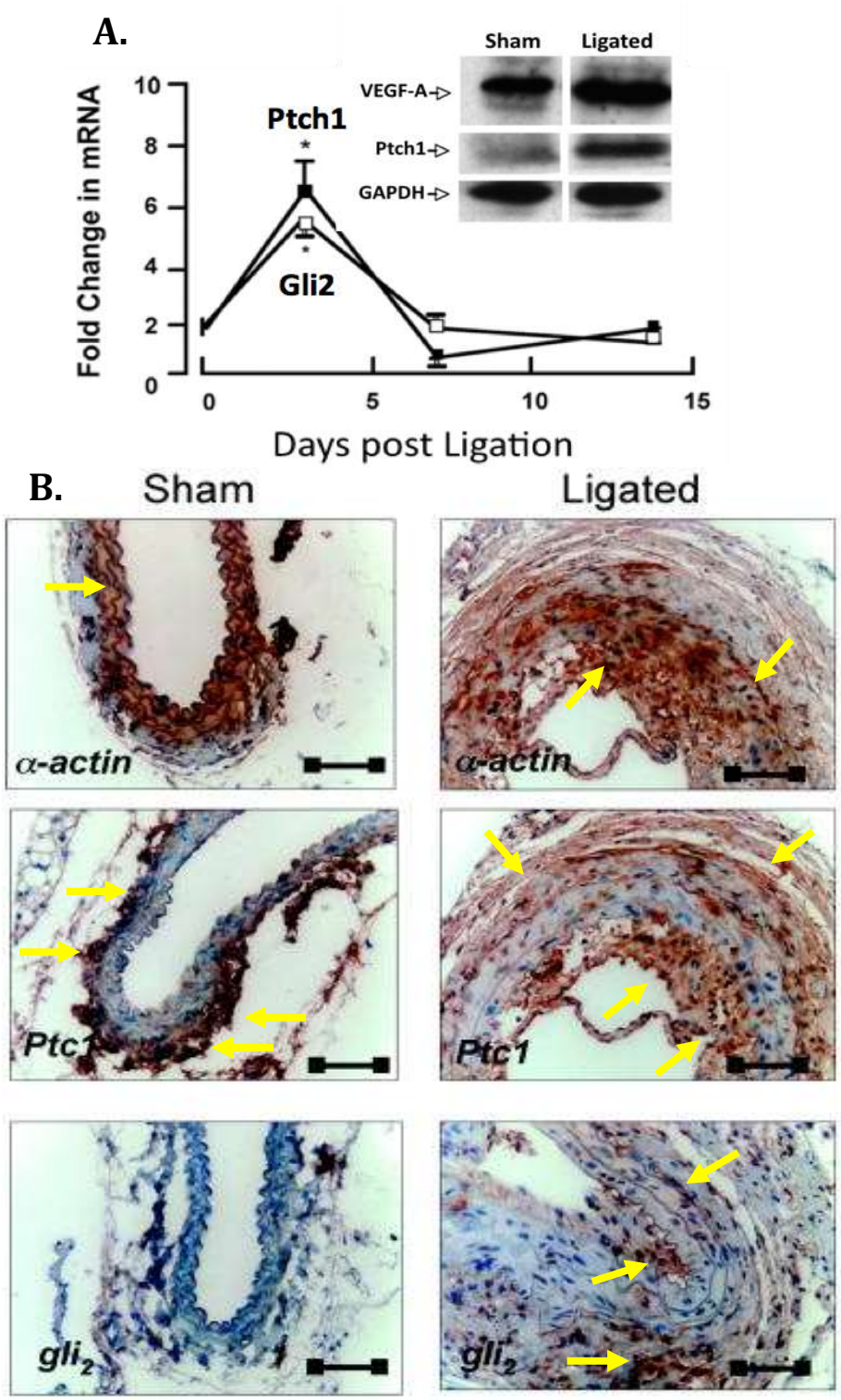

Figure 1.13: Hh signalling in healthy and injured vessels. A: mRNA levels of Shh receptor Patched 1 and Hh signalling target gene Gli 2 in healthy (sham) and injured (ligated) vessels. B: Protein detection of Shh receptor Patched 1 and Hh signalling target gene Gli 2 in healthy (left hand images) and injured (right hand images) vessels. Images taken from Morrow et al. 2009.

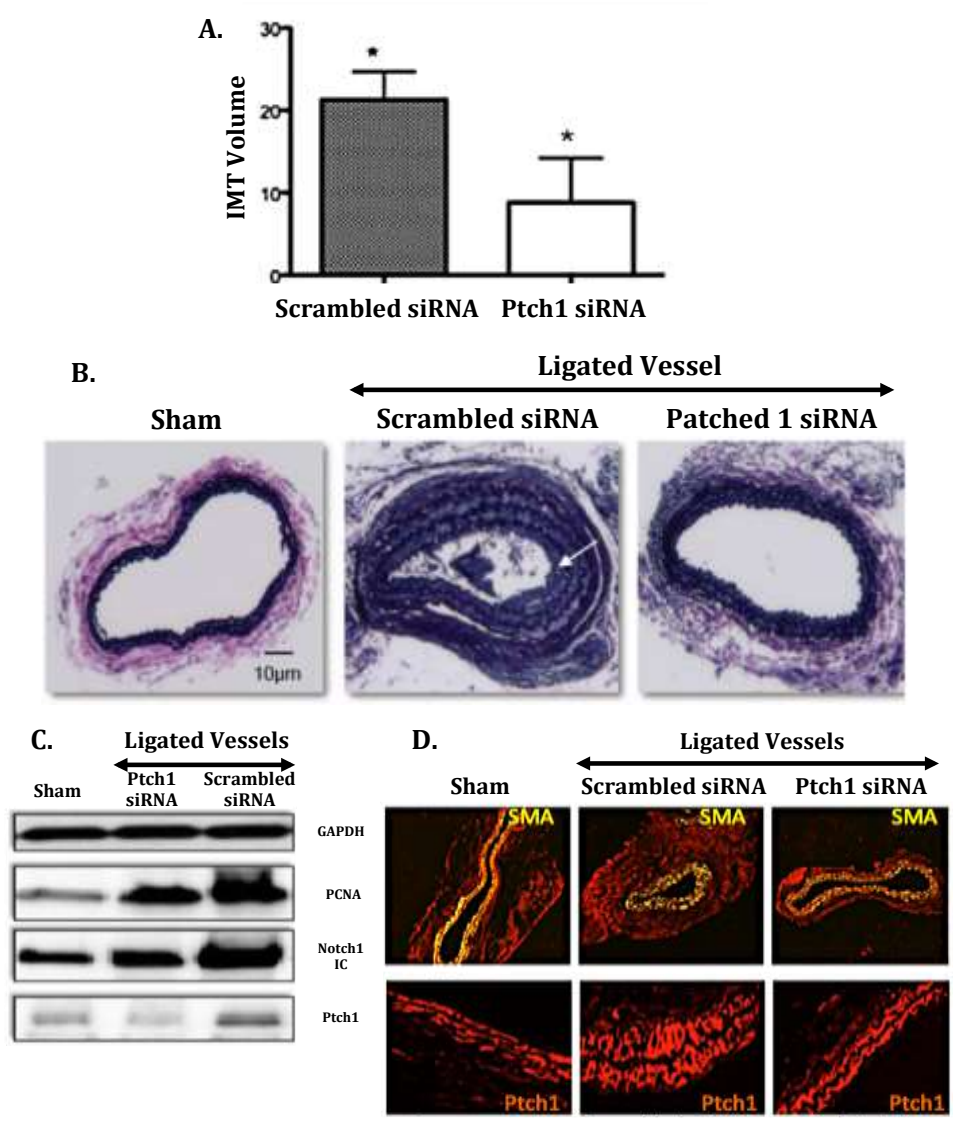

Figure 1.14: Patched 1 small interfering RNA (siRNA) inhibits injury-induced neointimal hyperplasia. Carotid arteries 14 days post sham operation or ligation ± Patched 1 siRNA. A: Intimal Medial Thickening (IMT) volume of control scrambled siRNA ligated carotid vessels and Patched 1 (Ptch1) siRNA ligated carotid vessels. B: Verhoeff van Gieson stain analysis of sham and ligated (scrambled siRNA and Patched 1 siRNA) carotid vessels. C: western blot analysis of sham and ligated (scrambled siRNA and Patched 1 siRNA) carotid vessels. D: immunofluorescence analysis of sham and ligated (scrambled siRNA and Patched 1 siRNA) carotid vessels (SMA = smooth muscle α-Actin and Ptch1 = Patched 1). Images taken from Redmond et al. 2013.

Contribution of Other Stem Cells to Vascular Remodelling

There are two other reported stem cell sources that may contribute to the cellular accumulation during vascular remodelling: 1. Bone Marrow-Derived Progenitor Cells and 2. Resident Medial Stem Cells.

Since 1987, circulatory bone marrow-derived progenitor cells (including mesenchymal stem cells – MSC) have been widely reported to contribute to post-injury vessel re-endothelialisation and vascular remodelling (Sata 2003; Shoji et al. 2004; Sahara et al. 2007; Doi et al. 2009; Shoji et al. 2014 and Moldovan et al. 2014). It has been reported that bone marrow contributes to vasculopathies (including vascular remodelling), by producing circulatory vascular progenitor cells that specifically target damaged vessels and begin differentiating and proliferating into the SMC, which ultimately results in vessel occlusion (Sata 2003 and Shoji et al. 2014). Studies have also shown that hematopoietic lineage cells attach to the luminal side of an injured vessel prior to vascular remodelling and SMC accumulation, and that neointimal SMC also express hematopoietic lineage markers (Sata 2003 and Shoji et al. 2004). However the data generated since these seminal studies suggests that the contribution of bone marrow-derived stem cells to the accumulation of neointimal SMCs at the site of injury depends on the level of injury and trauma to the vessel wall and the level of local inflammation (Sainz and Sata 2006 and Daniel et al. 2010).

The evidence for resident medial stem cells' contribution to vascular remodelling is relatively recent. Tang et al., present compelling evidence of the potential for resident medial multipotent stem cell contribution to vascular remodelling (Tang et al. 2012). The authors isolated a neural crest multipotent stem cell population ($Sox\,10^{+}$, $Sox\,17^{+}$ and $S100\beta^{+}$) with the ability to differentiate into SMC *in vivo* and *in vitro*. The group also show that these medial progenitor stem cells proliferate and differentiate into SMC in response to vascular injury, hence have the potential to contribute to vascular remodelling (Tang et al. 2012). Additionally, another report also shows a medial $Sca1^{+}$ progenitor cell type (with aortic prevalence of ~ 6 %) with EC and SMC differentiation capability (Sainz et al. 2006).

1.7 Project Objectives

The overall laboratory focus is to assess the specific role of resident vascular stem cell populations in contributing to vascular remodelling, with the ultimate aim of developing a specific therapy that could be incorporated into current drug eluting stent (DES) platforms. Due to the proposed specificity of the targeted therapeutic treatment, the current restenotic and thrombotic side effects of bare-metal stents and the current DES therapies (Sirolimus and Pacitaxel) could be circumvented, thereby increasing the success rate of post atherosclerotic intervention dramatically.

As part of the wider research project, my specific project aim was to:

"Assess hedgehog-responsive adventitial Sca1⁺ stem cells' contribution to vascular remodelling"

The project utilises three experimental strategies to address the overall aim:

1. Devise Cell Models for Sca1⁺ Cell Isolation and Characterisation
2. Evaluate Hedgehog Control of Sca1⁺ Cell Renewal and Differentiation *In Vitro*
3. Evaluate Hedgehog Control of Sca1⁺ Cell Renewal and Differentiation *In Vivo*

Aim 1: Devise Cell Models for Sca1⁺ Cell Isolation and Characterisation

This aim involved the following:

- Isolation, characterisation and Sca1 purification of adventitial progenitor cells (APC) from aortic explants
- Purification and characterisation of Sca1⁺ cells from mouse fibroblast cell C3H/10T1/2 origin (Model cell line 1: Sca1⁺ C3H)
- Generation, purification and characterisation of Sca1⁺ cells from mouse embryonic stem cell ES-D3 origin (Model cell line 2: Sca1⁺ mESC)

Note: As will be discussed in detail in chapter 3, establishing a Sca1⁺ APC cell line was not an easy feat, therefore two model cell lines were used in order to

conduct the proof of principle experiments. These cell lines (Sca1$^+$ C3H and Sca1$^+$ mESC) were chosen following scan of the literature. Briefly, the C3H cell line were chosen as they are a mouse embryonic fibroblast cell line of mesodermal origin; they are commercially sourced, low maintenance and have been previously widely used as a model cell line for molecular regulation of differentiation and gain- and loss-of-function studies due to their established ability to differentiate into vSMC (Hirschi et al. 1998). In order to control for any lineage bias, the second cell line of ESC were chosen; while ESC have also been shown to reproducibly differentiate into vSMC, they are a more delicate cell line (non-robust) to handle (Xiao et al. 2006 and Xiao et al. 2007).

Aim 2: Evaluate Hedgehog Control of Sca1$^+$ Cell Renewal and Differentiation *In Vitro*

This aim involved the following:

- Assessing Shh-induced Hh activation and inhibition in Sca1$^+$ cells
- Assessing Sca1$^+$ cell response to Shh with respect to differentiation
- Assessing Sca1$^+$ cell response to Shh with respect to maintenance of "stemness" (telomerase activity)

Aim 3: Evaluate Hedgehog Control of Sca1$^+$ Cell Renewal and Differentiation *In Vivo*

This aim involved the following:

- Assessing Sca1$^+$ cell response during vascular remodelling (partial ligation injury model)
- Assessing Sca1$^+$ cell response during vascular remodelling following treatment with cyclopamine (Hh inhibitor)
- Characterisation of vascular cell phenotypes during vascular remodelling
- Identify Sca1$^+$ cells in human vessels

Chapter 2

Materials and Methods

2.0 Materials

All materials were of the highest grade and purity available and were purchased from Sigma-Aldrich unless otherwise stated.

2.1 Cell Lines and Culture

2.1.1 Materials: Cell Lines

Cell Line	Organism	Strain	Tissue	Cell Type	Distributor
ES-D3 *(ATCC® CRL1934™)*	Mus musculus	129S2/ SvPas	Embryo	Embryonic multipotent stem cell	LGC
C3H/10T1/2 Clone 8 (ATCC®CCL-226™)	Mus musculus	C3H	Embryo	Fibroblast	LGC
Mouse Mesenchymal Stem Cell (S1502-100)	Mus musculus	C57BL/ 6	Bone Marrow	Mesenchymal Stem Cell	GIBCO
MOVAS (ATCC®CRL-2797™)	Mus musculus	C57BL/ 6	Aorta/smooth muscle	Smooth Muscle	LGC
A-10 *(ATCC® CRL1476™)*	Rattus norvegicus	DBIX	Embryo aorta, thoracic/medial layer	Myoblast	LGC

Table 2.1: Cell line details including organism, strain, tissue, cell type and distributor

2.1.2 Materials: Cell Line Culture Medium

Cell Line	Basal Medium	FBS	* S1	*S2	Cryo - preservation
ES-D3 *(ATCC® CRL1934™)*	ESC Basal Medium ATCC® SCRR-2011 (LGC)	10% ESC Qualified Fetal Bovine Serum (FBS) ATCC® SCRR-30-2020 (LGC)	1,000 U/mL mouse leukaemia inhibitory factor ESG1107 (Millipore)	0.1 mM 2-mercaptoethanol 21985-023 (Life Technologies)	10% Dimethyl sulfoxide (DMSO) 41639 (Sigma)
C3H/10T1/2 Clone 8 (ATCC®CCL-226™)	Eagle's Minimum Essential Medium (EMEM) ATCC® 30-2003 (LGC)	10% ESC Qualified FBS ATCC® SCRR-30-2020 (LGC)	n/a	n/a	10% DMSO 41639 (Sigma)
Mouse Mesenchymal Stem Cell (S1502-100)	EMEM Alpha Modification (α-MEM) with GlutaMax™-I 32571028 (Life Technologies)	MSC-Qualified FBS 12664025 (Life Technologies)	n/a	n/a	10% DMSO 41639 (Sigma)
MOVAS (ATCC®CRL-2797™)	Dulbecco's Modified Eagle's Medium	FBS F9665 (Sigma)	n/a	n/a	10% DMSO 41639 (Sigma)

	(DMEM) 30-2002 (LGC)				
A-10 ***(ATCC® CRL1476™)***	DMEM 30-2002 (LGC)	10% ESC Qualified FBS ATCC® SCRR-30-2020 (LGC)	n/a	n/a	10% DMSO 41639 (Sigma)

Table 2.2: Cell line medium components including FBS, supplements and cryopreservation medium.

*S1 – supplement 1; * S2 – supplement 2

2.1.3 Materials: Other

- Hanks Balanced Salt Solution (HBSS) H6648 (Sigma)
- Gelatin G1393 (Sigma)
- 1x TryPLE Select 12563029 (Life Technologies)
- Collagenase from Clostridium histolyticum C9891/C6885 (Sigma)
- Embryo extract 2850145 (MP Biomedical)
- Retinoic acid R2656 (Sigma)
- Soybean Trypsin inhibitor T6414 (Sigma)
- B27 17504-044 (GIBCO)
- rmFGF basic 3139-FB-025 (R&D Systems)
- Penicillin Streptomycin P4333 (Sigma)
- Elastase type III E0127 (Sigma)
- Fatty acid free BSA A7030 (Sigma)
- L-glutamine G7513 (Sigma)

2.1.4 Methods: Cell Line Culture, Cryostock Generation and Reanimation

All cell culture was carried out aseptically in a Biosciences Air 2000 Mac laminar flow cabinet. Cells were maintained in a Hera water-jacketed cell culture incubator at 37 °C and 5 % CO_2 and visualized using a Nikon Eclipse TS100 phase-contrast microscope. All cell lines were cultured in the same fashion, except for the mESC cell line (see section 2.1.5). Briefly, to subculture, medium was removed from 70-80 % confluent cells and washed

with HBSS balanced salt solution (HBSS), pH 7.4 which was subsequently removed. Cell dissociation was initiated using a 0.25 x TryPLE solution. Following dissociation HBSS was added to dilute the effect of TryPLE. Fresh medium was introduced into new culture vessels (i.e. flasks or plates) and the appropriate seeding density was then added to each vessel (in accordance with the manufacturers' recommendations) and the vessel placed at 37 °C 5 % CO_2. To generate cryostocks, cells were pelleted following dilution of TryPLE with HBSS at 300 X G for 5 min and re-suspended in 90 % complete medium 10 % DMSO and transferred to cryovials. The cryovials were then labeled appropriately, put into a Mr. Frosty™ freezing container for 12 hrs and following this placed for long term storage in liquid nitrogen. To reanimate, cells were defrosted quickly at 37 °C and transferred to pre-warmed complete medium in a centrifuge tube. The cells were then pelleted at 300 X G for 5 min, medium removed and then re-suspended in pre-warmed fresh medium. The cells were then seeded for culture.

2.1.5 Methods: Exception: mESC *(ES-D3 ATCC®* CRL1934™) Culture, Cryostock Generation and Reanimation

All work was carried out under the same conditions as outlined in section 2.1.4. Undifferentiated cells were fed every 2 days with fresh medium and passaged into gelatin coated culture vessels (plate or flask) in a 1: 4 – 1: 10 ratio every 2-4 days. Prior to subculture, the chosen culture vessels had 1:50 gelatin: HBSS added to cover the surface and incubated at 37 °C at 5 % CO_2 for 30 min. To subculture, medium was removed and cells washed with HBSS, which was subsequently removed. Cell displacement and dissociation occurred through the use of 0.25 x TryPLE and following dissociation, HBSS added in order to dilute the TryPLE and in effect cancel its affect. The gelatin: HBSS in the newly prepared culture vessels was removed and appropriate amount of fresh medium added. The appropriate seeding density was then added to each vessel and the vessel placed at 37 °C 5 % CO_2. To generate cryostocks, cells were pelleted following dilution of TryPLE with HBSS at 300 X G for 5 min and re-suspended in 90 % complete medium 10 % DMSO and transferred to cryovials. The cryovials were then labeled appropriately, put into a Mr. Frosty™ freezing container for 12 hrs and following this placed

for long term storage in liquid nitrogen. To reanimate, cells were defrosted quickly at 37 °C and transferred to pre-warmed complete medium in a centrifuge tube. The cells were then pelleted at 300 X G for 5 min, medium removed and then re-suspended in pre-warmed fresh medium. The cells were then seeded for culture.

2.1.6 Methods: Rat Adventitial and Medial Explant Generation

All work was carried out under the same conditions as outlined in section 2.1.4. Sprague Dawley rats were anesthetized with pentobarbital sodium (0.1 mg/g) and then perfused with 10 mL of PBS. Cervical dislocation was then conducted in order to confirm death before the animal was dissected. Prior to dissection the animal was thoroughly cleaned with 100 % IMS and the limbs pinned down to prevent movement. The dissection involved making a clean superficial incision medially from the abdomen to jaw. The skin was then separated from underlying muscle and pinned back. Another clean incision medially from the abdomen to jaw, penetrating the abdominal muscles (being careful not to damage the intestine) and ribcage exposed internal organs. All obstructing tissue was removed until only the heart and descending aorta were visible. Then under a dissection microscope, the heart was cut away to leave behind the aortic arch. The aortic arch was then supported by a fine tip forceps and the descending aorta released from the spine using gentle cuts and a fine scalpel blade and released at the end of the abdominal section. The tissue was then cut into its three regions: aortic arch, thoracic and abdominal (Figure 2.1). Following this, the tissue was placed in room temperature HBSS before the adipose tissue and blood was removed using two forceps. Blood was removed from the lumen by forcing HBSS through the lumen using a fine gauge needle. The adventitia was then separated from the medial layer by enzymatic digestion with 2.5 mg/mL of collagenase in medium for 15 - 20 min at 37 °C (Figure 2.2). After collagenase treatment, the adventitia was carefully peeled away from the media using fine tip forceps under a dissection microscope. The adventitia was then cut into 1 mm sections and placed in wells of 6 well plates and left to dry for 5 min in the laminar, then 2 mL complete MM2 medium (EMEM supplemented

with 2 mM L-glutamine and 10 % ATCC ESC qualified FBS) was added to each well containing tissue (Figure 2.3). The tissue was then placed at 37 °C 5 % CO_2 and left undisturbed for a minimum of 56 hr. The tissue was then monitored for explants. The tunic media was then cut open and the endothelial cells removed by scraping the surface with a scalpel. The medial layer was then washed in HBSS and treated in exactly the same manner as the adventitial sections however the medial tissue was placed in 94 % DMEM, 5 % FBS and 1 % penicillin streptomycin.

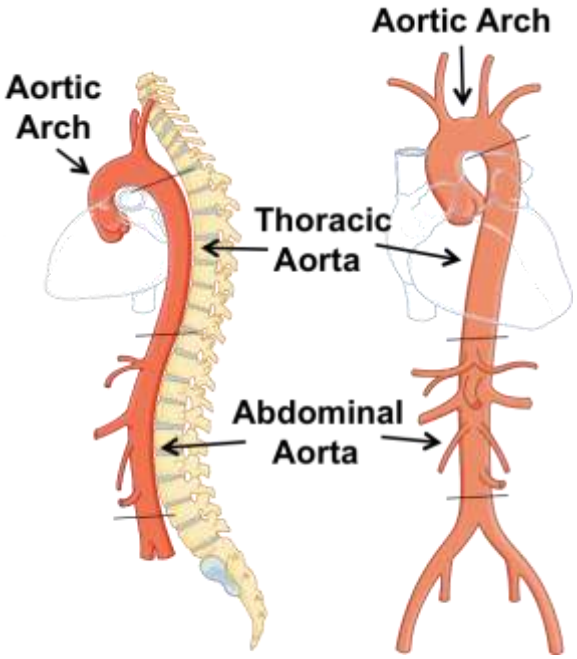

Fig 2.1: Aortic dissection.

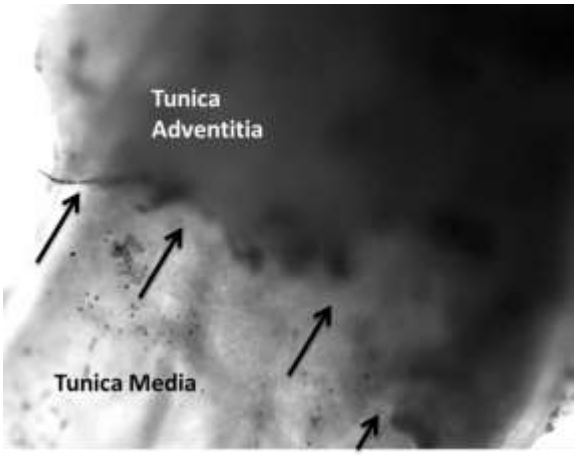

Fig 2.2: Vascular tissue dissection, separation of tunica adventitia from the tunica media.

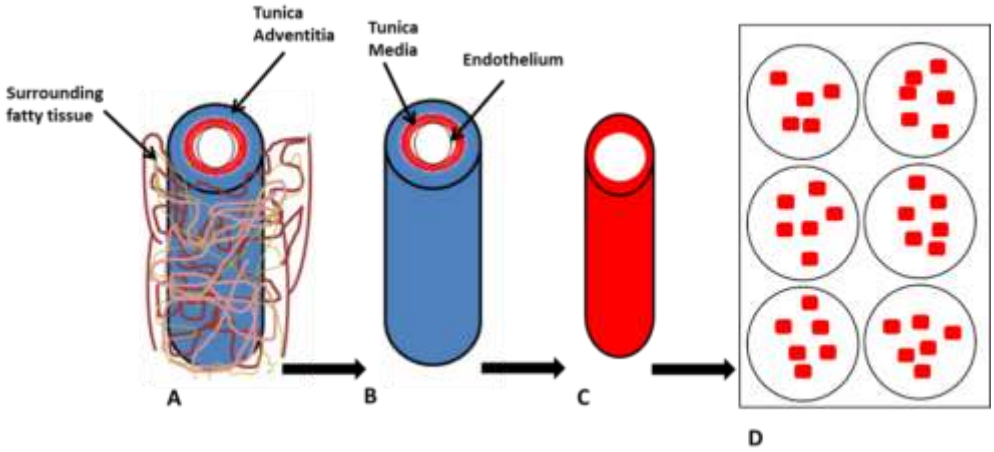

Fig 2.3: Vascular tissue dissection overview. Surrounding fatty tissue was removed, tunica adventitia, tunica media and endothelial layer were separated from one another, and tissue was cut into sections and plated.

2.1.7 Methods: Rat Adventitial and Medial Explant Cell Culture

Adventitial Explant Cell Culture

Adventitial progenitor cells (APC) derived from the adventitial layer explant were cultured in MM2 medium and passaged every 7 - 10 days depending on their original splitting ratio and when they reached ~ 70 % confluency. The APC quickly became recalcitrant to trypsin and TryPLE dissociation methods hence the cells were dissociated using cell scraping and conducted in the medium they were cultured in.

Sca1 Adventitial Progenitor Cell Generation and Culture

T175 flasks of APC were cultured to 70 % confluency prior to instigation of the Sca1 purification process. 20 ml was chosen for the cells to be dissociated into using a cell scraper. This volume was then transferred into two sterile tubes, one containing 1 – 2 ml of the cell suspension (purification control) and the second with the rest of the cell suspension (to be purified). These tubes were then centrifuged at 600 x g for 5 min. The medium was then carefully removed and the pellet resuspended in HBSS solution and centrifuged at 600 x g for 5 min. The HBSS solution was then removed and the cell pellet was treated in accordance with the EasySep® Mouse Sca1 Positive Selection Kit protocol from STEMCELL Technologies. Briefly, in the laminar flow cabinet, the cells were then re-suspended in 2 % FBS, 1 mM

EDTA and Ca^{2+} and Mg^{2+} free PBS (purification buffer) at a concentration of 1 x 10^8 cells/mL. This was then transferred to a flow cytometry tube. For samples containing 10^7 cells or less, 100 µL was used to re-suspend the cells. Following this 50 µL/mL of Sca1 PE labelling reagent was added, mixed and incubated at 15 – 25 °C for 15 min. Then 70 µL/mL of EasySep® PE Selection Cocktail was added, mixed and incubated at 15 – 25 °C for 15 min. Following this 50 µL/mL of magnetic nanoparticles was added, mixed and incubated at 15 – 25 °C for 10 min. The cell suspension was then brought to a total volume of 2.5 mL with purification buffer, gently pipetted twice and placed into the magnet for 5 min. The magnet was then picked up and in one continuous motion the tube and the magnet were inverted to dispel the supernatant fraction, taking note that the tube was not inverted for any longer than 2 sec. 2.5 mL of purification buffer was then added to the tube, gently pipetted and placed back in the magnet for a further 5 min. These steps of pouring off the supernatant and re-suspending in buffer were repeated for a total of 4 times. The final time the cells were placed into 1 mL of purification buffer and divided into two, one fraction would go on to be cultured in accordance with the APC culture protocol, the other would go on to be analysed for the Sca1 purity profile by flow cytometry. The sample mentioned previously as kept separate for the purification control was re-suspended in purification buffer containing the isotype control antibody IgG-PE. The samples destined for analysis by flow cytometry, were then assessed in the appropriate manner (see section 2.3) and the data analysed in accordance with section 2.3.3. Cultured post purification $Sca1^+$ APC were expanded and routinely re-purified in order to maintain a high $Sca1^+$ population.

Medial Explant Cell Culture

Three days after dissection and tissue preparation, cells were observed to migrate from the tissue explant. Once this was observed, the tissue pieces were removed and each well washed briefly with HBSS. The medium was replaced with a maintenance medium specifically designed to keep multipotent vascular stem cells (MVSCs) in a multipotent state. The medium was composed of DMEM supplemented with 2 % chick embryo extract (MP

Biomedical), 1 % FBS, 1 % N2 (Invitrogen), 2 % B27 (Invitrogen), 100 nM retinoic acid (Sigma-Aldrich), 50 nM 2-mercaptoethanol (Sigma-Aldrich), 1 % P/S and 20 ng/mL bFGF (R&D Systems). Cells were re-fed every 2-3 days and passaged every 3 days depending on confluency (~ 70 %). The cells exhibited low adherence rate post dissociation.

2.2 Sca1$^+$ Cell Line Generation, Purification and Cloning

2.2.1 Materials: Sca1$^+$ Cell Line Generation and Purification

- Collagen IV 734-0099 (VWR)
- α-MEM, GlutaMAX™, no nucleosides 32561-029 (GIBCO)
- FBS (GIBCO)
- 2-mercaptoethanol 21985-023 (Life Technologies)
- HBSS H6648 (Sigma)
- PBS without Calcium and Magnesium D8537 (Sigma)
- 1x TryPLE Select 12563029 (Life Technologies)
- Falcon™ 5 mL Polystyrene Round-Bottom Tubes 352058 (BD)
- EasySep Mouse Sca1 Positive Selection Kit 18756 (STEMCELL Technologies)
- PE Rat IgG2a, κ Isotype Ctrl Antibody 400507 (MSC)
- ClonaCell™ FLEX 03818 (STEMCELL Technologies)

2.2.2 Methods: Sca1^{+} Cell Line Generation and Purification

T75 flasks were pre-treated with 5 µg/mL mouse collagen IV for at least 2 hrs prior to seeding with mESC cells. The flasks were then gently washed with HBSS and basic differentiation medium was added to the flask. Each flask was seeded with 1 x 10^{6} cells for 2 – 6 days and medium was replaced every 2 – 3 days. Following this the medium was removed, cells washed with HBSS and TryPLE was added and left at 37 °C until all cells were disassociated. HBSS solution was then added, a fraction of cells were put into a separate tube for purification control purposes, and all cells centrifuged at 300 X G for 5 min. Sca1 purification was conducted as described in the aforementioned section 2.1.7 "Sca1 Adventitial Progenitor Cell Generation and Culture". Post purification Sca1^{+} mESC were expanded and routinely re-purified (by Sca1 purification, see section 2.1.7) in order to maintain a high Sca1^{+} population.

2.2.3 Methods: Sca1^{+} Cell Line Cloning

Cloning of Sca1^{+} cell lines were conducted in accordance with the recommended protocol detailed in the ClonaCell™ FLEX product manual. Briefly, the ClonaCell™ FLEX medium was thawed overnight at 2 – 8 °C and mixed well before aliquoted, excess aliquots of ClonaCell™ FLEX medium were then stored at - 20 °C. An equal volume of ClonaCell™ FLEX medium was vigorously mixed with 2 X stock of cell-specific medium. A cell suspension of desired concentration was then was then mixed with the ClonaCell ™ FLEX medium to make the final concentration 1 X. The medium containing the cells was then left to rest for 10 – 15 min to allow dissipation of generated bubbles. A syringe and blunt-end needle were then used to transfer the medium into a culture dish and incubated as outlined in section 2.1.6. The culture dish was checked the next day and individual cells were highlighted. The culture dish was then assessed every day in order to identify colonies deriving from a single cell; these colonies were then isolated using a pipette and transferred to fresh culture flasks for colony expansion.

2.3 Flow Cytometry

Flow cytometry was used throughout this body of work as it is a laser based technology employed for biomarker detection, whereby cells are corralled into single file using a fluidic stream, followed by optical and fluorescence measurement (Figure 2.4. A-B). Certain populations of cells can be resolved by comparing physical properties such as size (represented by the forward light scatter) and internal complexity (represented by side scatter), and antibodies with fluorescent particles conjugated to them were used for the biomarker detection (Figure 2.4 C). When a marker positive cell passes by the light source, the fluorescent particles become excited to a higher state of energy, and upon returning to their resting state emit light energy at a higher wavelength which is detected by multiple fluorescence emission detectors. The signal is then amplified and converted to a digital format for display on a computer, and ultimately analysis (Figure 2.4 D).

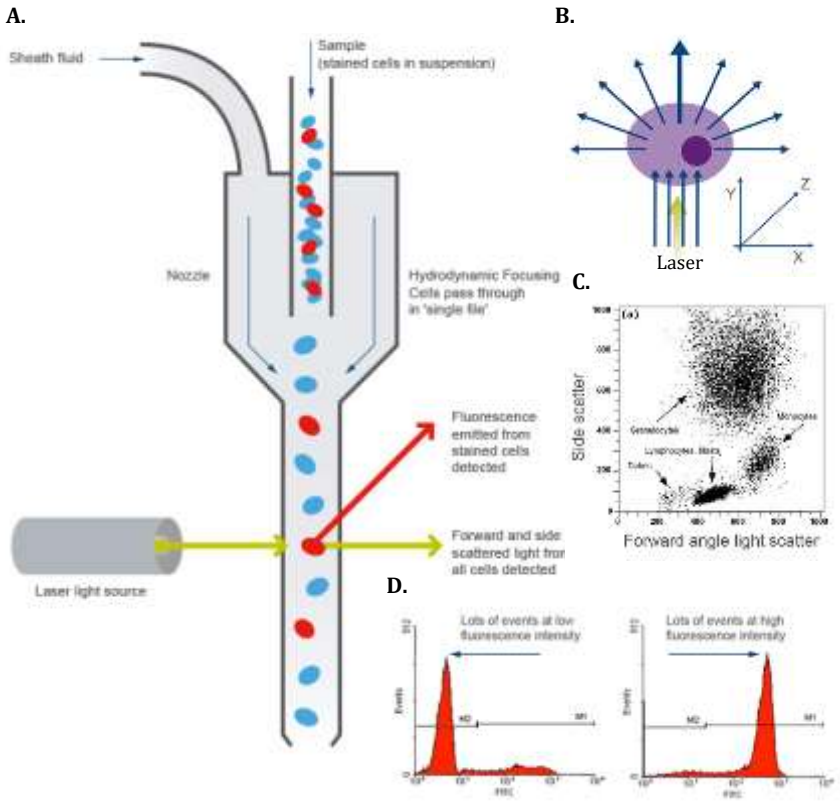

Figure 2.4: Overview of flow cytometry. A: Sheath fluid corrals cells into a single file prior to passing the path of a laser beam. Cells passing through the laser induce a scattering of the light source, B: forward scatter, side scatter and any fluorescence emitted from fluorescently stained cells are detected using filters and detectors, C and D: this analogue signal is then converted into a graphical representation of the data. Image edited from Abcam 2016a.

2.3.1 Materials: Flow Cytometry

- Cytofix/Cytoperm™ Fixation/Permeabilization Solution Kit 554714 (BD)
- Purified Rat IgG2a Kappa Isotype Control 400501 (BioLegend)
- Rabbit-IgG Alexa fluor 488, Isotype control bs-0295p-A488 (Bioss)
- FITC Rat IgG2a, κ Isotype Ctrl Antibody 400505 (BioLegend)
- PE Rat IgG2a, κ Isotype Ctrl Antibody 400507 (MSC)
- Alexa Fluor® 546 Goat anti-rabbit (H+L) A-11035 (Life Technologies)
- Alexa Fluor® 546 Goat anti-mouse (H+L) A-11030 (Life Technologies)
- Alexa Fluor® 488 Goat anti-rabbit (H+L) A-11008 (Life Technologies)
- Alexa Fluor® 488 Goat anti-mouse (H+L) A-11001 (Life Technologies)
- Alexa Fluor® 488 Donkey anti-goat (H+L) A-11055 (Life Technologies)
- Mouse Anti-Sca1 130-093-222 (Miltenyi Biotech)
- Anti-Mouse Sca1 Antibody, Clone E13-161.7 60032 (STEMCELL Technologies)
- Nestin Monoclonal Clone 10C2 Mouse IgG MA1-110 (Thermo Scientific)
- Pax 6 Polyclonal Rabbit Ab5790 (Abcam)
- Sox 10 Monoclonal Clone EPR4007 Rabbit IgG Ab155279 (Abcam)
- Sox 17 Polyclonal Rabbit 09-038 (Millipore)
- S100β Monoclonal Clone EP1576Y Rabbit IgG 04-1054 (Millipore)
- Smooth Muscle α-Actin Monoclonal Clone 1A4 Mouse IgG2a A5228 (Sigma)
- Calponin 1 Monoclonal Clone hCP Mouse IgG1 C2687 (Sigma)
- Smooth Muscle Myosin Heavy Chain 11 Monoclonal Clone 1G12 Mouse IgG1 Ab683 (Abcam)

2.3.2 Methods: Flow Cytometry: Marker Labelling

Flow cytometry was used to characterize cell lines for both stem cell and smooth muscle cell markers. Detection of membrane-associated markers were only put through the fixation step as permeabilization destroys the

membrane and hence interferes with the detection process. For this same reason, permeabilization is critical for the detection of intracellular antigens. Samples were prepared for antibody labelling using the BD Cytofix/Cytoperm kit and protocol. Briefly, 500,000 cells per purpose (control or marker) were aliquoted and pelleted at 500 X G for 10 min. Cells were then re-suspended in 100 µL of a 3.7 % formaldehyde solution at 4 °C for 10 - 20 min. Following this, cells were washed twice with 1 mL staining buffer. If appropriate to have permeabilized, cells were re-suspended in 100 µL 1 x Perm/Wash™ for 15 min before pelleting at 500 X G for 10 min and re-suspension in 50 µL of Perm/Wash™ solution containing the determined optimal concentration of primary antibody. Otherwise cells were immediately re-suspended in 50 µl of Perm/Wash™ solution containing the determined optimal concentration of primary antibody. Cell suspension in primary antibody was incubated at 4 °C for 30 min. Following this, cells were washed twice with 1 mL 1 x Perm/Wash™ solution and re-suspended in 50 µL of Perm/Wash™ solution containing the determined optimal concentration of fluorophore-conjugated secondary antibody. Cell suspensions in fluorophore-conjugated secondary antibody were incubated in darkness at 4 °C for 30 min. Cells were then washed twice again in 1 mL 1 x Perm/Wash™ solution and re-suspended in 700 µL staining buffer prior to analysis by flow cytometry.

2.3.3 Methods: Flow Cytometry: Data Analysis

Data analysis was performed using FloJo and De Novo software FCS Express 4 Flow Cytometry. Dot plot graphs were used to gate for uniform cell populations and fluorescent histograms generated to determine fluorescent profiles. Gating was used conducted in order to remove cell debris and other artifacts and prevent their skewing the experimental data.

2.4 Immunofluorescence

Immunofluorescence is an invaluable technique that allows for the localization of the marker being probed for by marker-specific probe. This technique is visualized by either light or confocal microscopy.

Immunofluorescence is a broad term encompassing the fluorescent labelling of tissue (immunohistochemistry) or cultured cells (immunocytochemistry).

2.4.1 Materials: Immunofluorescence

- Olympus CK30 microscope
- Purified Rat IgG2a Kappa Isotype Control 400501 (BioLegend)
- Rabbit-IgG Alexa fluor 488, Isotype control bs-0295p-A488 (Bioss)
- FITC Rat IgG2a, κ Isotype Ctrl Antibody 400505 (BioLegend)
- PE Rat IgG2a, κ Isotype Ctrl Antibody 400507 (MSC)
- Alexa Fluor® 546 Goat anti-rabbit (H+L) A-11035 (Life Technologies)
- Alexa Fluor® 546 Goat anti-mouse (H+L) A-11030 (Life Technologies)
- Alexa Fluor® 488 Goat anti-rabbit (H+L) A-11008 (Life Technologies)
- Alexa Fluor® 488 Goat anti-mouse (H+L) A-11001 (Life Technologies)
- Alexa Fluor® 488 Donkey anti-goat (H+L) A-11055 (Life Technologies)
- Mouse Anti-Sca1 130-093-222 (Miltenyi Biotech)
- Anti-Mouse Sca1 Antibody, Clone E13-161.7 60032 (STEMCELL Technologies)
- Nestin Monoclonal Clone 10C2 Mouse IgG MA1-110 (Thermo Scientific)
- Nestin Monoclonal Mouse Ab11306 (Abcam)
- Pax 6 Polyclonal Rabbit Ab5790 (Abcam)
- Patched 1 Monoclonal Mouse Ab55629 (Abcam)
- Sox 10 Monoclonal Clone EPR4007 Rabbit IgG Ab155279 (Abcam)
- Sox 10 Monoclonal Mouse Clone 20B7 MAB2864 (R&D Systems)
- Sox 17 Polyclonal Rabbit 09-038 (Millipore)
- Sox 17 Monoclonal Mouse Clone 245013 MAB1924 (R&D Systems)
- S100β Monoclonal Clone EP1576Y Rabbit IgG 04-1054 (Millipore)
- Smooth Muscle α-Actin Monoclonal Clone 1A4 Mouse IgG2a A5228 (Sigma)
- Calponin 1 Monoclonal Clone hCP Mouse IgG1 C2687 (Sigma)
- Smooth Muscle Myosin Heavy Chain 11 Monoclonal Clone 1G12 Mouse IgG1 Ab683 (Abcam)

- eNOS Polyclonal Rabbit PA1-037 (Thermo Scientific)
- Peripherin ab39374 (Abcam)
- DAPI D9542 (Sigma)
- Triton X-100 (Sigma)
- PBS D8662 (Sigma)
- BSA A2153 (Sigma)
- Glycine G8898 (Sigma)
- Ethanol E7023 (Sigma)
- Xylene 534056 (Sigma)
- Sodium Citrate Dihydrate W302600 (Sigma)
- Fluoroshield Histology Mounting Medium F6182 (Sigma)

2.4.2 Methods: Immunocytochemistry: Marker Labelling

Immunocytochemistry was used to characterize cell lines for both stem cell and smooth muscle cell markers. Detection of membrane associated markers were only put through the fixation step as permeabilization destroys the membrane hence interferes with the detection process. For this same reason, permeabilization is critical for the detection of intracellular antigens. Samples for this technique are traditionally seeded at low densities for maximum potential of marker structure and localization visualization to occur. These cells were seeded onto UV sterilized coverslips for high magnification convenience. All samples were fixed with 3.7 % formaldehyde at room temperature for 15 min. As mentioned previously, if samples required permeabilization for the detection of intracellular markers, samples were incubated in 0.025 % Triton X-100 PBS at room temperature for 15 min. Subsequently all samples were subjected to blocking using a 5 % BSA, 0.3 M Glycine, 1 % Tween PBS blocking solution. Blocking solution prevents unspecific binding of antibodies and is left to incubate at room temperature for 1 hr or 4°C overnight. Following this, marker-specific primary antibody at the recommended dilution is re-suspended in blocking buffer and left to incubate at room temperature for 1 hr or 4 °C overnight. Following this the samples were washed twice with PBS to remove any unbound primary antibody and the recommended concentration of secondary antibody was re-

suspended in blocking buffer. This secondary antibody was then added to the samples and left to incubate at room temperature for 1 hr or 4 °C overnight. Secondary antibodies specifically bound to the primary antibody and had a fluorophore conjugated which allowed for fluorescent detection of the marker of interest. Following this the samples were washed twice with PBS to remove any unbound secondary antibody and cell nuclei were stained using DAPI: PBS (dilution 1:1000) which was incubated at room temperature for 15 min. For each secondary antibody used, a no primary control was prepared to assess for unspecific binding of the secondary antibody to cells. An Olympus CK30 microscope and FCell software was used to take images. A threshold of negativity was defined by the no primary control and exposure rates were limited in order to rule out false positives. All results are representative of experiments that were repeated with n ≥ 3. Images from the Olympus CK30 microscopy were analysed with ImageJ software and confocal images were analysed using Zen 2008 software.

2.4.3 Methods: Confocal analysis of paraffinised carotid sections: Sca1-eGFP assessment

Paraffin rehydration was conducted at room temperature by immersing the slides in xylene for 20 minutes. The slides were then immersed in the following gradients of ethanol for 5 minutes respectively: 100 %, 90 %, 70 % and 50 % ethanol. The slides were then rinsed in distilled H_2O before leaving in 1x PBS for 10 minutes. The slides could then be stored in 1x PBS until ready to progress further. Following this the samples were stained using DAPI: PBS (dilution 1:1000) which was incubated at room temperature for 15 min. Prior to imaging, 1 drop of mounting medium was put onto the samples and a coverslip was placed gently on top to prevent the addition of bubbles. An Olympus FluoView™ FV1000 confocal microscope and FV10-ASW 4.2 Viewer software was used to take and compile images. All results are representative of experiments that were repeated with n ≥ 3.

2.4.4 Methods: Immunohistochemistry of paraffinised carotid sections: Marker Labelling

Paraffin rehydration was conducted at room temperature by immersing the slides in xylene for 20 minutes. The slides were then immersed in the following gradients of ethanol for 5 minutes respectively: 100 %, 90 %, 70 % and 50 % ethanol. The slides were then rinsed in distilled H_2O before leaving in 1x PBS for 10 minutes. The slides could then be stored in 1x PBS until ready to progress further. Before immunolabelling could begin it was necessary to conduct antigen retrieval which involved heating the slides at 80 – 100 °C for 20 minutes in antigen retrieval buffer (ARB – 10 mM sodium citrate, 0.05 % Tween 20, pH 6.0). Subsequent to the heat induced antigen retrieval, all samples were subjected to blocking using a 5 % BSA, 0.3 M Glycine, 1 % Tween PBS blocking solution. Blocking solution prevents unspecific binding of antibodies and is left to incubate at room temperature for 1 hr or 4 °C overnight. Following this, marker-specific primary antibody at the recommended dilution was re-suspended in blocking buffer and left to incubate at room temperature for 1 hr or 4 °C overnight. Following this the samples were washed twice with PBS to remove any unbound primary antibody and the recommended concentration of secondary antibody was re-suspended in blocking buffer. This secondary antibody was then added to the samples and left to incubate at room temperature for 1 hr or 4 °C overnight. Secondary antibodies specifically bound to the primary antibody and had a fluorophore conjugated which allowed for fluorescent detection of the marker of interest. Following this the samples were washed twice with PBS to remove any unbound secondary antibody and cell nuclei were stained using DAPI: PBS (dilution 1:1000) which was incubated at room temperature for 15 min. Prior to imaging, 1 drop of mounting medium was put onto the samples and a coverslip was placed gently on top to prevent the addition of bubbles. For each secondary antibody used, a no primary control was prepared to assess for unspecific binding of the secondary antibody. An Olympus CK30 microscope and FCell software was used to take images. A threshold of negativity was defined by the no primary control and exposure rates were limited in order to rule out false positives. All results are

representative of experiments that were repeated with n ≥ 3. Images from the Olympus CK30 microscopy were analysed with ImageJ software and confocal images were analysed using Zen 2008 software.

2.4.5 Methods: Immunohistochemistry of human cryopreserved sections: Marker Labelling

Both the human healthy artery tissue sections and human atherosclerotic plaque sections were cryopreserved by the manufacturer. Both these slides boxes were taken from the -80 °C and left unopened on the bench top for 30 minutes. The boxes were then opened and the slides left to adjust to room temperature for a further 15 minutes. The healthy artery tissue sections had been previously fixed by the manufacturer so these slides could then be stored in 1x PBS until ready to progress further. The human atherosclerotic plaque sections however required 4% ice cold acetone fixation which was conducted at -20 °C for 15 minutes prior to washing in 1 x PBS thrice. All samples then underwent antigen retrieval and immunostained in exactly the same manner as outlined in section 2.4.4.

2.5 Western Blot

Western blotting is an established qualitative technique for protein analysis. Its use of gels for the separation of proteins based on molecular size and antigen specific antibodies enables a target protein to be identified in the midst of complex cellular proteins.

2.5.1 Materials: Western Blot

- RIPA R0278 (Sigma)
- 2-mercaptoethanol M-7154 (Sigma)
- 30% bis/acrylamide solution A3699 (Sigma)
- 4 X SDS LaemmLi Buffer 161-0747 (BioRad)
- Protease inhibitor P8340 (Sigma)
- APS A3678 (Sigma)
- TEMED T7024 (Sigma)
- TMB T0565 (Sigma)
- Anti-goat 2° antibody, HRP conjugated A5420 (Sigma)

- Anti-mouse 2° antibody, HRP conjugated A5278 (Sigma)
- Anti-rabbit 2° antibody, HRP conjugated A0545 (Sigma)
- Gel Blotting Paper Z698172 (Sigma)
- Ponceau S stain P7170 (Sigma)
- Protran membrane Z670979 (Sigma)
- Tween P1379 (Sigma)
- Pierce BCA Assay kit 23227 (MSC)
- Pierce Page ruler ladder 26620 (MSC)
- Pierce 1 – step transfer buffer 84731 (MSC)
- Pre-cut nitrocellulose membrane A19020 (MyBio)
- ATTO system AE-6450 (ATTO)
- Pierce G2 Fast Blotter 62291 (MSC)
- 10% SDS 71736 (Sigma)
- Tris T1503 (Sigma)
- HCl H1758 (Sigma)
- Tris-Glycine-SDS Running Buffer G8898 (Sigma)

2.5.2 Methods: Western Blot

2.5.2.1 SDS-PAGE Single Gel Preparation

Chemical	Stacking Gel	7.5% Resolving Gel	10% Resolving Gel	12.5% Resolving Gel	15% Resolving Gel	20% Resolving Gel
30% Acrylamide (mL)	0.325	1.875	2.50125	3.12375	3.75	4.99875
1.5M Tris-HCl pH8.8 (mL)	n/a	1.875	1.875	1.875	1.875	1.875
0.5M Tris-HCl pH6.8 (µL)	625	n/a	n/a	n/a	n/a	n/a
10% SDS (µL)	25	75	75	75	75	75

H_2O (mL)	1.54	3.63375	3.0075	2.385	1.75875	0.51
10% APS* (µL)	12.5	37.5	37.5	37.5	37.5	37.5
TEMED (µL)	5	7.5	7.5	7.5	7.5	7.5

Table 2.3: Single SDS-PAGE gel formulation

10% APS*: Ammonium Persulfate was diluted in dH2O and stored at -20°C for long term storage

2.5.2.3 Preparation of SDS-PAGE gels

The ammonium persulfate and TEMED were always added to the mix as they are responsible for the polymerization of the gel. Upon addition of ammonium persulfate and TEMED, the solution was mixed and immediately poured. The gel was then overlaid with 50% ethanol and when the gel had set the ethanol was poured off and the boundary rinsed using distilled H_2O. Next stacking gel was prepared and poured immediately on top of the resolving gel. A comb was then inserted and any air bubbles were removed. The comb was removed when the gel had polymerized. Gels were pre-run at 30 mA for 30 min to equilibrate and calibrate.

2.5.2.4 Set up of SDS-PAGE gels in Electrophoresis Rig

The electrophoresis rig used was an ATTO system (model number AE-6450). Tris-Glycine-SDS Running buffer was poured into the rig until a third of the way up. The plastic gasket was then removed from the plates. The plates were then inserted into the rig at a slant so as to keep bubbles from the bottom of the gel, with the high sided glass on the outside so that when buffer was poured into the central cavity the gels were completely immersed in buffer. The plastic inserts that support the gel plates were then inserted. The central reserve was completely filled with buffer and bubbles were removed. Following this the plastic comb was removed gently vertically.

2.5.2.5 Sample preparation - preparation of whole cell protein lysates

Medium was removed from the cells growth vessels and cells were washed twice with ice cold HBSS solution. A small volume of ice-cold HBSS solution was added to each growth vessel and a cell scraper was used to detach the cells from the growth vessels surface. The cells were collected and pelleted at

300 X G for 5 min. The HBSS solution was removed and an appropriate volume of RIPA (depending on pellet size) was added to the pellet to lyse the cells. The RIPA had been supplemented with protease - phosphate inhibitor cocktails (1/100 dilution) beforehand. As minimal a quantity of RIPA was used to ensure as high a concentration of protein as possible. Samples were then stored at -20 °C overnight (short term) or -80 °C (long term). Subsequently samples were defrosted and centrifuged at 4 °C; 13,000 RPM for 15 min. Cellular cytosolic fractions resided in the supernatant fraction so were carefully pipetted off and stored in a fresh eppendorf. The pellet contained all nuclear proteins and was re-suspended in fresh RIPA and sonicated using a Branson Digital Sonifier (AGB Scientific) at 40 % for 15 sec four times in order to release any membrane bound proteins. For some experiments it was necessary to have equal protein loading so a ThermoScientific Pierce™ BCA Protein Assay was performed according to the manufacturers' recommendations. However, routinely protein loading was normalized using ponceau staining and beta actin expression at the end of the experiment. Samples were then mixed with 4 X LaemmLi buffer and boiled at 95 °C in a heating block for 5 min. Following this, samples were briefly centrifuged to gather the sample at the bottom of the eppendorfs.

2.5.2.6 Sample loading

20 µL PageRuler ladder were loaded at the start of each experiment. 25 µL of sample plus LaemmLi sample buffer were then loaded into subsequent lanes. Gels were run at 15 mA /gel until the loading dye was at the very bottom of the gel. For example 2 gels at 30mA took approximately 2.5 hrs.

2.5.2.7 Transfer of protein to nitrocellulose membrane using a semi-dry transfer system

Following gel electrophoresis, gels were equilibrated in Pierce 1 – step transfer buffer for at least 15 minutes. Equilibration facilitated the removal of electrophoresis salts and detergents. Salts if not removed, increase the conductivity of the transfer and the amount of heat generated during transfer. Pre-cut nitrocellulose membrane and pre-cut filter paper were also equilibrated in transfer buffer. Protein transfer was carried out on a Pierce

G2 Fast Blotter (model number 62291) semi-dry electrophoretic transfer system. A pre-soaked sheet of filter paper was placed onto the platinum anode. A pipette was rolled over the surface of the filter paper to exclude all air bubbles. This step was repeated with two to five more sheets of filter paper. Then the nitrocellulose membrane was placed on top of the filter paper and all bubbles rolled out. The equilibrated gel was carefully placed on top of the nitrocellulose membrane, aligning the gel on the center of the membrane. Any air bubbles were again rolled out. Another three to six sheets of pre-soaked filter paper were placed on top of the gel, with care taken to remove air bubbles. The cathode was placed on top of the stack and inserted into the transfer charge unit. Gels were transferred at 15 mA /gel for 14 min.

2.5.2.8 Staining of proteins immobilized on nitrocellulose filters

Ponceau S staining was employed to determine whether uniform transfer of proteins to the nitrocellulose membrane had taken place and to normalize for variations in protein loading. Transferred proteins were detected as red bands on a white background. This staining technique is reversible to allow further immunological analysis. Ponceau S is a negative stain, which binds to positively charged amino acid groups of proteins. It also binds non-covalently to non-polar regions of proteins. Following electrophoretic transfer, the nitrocellulose membrane was immersed in 20 mL Ponceau S solution and incubated at room temperature for 5 min with constant agitation. After protein visualization, a scan was taken for documentation and further analysis if necessary, and the membrane washed in several changes of dH_2O. The membrane was then used for immunological probing.

2.5.2.9 Immunological probing

Following Ponceau S staining, the membrane was incubated at constant agitation in blocking buffer at room temperature for 1 hr or 4°C overnight. The membrane was then washed three times for 5 min a piece with fresh TBS-T. Incubation with the appropriate primary antibody (diluted to recommended concentration in blocking buffer) was done at room temperature for 1 hr or 4 °C overnight. Following this the membrane was washed three times for 5 min a piece in fresh TBS-T. The membrane was then

incubated at constant agitation with the appropriate peroxidase-conjugated secondary antibody (again diluted to the recommended concentration in blocking buffer) at room temperature for 1 hr or 4 °C overnight. The membrane was then washed three times for 5 min a piece with fresh TBS-T. The membrane was then placed in a clean container and covered with 3, 3', 5, 5'-tetramethylbenzidine (TMB) which is used for the colorimetric detection of hydrogen peroxidase-conjugated molecules. When incubated, the peroxidase-bound to the secondary antibody catalyzed the production of a dark blue permanent colored product that was easily observable. The membrane was then rinsed in distilled water to stop the reaction and scanned.

2.5.2.10 Data analysis - normalization

Normalization was conducted using ImageJ software and graphical output was generated using Microsoft Office Excel.

2.6 Cell Manipulations

2.6.1 Materials: Cell Manipulations

- Recombinant Mouse Sonic Hedgehog/Shh (C25II), N-Terminus 464-SH-200 (R&D Systems)
- Recombinant TGFβ1 7666-MB-005 (R&D Systems)
- Recombinant PDGFBB 20-BB-050 (R&D Systems)
- Recombinant Shh 464-SH-025 (R&D Systems)
- StemPro® Adipogenesis Differentiation Kit A10070-01 (Invitrogen)
- StemPro® Osteogenesis Differentiation Kit A10072-01 (Invitrogen)
- Alizarin Red A5533 (Sigma)
- Oil Red O O0625 (Sigma)
- Cyclopamine hydrate C4116 (Sigma)
- HPI-4 H4541 (Sigma)
- Recombinant HIP-a 1568-HP-050 (R&D Systems)
- Anti-Patched 1 antibody ab55629 (Abcam)
- Anti-Shh antibody MAB4641 (R&D Systems)
- Cignal GLI Reporter (luc) Kit CCS-6030L (Qiagen)

- Attractene Transfection Reagent 301005 (Qiagen)
- Dual-Glo® Luciferase Assay System E2920 (Promega)

2.6.2 Methods: Cell Manipulations

2.6.2.1 Adipogenesis Differentiation

StemPro® adipogenesis differentiation medium was used to differentiate the $Sca1^{+}$ mESC and mouse mesenchymal stem cells to adipocytes. Cells were treated in accordance with the manufacturers recommendations; briefly, cells were cultured to between 60 – 80 % confluency in their maintenance medium before being washed with HBSS twice followed by feeding with the appropriate medium. A population of cells were cultured in maintenance medium as a control while the remaining cells were cultured in adipogenesis medium for 14 days, with medium replacement occurring every 3 – 4 days. On day 14, cells were fixed with 3.7 % formaldehyde at room temperature for 15 min. Following this the samples were washed twice with HBSS solution. If the samples were not going to be stained immediately, they were stored at 4 °C in HBSS. However, if they were going to be stained then they were washed thrice with deionized water and 2 mL of 60 % isopropanol was added to the cells for 2 min. Cells were then washed twice with deionized water and 1 mL of working stock Oil Red O* stain was added and allowed to incubate at room temperature for 15 min. Following this all samples were washed five times with deionized water, ensuring excess stain was removed. Samples were then assessed for the presence of adipose vesicles, which were stained by the 0.5 % Oil Red O solution and imaged using a Nikon microscope under phase contrast conditions.

*Oil Red O stain was prepared by adding 300 mg of Oil Red O powder to 100 mL of 99 % isopropanol. 30 mL of this Oil Red O stock solution was added to 20 mL of deionized water and the solution filter (0.2 µM) sterilized, this became the working Oil Red O solution.

2.6.2.2 Osteogenesis Differentiation

StemPro® osteogenesis differentiation medium was used to differentiate the Sca1^{+} mESC and mouse mesenchymal stem cells to osteocytes. Cells were treated in accordance with the manufactures' recommendations however; briefly, cells were seeded at a density of 10 x 10^3 cells/cm^2 in their maintenance medium and left for two days before being washed with HBSS twice, followed by feeding with the appropriate medium. A population of cells were cultured in maintenance medium as a control while the remaining cells were cultured in osteogenesis medium for 21 days, with medium replacement occurring every 3 – 4 days. On day 21, cells were fixed with 3.7 % formaldehyde at room temperature for 15 min. Following this the samples were washed twice with HBSS solution. If the samples were not going to be stained immediately, they were stored at 4 °C in HBSS. However if they were going to be stained immediately then 2 % Alizarin red in distilled water was prepared and put onto the cells at room temperature for 15 min. Following this all samples were washed five times with HBSS, ensuring excess stain was removed. Samples were then assessed for the presence of calcium deposits, which were stained by the 2 % Alizarin red and imaged using a Nikon microscope under phase contrast conditions. All results are representative of experiments that were repeated with n ≥ 3.

2.6.2.3 Vascular Smooth Muscle Cell Differentiation

Cells were seeded at a density of 1 x 10^3 cells/cm^2 in their maintenance medium and left for 24 hr before being washed with HBSS twice, followed by feeding with the appropriate medium. There were three populations investigated throughout this experiment. Firstly a population of cells were cultured in maintenance medium as a control (MM), another population were cultured in differentiation medium without the TGFβ1 and PDGF-BB, as a medium control (-DM). Lastly a population were cultured in differentiation medium which included TGFβ1 and PDGF-BB (+DM). The maintenance medium of each cell type is outlined in table 2.1. However the -DM cells were cultured in growth vessels pre-treated with 5 µg/mL mouse collagen IV for at least two hrs prior to seeding. The medium this population were cultured in

was composed of DMEM, 10 % GIBCO FBS and 0.05 mM mercaptoethanol. The +DM cells were also cultured in growth vessels pre-treated with 5 µg/mL mouse collagen IV for at least two hrs prior to seeding. The medium this population were cultured in was composed of DMEM, 10 % GIBCO FBS, 0.05 mM mercaptoethanol, 2 ng/mL TGFβ1 and 10 ng/mL PDGF-BB. Cells were cultured in their respective medium types for 2 – 6 days.

2.6.2.4 Other Cell Treatments

Cells were seeded in maintenance medium at a density appropriate for the duration of the experiment and left for 24 hr before being washed with HBSS twice, followed by feeding with the appropriate medium until the conclusion of the experiment. The following medium types were used:

Maintenance Medium – experimental control (MM): cell type dependent

Differentiation medium without supplementation – medium control (-DM): DMEM and 10 % GIBCO FBS

Differentiation medium with varying supplementation – experimental conditions (+DM): DMEM and 10 % GIBCO FBS base

Items supplemented into the differentiation medium

- Recombinant Shh (0.5 µg/ml)
- Cyclopamine (15 µM)
- HPI-4 (10 µM)
- Recombinant HIP-1 (1 µg/ml)
- Anti- Patched1 antibody (0.3 µg/ml)
- Anti-Shh antibody (2 µg/ml)

2.6.2.5 Gli Reporter Assay

Transfection

This protocol was conducted as per the manufacturers' recommendations (Cignal GLI Reporter (luc) Kit CCS-6030L (Qiagen)). In brief, cells were seeded 18 – 24 hrs prior to transfection in maintenance medium at an appropriate density to ensure ~ 80 % confluency of a 96 well plate at

commencement of transfection. On the day of transfection, the following tubes were prepared:

Experimental Transfections (Mix gently)

Tubes 1 – 4: 100 µl Opti-MEM® + 4 µl (400 ng) Cignal reporter (for every well dilute 1 µl (100 ng) Cignal reporter in 25 µl of Opti-MEM® serum free medium)

Control Transfections (Mix gently)

Tubes 5 – 8: 100 µl Opti-MEM® + 4 µl (400 ng) Cignal negative control (for every well dilute 1 µl (100 ng) Cignal negative control in 25 µl of Opti-MEM® serum free medium)

Tube 9: 25 µl of Opti-MEM® + 1 µl (100 ng) Cignal positive control

Following this, Attractene transfection reagent was prepared by warming the reagent to room temperature and vortexing it prior to use. The Attractene was diluted by adding 5.4 µl of Attractene to 225 µl of Opti-MEM® serum free medium in a sterile eppendorf (make 0.6 µl Attractene + 25 µl Opti-MEM® serum free medium per well). The solution was then gently pipetted and set aside at room temperature for 5 mins. Following the incubation:

100 µl of diluted Attractene was aliquoted into two eppendorfs containing 100 µl (equal volume) of diluted Cignal Reporter (Experimental Transfections)

25 µl of diluted Attractene was aliquoted into an eppendorf containing 25 µl (equal volume) of diluted Cignal negative control (Control Transfections)

25 µl of diluted Attractene was aliquoted into an eppendorf containing 25 µl (equal volume) of diluted Cignal positive control (Control Transfections)

The Attractene and construct containing tubes were then mixed gently and left to incubate at room temperature for 20 mins to allow complex formation to occur. During this incubation period, the cells were washed once in PBS (without Ca^{2+} and Mg^{2+}) and dissociated in accordance with the specific cell type see section 2.1. The cells were then suspended in 7 – 9 ml of Opti-MEM®

5 % FBS medium, centrifuged, medium removed and resuspended in fresh Opti-MEM® 5 % FBS medium supplemented with 1 % NEAA at a concentration of 4 x 10^5 cells/ml. Following the 20 min incubation, 50 µl of specific construct complex was aliquoted into the appropriate wells followed by 100 µl of prepared cell suspension. The plate was then gently tilted to mix the contents and incubated at 37 °C in a 5 % CO_2 incubator for 16 hrs. After the 16 hr transfection period the medium was replaced with assay medium (Opti-MEM® 0.5 % FBS, 1 % NEAA, 100 U/ml Penicillin and 100 µg/ml Streptomycin) and left for a further 8 hrs (to complete the 24 hr transfection process). After the 24 hr transfection mark, cells were treated in accordance with section 2.6.2.4 and harvested (see below) on completion for dual-luciferase assessment.

Dual-Glo® Luciferase Assay

Dual-Glo® luciferase assay assessment was conducted in accordance with the manufacturers' recommendations (Dual-Glo® Luciferase Assay System E2920). Briefly, the following reagents were prepared in advance of initiating the protocol:

1x PLB reagent was prepared by diluting 5x Passive Lysis Buffer (PLB) in 4 volumes of distilled water and mixed well. 1x PLB could be stored at 4 °C for ~ 1 month

LARII was prepared when Lyophilized Luciferase Assay Substrate was resuspended in Luciferase Assay Buffer II and could be stored at 20°C for ~ 1 month or -70 °C for ~ 1 year

Stop & Glo® Reagent was prepared when 2.1 ml of 50x Stop & Glo® Substrate was added to 105 ml of Stop & Glo® Buffer in the amber Stop & Glo® Reagent bottle provided, vortexed for 10 seconds and could be stored at -20°C for 15 days

After completion of the treatment protocol, the medium was removed from the wells and cells were washed twice with 1x PBS. The 1x PBS wash was removed and 20 µl of 1x PLB was added to each well of the 96 well plate and

incubated for 15 mins at room temperature on an agitation device (gentle agitation). Following incubation, 20 µl of the 1x PLB/cell solution was transferred to a black 96 well plate and 100 µl of LARII was added. The firefly luciferase activity (Gli) was then measured using a luminometer set at 560 nm. Following this 100 µl of Stop & Glo® Reagent was added to each well and Renilla luciferase (reaction control) activity was measured using a luminometer set at 480 nm. Data analysis was conducted exactly as per described in the manufacturers' protocol (Dual-Glo® Luciferase Assay System E2920 (Promega)).

Other important considerations were as follows:

Each sample was read 5 – 10 times to compensate for relative noise in background signals

The time set to quantify both the firefly luciferase activity and Renilla luciferase activity was 30 secs

Background firefly luciferase activity was assessed using non-transfected cells

The Cignal (transfection) positive control can be monitored on a luminometer set at 470 nm excitation and 515 nm emission.

2.7 Real time quantitative reverse transcription polymerase chain reaction (Real Time qRT-PCR)

Real time qRT-PCR enables quantitative gene expression studies. 1 step qRT-PCR was routinely conducted meaning that all components necessary for the reaction were contained in one tube, reducing the likelihood of contamination**.**

2.7.1 Materials: Real time quantitative reverse transcription polymerase chain reaction (Real Time qRT-PCR)

- MagCore® HF16 System (RBC Bioscience Corp.)
- MagCore® kit no. 610 (RBC Bioscience Corp.)
- Dnase I,Rnase-free 89836 (Pierce)

- Real Time Rotor-GeneRG-3000TM lightcycler (Corbett Research)
- SensiFast SYBR No-ROX One-Step Kit BIO-72005 (MSC)
- Rotor-Gene SYBR® Green RT-PCR Kit 204174 (Qiagen)
- Sensifast Probe No-ROX One-Step Kit BIO-76005 (MSC)
- primer set: SMA: Mm_Acta2_1_SG QT00140119 (Qiagen)
- primer set: SM-MHCII isoform 1: Mm_Myh11_1_SG QT01060843 (Qiagen)
- primer set: SM-MHCII isoform 2: Mm_Myh11_2_SG QT02327626 (Qiagen)
- primer set: Smoothened: Mm_Smtnl2_1_SG (QT00126455 (Qiagen)
- primer set: Calponin: Mm_Cnn1_1_SG QT00105420 (Qiagen)
- primer set: α-actin Mm.PT.58.16320644 (IDT)
- primer set: calponin 1 Mm.PT.58.12652862 (IDT)
- primer set: Sox 10 Mm.PT.58.42371609 (IDT)
- primer set: Sox 17 Mm.PT.58.41862449 (IDT)
- primer set: S100β Mm.PT.58.30112765 (IDT)
- primer set: smooth muscle myosin heavy polypeptide II transcript variant 2 Mm.PT.58.9236105 (IDT)
- primer set: smooth muscle myosin heavy polypeptide II transcript variant 1 Mm.PT.58.11741166 (IDT)
- primer set: gli1 Mm.PT.58.11933824 (IDT)
- primer set: gli2 Mm.PT.58.11001473 (IDT)
- primer set: gli3 Mm.PT.58.7351969 (IDT)
- primer set: patched1 Mm.PT.58.5305068 (IDT)
- primer set: notch1 Mm.PT.58.28794468 (IDT)
- primer set: notch3 Mm.PT.58.7794053 (IDT)
- primer set: hey1 Mm.PT.58.31332652 (IDT)
- primer set: hey2 Mm.PT.58.30516586 (IDT)
- primer set: heyl Mm.PT.58.17090120 (IDT)
- primer set: tbp Mm.PT.58.39a.22214839 (IDT)
- Agarose A9414 (Sigma)
- Tris-Acetate Buffer T8280 (Sigma)

- 1kb Plus DNA Ladder 10787-018 (Invitrogen)
- 6x Gel Loading Dye B7022S (New England BioLabs® Inc.)
- Ethidium Bromide E1510 (Sigma)

2.7.2 Methods: Real time quantitative reverse transcription polymerase chain reaction (Real Time qRT-PCR)

2.7.2.1 Preparation of total RNA

RNA was isolated from cells using the MagCore® HF16 System and kit, with samples prepared in accordance with the manufacturers' specifications. Briefly, medium was removed from the cells growth vessels and cells were washed twice with ice cold HBSS solution. Cells were then dissociated using the protocol outlined in section 2.1.2. The cells were then re-suspended at 1 x 10^6 cells /200 µL complete reaction buffer (for every 1 mL of reaction buffer, 10 µL 2-mercaptoethanol was added to complete it). The samples were then vortexed and either purified straight away or stored for 1 month maximum at -80°C. For every 200 µL aliquot, 10 µL DNase 1 and 190 µL DNase 1 reaction buffer was prepared and added to well 3 of the kits cartridge. The cartridge was then placed into the machine. The 200 µL sample aliquot was added to well 4, an empty elution tube to well 1, pipette tips to well 2 and a cuvette in the cuvette holder for post-purification RNA quantification and quality assessment (Figure 2.5). The machine was then set to run program 610, with an elution volume of 60 µL and the total time for automated RNA purification with DNase treatment was 73 min (Figure 2.5).

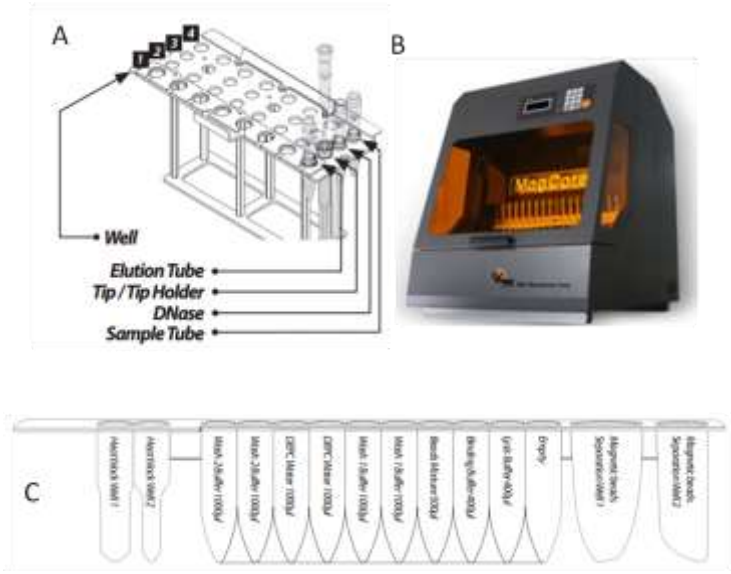

Figure 2.5: A. Rack containing wells, B. Magcore® HF16 system, C. Magcore® cartridge.

2.7.2.2 RNA concentration and quality assessment

The Magcore® instrument uses a spectrophotometric addition to calculate mRNA purity by taking absorbance readings at 230 nm, 260 nm and 280 nm. It then determines the ratio between them with pure RNAs 260 nm:280 nm ratio being 2.0. Lower than 2.0 260 nm: 280 nm ratios indicate proteins, phenol or another contamination from the purification process. The Magcore® also calculates the 230 nm:260 nm ratio, a second ratio indicator of RNA purity. These values can be higher and are generally between 2.0 - 2.2. If the ratio is lower it indicates the presence of EDTA, carbohydrate and phenolic contamination, all of which absorb at 230 nm. The instrument then generates a print out of the results.

2.7.2.3 Real Time qRT-PCR Reactions and Instrument Settings

Qiagen Rotor-Gene SYBR® Green RT-PCR Kit reaction components/tube

Component	Volume/reaction	Final Concentration
RNA	Variable	1 pg – 2 µg/reaction
Primer (F + R)	Variable	0.6 µM
SYBR Green	12.5 µL	1 x
Rnase free H_2O	Variable	-
RT	0.2 µL	-
Total Volume	50 µL	

Table 2.4: Qiagen real time qRT-PCR reaction component breakdown per tube.

The cycling program used was as follows:

Cycles	Temp. (°C)	Time	Notes
1	50	30 min	Reverse Transcription
1	95	15 min	Polymerase Activation
25 - 40	94	0.5 – 1 min	Denaturation
	50 - 68	0.5 – 1 min	Annealing*
	72	1 min	Extension (acquire at end of the step)
1	72	10 min	Final Extension

Table 2.5: Qiagen primer and mastermix cycling settings.

SensiFast SYBR No-ROX One-Step Kit reaction components/tube

Component	Volume/reaction	Final Concentration
RNA	Variable	1 pg – 1 µg/reaction
5 µM Primer (F + R)	1.6 µL	400 nM
SensiFast	10 µL	1 x
Ribosafe	0.4 µL	-
dH_2O	Variable	-
RT	0.2 µL	-

Table 2.6: Sensifast SYBR No-Rox One-Step Kit reaction component breakdown per tube.

The cycling program used was as follows:

Cycles	Temp. (°C)	Time	Notes
1	45	10 min	Reverse Transcription
1	95	2 min	Polymerase Activation
40	95	5 sec	Denaturation
	60	10 sec	Annealing
	72	5 sec	Extension (acquire at end of the step)

Table 2.7: IDT primer and sensifast mastermix cycling conditions.

SensiFast Probe No-ROX On-Step Kit reaction components/tube

Component	Volume/reaction	Final Concentration
RNA	Variable	1 pg – 1 µg/reaction
2 µM Probe	1 µL	100 nM
5 µM Primer (F + R)	1.6 µL	400 nM
SensiFast	10 µL	1 x
Ribosafe	0.4 µL	-
dH_2O	Variable	-
RT	0.2 µL	-
Final Volume	20 µL	

Table 2.8: Sensifast Probe No-Rox One-Step Kit reaction component breakdown per tube.

The cycling program used was as follows:

Cycles	Temp. (°C)	Time	Notes
1	45	10 min	Reverse Transcription
1	95	2 min	Polymerase Activation
40	95	5 sec	Denaturation
	60	20 sec	Annealing/Extension (acquire at end of step)

Table 2.9: IDT primer and sensifast mastermix cycling conditions.

2.7.2.4 Post qRT-PCR Product Assessment

Two indicative methods were employed in order to assess if correct and specific amplification was achieved, melt curve analysis and gel electrophoresis. Taken together they provide strong evidence for the correct amplification of the desired product as the only confirmatory method, Sequencing, is both expensive and timely, especially if conducted for every primer set and experiment.

If both indicative techniques complied with expectation then experimental samples were processed (see section 2.7.2.5).

Melt curve analysis

This technique involves including a melt curve step following the 40th RT-PCR cycles conclusion. In this step, the temperature is increased in small increments to 95 °C (complete double-strand oligonucleotide denaturation) at which points a fluorescent reading is taken. At the end of the 40th RT-PCR cycle, amplification of a single mRNA sequence should have occurred, with the resulting products in the form of double-stranded DNA (dsDNA) incorporated with the intercalating dye SYBR (which both the Qiagen and Sensifast methods use). As the dsDNA is heated the hydrogen bonds between the opposing connected nucleobases break releasing the SYBR molecules. Tm is the temperature at which 50% of the dsDNA has become single stranded (ssDNA) and two factors influence this:

- GC content: the GC bond with three hydrogen bonding points takes longer to denature; hence the higher the sequences GC content, the higher the temperature required to reach Tm
- The sequences length

With this in mind, a single product should theoretically produce one unique peak when the readings are plotted with respect to the increase in temperature, and multiple peaks produced if the reaction yields multiple products. The latter indicates an unspecific reaction primarily caused by inadequate primers, hence primer design is imperative for a successful investigation. However, this is not always true. The fact that this technique causes a flux whereby sequences are both in dsDNA and ssDNA forms and that the melt curve software interpretation

is based on the assumption that the product is in 1 of 2 states (dsDNA/ssDNA) with no intermediate, means that this technique cannot inherently be considered as confirmatory. An example of such discrepancies has been reported by Integrated DNA Technologies (IDT), where a single PCR product (as confirmed later by gel electrophoresis) yielded a two peaked melt curve profile.

Gel electrophoresis analysis

Gel electrophoresis was also used for the assessment of the post qRT-PCR products. It is considered another indicative technique since a single product will produce a single band, the predicted size of which can is inaccurately indicated by its' migration compared to a oligonucleotide ladder.

2 % agarose gel and 1X TAE running buffer were used in this analysis. The samples to be loaded onto the gel were mixed with loading dye in order to visualize the migration process during electrophoresis. A Bio-Rad electrophoresis instrument was set to the conditions of 120 volts for 25 minutes, following which the gels were stained by immersion in ethidium bromide solution for 15 minutes. The DNA bands were then visualized using an Amersham Bioscience Image Master® VDS UV trans-illuminator and the resulting image printed.

2.7.2.5 Post qRT-PCR Product Relative Quantification

Samples were run in triplicate with a no reverse transcriptase, and no mRNA control. TBP or HPRT were used as a reference gene to normalise and compare the results of the qRT-PCR samples (of all the reactions involved). Each experiment was conducted as a biological triplicate with each of test and control genes examined in technical triplicate to generate the Ct value. These Ct values were then graphed and the graphed error represents the deviation between three independent biological replicates. The amplification quantification data was analysed using both the comparative CT method (ΔΔCT), with both the results of which and their standard deviation inserted into PRISM version 6 to produce graphical representations of the data and the data was statistically analysed by ordinary one-way ANOVA. The second method of analysis was done by entering the Ct values into the Relative Expression Software Tool (REST;

http://rest.gene-quantification.info). The information resulting from this mathematical model was entered into PRISM version 6 in order to generate a graphical representation of the results and the data was statistically analysed by ordinary one-way ANOVA.

2.8 Telomerase Activity Assay

Telomeres are TTAGGG repeat structures which form at the end of eukaryotic chromosomes. Previously dubbed 'molecular clocks' these structures increasingly shorten with each cell division until such a point where adequate DNA replication to sustain function is no longer achievable and the cells line is terminated. Cells that succumb to such fate are considered to be terminally differentiated, however fortunately for the continuation of life, there exists a ribonucleoprotein called Telomerase. Telomerase contains an RNA component which it uses as a template to synthesize and direct the addition of telomeric repeats onto the 3' end of previously existing telomeres. Activity of this enzyme is found in traditionally considered immortal cells such as germ, cancer and stem cells and scientific advancements have lead to a commercially available kit with the ability to quantify its activity.

TRAPeze® XL Telomerase Detection Kit

The technology behind this protocol is too extensive to detail in this thesis however a brief summary is as follows:

1. A specific amount of sample protein (which includes telomerase) is added to a substrate oligonucleotide called TS. Any telomerase in the sample will add telomeric repeats onto the 3' end of the TS.
2. The TS-telomeric repeat sequences are next amplified by Taq Polymerase and FITC-labeled Amplifluor® RP (reverse) primers (RP for short).

Critical factors

- Internal control template TSK2: Used for telomerase activity quantification and as a PCR amplification positive control. The TSK2 primer is a sulforhodamine-labeled Amplifluor® K2 primer (K2 for short)

and generates a sulforhodamine containing product 56 bps in size. Semi-competitive amplification between the RP and K2 primers occurs.

- Telomerase activity quantification control template TSR8: TS primer sequence with an additional 8 telomeric repeats. A concentrated stock is provided with the kit and is serially diluted for quantification purposes.
- Telomerase positive extract control (provided in cell pellet form)
- Heat inactivated controls: Telomerase is thermo-sensitive and is inactivated when incubated for 10 min at 85 °C. Hence each sample for assessment must include a heat-inactivated control reaction.
- Telomerase negative control (achieved by using CHAPS buffer instead of sample)
- Taq polymerase negative control (achieved by using CHAPS buffer instead of Taq polymerase)

2.8.1 Materials: Telomerase Activity Assay

- Pierce BCA Assay kit 23227 (MSC)
- TRAPeze® XL Telomerase Detection Kit S7707 (Millipore)
- MyTaq DNA Polymerase BIO-21105 (MSC)
- Infinite 200 Plate Reader (Tecan)

2.8.2 Methods: Telomerase Activity Assay

2.8.2.1 Sample Preparation- Telomerase Extraction

Medium was removed from the cells growth vessels and cells were washed twice with ice cold HBSS solution. A small volume of ice-cold HBSS solution was added to each growth vessel and a cell scraper was used to detach the cells from the growth vessels surface. The cells were collected and pelleted at 600 X G for 5 min. The HBSS solution was removed and the cell pellet was then either flash frozen and stored at -80 °C (no longer than 12 months) or an appropriate volume of CHAPS (depending on pellet size) was added to the pellet to lyse the cells. The CHAPS had been supplemented with protease - phosphate inhibitor cocktails (1/100 dilution) beforehand. As minimal a quantity of CHAPS was used to ensure as high a concentration of protein as possible. Samples were then vortexed and flash frozen in liquid nitrogen and stored at -80 °C overnight or until ready to

progress with the protocol. Subsequently samples were defrosted on ice and centrifuged at 4 °C; 14,000 RPM for 15 min. Telomerase resides in the supernatant fraction so was carefully pipetted off and stored in a number of fresh eppendorfs in order to prevent more than 5 freeze thaw cycles.

2.8.2.2 Sample Quantification

The ThermoScientific Pierce™ BCA Protein Assay was performed according to the manufacturers' recommendations. Briefly:

Samples and BSA serial dilutions were prepared in triplicate as follows:

Sample Dilution

15µL 1/5 sample dilution + 65µL CHAPS

3 x 25µL = 75µL/assay

BSA Serial Dilutions (in CHAPS)

A. 1,000µL 1,000µg/mL BSA
B. 200µL CHAPS + 200µL 1,000µg/mL BSA = 500µg/mL BSA
C. 200µL CHAPS + 200µL 500µg/mL BSA = 250µg/mL BSA
D. 200µL CHAPS + 200µL 250µg/mL BSA = 125µg/mL BSA
E. 200µL CHAPS + 200µL 125µg/mL BSA = 62.5µg/mL BSA
F. 200µL CHAPS + 200µL 62.5µg/mL BSA = 31.25µg/mL BSA
G. 200µL CHAPS + 200µL 31.25µg/mL BSA = 15.625µg/mL BSA
H. 200µL CHAPS + 200µL 15.625µg/mL BSA = 7.8125µg/mL BSA
I. 1,000 µL CHAPS

3 x 25µL = 75µL/assay

Working Reagent (only usable within 7 days)

Required 200µL/well and made at 50:1 reagent A:B

Experimental Setup and Procedure

1. 25µL of either diluted sample or BSA dilution was added per well of a 96 well plate in triplicate

2. 200µL of working reagent was added to the above
3. Plate was covered in tin foil and placed on a shaker for 30 sec
4. Plate was incubated at 37 °C for 30 min
5. Plate was cooled to room temperature
6. Plate was read on a Tecan Infinite 200 set to measure absorbance at 562nm

Data Analysis and Protein Quantification

1. Absorbance readings were transferred to a new tab for manipulation
2. Each triplicates absorbance readings were averaged
3. A BSA standard curve graph was generated by plotting known BSA concentration (µg/mL) against averaged absorbance. The equation of the line and R^2 value were extracted from the graph.
4. The equation of the line was used to work out the unknown samples concentration (keeping in mind the dilution factor 1/5) and that the resulting figure was in µg/mL when later need to use µg/µL

2.8.2.3 Telomerase Assay Preparation

Prior to conducting the assay, it was critical to prepare the assays controls in an uncontaminated (product-free) room using uncontaminated (product-free) pipettes, tips and eppendorfs.

5x TRAPeze® XL Reaction Mix

Was aliquoted into 5 x 200µL and 1 x 120µL

Dilution of TSR8 control

1. 0.2 amoles/µL – concentration provided
2. 0.04 amoles/µL - 20µL CHAPS + 5µL 0.2 amoles/µL
3. 0.008 amoles/µL - 20µL CHAPS + 5µL 0.04 amoles/µL
4. 0.0016 amoles/µL - 20µL CHAPS + 5µL 0.008 amoles/µL

Telomerase Positive Control

200µL of CHAPS was added to the telomerase positive control cell pellet (10^6 cells). This was aliquoted into 10 x 20µL and stored at -80 °C. The stock was

then diluted 1:10 prior to the assay and any excess stored at-80 °C. 2µL of the 1:10 was used per reaction per assay.

2.8.2.3 Telomerase Assay Setup

The following was set up per assay:

Well/Tube 1 – 8 Duplicate of TSR8 controls (4 x 2)

Well/Tube 9 Telomerase Positive Control

Well/Tube 10 Telomerase Negative Control

Well/Tube 11 Taq Polymerase Negative Control

Samples and their heat inactivated controls were also ran in duplicate

2.8.2.4 Telomerase Assay Reaction Setup/Tube/Well

+ Taq polymerase mastermix – all tubes/wells bar - Taq polymerase control (+MM)

10.0µL	5x TRAPeze® XL Reaction Mix
0.4µL (2 units)	Taq Polymerase (5 units/µL)
37.6µL	dH_2O
48.0µL + MM/tube/well	
2.0µL	Cell Extract (10 – 750 ng/µL)
or	
2.0µL	Tissue Extract (10 – 500 ng/µL)
or	
2.0µL	1:10 Telomerase + control
or	
2.0µL	1:10 CHAPS (Telomerase - control)
or	

2.0µL	TSR8 control

- Taq polymerase mastermix – all tubes/wells bar – only 1/assay

10.0µL	5x TRAPeze® XL Reaction Mix
2.4µL (2 units)	CHAPS
37.6µL	dH_2O
48.0µL + MM/tube/well	

2.8.2.5 PCR Reaction Program Setting

An Applied Biosystems Verti™ 96 - well thermal cycler instrument was utilized.

Cycles	Step:	Temperature:	Time (hr:min:sec):
Hold	TS Extension	30 °C	00:30:00
35	Denaturation	94 °C	00:00:30
	Annealing	54 °C	00:00:30
	Extension	72 °C	00:01:00
Hold	Final extension	55 °C	00:25:00
Hold	Storage	4 °C	∞

Table 2.10: Telomerase assay PCR reactions program settings after optimization.

2.8.2.6 Fluorescence Measurement

A Tecan SAFIRE II fluorescent plate reader and XFLUOR4SAFIREII Version V 4.62b software were utilized. The following settings were used:

Telomerase Activity (FITC-labeled Amplifluor® RP primers)

Excitation wavelength:	485	Nm
Emission wavelength:	535	Nm
Excitation bandwidth:	20	Nm

Emission bandwidth:	20	Nm

Internal Control (Sulforhodamine-labeled Amplifluor® K2 primers)

Excitation wavelength:	585	Nm
Emission wavelength:	620	Nm
Excitation bandwidth:	20	Nm
Emission bandwidth:	20	Nm

2.8.2.7 Fluorescence Data Analysis

The duplicate readings from the fluorescent measurement were then averaged before undergoing the below analysis. Table 2.11 outlines the calculations required to generate a standard curve required to obtain the equation of a line and R^2 values critical for the calculation of the telomerase activity of the samples (Figure 2.6).

Standard Curve Data and Calculations

R8 (amole/Rx)	R8 (TPG Unit)	Log [TPG]
0.4	400	2.60205999
0.08	80	1.90308999
0.016	16	1.20411998
0.0032	3.2	0.50514998
No Telomerase Control	-	-
No Taq Control	-	-
R8 (amole/Rx)	**FL (RFU)**	**ΔFL**
0.4	48295	38760
0.08	28320	18785
0.016	16709	7174
0.0032	12405	2870
No Telomerase Control	9535	-
No Taq Control	-	-
R8 (amole/Rx)	**R (RFU)**	**ΔR**
0.4	26395	20510
0.08	38274	32389
0.016	43446	37561
0.0032	48818	42933
No Telomerase Control	-	-
No Taq Control	5885	-
R8 (amole/Rx)	**ΔFL/ΔR**	**Log [ΔFL/ΔR]**
0.4	1.889809849	0.276418108
0.08	0.579980858	-0.23658634
0.016	0.19099598	-0.718975774

0.0032	0.066848345	-1.17490934
No Telomerase Control	-	-
No Taq Control	-	-

Table 2.11: Calculations for the generation of the telomerase assay standard curve. R8 (amole/Rx): known concentration range of the telomerase activity quantification control template TSR8 expressed as amoles/reaction, no Telomerase and Taq controls also indicated. R8 (TPG Unit): Conversion of amole/Rx to TPG units - 1 amole of TSR8 = 1,000 TPG units. Log [TPG]: Log of R8 (TPG Unit) values. FL (RFU): Fluorescence readings of FITC -labeled Amplifluor® RP primer samples (telomerase activity). ΔFL: 0.4 – 0.0032 FL (RFU) readings minus No Telomerase Control FL (RFU) reading. R (RFU): Fluorescence readings of sulforhodamine-labeled Amplifluor® K2 primer samples (internal control). ΔR: 0.4 – 0.0032 R (RFU) readings minus No Taq Control R (RFU) reading. ΔFL/ΔR: ΔFL values divided by ΔR values. Log [ΔFL/ΔR]: Log of ΔFL/ΔR values.

Generated Standard Curve Graph

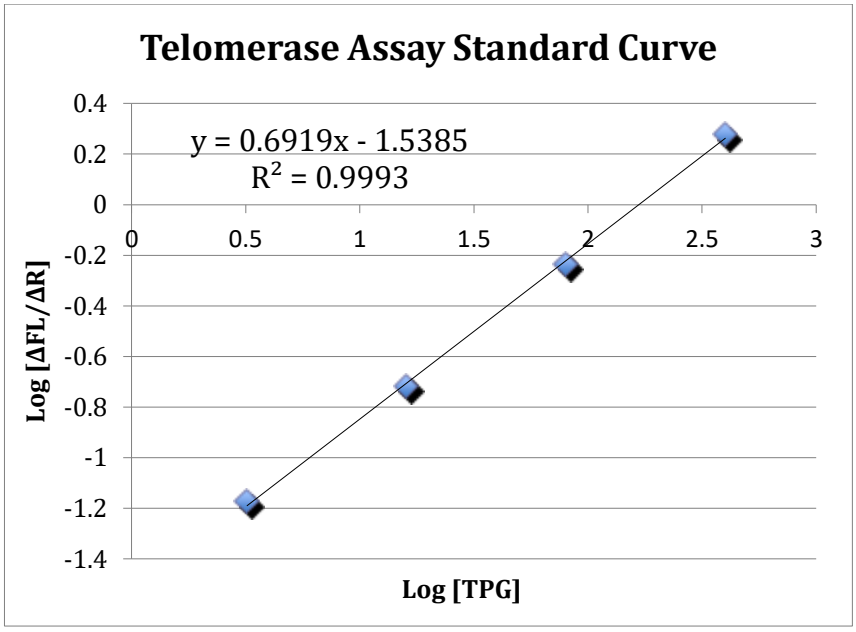

Fig 2.6: Generated standard curve from data in table 2.8. Also included are the R^2 value and the equation of the line.

Quantifying Unknown Samples Telomerase Activity

The unknown samples were then processed in the same manner as the standards shown in table 2.8. and the resulting Log [ΔFL/ΔR] reading is inserted into the equation of the line as y, this leaves the result x which equals the log[TPG Unit]. The TPG units can then be calculated by using an exponential function calculator to function 10 the log[TPG Unit] value resulting in TPG units. The standard deviation between each biological samples TPG units can be determined and factored into the graphing process.

Graphing Telomerase Activity Data

The TPG units plus their standard deviation results were inserted into PRISM version 6 to produce graphical representations of the data and statistically analysed by ordinary one-way ANOVA.

2.9 Sca1-eGFP Animal Model Study (B6.Cg-Tg(Ly6a-EGFP) G5Dzk/J)

2.9.1 Methods: Surgery and Tissue Preparation

2.9.1.1 Partial Carotid Ligation Surgical Procedure

Aseptic techniques were strictly adhered to throughout the surgical procedure, starting with the sterilization of all surgical instruments, cue tips, gauze and ligation silk (autoclave 121 °C for 15 minutes). The surgical station was covered with sterile drapes and all the surgical surfaces and instruments sprayed with 70% isopropyl alcohol. A heating pad was placed under the sterilized surgical stage and allowed to heat up prior to continuation of the procedure. The animal was quickly anesthetized (inhalation: 4 % isoflurane 2 L/min oxygen) in an enclosed container then rapidly transported to the surgical stage and maintained under anesthetic (inhalation: 1.7 - 3 % isoflurane 1 L/min oxygen) for the duration of the procedure (Figure 2.7). Following initial anthesization, the mouse was injected with analgesic (subcutaneous injection: 0.075 mg/kg buprenorphine) and ocular protection applied in the form of ophthalmic solution prior to securement to the surgical stage in the supine position using surgical tape. The mouse was then covered in sterile drape excluding the zone of surgery, face (which was contained within the anesthesia mask) and a foot (in order to continually assess for responsiveness). Hair removal cream was then applied to the area of surgery and cleaned off with sterile gauze when hair removal was achieved. The surface was then gently cleaned to remove hair removal residue using more sterile gauze dipped in sterile water. Iodine was then applied thrice to the surgical area and allowed to sit for 10 minutes. Prior to incision, 3 applications of iodine were applied to the surgical area and left for 5 minutes. The rodents chin spot was then identified and a 1 cm vertical incision was made 2 cms from the rodents chin spot (Figure 2.8). The salivary glands were then pushed to either side and when the rodents left hand side muscular triangle was identified retractors were implanted to assist with clearance of view and ease of

access. Using the fine forceps, the carotid artery was located to the left hand side of the trachea under adipose and muscular tissue. The carotid was then loosened away from the surrounding adipose tissue in zones denoted as clearance zones of which there were 4. All of the clearance zones are shown in fig. 2.10. Briefly, the first clearance zone ran to the left hand side of the superficial temporal artery and external carotid artery; the second zone of clearance ran just above the internal carotid artery; the third zone of clearance ran below the internal carotid artery; lastly the fourth zone of clearance ran to the right hand side of external carotid artery above the internal carotid artery. The next step was to begin the ligation (tie off) phase of the procedure which is shown in fig. 2.10. Briefly, the internal carotid artery was ligated first followed by the superficial temporal artery ligated to the external carotid artery. Following ligation all disturbed tissue was readjusted back into place and the two sides of the original incision repositioned in preparation for suturing. The interrupted suturing technique was employed in order to close the incision, and once completed a generous amount of iodine was applied to the site. The mouse was then given a subcutaneous injection of 500 μL saline 0.9 % NaCl and buprenorphine every 6 - 12 hours as necessary. The mouse was then placed in a clean cage under a heat lamp and monitored until recovered enough to return to the housing facility (usually 1.5 hrs later).

Cyclopamine treatment of Sca1-eGFP mice if required

Vehicle and cyclopamine or vehicle alone animals were injected one day prior to ligation, then every other day until culled. The vehicle for cyclopamine, 2-hydropropyl-β-cyclodextrin (HPCD), was diluted from stock to 45 % with PBS. Cyclopamine was dissolved in HPCD for a final concentration of 1 mg/ml by incubation at 65 °C for 1 hr. Aliquots were then stored at -20 °C until use and animals were injected with 10 mg/kg of HPCD or HPCD-cyclopamine intraperitoneally.

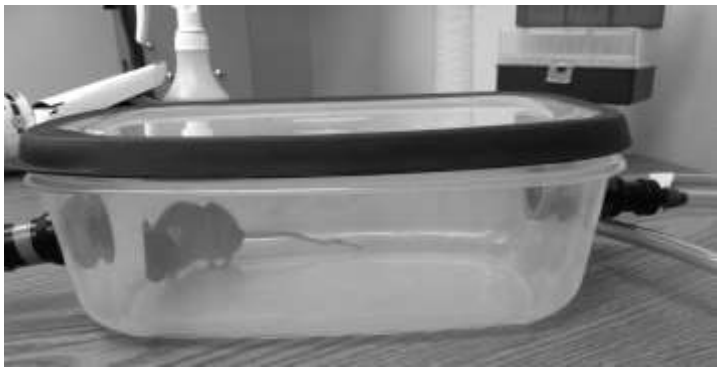

Figure 2.7: 4 % isoflurane 2 L/min oxygen anesthesia chamber.

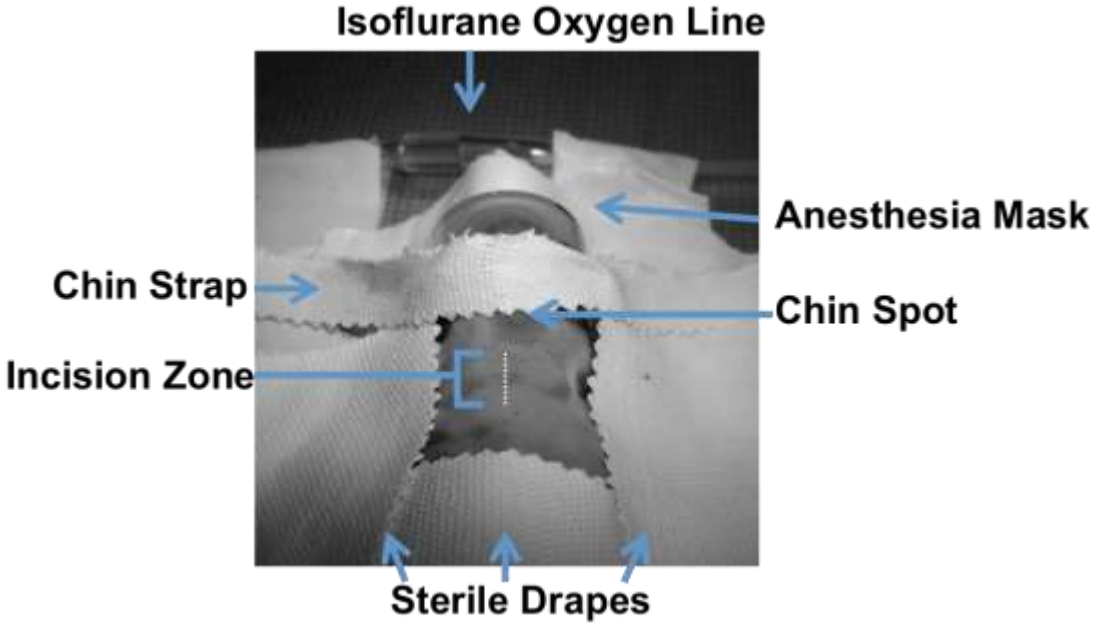

Figure 2.8: Surgical area following preparation.

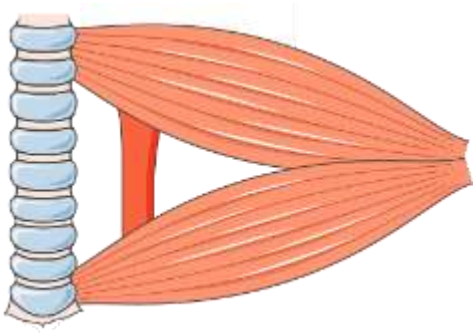

Figure 2.9: Muscular triangle.

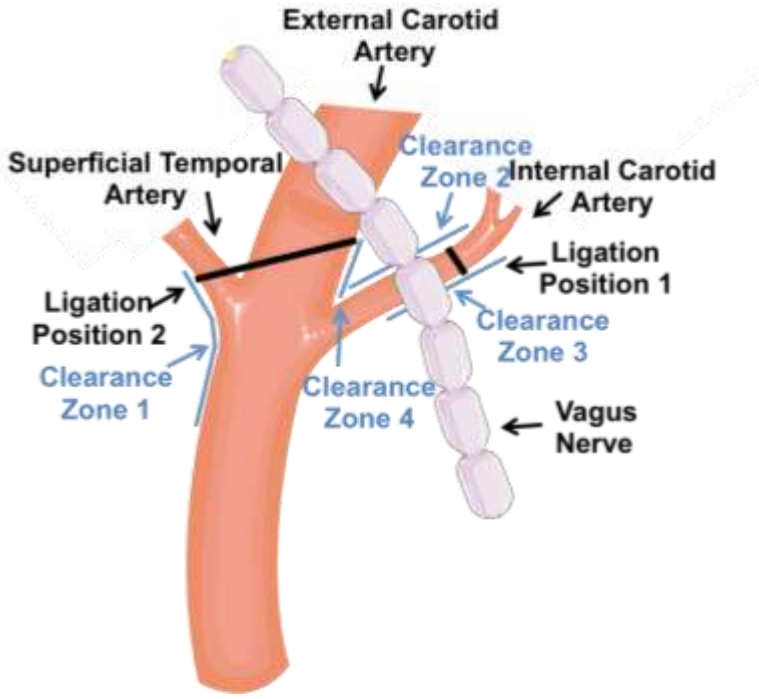

Figure 2.10: Left hand side carotid ligation.

2.9.1.2 Paraffin Preservation

The anesthetized mouse (100mg/kg Ketamine/ 16 mg/kg Xylazine) was PBS perfused. Tissue was dissected from the animal and any extraneous tissue gently removed under a dissection microscope using fine tipped forceps; the latter was conducted in a small volume of 1x PBS. The tissue kept moist in a small quantity of 1x PBS was then stained with a toothpick dipped in histology dye; excess dye was then washed off by transferring the tissue to an eppendorf of 1x PBS and inverted thrice. The tissue was then transferred into 10% neutral buffered formalin (estimated 20 - 30 times the volume of the tissue) and incubated at 4 °C overnight. The sample was then handed to pathology for paraffin embedding and sectioning using a microtome. See immunofluorescence section 2.4.3. and 2.4.4. for downstream analysis.

2.9.1.3 Cryopreservation

The mouse was anesthetized and the tissue dissected and cleaned as previously described in section 2.9.1.2. The appropriate size cryomold was then half filled with optimal cutting temperature (OCT) compound, being careful not to introduce bubbles to the chamber. Any bubble could be pulled to the outermost edges of the sample using a toothpick. The tissue was then blot dry and gently

added to the OCT compound; orientated in the same manner as documented on the tab. More OCT compound was gently added until the chamber was full and bubbles removed from the vicinity of the tissue was previously described. The cryomold was then placed in a petri dish previously left floating on liquid nitrogen in a closed container (e.g. Styrofoam box) and left to set for 1 minute. When the O.C.T compound set it turned from a clear gel to a white solid which was stored at -80 °C until sectioned using a cryomicrotome. The samples were sectioned by removing the O.C.T sample from the cryomold, placed in the correct orientation and 'glued' into the cryomicrotome sing a small amount of fresh O.C.T. The sample was then processed until the histology dye could be seen and resulting shavings were carefully put onto a positively charged glass histology slide. The glass slides were then labeled and stored in a non-transparent slide box at -80 °C until ready for further analysis. Prior to immunofluorescence, the slides were taken out of the -80 °C and immersed in 10 % neutral buffered formalin for 15 minutes at room temperature. The sample was then washed with 1x PBS and mounted using DAPI containing fluoroshield mounting medium. A coverslip was then placed on top and sealed in place using extreme wear clear nail varnish prior to confocal analysis using an Olympus FluoView™ FV1000 confocal microscope and FV10-ASW 4.2 Viewer software.

2.9.1.4 Whole Tissue - Aorta

The anesthetized mouse (100 mg/kg Ketamine/ 16 mg/kg Xylazine) was perfused with PBS. The dissection involved making a clean superficial incision medially from the abdomen to jaw. The skin was then separated from underlying muscle and pinned back. Another clean incision medially from the abdomen to jaw, penetrating the abdominal muscles (being careful not to damage the intestine) and ribcage exposed internal organs. All obstructing tissue was removed until only the heart and descending aorta were visible. Then under a dissection microscope, the heart was cut away to leave behind the aortic arch. The aortic arch was then supported by a fine tip forceps and the descending aorta released from the spine using gentle cuts using a fine scalpel blade and released at the end of the abdominal section. Any extraneous tissue was gently removed under a dissection microscope using fine tipped forceps; the latter was conducted in a small volume of 1x PBS. The tissue was then transferred into 10 % neutral buffered formalin (estimated 20 - 30 times the volume of the tissue) and incubated at 4 °C overnight. The tissue was then washed thrice in 1x PBS before mounting on histology slides using DAPI containing fluoroshield mounting medium. The whole tissue was then imaged using a Nikon Eclipse TS100 inverted microscope, EXFO X-Cite™ 120 fluorescence system and assessed using SPOT imaging software.

2.10 Histological Staining of Human and Mouse Tissue

Histological staining techniques are employed to investigate certain properties of animal tissue. This research involved two histological stains:

1. **Haematoxylin/hematoxylin and eosin (H+E) stain**

- The simplest way to describe this stain is to understand what each of its components stain during this procedure.
  - Haematoxylin is supplemented with aluminum salts to make what is considered a basic pH dye which stains acidic pH structures blue/purple. DNA and RNA are both examples of acidic pH structures within cells, hence the nucleus of cells classically stain blue/purple.

– Eosin is an acidic pH dye which stains basic pH structures pink/red. Cytoplasmic proteins are a typically examples of basic pH structures within cells, hence the cytoplasm classically stain pink/red.

2. Verhoeff's Van Gieson stain

- This dye is excellent for differentiating between collagen and other connective tissues. It is particularly excellent in highlighting elastic fibers which are not typically obvious following H+E staining. Elastic tissue atrophy is classically seen in emphysema and vascular diseases, a notable example of which is the degradation of elastic fibers in arteriosclerosis. However for the purpose of this research, Verhoeff's Van Gieson stain was employed to distinguish between the different arterial layers, with the medial layer consisting of cells contained within defined elastin layers.
- This staining procedure results in the following staining profile:

– elastic fibers: black
– nuclei (DNA and RNA): blue/black
– collagen: red
– other tissue elements: yellow

2.10.1 Materials: Histological Staining of Human and Mouse Tissue

- PBS D8662 (Sigma)
- Acetone 439126 (Sigma)
- Ethanol E7023 (Sigma)
- Xylene 534056 (Sigma)
- Ferric Chloride 451649 (Sigma)
- 1% Acid Alcohol: 1ml HCl H1758 (Sigma); 50ml 70% ethanol
- Sodium bicarbonate S6297 (Sigma)
- DPX 06522 (Sigma)
- Histoclear AGR1345 (Agar Scientific)
- Van Gieson's Solution: 100ml Picric Acid P6744 (Sigma); 0.1g Acid Fuchsin HT254 (Sigma)
- Verhoeff's Solution: 20ml 5% Alcohol Hematoxylin: 1g Hematoxylin H3136 (Sigma); 20ml Ethanol (above); 10ml 10% Ferric Chloride: 1g

Ferric Chloride (above); 10ml dH_2O; 10ml; 10ml Lugol's iodine: 0.4g Potassium Iodide 60399 (Sigma);0.2g Iodine 207772 (Sigma); 10ml dH_2O

- Human Normal Adult Artery - Frozen Tissue Section T1234013 (Amsbio)
- Human Aortic Atherosclerotic Plaque - Frozen Tissue Section CS515570 (Amsbio)

2.10.2 Methods: Histological Staining of Human and Mouse Tissue

2.10.2.1 Haematoxylin and Eosin (H+E) Staining of Human Tissue

The human tissue sections (atherosclerotic and healthy) were taken out of the -80°C freezer and left on the bench top while still in their containers for 30 min. The container lids were then opened and the slides left at room temperature for a further 15 min. The appropriate number of slides were then removed from their containers and dipped in PBS (the healthy tissue was left in PBS until the completion of the next step). The atherosclerotic slides were then placed in ice-cold acetone and held in a – 20 °C freezer for 15 min. Both the human atherosclerotic and healthy tissue were then dipped in PBS thrice before submersion in Harris Haematoxylin at room temperature for 8 min. All samples were then subjected to the following sequenced routine conducted at room temperature: washed under running tap water for 5 min; dipped in 1 % acid alcohol for 30 sec; washed under running tap water for 1 min; submerged in 0.1 % sodium bicarbonate for 1 min; washed under running tap water for 5 min; dipped 10 times in 95 % ethanol; dipped continuously in Eosin for 1 min; submerged in 75 % ethanol for 3 min; submerged in 95 % ethanol for 3 min; submerged in a second container of 95 % ethanol for 3 min; submerged in 100 % ethanol for 3 min; submerged in Histoclear for 3 min; submerged in a second container of Histoclear for 3 min and finally, each slide was permanently mounted using 3 drops of DPX (while being careful not to introduce bubbles). The slides were then pressed to remove any bubbles, cleaned with 100 % ethanol and left in the fume hood for several hours (to allow any noxious chemical fumes to evaporate) before analysis or storage at room temperature.

2.10.2.2 Haematoxylin and Eosin Staining of Mouse Tissue

Paraffin rehydration was conducted at room temperature by immersing the slides in xylene for 20 minutes. The slides were then immersed in the following gradients of ethanol for 5 minutes respectively: 100 %, 90 %, 70 % and 50 % ethanol. The slides were then rinsed in distilled H_2O before leaving in 1x PBS for 10 minutes. The slides could then be stored in 1x PBS until ready to progress further or could be immediately submersed in Harris Haematoxylin at room temperature for 8 min, followed by the same sequence of events as described above in section 2.10.2.1.

2.10.2.3 Verhoeff's Van Gieson Staining of Mouse Tissue

Paraffin rehydration was conducted as previously described in section 2.10.2.2. The slides were then submersed in Verhoff's staining solution for 10 min and briefly washed under running tap and rinsed in two changes of distilled H_2O. Black elastic fiber differentiation was achieved by immersion in 2 % ferric chloride for 15 sec followed by two washes with distilled H_2O (the latter was repeated if adequate differentiation had not occurred however less was more with subsequent Van Gieson's solution extracting elastic stain). The samples were then immersed in Van Gieson's counterstain for 1 min followed by dehydration by submersion in 95 % ethanol for 3 min; submersion in a second container of 95 % ethanol for 3 min; submersion in a third container of 95 % ethanol for 3 min and submersion in a container of 100 % ethanol for 3 min. The samples were then subjected to three submersions in separate containers of xylene for 3 minutes each and finally, each slide was permanently mounted using 3 drops of DPX (while being careful not to introduce bubbles). The slides were then pressed to remove any bubbles, cleaned with 100 % ethanol and left in the fume hood for several hours (to allow any noxious chemical fumes to evaporate) before analysis or storage at room temperature indefinitely

2.10.2.4 Morphometric Analysis of Histologically Stained Sections

Morphometric analysis was conducted in accordance with the previously published method described by Korshunov and Berk 2003, however briefly, H + E and Van Gieson stained sections images were assessed using microcomputer imaging device software (MCID Elite 6.0, Imaging Research). Data was obtained by tracing the appropriate thresholds and these reading were used to inform the morphometric analysis. The following trace readings were used: the circumference of the lumen (which is circular) was used to calculate the lumen area; the luminal surface and internal elastic lamina were used to define the intimal area; the internal elastic lamina and external elastic lamina were used to define the medial area; and the external elastic lamina and the outer edge was used to define the adventitial area. In order to get a complete picture of the vessels under investigation, three or four 4 µm cross sections were analysed every 200 µm over the entire length of each 2 mm vessel, and the mean for each of 10 divisions were calculated and the following equation as used on order to more accurately evaluate remodeling over the length of each vessel:

$$Volume = \sum_{i=8} (Area_i * 200), \mu m^3$$

Where v*olume* is the area volume of a 1,600 µm length of vessel; $Area_i$ is the area at one division and 200 is the length between divisions. A minimum of four animals per group was assessed and results expressed as mean ± SEM. Differences between groups were assessed by one-way ANOVA and a reading of $P < 0.05$ was considered significant.

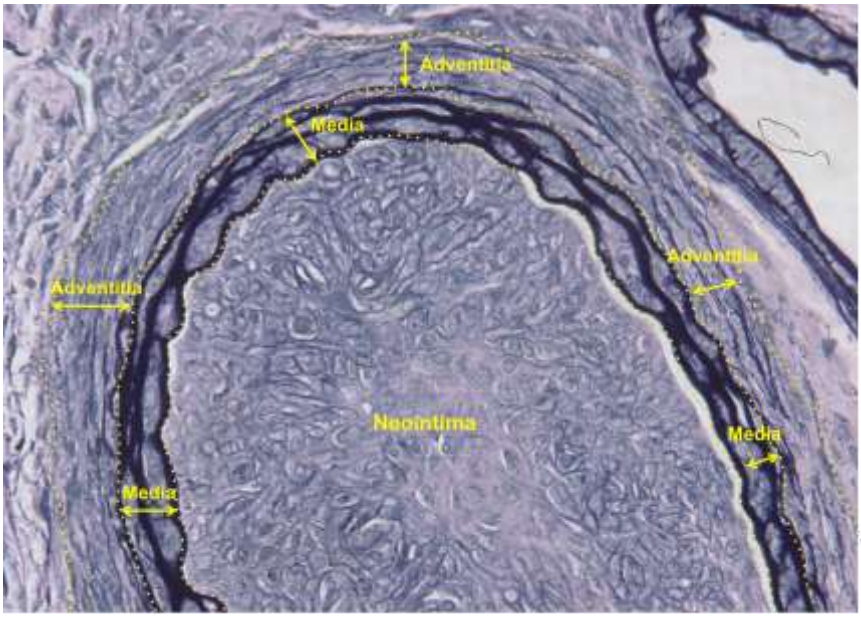

Figure 2.11: Carotid section 14 days post ligation and Verhoeff's Van Gieson staining. The adventitial and medial layers of the artery are demarcated.

2.11 Data Analysis and Management

Data was assessed blind in order to remove observer bias, and data was routinely re-assessed by a second individual in order to rule out any potential human error. PRISM version 6 was used to conduct all statistical analysis, and a student *t* test used for the comparison of two groups whereas an ordinary one-way ANOVA was used to assess variance between different groups. See appropriate section for details on specific technique related analysis, however data was assessed in accordance with best current practices.

See the following sections for further details on data analysis:

qRT-PCR: 2.7.2.5

Telomerase Assay: 2.8.2.7

Morphometric Analysis of Carotid Sections: 2.10.2.4

Chapter 3

Cell Models for Sca1^{+} Cell Isolation and Characterisation

3.1 Introduction

3.1.1 Rationale

Stem Cell Antigen 1 (Sca1)

Stem cell antigen 1 (Sca1) is an 18-kDa external membrane protein that is anchored to the phospholipid bilayer (membrane) by a glycerophosphatidylinositol (GPI); therefore, Sca1 is known as a GPI-anchored protein. GPI anchors are glycolipid structures added to proteins C-termini post-translationally; the only confirmed biological function of GPIs are to provide a stable membrane-anchoring device for proteins (Paulick and Bertozzi 2008 and Yuan et al. 2012). Sca1, also known as lymphocyte activation protein-6A (Ly-6A), is a member of the *Ly6* gene superfamily and is encoded by two strain-specific alleles. The murine *Ly6* gene family alone encodes at least 18 homologs, which for the most part demonstrate more than 80 % sequence similarity to Sca1. Sca1 structure is similar to cobra toxin proteins (another member of the *Ly6* superfamily), in that it contains two/three protruding fingers and is localised to membranous lipid rafts. Sca1 is also related to a family of proteins that contain a urokinase plasminogen activator receptor (UPAR) domain, and UPAR proteins play key roles in cell adhesion, signalling and migration. While the location and structure of Sca1 is ideal for protein-protein interaction and cell signalling, a specific molecular action of Sca1 is yet to be elucidated. Nevertheless, Sca1 is currently used as a marker for stem cell populations and the following summarises briefly what we currently know about Sca1 apart from its use as a stem cell marker (Bradfute et al. 2005; Holmes and Stanford 2007 and Yuan et al. 2012).

- Sca1 expression is upregulated in activated lymphocytes (Van de Rijn et al. 1989)
- Sca1 plays a role in hematopoietic stem cell (HSC) lineage fate (as HSC commit to lymphoid progenitors, Sca1 expression is decreased and as HSC commit to prothymocytes, Sca 1 expression is increased; Sca1-null HSC exhibit lineage skewing in B, natural killer and

macrophage cells and Sca1 overexpression decreases human and mouse myeloid activity *in vitro*; Sca1 null mice display mild thrombocytopenia (reduced platelet count) concomitant with decreased megakaryocyte progenitor and megakaryocyte levels), Sca1 null mice also display reduced self-renewal and multipotency of bone marrow progenitors (Spangrude et al. 1989; Kondo et al. 1997; Ito et al. 2003 and Bradfute et al. 2005)

- Sca1 is crucial for myoblast cell-cycle withdrawal and differentiation (Sca1 downregulation/knockdown promotes proliferation and inhibits myotube formation (Epting et al. 2004)
- Sca1 is necessary for extracellular matrix remodelling during skeletal muscle regeneration (Sca1 null mice exhibit defective muscle regeneration, post-injury fibrosis and reduced matrix metalloproteinase (critical extracellular matrix remodelling regulators) activity (Kafadar et al. 2010)
- Sca1 is required for exercise-induced muscle conditioning (Sca1 knockout mice exhibit reduced stamina and do not improve with practise (compared to control mice) (Bernstein et al. 2016)
- Sca1 has a protective effect against cardiac hypertrophy and fibrosis (Sca1 knockout mice display dramatically worse cardiac hypertrophy, fibrosis and dysfunction post-injury (pressure overload) (compared to control mice); conversely, Sca1 overexpression significantly attenuates cardiac hypertrophy and restores cardiac function post-injury (pressure overload)) (Zhou et al. 2012)
- Sca1 deficiency is known to reduce mammary epithelial proliferation and enhance chemopreventative drug-associated effects (Yuan et al. 2012).
- Sca1 attenuates tumour suppression (Yuan et al. 2012)

APC Model Cell Lines

There are currently several *in vitro* model cell lines used for the study of stem cell transition to vascular SMC (Hirschi et al. 1998; Jain et al. 1998; Manabe and Owens 2001 and Xie et al. 2011). These were reviewed most recently by Xie et al., who published a comprehensive paper detailing the pros and cons of each model cell line (Xie et al. 2011). The Xie et al., review provided an excellent resource for deciding the two best model cell lines to conduct proof of principal experimentation in this study (Xie et al. 2011). The two chosen cell lines were C3H-10T1/2 and Sca1^{+} ES-D3 mESC.

The C3H-10T1/2 cell line (denoted C3H) is a mouse embryonic fibroblast cell line of mesodermal origin shown previously to differentiation into SMC (Hirschi et al. 1998). C3H are easy to procure (from ATCC), do not require a demanding culture regime and can be reproducibly differentiated into SMC. The only caveat reported is the varying degree of differentiation depending on the protocol used, making it an attractive *in vitro* cell line. Hence C3H cells have been widely used as a model cell line for molecular regulation of differentiation and gain- and loss-of-function studies.

The second model cell line, ES-D3 mESC was prudently chosen to prevent any lineage bias associated with choosing a particular cell line. The mESC have mesodermal, endodermal and ectodermal lineage potential and therefore the experimental results will not be influenced by lineage determination (such as C3H which are purported to be of a mesodermal background). Adherent monolayer culture of mESC was chosen over embryoid body cultures due to differentiation limitations which can occur due to spacial availability of differentiation factors (Xie et al. 2011). Adherent cultured mESC have previously been successfully differentiated into SMC with a differentiation efficiency of approximately 50 % combined with an increase in mRNA levels for the SMC maker SMMHC (Xie et al. 2009). Critically, mESC cultured on collagen IV induces Sca1 expression and these Sca1^{+} mESC were also shown to differentiate into SMC with over 95 %

SMC marker expression as well as having the potential to differentiate into endothelial cells (Xiao et al. 2006 and Xiao et al. 2007).

Resident Vascular Adventitial Progenitor Cells (APCs)

Several distinct sub-populations of vascular progenitors have previously been reported, namely: $Sca1^+$ and $CD31^+$ endothelial progenitor cells, $Sox17^+$, $Sox10^+$ and $S100\beta^+$ medial progenitor cells, $CD31^+$, $CD34^+$, $CD105^+$, $CD144^+$, $VEGFR2^+$ and $CD45^+$ medial progenitor cells, and $Sca1^+$ adventitial progenitor cell (Liang et al. 2011; Tang et al. 2012; Potter et al. 2014, Tigges et al. 2013 and Passman et al. 2008). The potential of $Sca1^+$ APC to contribute to neointimal formation following vascular injury has been reported numerous times since the seminal paper published by Li et al., which provided evidence for APC migration following vascular injury and their presence in resulting intimal formation. $Sca1^+$ APC accounted for 21 % of APC when Hu et al., characterized aortic root adventitia; however critically they also showed that the $Sca1^+$ APC differentiated into SMC and EC *in vitro*, and contribute to neointimal formation *in vivo* (Li et al. 2000 and Hu et al. 2004). Despite their identification, it wasn't until data from Passman et al., and work published from our lab (Morrow et al. 2009) that the mechanism leading to their differentiation and ultimate contribution to neointimal formation was initially hypothesized (Passman et al. 2008).

$Sca1^+$ APC and the Hh Signalling System

The Hh signalling pathway is highly conserved in invertebrates and plays a fundamental role in embryonic development, specifically, the control of cell growth and arterial differentiation, and ensures the correct size and location, as well as the maintenance of tissue polarity and cellular content (Ma et al. 1993; Farrington et al. 1997; Lawson et al. 2002; Vyas et al. 2008; Dyer and Kirby 2009; Wilson and Stainier 2010 and Rimkus et al. 2016). We therefore hypothesised that $Sca1^+$ APC could contribute to intimal formation and vascular remodelling through their responsiveness to Hh signalling. In this context, Passman et al., had previously reported that $Sca1^+$ cells co-localize with Shh (the Hedgehog signalling pathway activating

ligand) and Patched 1^+ (Shh receptor) cells in young healthy vessels (Passman et al. 2008). In addition, work from our research group investigated Hh signalling components in both older healthy and injured vessels and confirmed that Patched 1^+ cells are present in the adventitia but lack active Hh signalling (very little Gli 2 levels) in healthy vessels. However, following injury, Patched 1 and Gli 2 levels are significantly increased within the initma and adventitial layers of remodelled vessels, indicating activated Hh signalling downstream of the Patched 1 receptor (Morrow et al. 2009 and Redmond et al. 2013).

3.1.2 Strategy: Addressing Thesis Aim 1: Devise Cell Models for Sca1⁺ Cell Isolation and Characterisation

Before detailing the strategies for the outlined aims, the following table details the cell markers of interest used throughout the characterisation studies.

Cell Marker	Other Aliases	Description	References
Stem Cell Antigen 1 (Sca1)	Ly-6A.2, Ly-6E.1, Ly-6A/E, TAP	Stem Cell Marker Exact function is unknown	National Centre for Biotechnology 2016 a
Smooth Muscle α-Actin (α-Actin)	a-SMA, ACTA-2	Pericyte/SMC marker Critical component of contractile apparatus involved in cell structure, integrity and motility	National Centre for Biotechnology 2016 b
Calponin 1	Cnn1	Early Differentiated SMC Marker Regulates actomyosin structure organisation and smooth muscle contraction	National Centre for Biotechnology 2016 c
Smooth Muscle Cell Myosin Heavy Chain (SMMHC)	Myh11, SM-MHC, SMHC	Differentiated SMC Marker Contractile Protein	National Centre for Biotechnology 2016 d

SRY-box 10 (Sox 10)	DOM, WS4, PCWH	Neural Stem Cell Marker Transcription factor involved in regulating embryonic development and cell fate determination	National Centre for Biotechnology 2016 e
SRY-box 17 (Sox 17)	VUR3	Endodermal and Hematopoietic Cell Marker Transcription factor involved in regulating embryonic development and cell fate determination	National Centre for Biotechnology 2016 f
S100 Calcium Bind Protein B (S100β)	NEF, S100, S100-B	Glial Cell Marker Involved in the regulation of differentiation and cell cycle progression	National Centre for Biotechnology 2016 g
Nestin	NES	Neural Stem Cell Marker Intermediate filament protein involved in cell cycle transition	National Centre for Biotechnology 2016 h
Paired Box 6 (Pax6)	AN, MGDA, WAGR	Neuroectodermal Marker Transcription factor and homeobox involved in neural tissue development	National Centre for Biotechnology 2016 i
Paired Box 1 (Pax1)	OFC2, HUP48	Mesodermal Marker Transcription factor involved in embryogenesis (pattern formation and vertebral column development)	National Centre for Biotechnology 2016 j

Table 3.1: Characterization study cell markers and descriptions

1. Isolation, characterisation and Sca1 purification of adventitial progenitor cells (APC) from aortic explants

In order to gain insight into all APC-derived cells from aortic adventitial explants, migratory resident APC were isolated and characterized by immunofluorescent staining (section 2.4) for specific protein markers to elucidate their embryonic origin (which may dictate a lineage-specific response to common stimuli in vascular SMC), stem cell and differentiated vascular smooth muscle cell identity (Topouzis and Majesky 1996; Gadson et al. 1997 and Nakamura et al. 2006). The phenotypic markers chosen were as follows (table 3.1):

- Sca1
- α-Actin
- SMMHC
- Calponin 1
- Sox 10
- Sox 17
- S100β

$Sca1^+$ APC were isolated, purified, cultured and cloned (sections 2.1 and 2.2) in order to establish a homogenous $Sca1^+$ APC cell line for future experiments to address Hh responsiveness (see chapter 4).

2. Purification and characterisation of $Sca1^+$ cells from mouse fibroblast cell C3H/10T1/2 cells (Model cell line 1: $Sca1^+$ C3H)

This robust cell line provided an excellent resource for protocol generation, optimisation and potential insight into stem cell responses to Hh signalling. C3H were firstly assessed for Sca1 without manipulation and were found to be natively homogenous high expressers of Sca1. Following this, the C3H cell line were characterised by flow cytometry (section 2.3) and western blot (section 2.5) for the following phenotypic markers (table 3.1):

- α-Actin
- SMMHC

- Calponin 1
- Sox 10
- Sox 17
- S100β
- Nestin
- Pax 6
- Pax 1

Following characterisation, confirmation of $Sca1^+$ C3H differentiation to SMC was conducted by analysis of SMC marker protein levels by western blot (see section 2.6 and 2.5 respectively).

3. Generation, purification and characterisation of $Sca1^+$ cells from mouse embryonic stem cell ES-D3 origin (Model cell line 2: $Sca1^+$ mESC)

Briefly, this cell line was generated by culturing mESC on collagen IV before being purified for Sca1 (sections 2.6 and 2.2 respectively). The characterization study included assessing $Sca1^+$ mESC anchorage dependence and phenotype by flow cytometry (section 2.3) and western blot (section 2.5). The phenotypic markers included in the characterization study were as follows (table 3.1):

- SMMHC
- Calponin 1
- Sox 10
- Sox 17
- S100β
- Nestin
- Pax 6

Following characterization, the $Sca1^+$ mESC were assessed for their multipotency, which was conducted to identify if the $Sca1^+$ generation process affected the multipotency of the mESC (section 2.6). The term

multipotency defines the cells ability to differentiate into at least 3 different lineages:

- Adipocytes – assessed by Oil Red O staining and brightfield microscopy (section 2.6)
- Osteocytes – assessed by Alizarin Red staining and brightfield microscopy (section 2.6)
- Vascular Smooth Muscle Cells (SMC)– assessed by SMMHC marker phenotyping by flow cytometry, immunofluorescence and western blot (sections 2.3, 2.4 and 2.5)

3.2 Results

3.2.1 APC Explant Generation and Characterisation

Rats were dissected, aorta was isolated and prepared as described in materials and methods before the adventitial tissue was prepared and plated in accordance with section 2.1.6. After approximately 6 days, cells began to migrate from the dissected tissue as clearly demonstrated by phase contrast microscopy and DAPI nuclei staining (Figure 3.1).

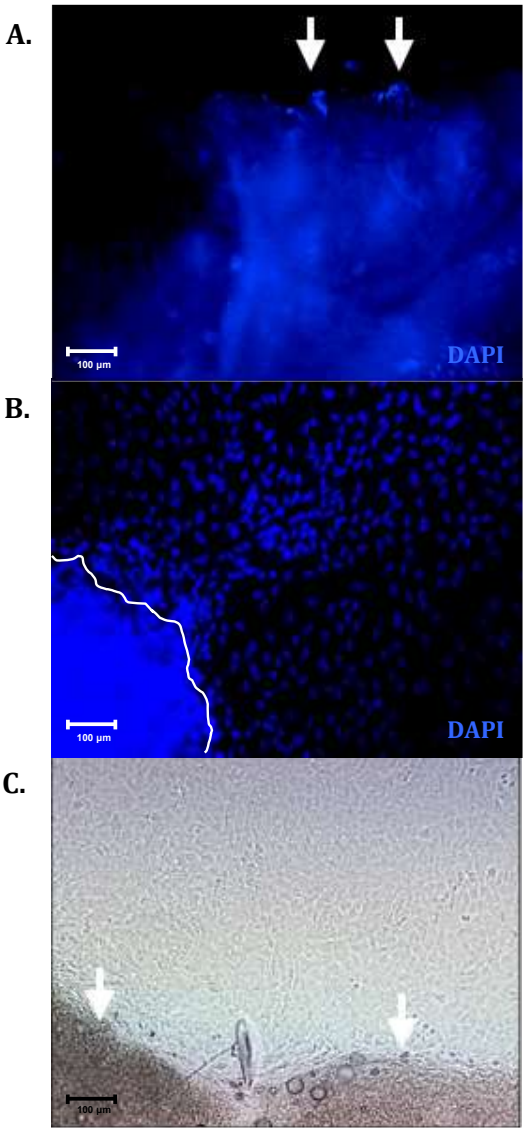

Figure 3.1: Adventitial Cells Migrating From Adventitial Explants. A: Representative fluorescent image of cell nuclei stained with DAPI as they begin to migrate from the adventitial explant, B: Representative fluorescent image of APC nuclei stained with DAPI following extensive migration from the adventitial explant, C: Representative phase contrast microscopic image of APC following successful explant from the adventitia. All images are representative of n≥4. Scale bars represent 100 microns.

The APCs were then analysed for the presence of embryological origin markers, stem cell markers and SMC differentiation markers by fluorescent immunocytochemistry as described in section 2.4. However, prior to this, it was important to establish the optimum imaging parameters and assess for secondary antibody associated background staining (Figure 3.2). While adventitial cells from the explant alone did not exhibit background staining associated with the secondary IgG, there was significant secondary IgG staining associated with adventitial tissue itself (Figure 3.2). For this

reason, in some instances, the explanted tissue was removed prior to the immunocytochemical analysis. In reference to the diagrams located in the centre of Figures 3.2 – 3.9, the location of each image was meticulously mapped in relation to the explant tissue and a white boundary was added for explant boundary recognition. When the adventitial tissue remained in some of the images, the secondary background staining is clearly visible, whereas in other cases when the adventitial tissue washed away during preparation, there is no associated background staining, however the demarcation was left in place.

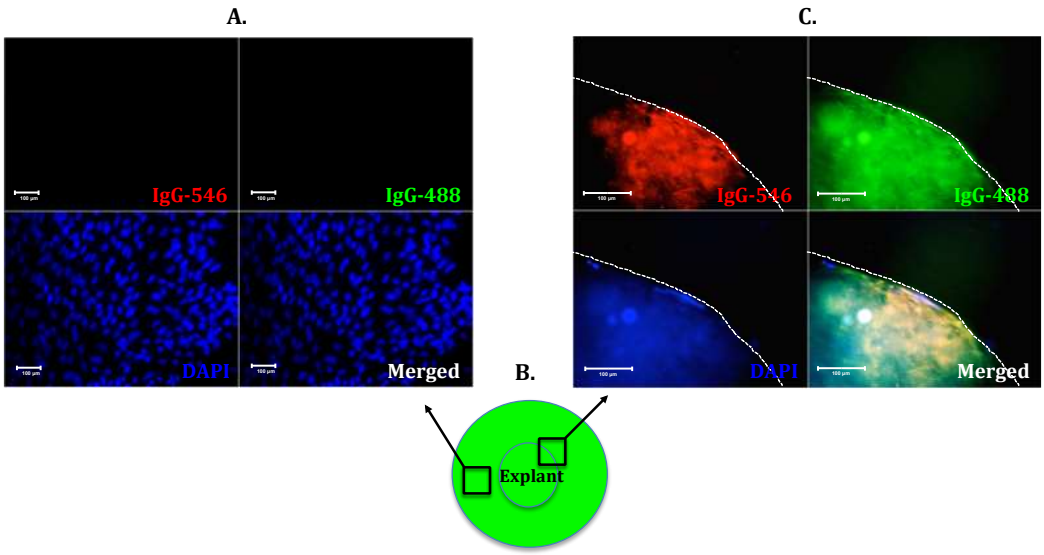

Figure 3.2: IgG Controls. A: Representative image of fluorescent signature of IgG control labelled cells, B: Representative image of fluorescent signature of IgG control labelled adventitial tissue. All images are representative of n≥4. Scale bars represent 100 microns.

When the numerous tissues sections were analysed using anti-Sca1, there is clear evidence of $Sca1^{+}$ cells migrating from the adventitia tissue (Figure 3.3).

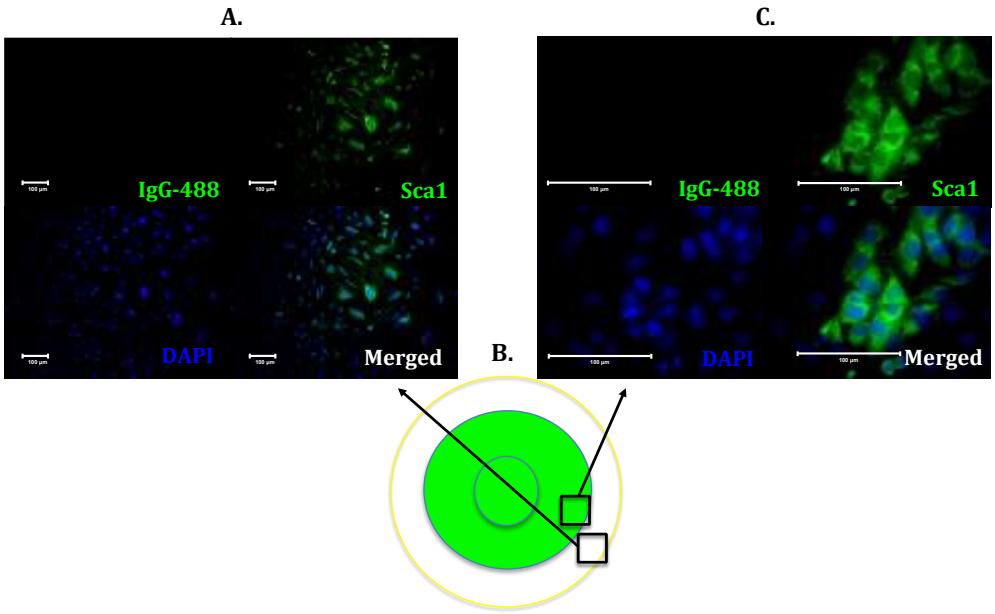

Figure 3.3: Sca1⁺ expression in explanted adventitial cells. A: Representative image of cells labelled with anti-Sca1, B: Schematic to illustrate the location of images taken with respect to tissue, C: Representative image of cells labelled with anti-Sca1. All images are representative of n≥4. Scale bars represent 100 microns.

It was subsequently imperative to assess the APCs for the presence of SMC markers to confirm that no medial cells remained attached to the separated adventitial layer. Differentiated SMCs express α-Actin, Calponin1 and SMMHC markers. Analysis of the APCs shows a large percent of cells coming from the explant are positive for the pericyte/smooth muscle cell (SMC) marker α-actin (Figure 3.4). However, there are negative for SMMHC (Figure 3.5) and Calponin 1 (Figure 3.6). It is important to note that α-Actin is also a pericyte stem cell marker and does not confirm SMC lineage. The critical indicators of differentiated SMC are the presence of Calponin 1 and SMMHC and since these cells are negative for both of these markers, the lack of differentiated SMC in culture was confirmed.

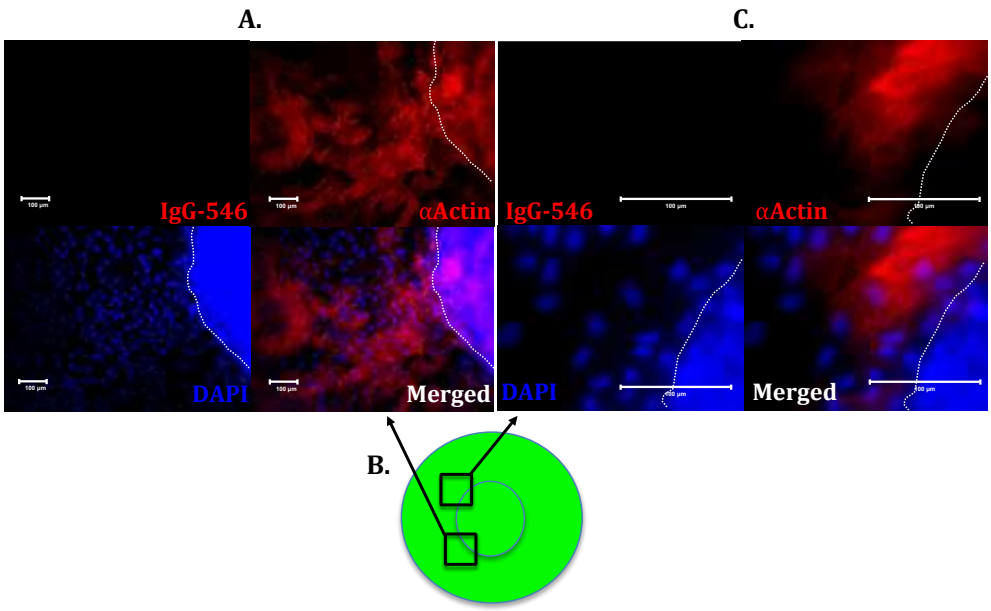

Figure 3.4: α–Actin expression in explanted adventitial cells. A: Representative image of cells labelled with anti-α-Actin, B: Schematic to illustrate the location of images taken with respect to tissue, C: Representative image of cells labelled with anti-α-Actin. All images are representative of n≥4. Scale bars represent 100 microns.

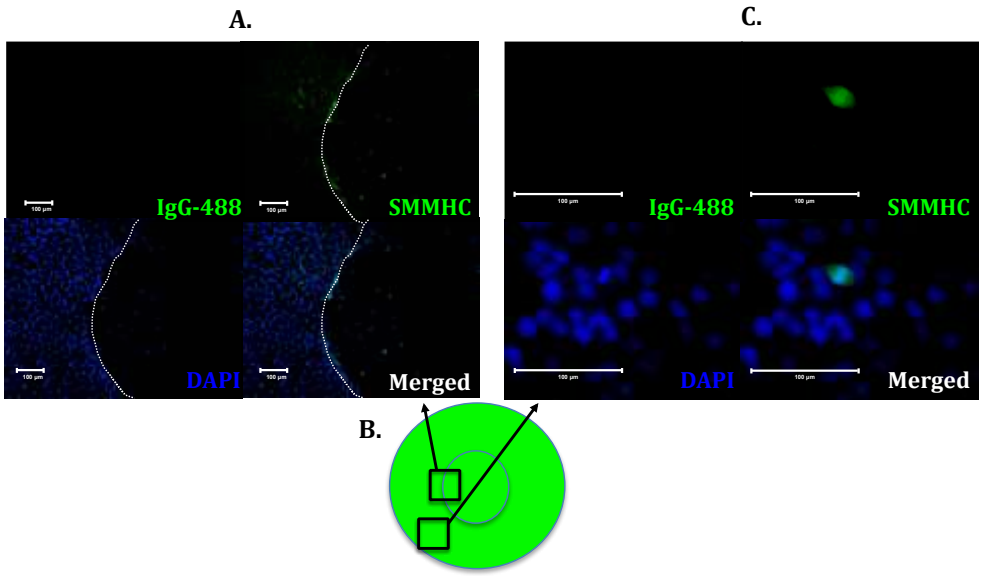

Figure 3.5: SMMHC expression in explanted adventitial cells A: Representative image of cells labelled with anti-SMMHC, B: Schematic to illustrate the location of images taken with respect to tissue, C: Representative image of cells labelled with anti-SMMHC. All images are representative of n≥4. Scale bars represent 100 microns.

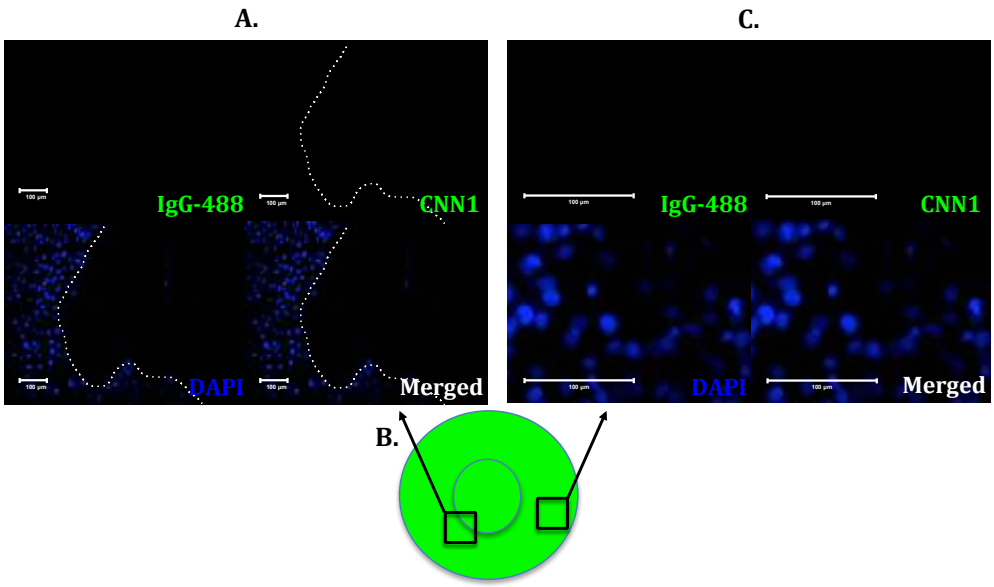

Figure 3.6: Calponin 1 expression in explanted adventitial cells. A: Representative image of cells labelled with anti-Calponin1 (CNN1), B: Schematic to illustrate the location of images taken with respect to tissue (central purple circle), C: Representative image of cells labelled with anti-Calponin1 (CNN1). All images are representative of n≥4. Scale bars represent 100 microns.

Explanted cells were also assessed for stem cell markers other than Sca1. APCs express the neural stem cell marker Sox 10 (Figure 3.7), the endodermal and hematopoietic cell marker Sox 17 (Figure 3.8) and the glial cell marker S100β (Figure 3.9). The presence of Sox 10, Sox 17 and S100β in addition to the Sca1^{+} cells suggests that the adventitial layer harbours stem cells of neural hematopoietic and endodermal origin similar to the adjacent medial layer (Tang et al. 2012).

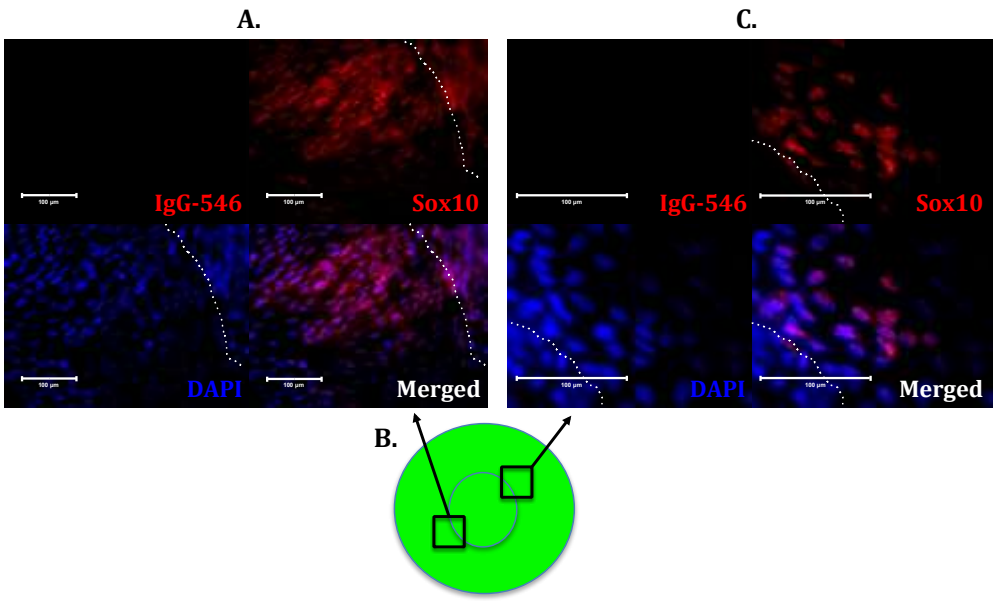

Figure 3.7: Sox 10 expression in explanted adventitial cells. A: Representative image of cells labelled with anti-Sox 10, B: Schematic to illustrate the location of images taken with respect to tissue (central purple circle), C: Representative image of cells labelled with anti-Sox 10. All images are representative of n≥4. Scale bars represent 100 microns.

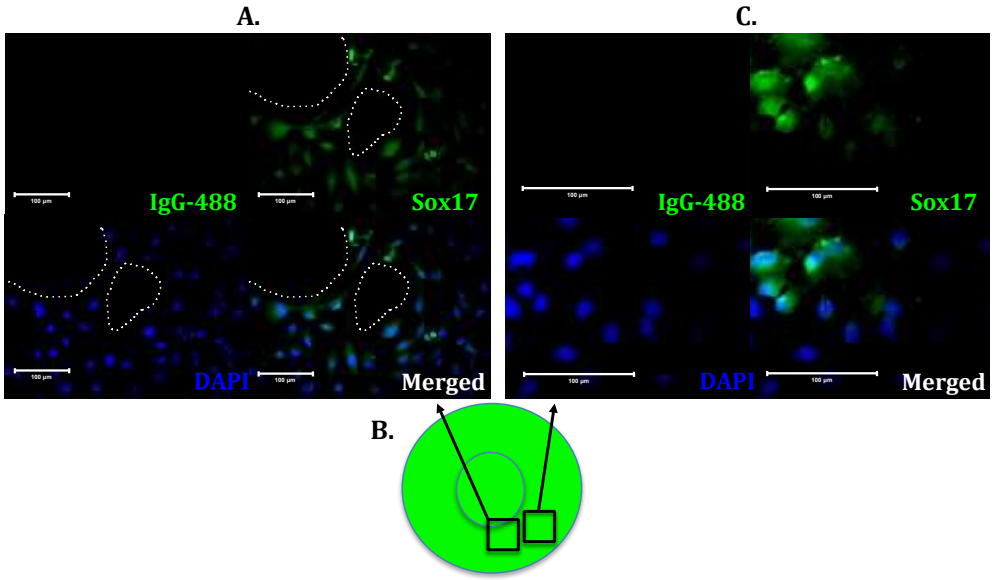

Figure 3.8: Sox 17 expression in explanted adventitial cells. A: Representative image of cells labelled with anti-Sox 17, B: Schematic to illustrate the location of images taken with respect to tissue (central purple circle), C: Representative image of cells labelled with anti-Sox 17. All images are representative of n≥4. Scale bars represent 100 microns.

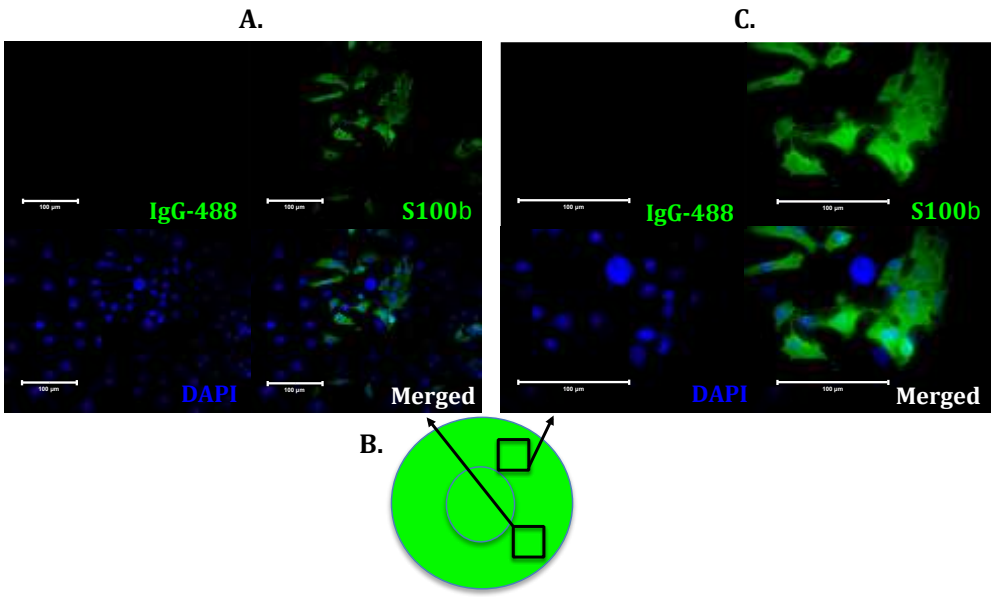

Figure 3.9: S100β⁺ expression in explanted adventitial cells A: Representative image of cells labelled with anti-S100β, B: Schematic to illustrate the location of images taken with respect to tissue (central purple circle), C: Representative image of cells labelled with anti-S100β. All images are representative of n≥4. Scale bars represent 100 microns.

3.2.2 Sca1⁺ Adventitial Progenitor Cell Purification

Following characterization of explanted cells, APCs were Sca1⁺ purified using an EasySep™ system as described in section 2.2 with the aim of establishing a purified Sca1⁺ APC cell line. The enrichment of Sca1⁺ cells following EasySep™ purification was determined by flow cytometry analysis as described in section 2.2

The flow cytometry data confirmed that Sca1⁺ APC purification resulted in a 51.4 % Sca1 positive population. The purification process had to be repeated 4/5 times in order to eventually get a pure Sca1 positive population, which was confirmed by flow cytometry analysis (Figure 3.10.D). Once purified, the Sca1⁺ APC were cloned as per section 2.2.2 and a resulting clone that was confirmed to be 100 % Sca1⁺ was used for all subsequent experiments (Figure 3.10.E).

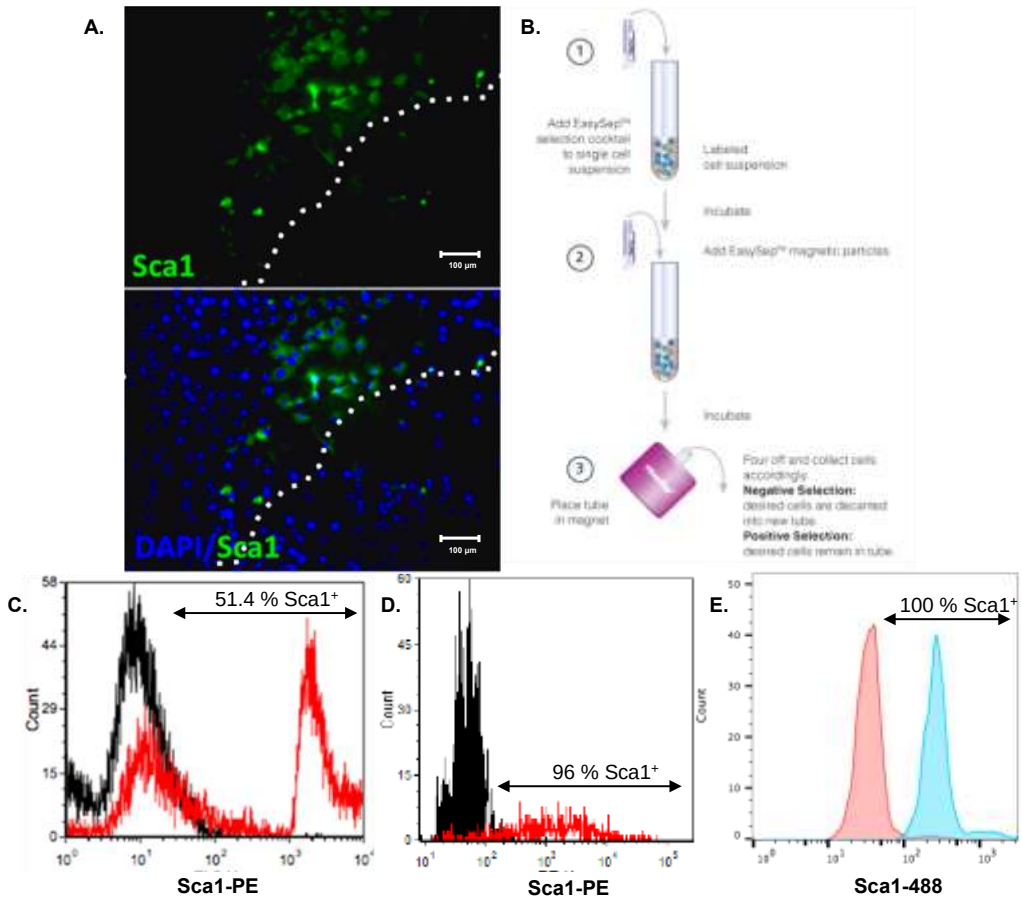

Figure 3.10: Establishment of a Sca1⁺ APC Cell Line. A: Representative image of APCs labelled with anti-Sca1, B: Schematic of the Sca1 purification process, C: Flow Cytometry analysis of APC Sca1 profile prior to obtaining a pure Sca1 APC cell line (Black histogram is IgG control, Red is anti-Sca1), D: Flow Cytometry analysis of APC Sca1 profile after obtaining a pure Sca1 APC cell line (Black histogram is IgG control, Red is anti-Sca1), E: Flow Cytometry analysis of a Sca1⁺ APC clone (Red histogram is IgG control, Blue is anti-Sca1). Scale bars represent 100 microns.

3.2.3 C3H/10T1/2 (C3H) Cell Line Characterisation: Sca1 Status

A master stock of C3H/10T1/2 (C3H) was generated and the C3H cells were screened for the Sca1 antigen before and after EasySep™ purification. Prior to purification, the C3H population were assessed as 86 % Sca1 antigen positive; this purity was slightly enhanced (to 91 %) following the purification process (Figure 3.11). The loss of Sca1 antigen expression was evident when cells were not grown in their maintenance medium but allowed to differentiate in differentiation medium (Figure 3.12).

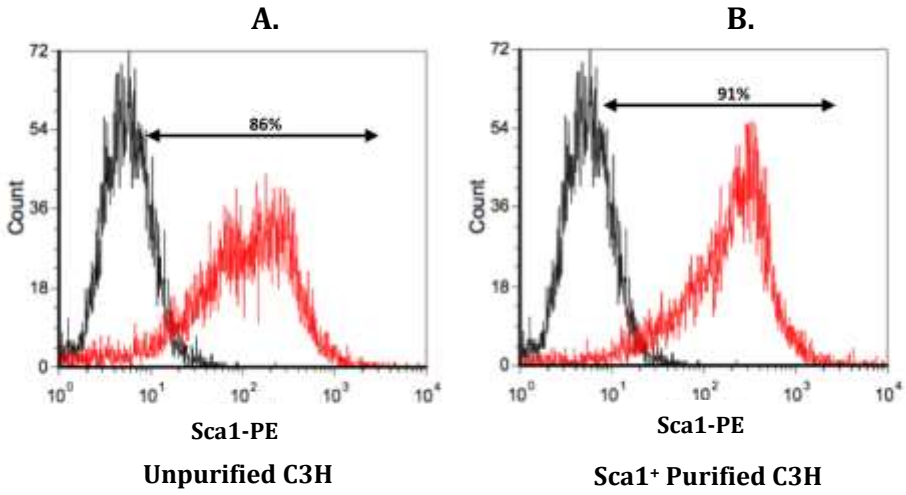

Figure 3.11: The expression of Sca1 in C3H cells in maintenance media. A: Representative flow cytometry analysis of the Sca1 profile in C3H cells prior to Sca1 purification using EasySep™. (Black histogram is IgG control, Red is anti-Sca1) n = 3, B: Representative flow cytometry analysis of Sca1 profile in C3H cells after Sca1 purification (Black histogram is IgG control, Red is anti-Sca1) n = 3.

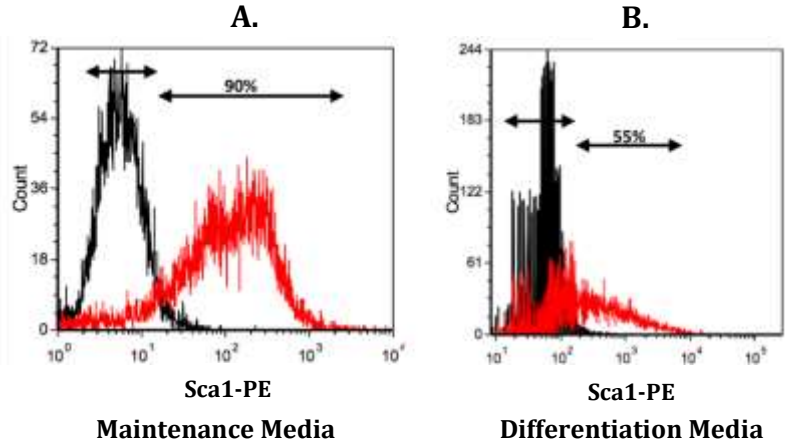

Figure 3.12: Sca1 profile for C3H cells is dependent on the culture media. A: Representative flow cytometry analysis of Sca1 profile following culture of cells in stem cell maintenance medium (Black histogram is IgG control, Red is anti-Sca1) n = 3, B: Representative flow cytometry analysis of Sca1 profile following culture of C3H cells in non-stem cell maintenance medium [differentiation media, Black histogram is IgG control, Red is anti-Sca1) n = 3.

3.2.4 C3H/10T1/2 (C3H) Cell Line Characterisation: Neural Stem, Neuroectodermal, Glial, SMC, Endodermal and Hematopoietic Marker Status

The characterisation of C3H cells was conducted following purification of the Sca1 population using EasySep™. Flow cytometry scatter analysis and overlay plots were used to analyse the staining patterns. With this approach, individual samples can be compared based on a particular fluorescent or light scatter parameter, or control data can be overlayed against test samples to distinguish experimental significance. This type of analysis is suitable when monitoring marker expression of a population before and after differentiation. The FACS analysis revealed that these C3H cell populations robustly express α-Actin, but weakly express Calponin 1 and SMMHC (Figure 3.13). Similarly, overlay plots were generated and revealed that C3H cells also robustly express the neural stem cell marker, Sox 10, the endodermal and hematopoietic marker Sox 17, the glial cell marker, S100β (Figure 3.14) and the neural stem cell marker nestin and neuroectodermal marker Pax 6 (Figure 3.15). In parallel studies, using immunoblot analysis, the C3H cells were shown to express the aforementioned antigens validating the antibodies and further confirming the flow cytometry data (Figure 3.16). C3H also expressed Shh and the Shh receptor, Patched 1.

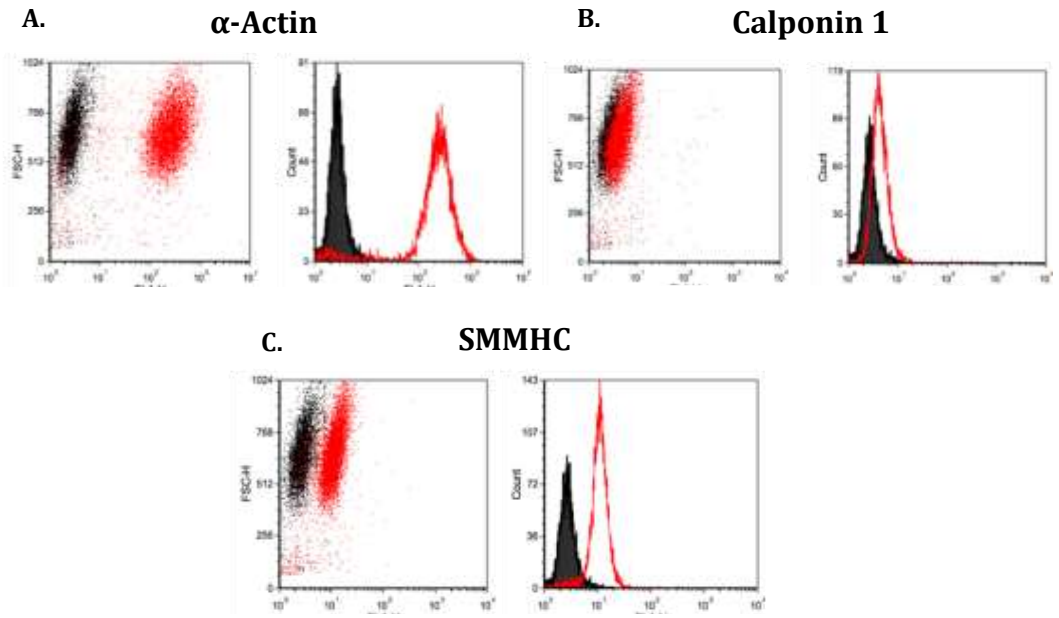

Figure 3.13: SMC Differentiation Marker Expression in C3H cells A: Representative flow cytometry analysis of Sca1⁺ C3H labelled with anti-α-Actin (Black histogram is IgG control, Red is anti-α-Actin) n = 3, B: Representative flow cytometry analysis of Sca1⁺ C3H labelled with anti-Calponin 1 (Black histogram is IgG control, Red is anti-Calponin 1) n = 3, C: Representative flow cytometry analysis of Sca1⁺ C3H labelled with anti-SMMHC (Black histogram is IgG control, Red is anti-SMMHC) n = 3.

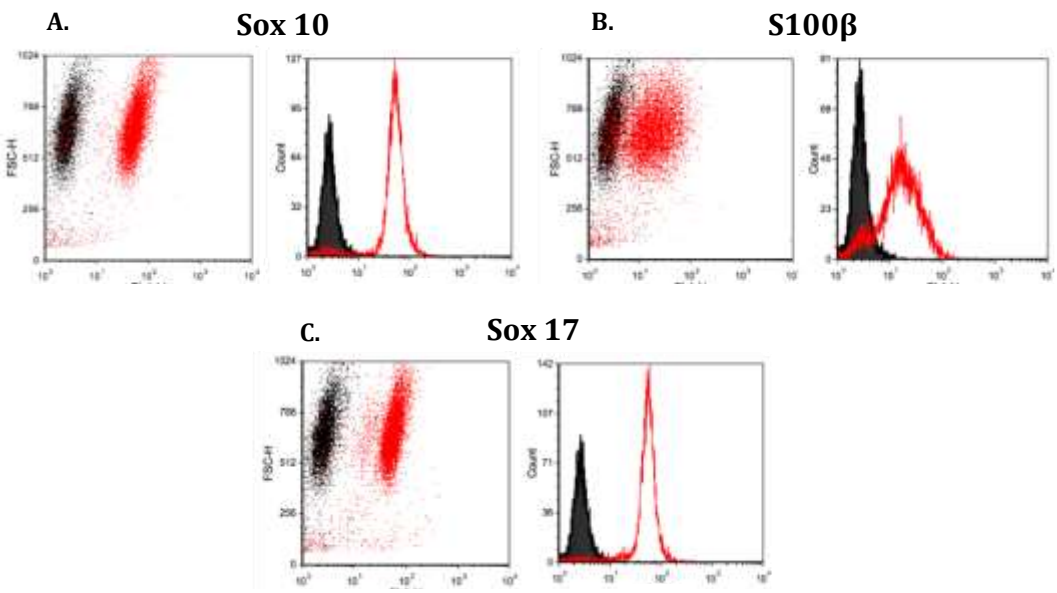

Figure 3.14: Sca1⁺C3H Express Markers for Neural Stem (Sox 10), Endodermal and Hematopoietic (Sox 17) and Glial Cell (S100β) Lineages. A: Representative flow cytometry analysis of Sca1⁺ C3H labelled with anti-Sox 10 (Black histogram is IgG control, Red is anti-Sox 10) n = 3, B: Representative flow cytometry analysis of Sca1⁺ C3H labelled with anti-S100β (Black histogram is IgG control, Red is anti-S100β) n = 3, C: Representative flow cytometry analysis of Sca1⁺ C3H labelled with anti-Sox 17 (Black histogram is IgG control, Red is anti-Sox 17) n = 3.

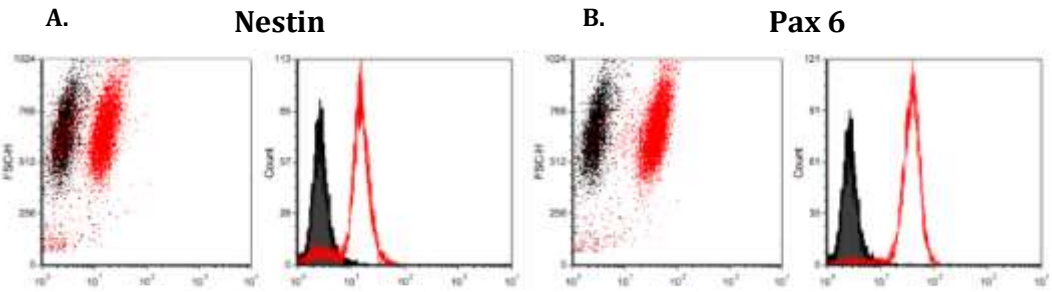

Figure 3.15: Sca1⁺ C3H Express Markers for Neural Stem (Nestin) and Neuroectodermal (Pax 6) Lineages. A: Representative Flow Cytometry analysis of Sca1⁺ C3H labelled with anti-Nestin (Black histogram is IgG control, Red is anti-Nestin) n = 3, B: Representative Flow Cytometry analysis of Sca1⁺ C3H labelled with anti-Pax 6 (Black histogram is IgG control, Red is anti-Pax 6) n = 3.

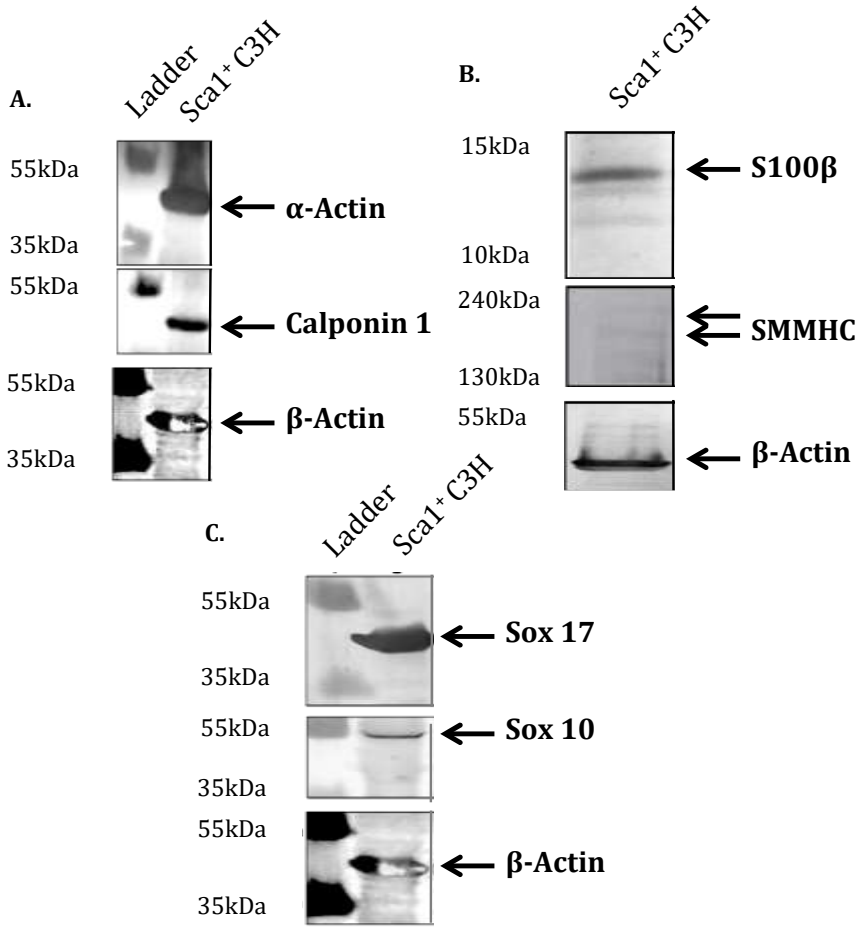

Figure 3.16: Expression of SMCs, Neural Stem, Endodermal and Hematopoietic and Glial Cell Lineage Markers. A: Western blot analysis of Sca1⁺ C3H using anti-α-Actin and anti-Calponin1 antibodies for the detection of pericyte and early SMC (anti-β-Actin control), B: Western blot analysis of Sca1⁺ C3H using anti-S100β and anti-SMMHC antibodies for the detection of Glial Cell and differentiated SMC respectively (anti-β-Actin control), C: Western blot analysis of Sca1⁺ C3H using anti-Sox 17 and anti-Sox 10 antibodies for the detection of endodermal and hematopoietic and neural stem cell markers respectively (anti-β-Actin control).

3.2.5 C3H/10T1/2 (C3H) Cell Line SMC Potential

It was then decided to assess if C3H cells could be further driven towards a SMC lineage. Despite background α-Actin and Calponin 1 expression levels, a higher expression can be achieved with the addition of the SMC differentiation inductive factors, TGF-β1 and PDGF-BB (Figure 3.17). The critical SMC marker SMMHC can be increased with incrementing concentrations of TGFβ1 (Figure 3.17). The levels of the neural stem cell marker Nestin are maintained following the transition (Figure 3.18). The mesodermal marker Pax 1 is also maintained following SMC differentiation (Figure 3.18). The Glial cell marker S100β is lost following SMC differentiation (Figure 3.18).

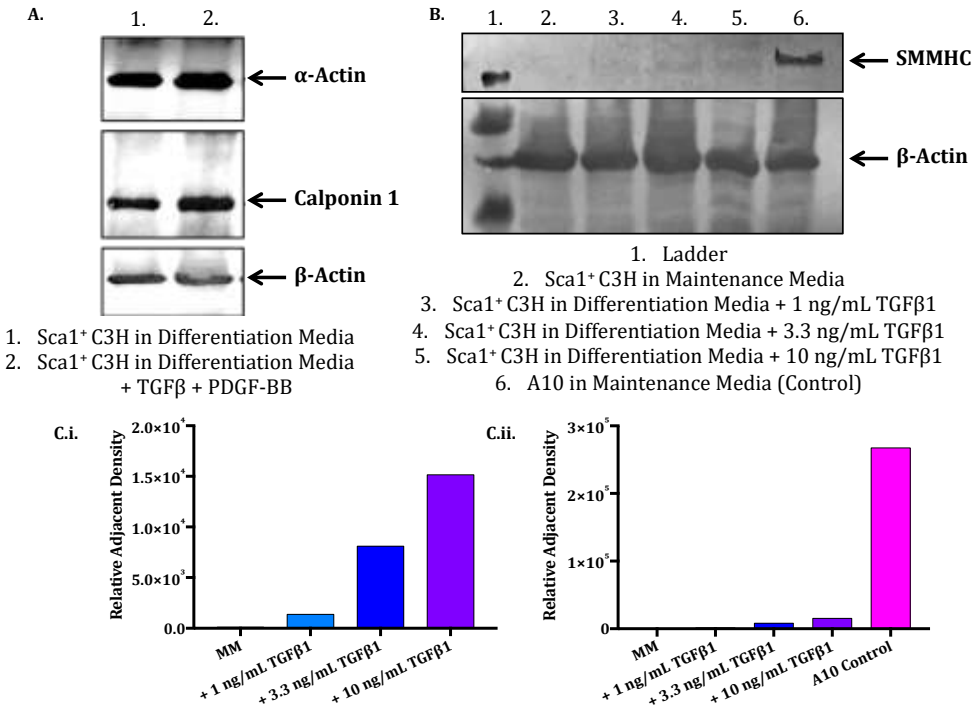

Figure 3.17: Induction of SMC differentiation in C3H cells A: Western blot analysis of Sca1⁺ C3H using anti-α-Actin and anti-Calponin1 antibodies for the detection of SMC markers (anti-β-Actin control), B: Western blot analysis of Sca1⁺ C3H using an anti-SMMHC antibody for the detection of the SMC marker (anti-β-Actin control), C: Densitometry assessment of B (C.i: without A10 cell line SMMHC control and C.ii: A10 cell line SMMHC control).

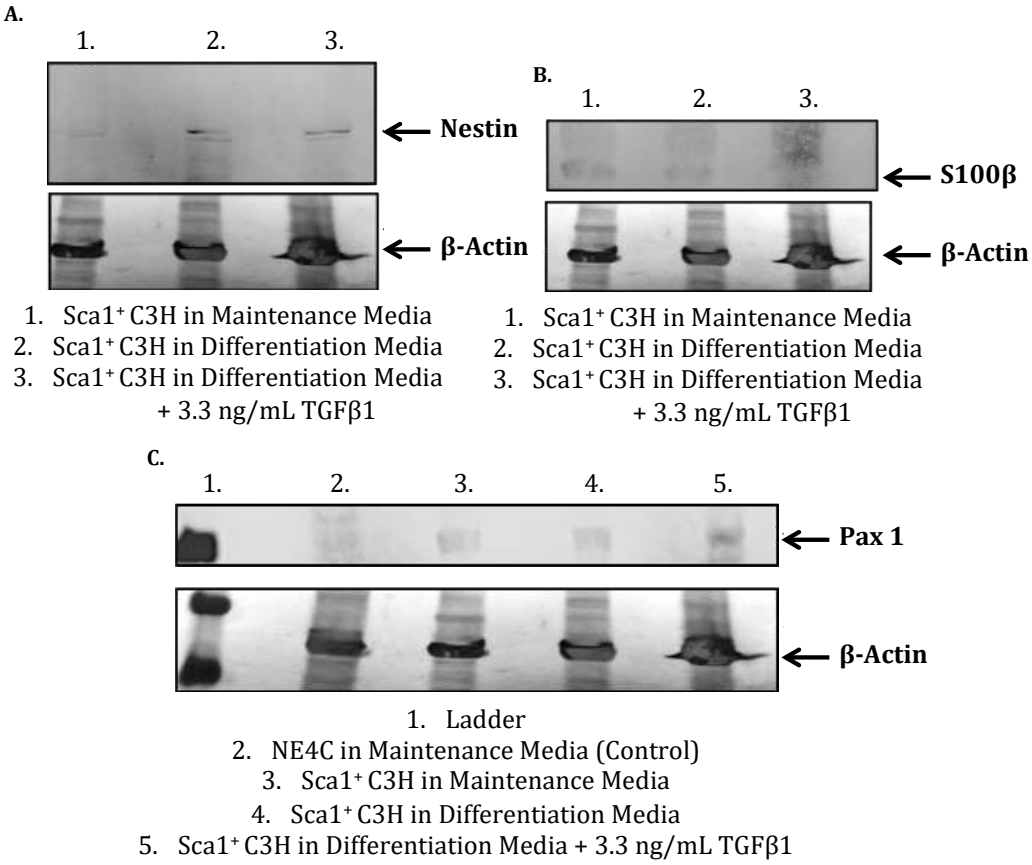

Figure 3.18: Neural stem, glial cell and mesodermal lineage marker expression after induction of SMC differentiation in C3H cells A: Western blot analysis of Sca1⁺ C3H using anti-Nestin antibody for the detection of the Neural Stem Cell marker, B: Western blot analysis of Sca1⁺ C3H using anti-S100β antibody for the detection of the Glial cell marker, C: Western blot analysis of Sca1⁺ C3H using anti-Pax 1 antibody for the detection of the Mesodermal marker.

3.2.6 Sca1⁺ mESC Generation and Optimisation

Firstly, a time course analysis of Sca1⁺ expression was conducted by immunocytochemistry using an anti-Sca1 antibody as per section 2.2.1, in order to determine the optimum time period to seek to enrich the number of Sca1⁺ cells using an EasySep™ purification system. Growth of mESC cells on collagen IV in differentiation medium for 4-5 days was clearly the optimal time for the appearance of Sca1 positive cells and hence the EasySep™ purification (Figure 3.19).

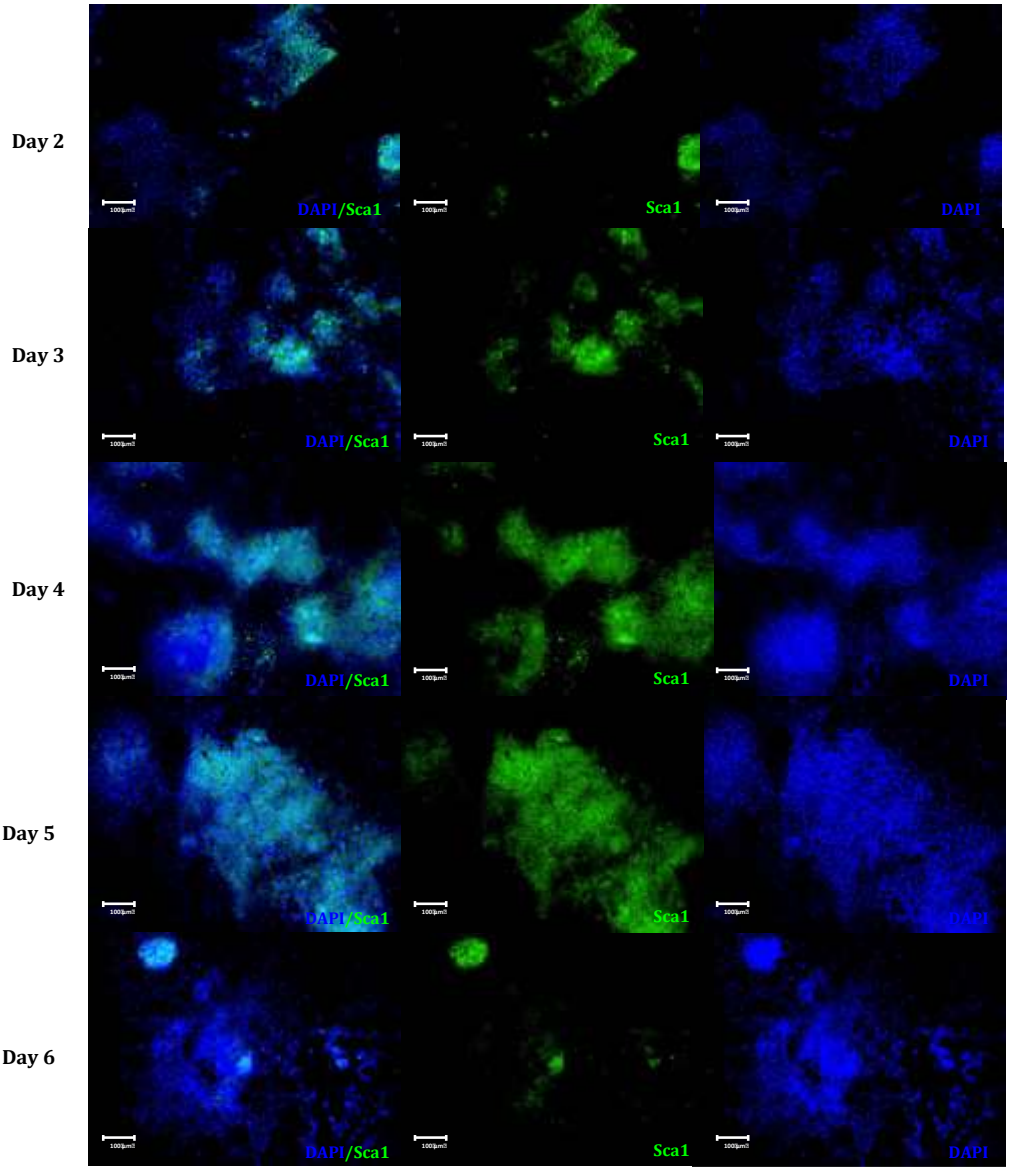

Figure 3.19: Temporal Appearance of Sca1⁺ mESC progenitors when grown on collagen IV. Representative images of mESC cultured on Collagen IV up to 6 days. Sca1⁺ mESC were labelled with anti-Sca1 and DAPI nuclear stain (n ≥ 4). Scale bars represent 100 microns.

3.2.7 Sca1⁺ mESC Purification

In order to generate a pure Sca1⁺ cell population for future experiments, it was necessary to initially employ a Miltenyi Biotech Sca1⁺ purification kit to establish an enriched population. However, loss of cellular viability, perhaps as a result of one of the kits steps that involved creating flow force to push cells through a column, mitigated against the continued use of this purification kit. Hence a second Sca1 EasySep™ purification kit developed

by STEMCELL Technologies was employed to generate a pure Sca1⁺ cell population. Flow cytometry analysis during the EasySep™ Sca1⁺ purification process was used to monitor the purity of the cell populations. The pre-purification purity of the cells was 11.8 % Sca1⁺ as assessed by FACS (which is in line with Xiao et al. 2007) but dramatically increased following EasySep™ purification to a 91.3 % Sca1⁺ population (Figure 3.20). This population was expanded and continuously re-purified immediately prior to experimentation in order to ensure the population under investigation were ≥ 98 % Sca1⁺.

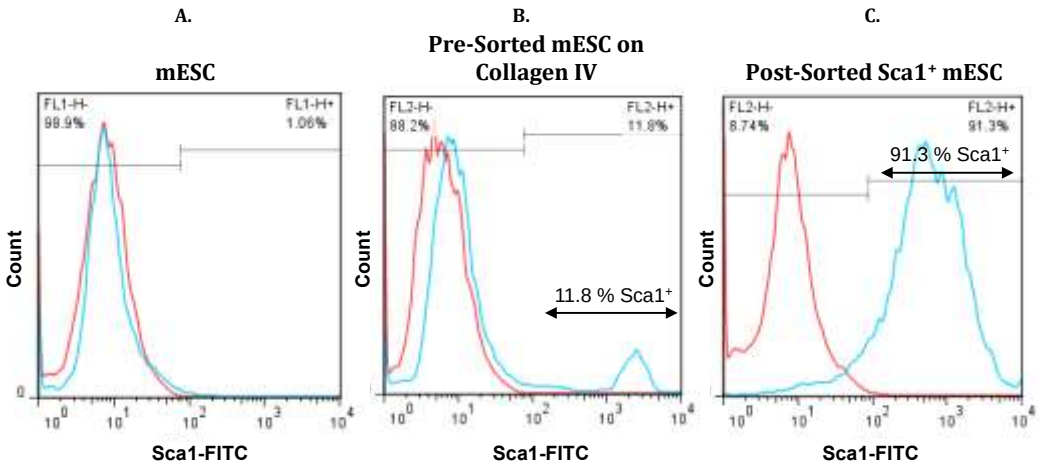

Figure 3.20: Sca1⁺ mESC generation and purification. A: Flow Cytometry analysis of mESC Sca1 profile (Red histogram is IgG control, Blue is anti-Sca1), B: Flow Cytometry analysis of mESC cultured on Collagen IV Sca1 profile (Red histogram is IgG control, Blue is anti-Sca1), C: Flow Cytometry analysis of B. post Sca1 purification (Red histogram is IgG control, Blue is anti-Sca1).

3.2.8 Sca1⁺ mESC Characterisation: Anchorage Independence

The Sca1⁺ mESC cell line was then assessed for anchorage dependency, one of the initial signs of multipotency (Welte et al. 2010). Sca1⁺ mESC cultured routinely on gelatin are phenotypically adherent (Figure 3.21), however, these cells can also become anchorage-independent 3D spheroids when cultured on non- gelatinized (adherent) plates (Figure 3.21).

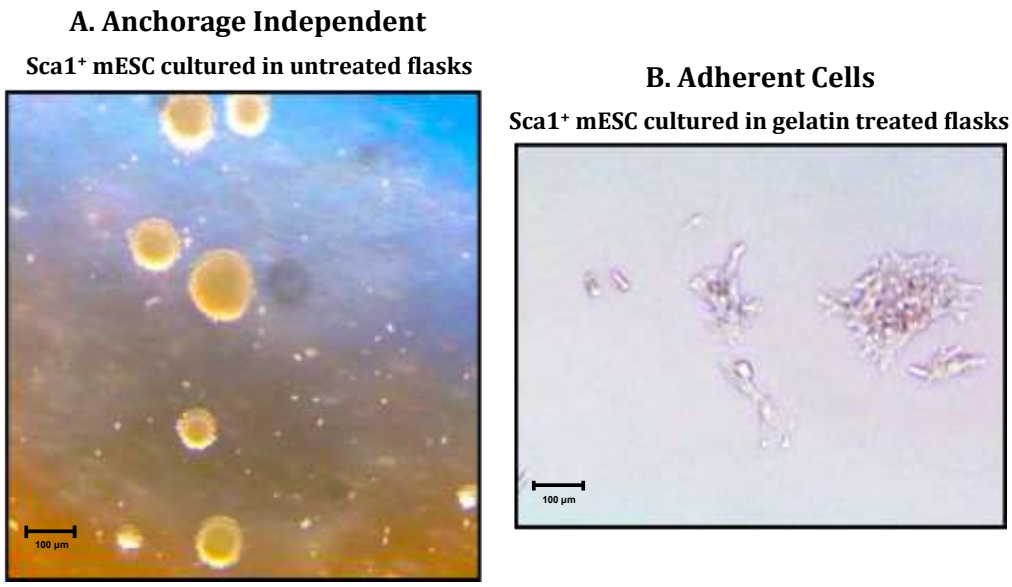

Figure 3.21: Sca1⁺ mESC Display Anchorage Independence. A: Representative 20x phase contrast image of Sca1⁺ mESC cultured in the absence of gelatin, (n ≥ 4) B: Representative 20x phase contrast image of Sca1⁺ mESC cultured in the presence of gelatin (n ≥ 4). Scale bars represent 100 microns.

3.2.9 Sca1⁺ mESC Characterisation: SMC Marker Status

The Sca1⁺ mESC population were initially characterised for the absence of SMC differentiation markers when cultured in their maintenance media. Flow cytometry and western blot analysis revealed that Sca1⁺ mESC do not express the smooth muscle cell markers Calponin 1 (CNN1), α-Actin and Smooth Muscle Myosin Heavy Chain II (SMMHC) (Figure 3.22). The lack of a peak shift in flow cytometry and discrete bands in the western blot indicate that Sca1⁺ mESC do not possess these smooth muscle cell markers (Figure 3.22).

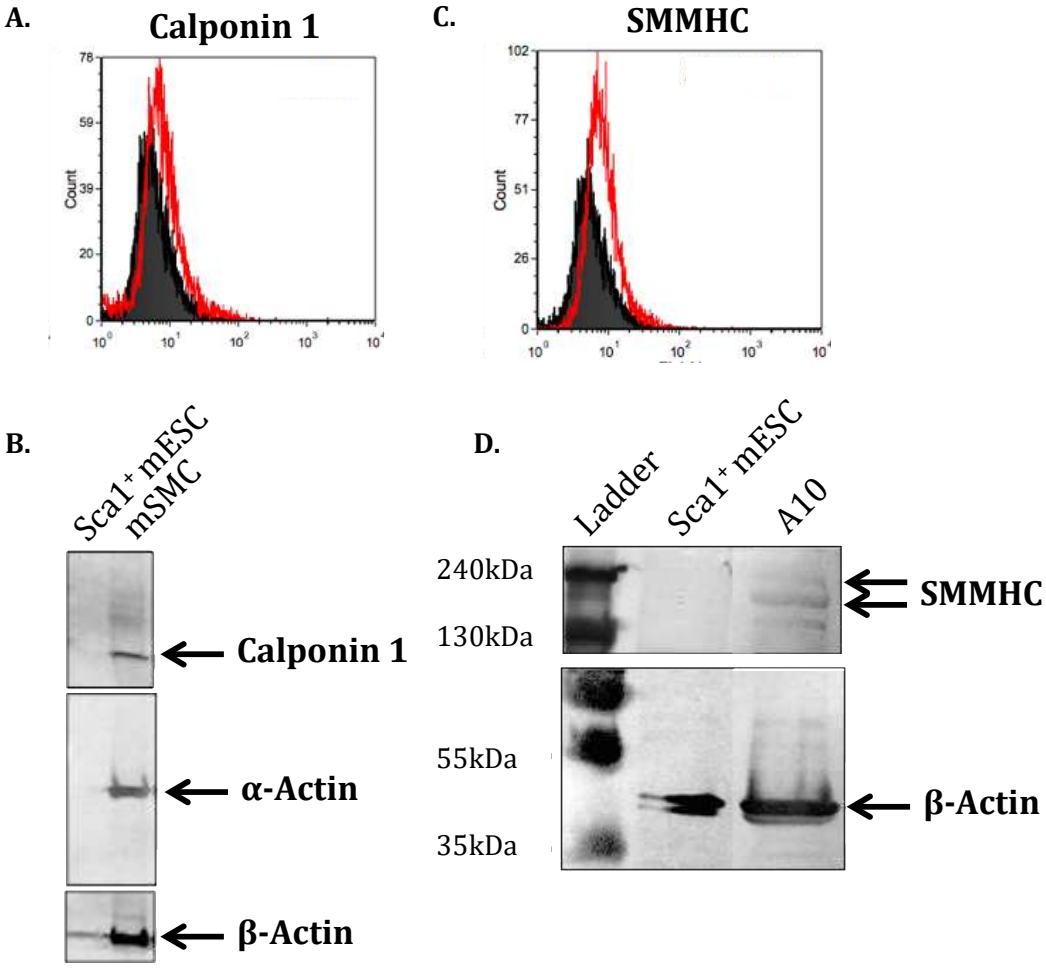

Figure 3.22: Sca1⁺ mESC Do Not Express SMC Markers. A: Representative Flow Cytometry analysis of Sca1⁺ mESC labelled with anti-Calponin 1 (Black histogram is IgG control, Red is anti-Calponin 1) n = 3, B: Western blot analysis of Sca1⁺ mESC using anti-Calponin 1 and anti-α-Actin antibodies for the detection of early SMC and pericyte markers (anti-β-Actin control), C: Representative Flow Cytometry analysis of Sca1⁺ mESC labelled with anti-SMMHC (Black histogram is IgG control, Red is anti-SMMHC) n = 3, D: Western blot analysis of Sca1⁺ mESC and A10 cell line (positive control) using anti-SMMHC antibody for the detection of differentiated SMC (anti-β-Actin control).

3.2.10 Sca1⁺ mESC Characterisation: Neural Stem and Neuroectodermal Marker Status

The expression of the neural stem cell marker, Nestin and neuroectodermal marker, Pax 6 were both assessed by flow cytometry and western blot analysis. There was a peak shift in flow cytometry for both markers when analysed by FACS and discrete bands in the western blot analysis for these antigens to suggest that Sca1⁺ mESC possess these neural stem and neuroectodermal cell markers (Figure 3.23).

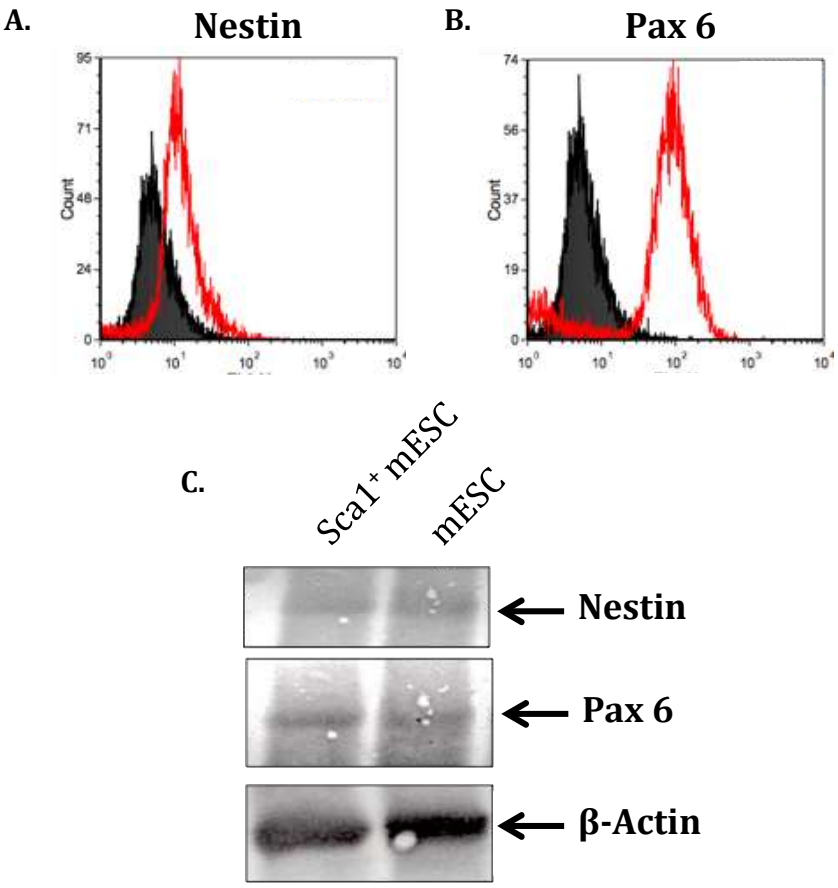

Figure 3.23: Sca1⁺ mESC Express Neural Stem and Neuroectodermal Markers. A: Representative Flow Cytometry analysis of Sca1⁺ mESC labelled with anti-Nestin (Black histogram is IgG control, Red is anti-Nestin) n = 3, B: Representative Flow Cytometry analysis of Sca1⁺ mESC labelled with anti-Pax 6 (Black histogram is IgG control, Red is anti-Pax 6) n = 3, C: Western blot analysis of Sca1⁺ mESC using anti-Nestin and anti-Pax 6 antibodies for the detection of Neural Stem and Neuroectodermal markers (anti-β-Actin control).

3.2.11 Sca1^{+} mESC Characterisation: Neural Stem, Endodermal, Hematopoietic and Glial Marker Status

In parallel studies, the expression of stem cell marker Sox 10, the endodermal and hematopoietic marker Sox 17 and glial cell marker S100β were also assessed by FACS analysis and western blot. There was a peak shift in flow cytometry analysis and presence of discrete bands in the western blot to indicate that Sca1^{+} mESC possess Sox 10 and Sox 17 (Figure 3.24). Follow-up immunocytochemical analysis confirmed the expression of Sox 10, which as a transcription factor, is localised to the nucleus (Figure 3.24).

However, the lack of a peak shift in flow cytometry and a discrete band in the western blot analysis for S100β indicates that Sca1^{+} mESC do not possess the glial cell marker, S100β.

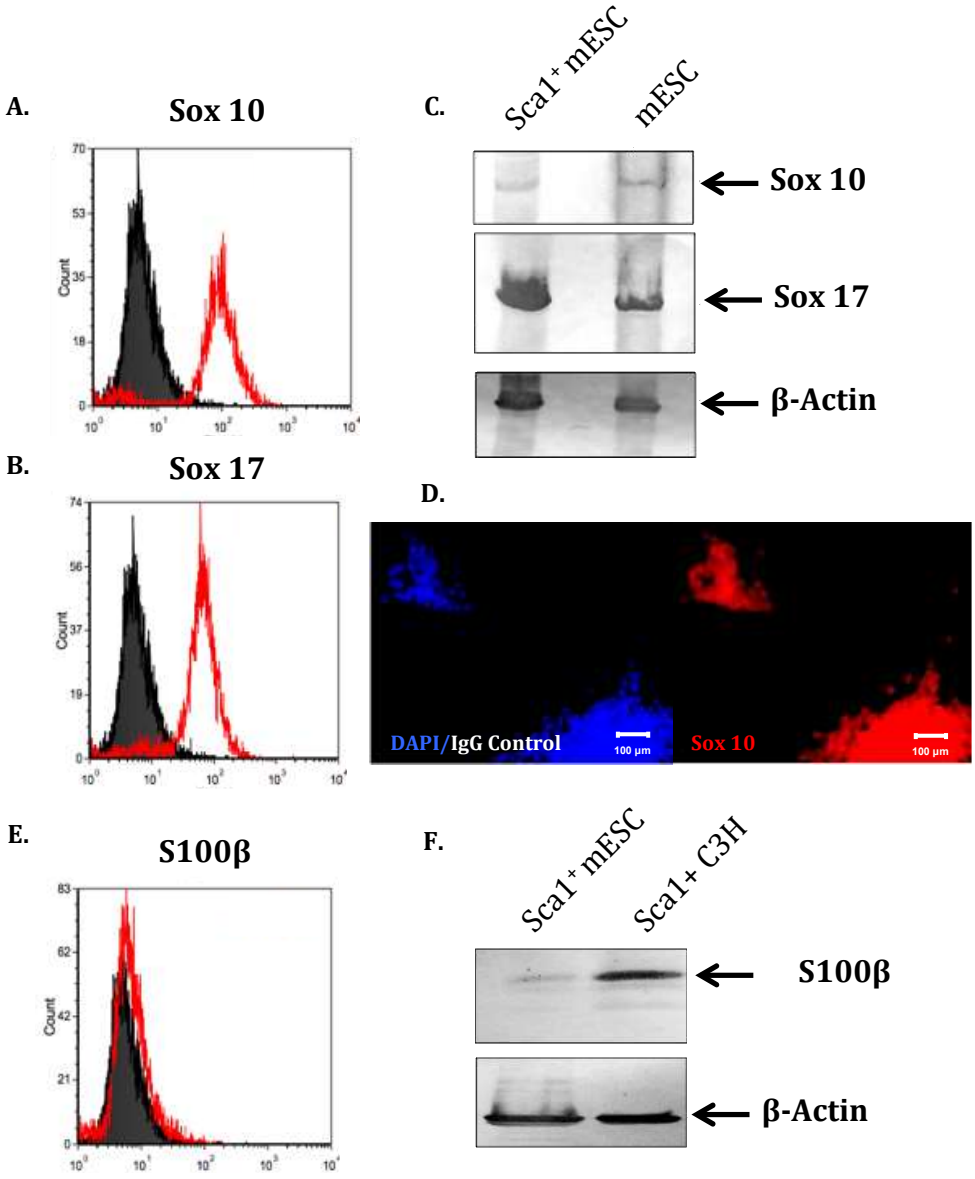

Figure 3.24: Sca1⁺ mESC Express Markers For Neural Stem (Sox 10) and Endodermal and Hematopoietic (Sox 17) But Not Glial Cells (S100β). A: Representative Flow Cytometry analysis of Sca1⁺ mESC labelled with anti-Sox 10 (Black histogram is IgG control, Red is anti-Sox 10) n = 3, B: Representative Flow Cytometry analysis of Sca1⁺ mESC labelled with anti-Sox 17 (Black histogram is IgG control, Red is anti-Sox 17) n = 3, C: Western blot analysis of Sca1⁺ mESC using anti-Sox 10 and anti-Sox 17 antibodies for the detection of Neural Stem and Endodermal and Hematopoietic markers respectively (anti-β-Actin control), D: Representative 20x images of Sca1⁺ mESC were labelled with anti-Sox and DAPI nuclear stain (n ≥ 4). Scale bars represent 100 microns, E: Representative Flow Cytometry analysis of Sca1⁺ mESC labelled with anti-S100β (Black histogram is IgG control, Red is anti-S100β) n = 3, F: Western blot analysis of Sca1⁺ mESC using anti-S100β antibody for the detection of the Glial Cell marker (anti-β-Actin control).

3.2.12 Sca1⁺ mESC Multipotency: Adipogenesis and Osteogenesis

In order to examine whether Sca1⁺ mESC exhibit multipotency, purified cells were treated with adipogenic and osteogenic inductive for prescribed times as outlined in Section 2.6 before differentiation to adipocytes and osteoblasts was assessed by oil red O and alizarin red, respectively to confirm lipid vesicle formation (adipogenic) and calcium deposit formation (osteogenic). Mouse mesenchymal stem cells (mMSC) were treated in a similar manner providing a positive control for both adipogenic and osteogenic differentiation. The mMSC control cells and the Sca1⁺ mESC both exhibited robust adipogenic and osteogenic potential, respectively in vitro (Figure 3.25).

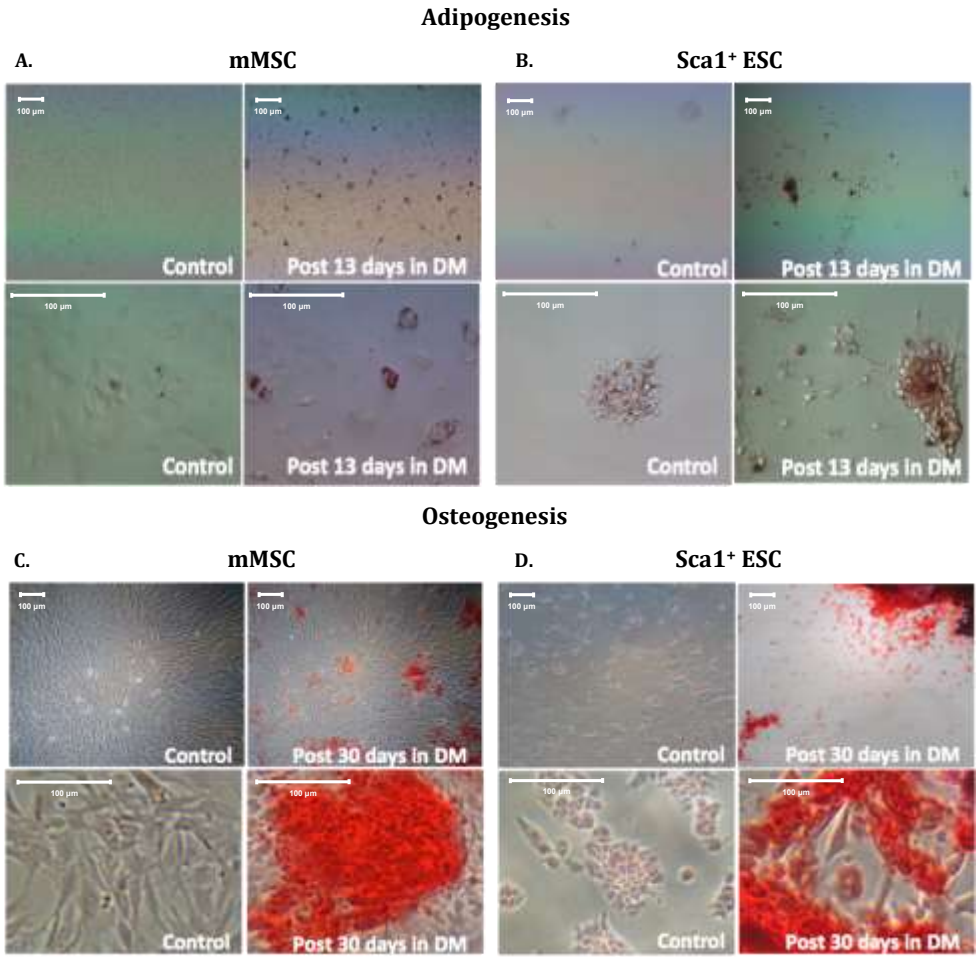

Figure 3.25: Sca1⁺ mESC Display Adipogenic and Osteogenic Potential. A - B: Representative 10x and 40x phase contrast image of mMSC and Sca1⁺ mESC cultured in adipogenic differentiation medium and stained with Oil Red O, (n ≥ 4) C - D: Representative 10x and 40x phase contrast image of mMSC and Sca1⁺ mESC cultured in osteogenic differentiation medium and stained with Alizarin Red, (n ≥ 4). Scale bars represent 100 microns.

3.2.13 Sca1^{+} mESC Multipotency: SMC Generation

In order to examine whether Sca1^{+} mESC exhibit myogenic capacity, purified cells were treated with myogenic inductive medium for prescribed times as outlined in section 2.6 before differentiation to SMCs was assessed by determining the expression of SMC differentiation markers (α-Actin, CNN1 and SMMHC). The definitive presence of SMMHC filaments after 4 – 6 days treatment confirmed that Sca1^{+} mESC can transition and differentiate to SMC. Subsequent flow cytometry and western blot analysis for the SMC markers α-Actin, Calponin 1 and SMMHC further validated Sca1^{+} mESC transition and differentiation to SMC following treatment with vascuolgenic inductive stimuli (Figure 3.26).

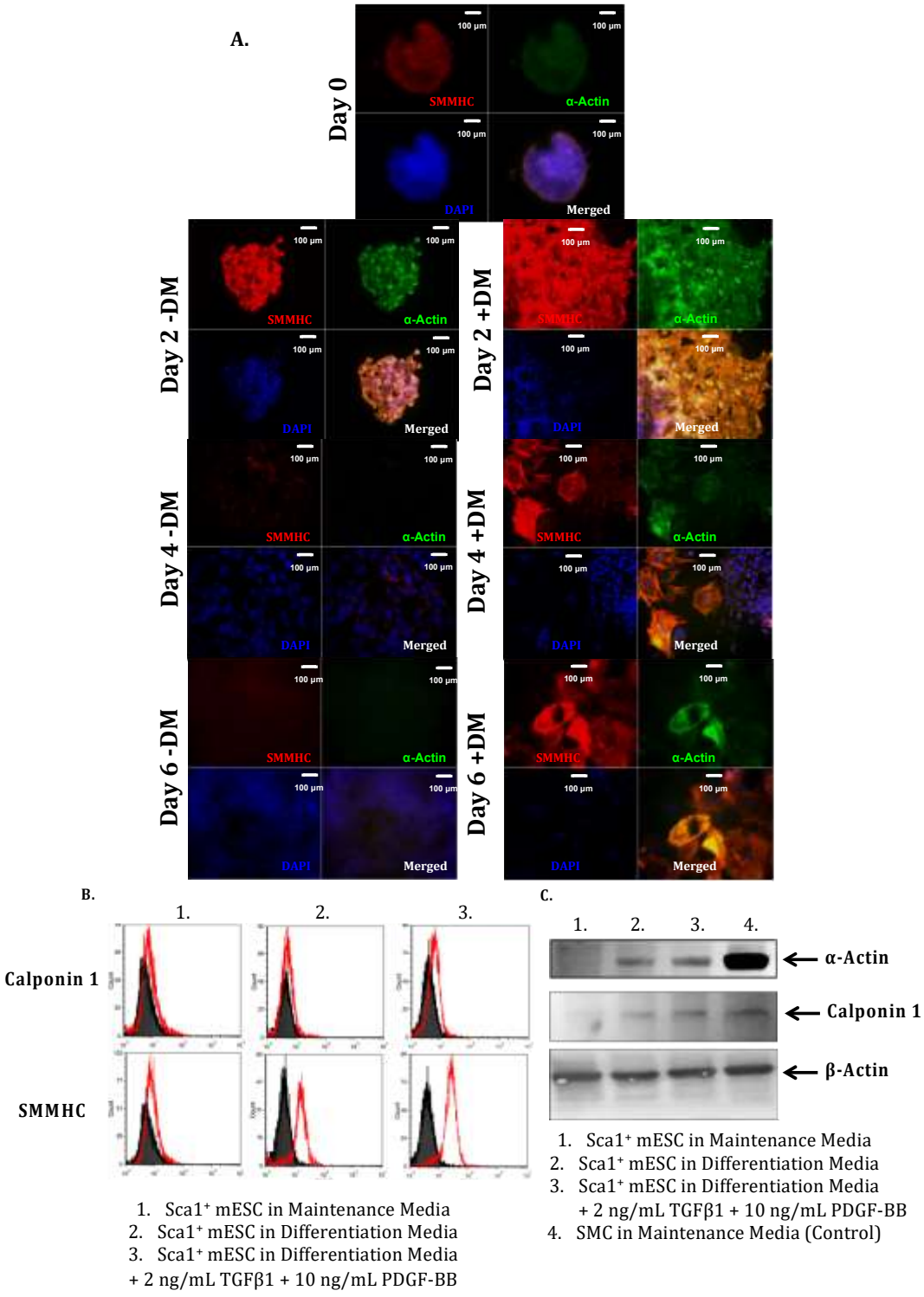

Figure 3.26: Sca1⁺ mESC differentiation to SMC A: Representative images of time course of Sca1⁺ mESC differentiation to SMC using anti-SMMHC and anti-α-Actin antibodies and DAPI nuclear stain, (-DM = Differentiation Media, +DM = Differentiation medium + 2 ng/mL TGFβ1 + 10 ng/mL PDGF-BB) (n ≥ 4), B: Representative Flow Cytometry analysis of Sca1⁺ mESC differentiation to SMC labelled using anti-Calponin 1 and anti-SMMHC antibodies (Black histogram is IgG control, Red is anti-Calponin1/SMMHC) n = 3, C: Western blot analysis of Sca1⁺ mESC differentiation to SMC using anti- α-Actin and anti-Calponin 1 antibodies for the detection of the SMC/pericyte and early SMC markers respectively (anti-β-Actin control). Scale bars represent 100 microns.

3.3 Discussion

The following section will discuss all three cell lines individually and culminate following their comparison.

APC

The adventitia has been considered a complex tissue and home to a variety of cell types for nearly two decades. Subsequently there have been proposals put forward of adventitial cells (including vascular myoblasts and fibroblasts) having SMC differentiation capabilities (Shi et al. 1996; Van der Loo and Martin 1997; Shi et al. 1997; Zalewski and Shi 1997 and Hu et al. 2004). However Hu et al., were the first to provide solid evidence of an adventitial progenitor exhibiting vSMC potential, and where $Sca1^+$ APCs have SMC potential both *in vitro* and *in vivo* (Hu et al. 2004). It is worth noting that these authors used enzyme digestion, Sca1 purification and immediate experimentation, and do not report any attempts at explanting, culturing or characterisation of the $Sca1^+$ APC (Hu et al. 2004). Nevertheless, Hu et al., examined the adventitia for Sca1, the stage specific embryonic antigen-1 (SSEA-1), lateral plate mesodermal marker (earliest marker for blood and endothelial cells) Flk1, cardiac stem cell and mast marker c-Kit (also known as CD117), the diverse progenitor/stem cell marker CD34 and the platelet, blood leucocyte and EC marker CD31, and reported adventitial expression of all bar SSEA-1 (Yamashita et al. 2000; Hu et al. 2004; Zhou et al. 2010; Liu and Shi 2012; Sidney et al. 2014; National Centre for Biotechnology Information 2016k).

Since then Klein et al., identified another APC ($CD44^+CD90^+CD34^-CD45^-$ APC) demonstrating multipotency and SMC potential (with TGFβ1 induction) (Klein et al. 2011). Taken together $CD44^+CD90^+$ cells are indicative of a mesenchymal stem cell (CD44 is a cell-surface glycoprotein known to participate in cell-cell interactions, as well as cellular adhesion and migration; CD90 also known as Thy-1 is widely used as a hematopoietic stem cell marker however it is also found in immune and nerve cells) (Ramos et al. 2016; Centre for Biotechnology Information 2016o and Centre

for Biotechnology Information 2016p). Klein et al., show that $CD44^{+}CD90^{+}CD34^{-}$ APC also express the pericyte/SMC marker α-Actin and the neural stem cell marker Nestin (interestingly our results show similar observations (i.e. the presence of a pericyte/SMC (α-$Actin^{+}$) and neural stem cell ($Sox\ 10^{+}$) populations migrating from the adventitia)) (Klein et al. 2011). Unfortunately, they did not assess these multipotent neural stem cell marker expressing mesenchymal APC for Sca1, however regardless, they provide evidence of APC populations with potential for multipotency and contribution to vessel remodelling (Klein et al. 2011).

Nevertheless, there has been limited characterisation of all potential APCs to date, therefore it was decided to characterise explanted APC for pericyte, SMC, neural stem, endodermal, hematopoietic and glial cell markers. Interestingly $Sca1^{+}$ APCs were observed migrating from the adventitial explant, confirming a potential for $Sca1^{+}$ APC migration and/or proliferation. There was no evidence to suggest that APC contained differentiated SMC (as contaminants or otherwise) as they lacked the expression of the key SMC differentiation markers, Calponin 1 and SMMHC. A population of APC express the pericyte/SMC marker α-Actin and additional APC analysis showed marked expression of neural stem, endodermal, hematopoietic and glial cell markers. The expression of neural stem and endodermal markers highlights that APC harbour non-mesodermal progenitor cells (also observed by Klein et al.,), which is important to note considering as mentioned previously (section 1.4.2), the embryonic origin of cells can influence both contribution to disease susceptibility and response to common stimuli (Woyda et al. 1960; Haimovici and Maier 1964; Haimovici and Maier 1971; Topouzis and Majesky 1996; Gadson et al. 1997; Debakey 2000; Nakamura et al. 2006; Tanous et al. 2009; Leroux-Berger et al. 2011; Majesky, Dong and Hoglund 2011 and Klein et al. 2011). Interestingly, Tang et al., showed multipotent vascular stem cells (MVSC) derived from the medial layer express these same markers which raises the intriguing question as to whether medial MVSC and APC derive from a similar origin (Tang et al. 2012).

Investigating surface membrane receptors does not always permit additional probing for intracellular proteins, as permeabilization of the membrane necessary for the detection of the intracellular proteins permanently disrupts membrane structure, i.e. removes or alters surface proteins and/or interferes with surface protein epitope binding (Vernay and Cosson 2013 and Abcam 2016b). In this context, dual probing for Sca1 and other phenotypic markers was not possible at the time.

Additionally, APC explant culture proved to be a challenging task with cells repeatedly becoming senescent prior to establishment of a $Sca1^+$ pure culture. It was hypothesized that the advanced age of the animals (16 months) was the limiting factor, a consequence of obtaining tissue as part of the 3Rs initiative. Another purely practical limitation was the lack of accessible animal tissue therefore there was extended periods of time in between attempts. Despite this, explanted cells were methodically cultured in different medium conditions and fortuitously a cloned $Sca1^+$ APC population was obtained eventually by culturing them in MM2 medium as described in section 2.1.6.

The fact that few laboratories to date have published anything on explanted $Sca1^+$ APC suggests that the adventitial niche contains critical signals for their survival and self-renewal, or that the parental stem cell population is diluted during the culturing process (i.e. other stem cell populations dominate and become established). However, those that have published on $Sca1^+$ APC have already confirmed some interesting phenomenon. Passman et al., examined freshly isolated $Sca1^+$ APC for a number of markers and established that they express Shh signalling markers (including *shh*, *hhip1*, *cdo*, *boc*, *patched 1*, *patched 2*, *smoothened*, *gli1*, *gli2* and *gli3*), the diverse progenitor/stem cell marker *cd34* (also observed by Hu et al. 2004) and platelet derived growth factor β (PDGFβ: PDGFβ is a mitogen (induces cell proliferation)) receptor *cd140b*, but do not express the cardiac stem cell and mast marker *c-kit* (contrary to observation by Hu et al. 2004), the regulatory immune (T- and B-) cell antigen receptor signalling molecule *cd45*, and the monocyte and tissue macrophage scavenger receptor *cd68*

(Meloche et al. 2007; Passman et al. 2008; Sidney et al. 2014; Centre for Biotechnology Information 2016k; Centre for Biotechnology Information 2016l; Centre for Biotechnology Information 2016m and Centre for Biotechnology Information 2016n). Passman et al., also report that during the *in vitro* culturing process, their $Sca1^{+}c\text{-}Kit^{-}CD45^{-}$ APC lost Sca1 expression and began differentiating into SMC (gained Calponin 1 and SMMHC expression) (Passman et al. 2008). Interestingly Shikatani et al., examined $Sca1^{+}CD45^{-}$ APC proliferation *in vitro* (CD45 is a regulatory immune (T- and B-) cell antigen receptor signalling molecule) and observed that proliferating $Sca1^{+}$ APC were predominantly $c\text{-}Kit^{+}$, indicating that c-Kit expression may be a marker for the parental stem cell phenotype (Centre for Biotechnology Information 2016l and Shikatani et al. 2016). Crucially Shikatani et al., also show that $Sca1^{+}$ APC can be differentiated into SMC using TGFβ1; establishing their capability to transition into SMC (Shikatani et al. 2016). Considering that the cloned $Sca1^{+}$ APC population generated during this research retained a proliferative phenotype and did not gain SMC marker expression without induction (see section 4.2 and 4.3), it is likely they too express c-Kit. It is also important to note that Chen et al., also report differentiating $Sca1^{+}$ APC into SMC (significant induction of SMC markers Calponin1 and SMMHC) however they did not clone the cells (which were generated from vein graft arteriosclerosis) and used Collagen IV (Chen et al. 2013). Interestingly, Chen et al., also report concomitant reduction of progenitor cell markers (Sca1, the cardiac stem cell and mast marker c-Kit and the diverse progenitor/stem cell marker CD34) following the differentiation process (Chen et al. 2013). Therefore, there is substantial evidence from both Chen et al., and Shikatani et al., that $Sca1^{+}$ APC have potential to become SMC and hence contribute to the accumulation of SMC observed in vascular remodelling as described in section 1.6 (Chen et al. 2013 and Shikatani et al. 2016).

Intriguingly, Psaltis et al., isolated the previously unstudied $Sca1^{+}CD45^{+}$ APC subpopulation and showed that they can be differentiated towards macrophage or dendritic cells using macrophage colony-stimulating factor

or granulocyte macrophage colony-stimulating factor and interleukin-4 respectively, indicating that a population of $Sca1^+$ APC (they report aortic $Sca1^+CD45^+$ APC accounts for 35.9 ± 4.7 % of total aortic $Sca1^+$ APC) has potential to become immune modulating cell types (Psaltis et al. 2014). Psaltis et al., also provide evidence that indicates arterial macrophage colonies are not derived from monocytes (consistent with other recent publications) but locally maintained resident $Sca1^+CD45^+$ APC, and concludes that the adventitia is enriched with macrophage progenitors (responsible solely for the maintenance of the adventitia) that originate from $Sca1^+CD45^+$ APC (Jenkins et al. 2011; Schulz et al. 2012; Hashimoto et al. 2013 and Psaltis et al. 2014). Therefore, it is a possibility that the cloned $Sca1^+$ APC generated during this study may also be of the macrophage progenitor $Sca1^+CD45^+$ APC subpopulation. However, it is more likely that they are $Sca1^+CD45^-$ considering $Sca1^+CD45^-$ APC are previously known to have SMC potential but not hematopoietic, and upon induction (see section 4.2 and 4.3) the cloned $Sca1^+$ APC generated during this research acquired SMC markers. Nevertheless, it is possible that some of the originally identified $Sca1^+$ APC may be the macrophage progenitor $Sca1^+CD45^+$ APC subpopulation (however not confirmed).

C3H

Previous studies investigated the molecular mechanisms behind the SMC differentiation process and have all shown that C3H have vSMC potential (Hirschi et al. 1998; Yoshida et al. 2003 and Brunelli et al. 2004). However, none of these papers shed any light on whether or not the C3H cell line (despite recommendation) is an appropriate model of choice for assessing resident stem differentiation to vSMC, and the question of their validity still remains (Xie et al. 2011). The aim to characterise the C3H cell line begins to address this question. Interestingly, C3H are ≥ 80 % Sca1 positive without any Sca1 enrichment through EasySep™ purification and protein analysis by flow cytometry and western blot analysis shows that these cells are positive for pericyte, SMC, glial, neural stem, mesodermal, endodermal and hematopoietic cell markers. C3H are considered a “mesoderm-derived

model" however the fact that they also express neural stem and glial markers brings this into question (Pinney and Emerson 1989; Kubo 1991 and Xie et al. 2011). Prior to assessment of C3H response to Hh signalling, confirmation of C3H differentiation to vSMC was conducted. It is noteworthy to point out that neural stem and mesodermal markers were maintained following the vSMC differentiation process and that the glial cell marker was lost.

mESC

Embryonic (mESC) derived progenitors are also recommended as a model for investigating the differentiation of resident stem cell populations into SMC. As mentioned in section 3.1, the use of mESC prevents any lineage bias associated with experimenting on cells-derived from any one given embryonic germ layer.

Xiao et al., were the first to present a method of obtaining $Sca1^+$ mESC (by culturing mESC on collagen IV) and showed that these $Sca1^+$ mESC could be differentiated into EC (Xiao et al. 2006). The group also presented data suggesting that these $Sca1^+$ mESC derived-EC repair damage after an arterial injury (Xiao et al. 2006). They furthered this research and presented data whereby $Sca1^+$ mESC were differentiated into SMC (SMC induction lead to over 95 % SMC marker expression) (Xiao et al. 2007). Therefore, following evidence that $Sca1^+$ mESC could be differentiated into the vascular lineage, it was decided that the first aim would be to replicate $Sca1^+$ mESC production. Immunocytochemical analysis of the temporal expression of Sca1 showed the optimal time frame for $Sca1^+$ mESC cell generation to be 4/5 days. Flow cytometry analysis showed this generation process results in ~11 % of the population expressing the antigen of interest (similar to data presented by Xiao et al. 2006 and Xiao et al. 2007) which can be purified to ≥ 95 % purity on a routine basis. As mentioned in the case of the C3H, the $Sca1^+$ mESC have also not been previously characterised either (apart from their ability to differentiate into EC and SMC). Therefore prior to initiating further experimentation on this cell line,

the Sca1⁺ mESC were characterised for their stem cell profile and their multipotency. Phase contrast images show that the Sca1⁺ mESC cells can grow as 3D spheroids in the absence of gelatin, or as a clustered monolayer in its presence, proving anchorage independence (a characteristic of stem cells) (Welte et al. 2010). Protein analysis by flow cytometry and western blot show they are negative for differentiated SMC makers and the glial cell marker S100β, however they are positive for the neural stem, neuroectodermal, endodermal and hematopoietic cell markers. Sca1⁺ mESC cells are multipotent, as shown by their adiopogenic, osteogenic and SMC lineage potential.

Cell Lines Comparison

Cell Marker	Cell Line	+/-	Cell Line	+/-	Cell Line	+/-
Sca1 Stem Cell	APC	+	Sca1⁺ C3H	+	Sca1⁺ ESC	+
α-Actin Pericyte/SMC	APC	+	Sca1⁺ C3H	+	Sca1⁺ ESC	-
Calponin 1 Early Differentiated SMC	APC	-	Sca1⁺ C3H	+	Sca1⁺ ESC	-
SMMHC Differentiated SMC	APC	-	Sca1⁺ C3H	+	Sca1⁺ ESC	-
Sox 10 Neural Stem Cell	APC	+	Sca1⁺ C3H	+	Sca1⁺ ESC	+
Sox 17 Endodermal and Hematopoietic Cell	APC	+	Sca1⁺ C3H	+	Sca1⁺ ESC	+
S100β Glial Cell	APC	+	Sca1⁺ C3H	+	Sca1⁺ ESC	-
Nestin	APC	?	Sca1⁺	+	Sca1⁺	+

Neural Stem Cell			C3H		ESC	
Pax 6 Neuroectodermal	APC	?	Sca1⁺ C3H	+	Sca1⁺ ESC	+
Pax 1 Mesodermal	APC	?	Sca1⁺ C3H	+	Sca1⁺ ESC	?

Table 3.2: Cell line characterization study summary

Sca1⁺ mESC display the following similarities to APC (negative expression of early differentiated SMC and differentiated SMC markers; positive expression of neural stem and endodermal and hematopoietic cell markers) there are two dissimilarities known so far (expression of pericyte/SMC and glial cell markers). Sca1⁺ mESC and Sca1⁺ C3H display the following similarities (positive expression of neural stem, neuroectodermal and endodermal and hematopoietic cell markers) and dissimilarities (expression of pericyte/SMC, early differentiated SMC, differentiated SMC and glial cell markers) (Table 3.2). Sca1⁺ C3H display the following similarities to APC (positive expression of pericyte, neural stem, glial and endodermal and hematopoietic cell markers) and dissimilarities (expression of early differentiated SMC and differentiated SMC) (Table 3.2).

Due to the aforementioned issues involving the procurement of a Sca1⁺ APC cell line, characterisation of these cells was not possible due to time constraints. However, despite the fact that Sca1⁺ mESC and Sca1⁺ C3H are not comparable with each other, both have merits for comparison to APC. Based on these characterization studies, the cell line most appropriate as the cell line for mimicking APC in the Hh studies going forward was the Sca1⁺ C3H. Sca1⁺ C3H cells have the added advantage of being more convenient to culture and are Sca1⁺ without manipulation.

3.4 Conclusion

The generation and characterization of all three Sca1⁺ cell lines provide important insights into the variable expression profiles of each cell line. Interestingly the SMC characterization analysis of Sca1⁺ APC shown here corroborates with Hu et al., reporting that Sca1⁺ APC do not express

differentiated SMC marker expression (SMMHC). Our stem cell marker analysis also confirms work done by Hu et al., that Sca1$^+$ APC show significant stem cell marker expression, and that Sca1$^+$ APC may be a non-mesodermal progenitor cell type considering neural stem cell marker profile (also observed by Klein et al., in APC) (Hu et al. 2004 and Klein et al. 2011). The similar expression profiles between Sca1$^+$ APC and the multipotent vascular stem cells (MVSCs) described by Tang et al., also alludes to the possibility that medial MVSC and Sca1$^+$ APC derive from a similar origin (Tang et al. 2012). Also, going forward, Sca1$^+$ C3H will be the model cell line of choice for any Hh signalling studies considering its comparable characteristics and robust culturing nature.

Chapter 4

Hedgehog Control of Sca1^{+} Cell Renewal and Differentiation *In Vitro*

4.1 Introduction

4.1.1 Rationale

Hedgehog Signalling in Stem Cells

Several factors have been described as positive and negative regulators of stem cell self-renewal and differentiation. Most of the hematopoietic cytokines studied promote either survival or differentiation or both in hematopoietic stem cells *ex vivo*, whereas morphogens (Wnt, Notch, and Hedgehog) signify a class of hematopoietic stem cell regulators that support expansion of the hematopoietic stem cell pool by a combination of survival and induced self-renewal (Zon et al. 2001).

Hedgehog (Hh) is one key morphogen regulating embryonic development and tissue repair that has been shown to govern adult stem cell fate (Briscoe et al., 2013). While embryonic Hh signalling controls cell patterning and differentiation, Hh has been shown to promote stem cell self-renewal and differentiation. The following studies are just some of those that describe this phenomenon.

Hh signalling and neural stem cell regulation is apparent as Shh is expressed at birth in two key neurogenic regions: hippocampus and lateral ventricle wall (Favaro et al. 2009). It has previously been reported that neural stem cells in the lateral ventricles subventricular zone and hippocampal subgranular zone respond to Shh activity (Ahn and Joyner 2005). They also show that $Sox2^{+}$ neural stem cells are surrounded by Shh, and that in $Sox2^{-}$ null mutant mice, Shh expression is also lost (Favaro et al. 2009).

Shh has been shown to promote anaplastic thyroid cancer stem cell self-renewal, and interestingly, nicotine has been shown to induce the production of Shh in pancreatic cancer stem cells which in turn induces their self-renewal (Heiden et al. 2014 and Al-Wadei et al. 2016). Shh has also been shown in cerebellar granule cell precursors to promote proliferation and inhibit differentiation, and Shh has also been demonstrated to maintain self-renewal capacity in murine midbrain neural stem cells (Wechsler and Scott

1999; Argenti et al., 2005; Doe et al. 2008 and Martinez et al. 2013). Yu et al., have also suggested that Shh establishes and/or maintains ureteral subepithelial mesenchymal stem cells by actively inhibiting their differentiation into urethral SMC (Yu et al. 2002). Interestingly however Agathocleous et al., has suggested that Shh might promote stem cell transition to an activated proliferative population of progenitors rather than strictly induce self-renewal (Agathocleous et al. 2007). Other studies have shown that Shh induces differentiation. For example rats treated with Shh expressing bone marrow stem cells recover significantly better following spinal cord injury (Jia et al. 2014). Shh has also been shown to activate retinal stem cells resulting in retinal regeneration following removal (Spence et al. 2004). Shh also promotes bone marrow derived mesenchymal stem cell proliferation and chondrogenic differentiation, and Shh has also been shown to promote cementoblastic (peridonal progenitor) differentiation (Wazecha et al. 2006 and Bae et al. 2016).

Hedgehog (Hh) Signalling in SMC

Static rat SMC *in vitro* express key Hh signalling components Shh, Patched 1, Smoothened and Gli 2 (both protein and mRNA), and immunocytochemistry analysis has demonstrated that Shh is localized in the cytoplasmic space and native Patched 1 is localized in intracellular lysosomes (as indicated by the discrete vesticular pattern) (Morrow et al. 2007). Morrow et al., also reported that Shh induces Hh signalling activation and stimulates SMC proliferation as well as reduces apoptotic nuclei levels, all of which are attenuated following the addition of the Hh inhibitor cyclopamine (Morrow et al. 2007). Importantly, in a follow up study, Morrow et al., confirmed their previous evidence that Shh induces Hh signalling activation and increases SMC growth and survival in SMC *in vitro* (Morrow et al. 2009). In both reports Bax and Bcl-X_L (apoptosis mediators) were assessed and it was observed that Shh induced a significant increase in Bcl-X_L (prosurvival) while concurrently decreasing Bax (proapoptotic) mRNA and protein levels

(Morrow et al. 2007; Morrow et al. 2009 and Westphal et al. 2010). Interestingly, they also found that Shh induced Notch target gene expression through vascular endothelial growth factor A (VEGF-A – Hh target gene), and that Shh induced effects were attenuated using Notch inhibitors and the Hh inhibitor cyclopamine *in vitro* (Nakagawa et al. 2000 and Morrow et al. 2009).

Hh signalling activation has also been found to induce cellular proliferation by Li et al., who used platelet-derived growth factor (PDGF), a known stimulus for vSMC proliferation and intimal formation, to treat cultured primary human vSMC (Li et al. 2010). They observed the upregulation of key Hh target genes (Shh, Patched 1 and Gli 2), and subsequently assessed the effect of Hh inhibition (using cyclopamine and lentivirus-*Gli 2* siRNA) on PDGF treated SMC. Importantly, Hh signalling inhibition resulted in markedly lower human vSMC numbers (50 % reduction in cyclopamine, and 54 % reduction in lentivirus-*Gli 2* siRNA treated cells), which was confirmed by BrdUrd incorporation assay analysis (53 % reduction in cyclopamine, and 56 % reduction in lentivirus-*Gli 2* siRNA treated cells), and cellular proliferation using Ki-67 was also significantly reduced (Li et al. 2010). Crucially, they also showed that Hh signalling activation (using Shh or *Gli 2* cDNA) resulted in the complete opposite (marked increase in cell proliferation (60 % increase in Shh, and 67 % increase in *Gli 2* cDNA treated cells), which was confirmed by BrdUrd incorporation assay analysis (42 % increase in Shh, and 39 % increase in *Gli 2* cDNA treated cells). Cellular proliferation using Ki-67 was also significantly increased (Li et al. 2010). It is also crucial to highlight that human vSMC treated with Shh or *Gli 2* cDNA without prior PDGF stimulation, have increased Ki-67 expression levels comparable to PDGF stimulated cells, supporting the conclusion that Shh/Gli 2 promotes mitogenic activity in human vSMC (Li et al. 2010). Additionally, Li et al., reported that inhibition of Shh/Gli 2 signalling interfered with the cell cycle (prevented G_1-S transition resulting in G_1 arrest) with reduced cyclin D1 levels; knockdown of cyclin D1 also abolished Shh induced human vSMC proliferation (Li et al. 2010).

Interestingly, Hh signalling has also been observed to be activated in human pulmonary artery SMC (hpaSMC) and induced proliferation in response to hypoxia. SMC wrapping/layering in the development of neovessels have been shown to be driven by Shh induced upregulation of platelet-derived growth factor (PDGF - a known stimulus for vSMC proliferation and intimal formation) (Wang et al. 2010; Li et al. 2010 and Frontini et al. 2011).

Critically, it has also been demonstrated that the key Hh activation components (Patched 1 and Gli 2), Notch and VEGF-A are upregulated during vascular remodelling *in vivo*. It is also important to note that Patched 1 expression is limited to the adventitia, and there is little to no Gli 2 expression in uninjured vessels. However, during vascular remodelling, there is a significant increase in adventitial and neointimal Patched 1 and Gli 2 expression (Morrow et al. 2009).

Interestingly, it has also been reported that cyclic strain (mimetic of hemodynamic force) analysis on SMC *in vitro* induces a significant decrease in SMC cell number (observed 10 days post treatment), a significant increase in apoptotic nuclei, concomitant with an increase in Bax (proapoptotic protein) and a decrease in Bcl-X_L (prosurvival protein). Most importantly, a significant reduction in key Hh signalling target proteins and genes (Shh and Patched 1 protein and mRNA, and Smoothened and Gli 2 mRNA levels) was found (Morrow et al. 2007). Following this, Shh treatment significantly recovers (increases) strain induced Hh target levels, increases cellular levels of proliferation cell nuclear antigen (PCNA – cell proliferation protein), and decreases the number of apoptotic nuclei (detected by annexin V/propidium iodide analysis by flow cytometry) (Morrow et al. 2007).

Hedgehog (Hh) Signalling in Intimal Cells

Key Hedgehog signalling components in restenotic (remodeling) vessels 2 weeks post vein grafting have also been examined. Li et al., reported a significant increase in Shh, Patched 1 and Gli 2 protein levels during vascular remodelling in comparison to control vessels, confirming that Hh signalling is

activated in remodelling (restenotic) vessels (Li et al. 2010). Additionally they suggest that Shh/Gli 2 may promote proliferation from their observation that Shh/Gli 2 signalling coincides with increased proliferating cell nuclear antigen (PCNA) in remodelling vessels (Li et al. 2010).

Daniels et al., also reported that Shh signalling is crucial to neointimal formation as inhibition of Shh signalling impedes perivascular cell signalling (and differentiation) and prevents neointimal formation (Daniel et al. 2013). This conclusion was formed following examination of their wire-mediated induced vascular remodelling. They observed significant increases in Shh in neointimal SMC and Sca1$^+$ perivascular stem cells 4 and 7 days post injury (by both immunohistochemistry and mRNA analysis). Daniels et al., also applied a Shh inhibitor (GCD-0449) using pluronic gel to vessels following injury and observed that treatment resulted in a significant reduction of neointimal formation as well as a significant reduction in the accumulation of adventitial Sca1$^+$ cells (Daniel et al. 2013).

Based on the aforementioned studies, it was important to understand the role of Hh signalling in dictating Sca1$^+$ stem cell fate *in vitro.*

4.1.2 Strategy: Addressing Thesis Aim 2: Evaluate Hedgehog Control of Sca1$^+$ Cell Renewal and Differentiation In Vitro

The strategy was to use 3 different Sca1$^+$ stem cells (APCs, C3H and ESC-derived Sca1 cells) and determine (i) whether Hh signalling components were present in these cells (ii) whether activation of Hh signalling with Shh resulted in increases in Hh target gene expression before assessing whether this promoted myogenic differentiation and/or maintenance of stemness.

Western blot analysis was used to assess if Sca1$^+$ APC express Shh and its receptor Patched 1 prior to assessing them for Hh responsiveness.

Sca1$^+$ APC responsiveness to Hh signalling was investigated in the following culture conditions:

- Maintenance medium control – contained embryonic qualified FBS (does not induce differentiation of embryonic stem cells)
- Differentiation medium control – non embryonic qualified FBS
- Differentiation medium + recombinant Shh
- Differentiation medium + recombinant Shh + Hh signalling inhibitor (cyclopamine – Smoothened inhibitor)

Based on previous studies of the Hh signalling pathway, Shh treatment had potential to induce the following responses (Briscoe and Thérond 2013):

1. Stem cell maintenance – prevent stem cell niche depletion
2. Proliferation/differentiation
3. Have no effect

To address the question of Shh inducing stem cell maintenance, the telomerase activity of each medium culture type was assessed. Telomerase activity levels serve as a marker for "stemness" with activity occurring exclusively in stem cells (Skvortsov et al. , 2011). To assess if Shh induced differentiation of $Sca1^+$ APC to SMC, mRNA levels and protein expression of the SMC marker Calponin 1 were assessed by qRT-PCR and immunocytochemistry respectively. Immunocytochemistry images were also used to assess if Shh treatment induced proliferation by means of nuclei quantification following DAPI staining. Additionally, to assess if Shh treatment activated Hh signalling, *Gli 1* mRNA levels (constitutive activator of Hh signalling) were assessed by qRT-PCR.

$Sca1^+$ C3H

Western bot analysis was used to assess if $Sca1^+$ C3H express Shh and its receptor Patched 1 prior to assessing them for Hh responsiveness.

$Sca1^+$ C3H responsiveness to Hh signalling was investigated in the following culture conditions:

- Maintenance medium control – contained embryonic qualified FBS (does not induce differentiation of embryonic stem cells)

- Differentiation medium control – non embryonic qualified FBS
- Differentiation medium + recombinant Shh
- Differentiation medium + recombinant Shh + Hh signalling inhibitor

To address the question of Shh inducing maintenance of the stem cell population, the Sca1 profile and telomerase activity of each medium culture type was assessed. The maintenance or loss of the Sca1 antigen would be indicative of change but telomerase activity serves as a marker for "stemness", and so would provide significant evidence towards elucidating this issue.

In parallel studies to the assessment of stem cell maintenance, the effect of Shh treatment on downstream Hh signalling was established along with the assessment of various potential Hh signalling inhibitors. Downstream Hh signalling was assessed by relative quantification of the following Hh signalling target genes by qRT-PCR:

1. Hh signalling activator: *Gli 1* mRNA
2. Hh signalling activator and repressor: *Gli 2* mRNA
3. Hh signalling repressor: *Gli 3* mRNA

Critically, blockade of Hh signalling target gene expression using Hh signalling specific inhibitors would substantiate any effects observed with recombinant Shh and confirm that the changes were as a result of Hh signalling thereby providing controls for future experiments. Additionally, the identified inhibitors could also become potential prototype therapeutic agents to target recapitulation of Hh signalling within the vessel wall during disease progression (intimal formation).

A range of potential and known Hh signalling specific inhibitors were investigated and are outlined below:

1. Cyclopamine – A steroidal alkaloid (small molecule) that blocks Hh signalling by directly binding the signal transducer Smoothened (Chen et al. 2002).

2. HPI 4 – Another small molecule inhibitor; acts downstream of Smoothened and is hypothesized disrupt Gli 1/2 activity (processing and stability) through perturbation of ciliogenesis (Firestone et al. 2012 and Xiang et al. 2014).
3. Recombinant Hedgehog Inhibitory Protein 1 (Hip-1) – Downstream Hh signalling target involved in negative-feedback; competitively binds Hh signalling ligands to prevent binding to Patched 1 receptor and signal activation (Holtz et al. 2013).
4. An anti-Patched 1 antibody – potential Hh signalling inhibitor by competitively binding the Patched 1 receptor and preventing Hh signalling activation, however may also activate Hh signalling or have no effect at all. In 2007 Nakamura et al. reported Hh inhibition using rabbit derived antibodies produced after exposure to a custom made oligo-peptide antigen containing the amino acid sequence KADYPNIQH of the Patched 1 receptor (Nakamura et al. 2007). Bioinformatic analysis of this sequence indicated the sequence to be amino acids 809 – 817. Similar analysis of commercially available antibodies showed two possible candidate antibodies, Abcam's ab55629 which was raised against amino acid sequence 841 – 941 and Abnovas H00005727-M02 raised against amino acid sequence 841 – 940.
5. An anti-Shh antibody – a Hh signalling inhibitor by competitive neutralization of Shh preventing Shh activation of the Hh signalling pathway.

Sca1$^+$ mESC

To address the question of Shh inducing maintenance of the stem cell population, the preservation/maintenance of Sca1 expression was assessed. This involved investigating the effects of differentiation medium and serum concentrations on the number of Sca1$^+$ cells in a population before assessing the effect of Shh treatment.

4.2 Results

4.2.1 Native Hedgehog Components - Expression in Sca1⁺ APC

Once a pure population of Sca1⁺ APC was established, the cells were assessed by western blot for the hedgehog signalling components, namely the proteins Shh and Patched 1. The presence of the Hh signalling ligand, Shh and its corresponding receptor Patched 1 was confirmed (Figure 4.1). Shh was detected in the conditioned culture medium and Patched 1 receptor was detected in the cell lysate.

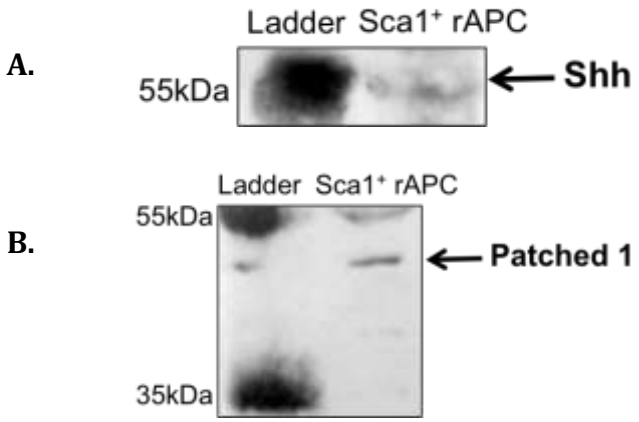

Figure 4.1: Sca1⁺ APC express the Hedgehog Signalling Components, Shh and Patched 1. A: Western blot analysis of Sca1⁺ APC using an anti-Shh antibody for the detection of the Hh signalling ligand Shh in the conditioned media, B: Western blot analysis of Sca1⁺ APC cell lysates using an anti-Patched 1 antibody for the detection of the Hh signalling receptor Patched 1.

4.2.2 Sca1⁺ APC Hh Responsiveness: Shh stimulation of Hedgehog target gene Gli 1 mRNA levels

Since key native hedgehog signalling components are present in Sca1⁺ APCs, the effect of Shh treatment on Gli 1 (constitutive Hh signalling activator) mRNA levels was assessed by real-time qRT-PCR. It was confirmed that Shh increased Gli 1 mRNA levels after 24 hrs, an effect that was blocked by co-treatment of cells with the Hh signalling inhibitor cyclopamine (Smoothened antagonist) (Figure 4.2).

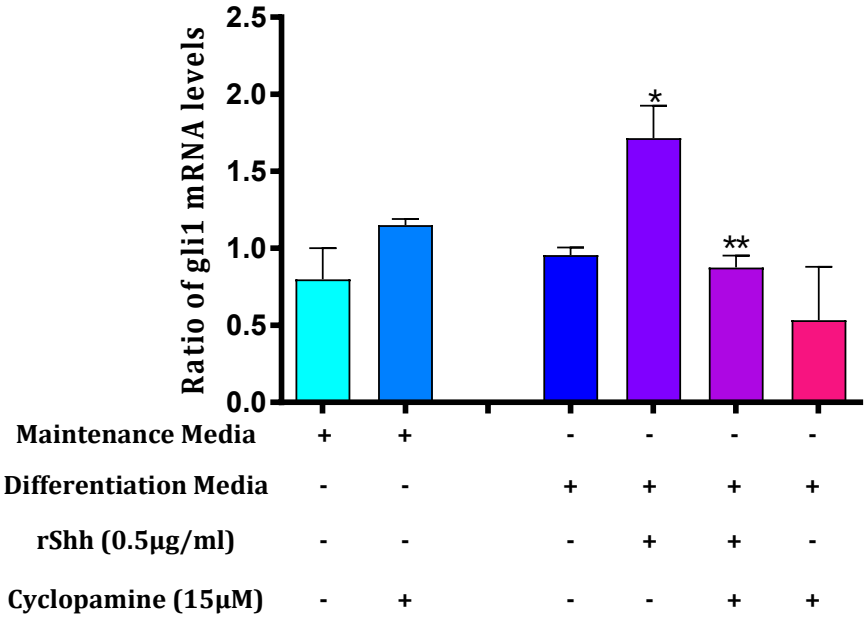

Figure 4.2: The effect of Shh on *Gli 1* (Hh signalling activator) mRNA levels in Sca1⁺ APC in the absence or presence of a Hh inhibitor. qRT-PCR analysis of *Gli 1* mRNA levels. n = 3, one-way ANOVA statistical analysis result: * p = 0.034, **: p = 0.0060.

4.2.3 Sca1⁺ APC Stem Cell Maintenance Analysis: Shh treatment does not increase telomerase activity, however blocking Hh signalling using cyclopamine prevents the media-associated reduction in telomerase activity

As Sca1⁺ APC express the Hh signalling components Shh and Patched 1 to promote Gli 1 expression, the effect of recombinant Shh treatment on telomerase activity ("stemness") was assessed. Telomerase activity analysis was performed on cells cultured in maintenance media, differentiation medium and differentiation medium in the presence of Shh (500 ng/ml) with or without cyclopamine (15µM) for 9 days. There was a significant decrease in telomerase activity upon treatment of APCs with SMC differentiation media, when compared to cells grown in maintenance medium for 9 days (Figure 4.3). However, there was no significant difference between differentiation medium with and without recombinant Shh treatment. In contrast, there was a significant increase in telomerase activity in cells treated with Shh in the presence of cyclopamine when compared with differentiation medium alone and differentiation medium with Shh, indicating that inhibition of Hh signalling increases "stemness" (Figure 4.3).

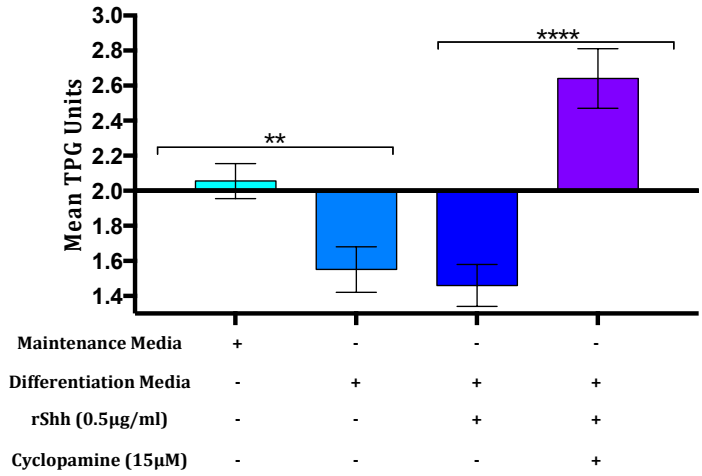

Figure 4.3: The effect of Shh on telomerase activity in Sca1 APCs. Telomerase activity was measured in APCs in the absence or presence of rShh (0.5µg/ml) with or without Cyclopamine (15µM) after 9 days using the TRAPEZE® XL Telomerase Detection Kit. n = 3, one-way ANOVA statistical analysis result: **: $p = 0.007$, ****: $p < 0.0001$.

4.2.4 Sca1$^+$ APC Proliferation/Differentiation Analysis: Shh induces SMC marker Cnn1 Expression

As Sca1$^+$ APC express the Hh signalling components Shh and Patched 1 to promote Gli 1 expression and inhibit telomerase activity, the effect of recombinant Shh treatment on stem cell transition and differentiation to SMC was conducted. Shh increases *Cnn1* (SMC marker) mRNA levels compared to the medium alone (Figure 4.4.A), an effect attenuated by cyclopamine. Parallel immunocytochemistry analysis concurs with the mRNA data and demonstrates that Shh induces an increase in the number of Cnn1 positive cells, which is attenuated following treatment with cyclopamine (Figure 4.4.B and C). Shh treatment also increases Sca1$^+$ APC proliferation an effect significantly attenuated by cyclopamine (Figure 4.4.D).

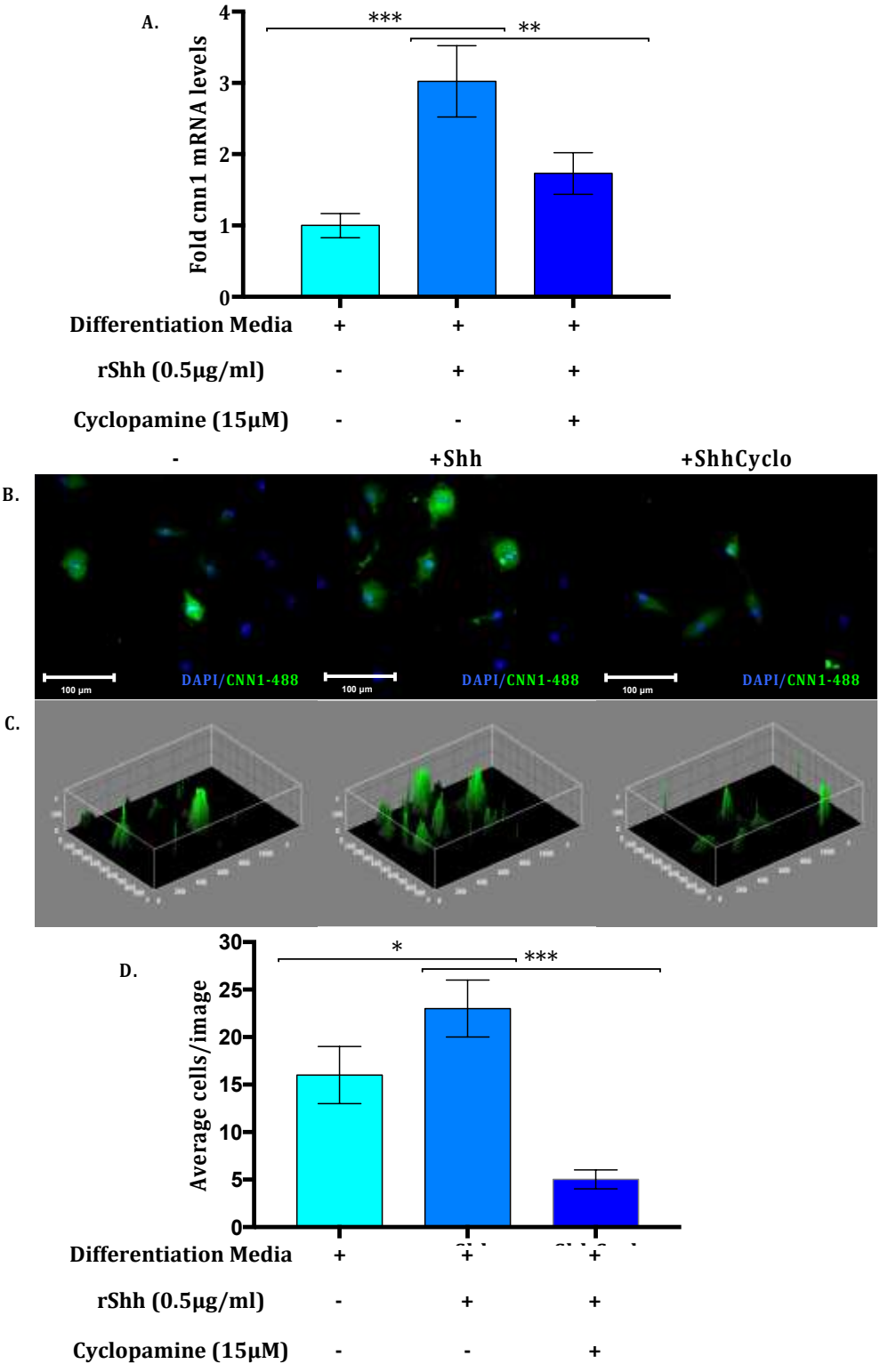

Figure 4.4: The effect of Shh treatment on APC growth and differentiation to SMC. The number of Calponin 1 positive cells was determined by fluorescent immunocytochemistry following treatment of APCs with Shh (0.5µg/ml) in the absence or presence of cyclopamine (15µM) after 9d. A: qRT-PCR analysis of *Cnn1* mRNA levels (n = 3), one-way ANOVA statistical analysis result: ***: p = 0.0009, **: p = 0.0093, B. Representative image of Sca1$^+$ APCs labeled with anti-Cnn1 and DAPI nuclear stain (n ≥ 4), C: 3D plots corresponding to B, D: The number of DAPI nuclei cell/hpf in pre- and post-treated Sca1$^+$ APCs, one-way ANOVA statistical analysis result: *: p = 0.0332, ***: p = 0.0003.

4.2.5 Native Hedgehog Components - Expression in Sca1⁺ C3H/10T1/2

Sca1⁺ C3H also expressed Shh and the Shh receptor, Patched 1. Sca1⁺ C3H cells were assessed by western blot for the hedgehog signalling components. The presence of the Hh signalling ligand, Shh and its corresponding receptor Patched 1 was confirmed (Figure 4.5). Shh was detected in the conditioned culture medium while the Patched 1 receptor was present in the cellular fraction.

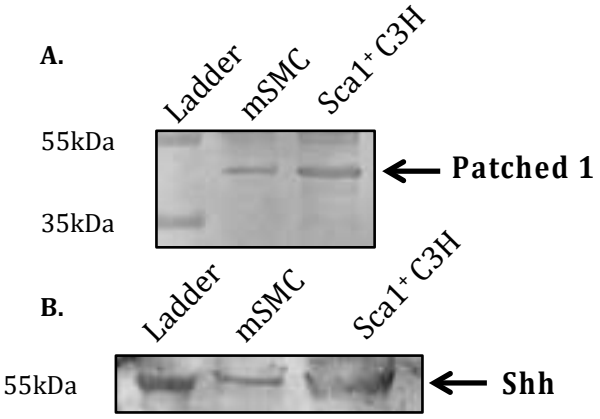

Figure 4.5: Sca1⁺ C3H express the Hedgehog Signalling Components, Shh and Patched 1. A: Western blot analysis of Sca1⁺ C3H using an anti-Patched 1 antibody for the detection of the Hh signalling receptor Patched, B: Western blot analysis of Sca1⁺ C3H using an anti-Shh antibody for the detection of the Hh signalling ligand Shh in the conditioned media.

4.2.6 C3H/10T1/2 (C3H) Cell Line Hh Responsiveness: Shh maintains Sca1 expression and increases telomerase activity (self-renewal/ stem cell maintenance/ "stemness")

The effect of Shh on the self-renewal of Sca1⁺ C3H stem cells was also investigated, and was approached by assessing the effect of Shh on Sca1 expression and telomerase activity. Sca1 expression was assessed in C3H cells maintained in 0.5% serum concentrations in both maintenance medium and non-maintenance medium (differentiation media). However, it was not possible to culture C3H cells in 0.5% serum for extended periods of time. When C3H cells were grown in 10 % serum containing differentiation medium for 48 hrs, there were significant changes to the population of Sca1⁺

cells (Figure 4.6.A). Treatment of C3H cells with low concentrations of Shh (75 ng/mL) in differentiation medium with 10 % FBS for 48 hrs also resulted in a change in Sca1⁺ cells in the Shh treated population in comparison to the untreated cells (Figure 4.6.B). In parallel studies, Shh significantly increased telomerase activity in C3H cells when compared to untreated cells (Figure 4.6.C).

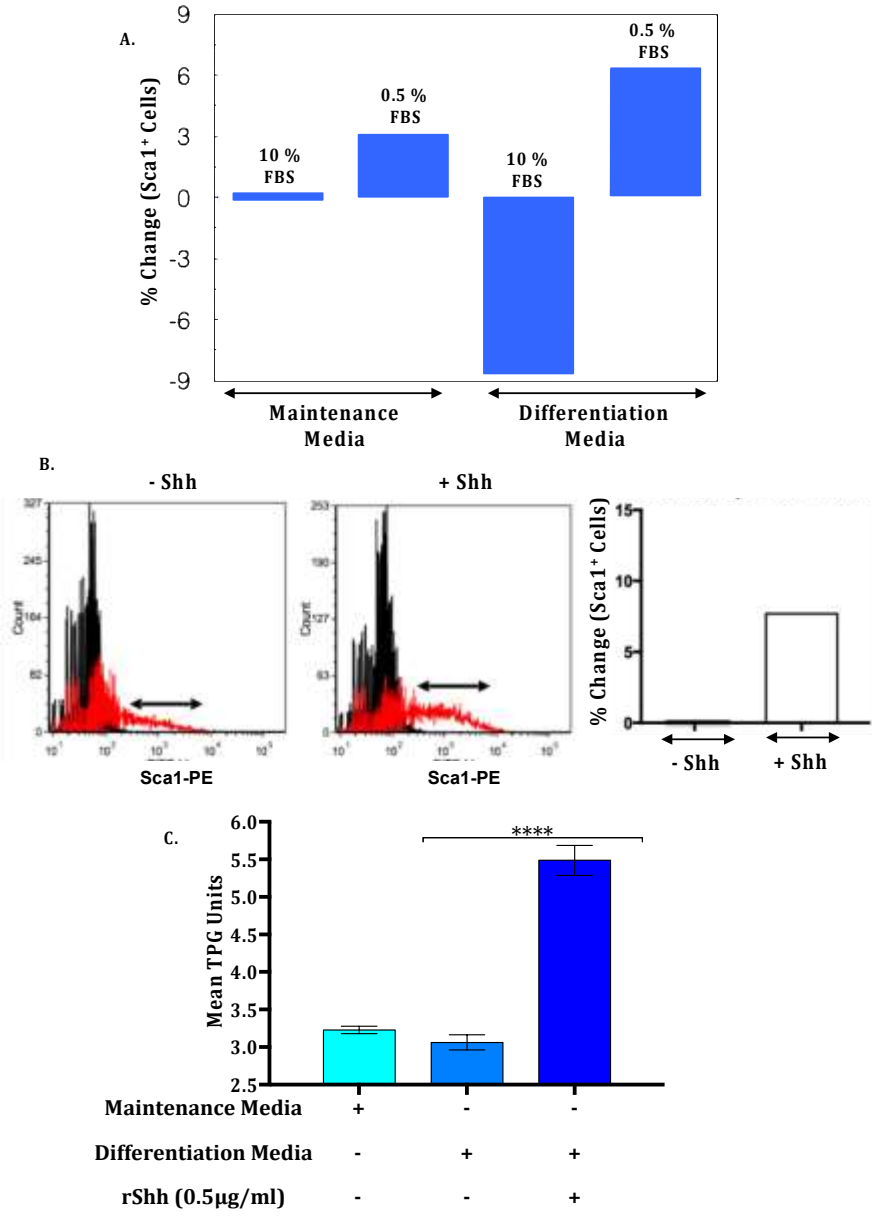

Figure 4.6: Shh Maintains Sca1 Expression and Increases Telomerase Activity ("Stemness") in Sca1⁺ C3H after 24 hrs. A: Graphical representation of Flow Cytometry analysis of C3H Sca1 profile showing C3H Sca1 expression is FBS dependent, B: Flow Cytometry analysis of C3H Sca1 profile with/without 75 ng/mL Shh after 48 hrs in differentiation medium (Black histogram is IgG-PE control, Red is Sca1-PE), C: Telomerase Activity Assay of Sca1⁺ C3H treated with/without 500 ng/mL Shh for 24 hrs. n = 3, one-way ANOVA statistical analysis result: ****: $p < 0.0001$.

4.2.7 C3H/10T1/2 (C3H) Cell Line Hh Responsiveness: Shh stimulation of Hedgehog target gene mRNA levels

The effect of Shh treatment on Gli 1 (constitutive Hh signalling activator) mRNA levels was assessed by real-time qRT-PCR. Shh increased Gli 1 mRNA levels after 24 hrs, an effect that is blocked by co-treatment of cells with the Hh signalling inhibitor cyclopamine (Smoothened antagonist) and an anti-Patched 1 monoclonal antibody (Figure 4.7).

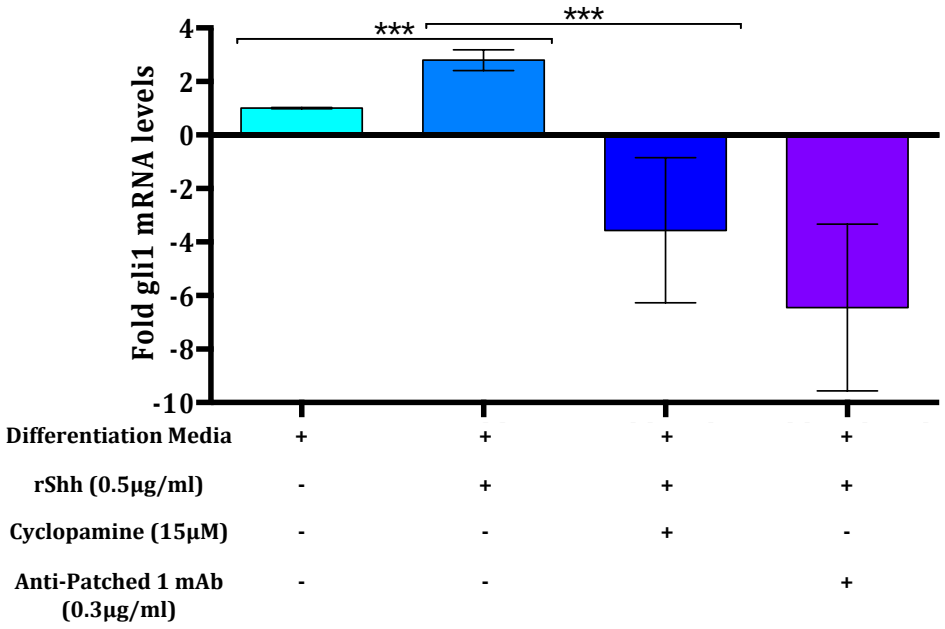

Figure 4.7: The effect of Shh on *Gli 1* (Hh signalling activator) mRNA levels in Sca1⁺C3H cells in the absence or presence of Hh Inhibitors. qRT-PCR analysis of *Gli 1* mRNA levels. n = 3, one-way ANOVA statistical analysis result: ***: $p < 0.001$.

4.2.8 C3H/10T1/2 (C3H) Cell Line Hh Responsiveness: Shh increases the signal activator and repressor Gli 2 mRNA levels which is attenuated by the addition of cyclopamine and an Anti-Patched mAb

The effect of Shh treatment on Gli 2 (Hh signalling activator and repressor) mRNA levels was assessed by real-time qRT-PCR. Shh increased Gli 2 mRNA levels after 24 hrs, an effect that is blocked by co-treatment of cells with the Hh signalling inhibitor cyclopamine (Smoothened antagonist) and an anti-Patched 1 monoclonal antibody (Figure 4.8).

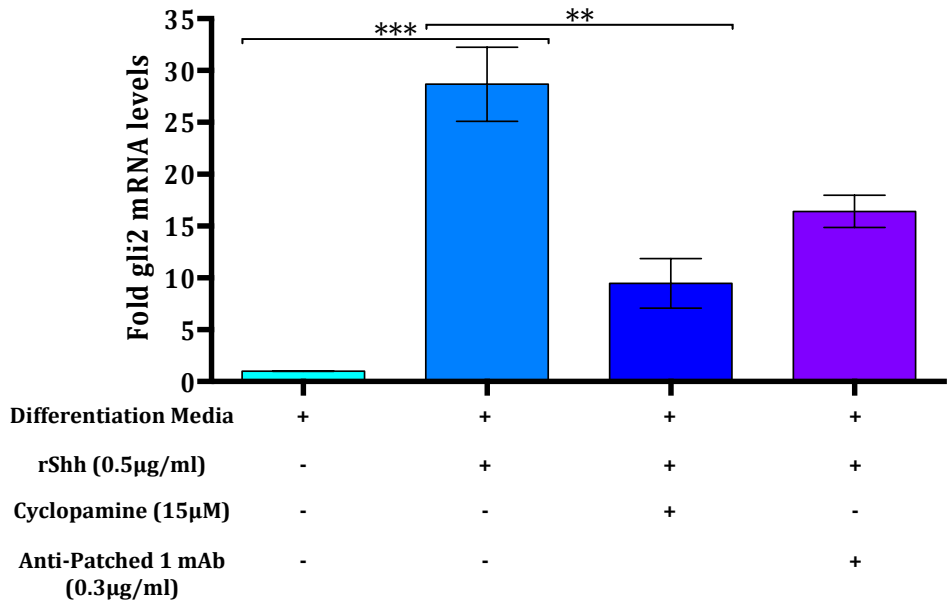

Figure 4.8: The effect of Shh on *Gli 2* (Hh signalling activator) mRNA levels in Sca1⁺ C3H cells in the absence or presence of Hh Inhibitors. qRT-PCR analysis of *Gli 2* mRNA levels. n = 3, one-way ANOVA statistical analysis result: ***: p = 0.00028, **: p = 0.0064.

4.2.9 C3H/10T1/2 (C3H) Cell Line Hh Responsiveness: Shh decreases the signal repressor Gli 3 mRNA levels which is prevented with the addition of cyclopamine but not an Anti-Patched mAb

The effect Shh treatment on Gli 3 (Hh signalling activator and repressor) mRNA levels was assessed by real-time qRT-PCR. Shh decreased Gli 3 mRNA levels after 24 hrs, an effect that is blocked by co-treatment of cells with the Hh signalling inhibitor cyclopamine (Smoothened antagonist) but unaffected by the anti-Patched 1 monoclonal antibody (Figure 4.9).

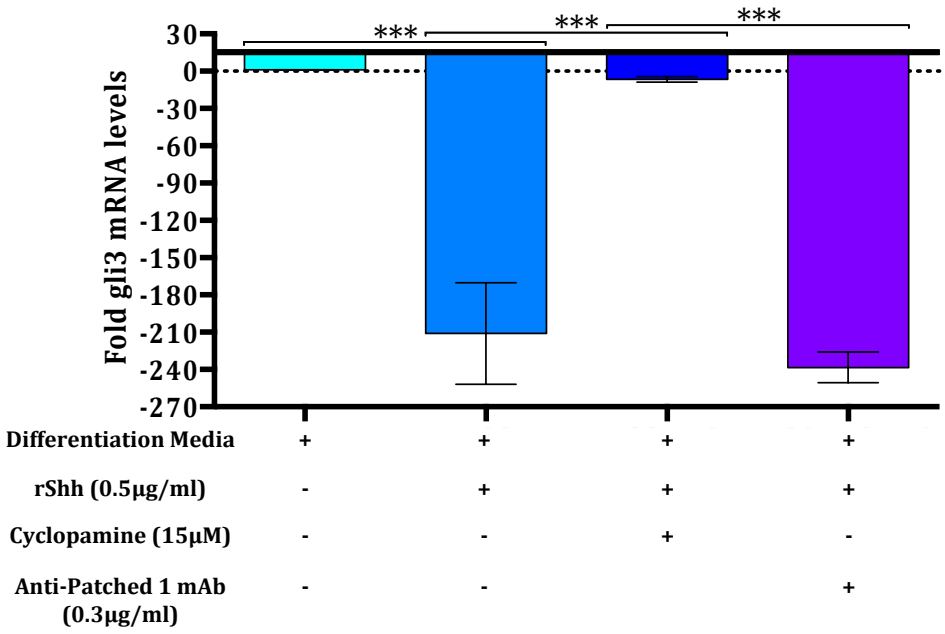

Figure 4.9: The effect of Shh on *Gli 3* (Hh signalling activator) mRNA levels in Sca1⁺ C3H cells in the absence or presence of Hh Inhibitors. qRT-PCR analysis of *Gli 3* mRNA levels. n = 3, one-way ANOVA statistical analysis result: ***: $p < 0.001$.

4.2.10 C3H/10T1/2 (C3H) Cell Line Hh Responsiveness: Shh increases the signal activator Gli 1 mRNA levels which is prevented with the addition of cyclopamine and an Anti-Shh mAb

The effect of other Hh signalling inhibitors on Shh activation of Hh target gene expression was also assessed by real-time qRT-PCR. Shh treatment increased Gli 1 (constitutive Hh signalling activator) mRNA levels after 24 hrs, an effect that is blocked following treatment of cells with the Hh signalling inhibitor cyclopamine (Smoothened antagonist) and a neutralizing anti-Shh monoclonal antibody (Figure 4.10).

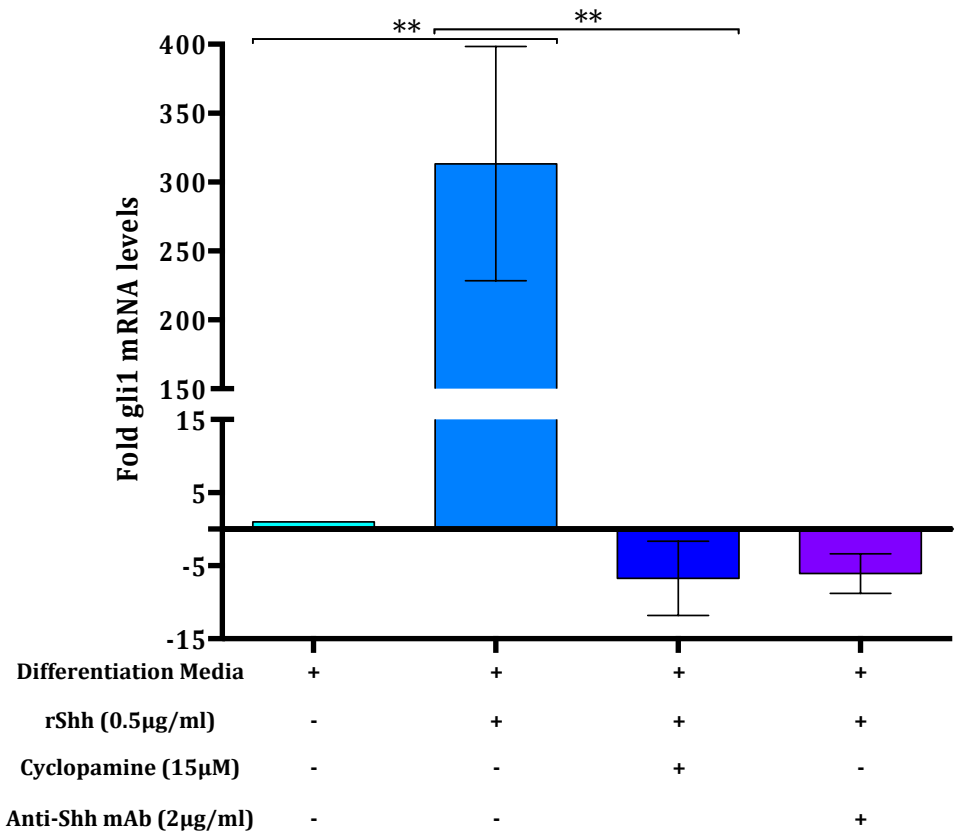

Figure 4.10: The effect of Shh on *Gli 1* (Hh signalling activator) mRNA levels in Sca1⁺ C3H cells in the absence or presence of Hh Inhibitors. qRT-PCR analysis of *Gli 1* mRNA levels. n = 3, one-way ANOVA statistical analysis result: **: $p < 0.03$.

4.2.11 C3H/10T1/2 (C3H) Cell Line Hh Responsiveness: Shh increases the signal activator and repressor Gli 2 mRNA levels which is attenuated by the addition of cyclopamine and an Anti-Shh mAb

The effect of other Hh signalling inhibitors on Shh activation of Hh target gene expression was also assessed by real-time qRT-PCR. Shh treatment increased Gli 2 (constitutive Hh signalling activator) mRNA levels after 24 hrs, an effect that is blocked following treatment of cells with the Hh signalling inhibitor cyclopamine (Smoothened antagonist) and a neutralizing anti-Shh monoclonal antibody (Figure 4.11).

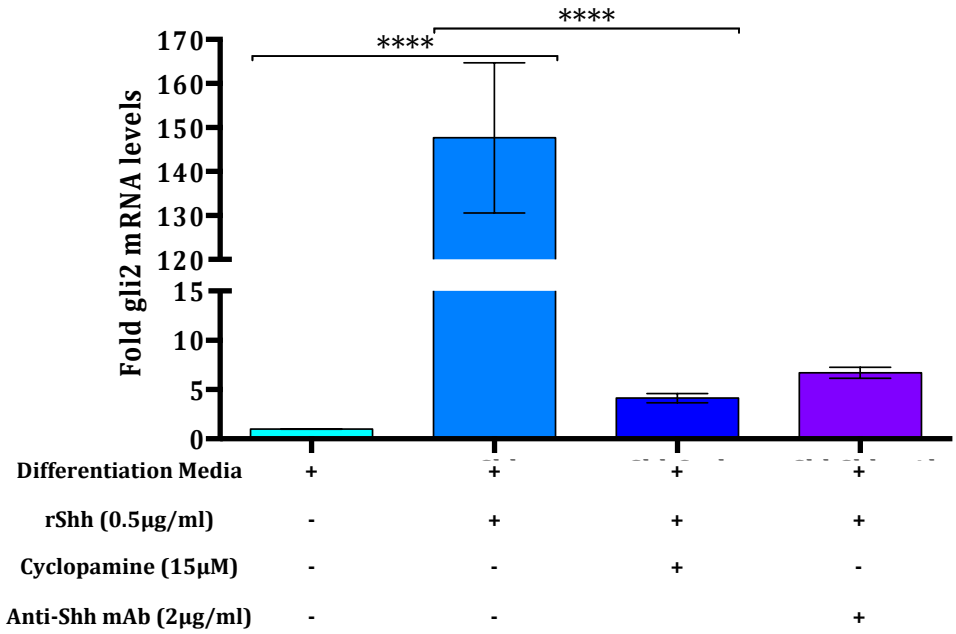

Figure 4.11: The effect of Shh on *Gli 2* (Hh signalling activator) mRNA levels in Sca1⁺ C3H cells in the absence or presence of Hh Inhibitors. qRT-PCR analysis of *Gli 2* mRNA levels. n = 3, one-way ANOVA statistical analysis result: ****: $p < 0.0001$.

4.2.12 C3H/10T1/2 (C3H) Cell Line Hh Responsiveness: Shh decreases the signal repressor Gli 3 mRNA levels which is attenuated by the addition of cyclopamine and an Anti-Shh mAb

The effect of other Hh signalling inhibitors on Shh activation of Hh target gene expression was also assessed by real-time qRT-PCR. Shh treatment decreased Gli 3 (constitutive Hh signalling activator) mRNA levels after 24 hrs, an effect that is blocked following treatment of cells with the Hh signalling inhibitor cyclopamine (Smoothened antagonist) and a neutralizing anti-Shh monoclonal antibody (Figure 4.12).

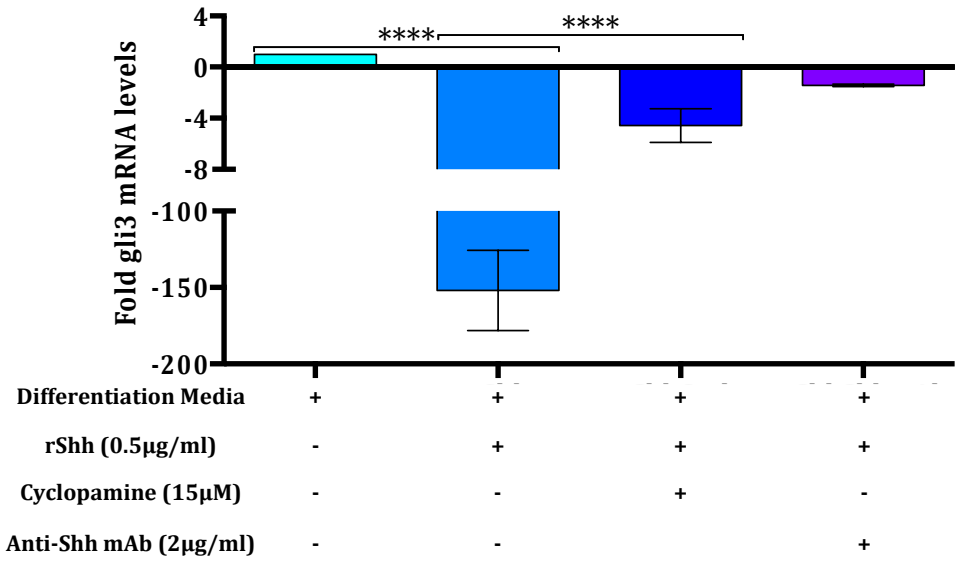

Figure 4.12: The effect of Shh on *Gli 3* (Hh signalling activator) mRNA levels in Sca1⁺ C3H cells in the absence or presence of Hh Inhibitors qRT-PCR analysis of *Gli 3* mRNA levels. n = 3, one-way ANOVA statistical analysis result: ***: $p < 0.001$.

4.2.13 C3H/10T1/2 (C3H) Cell Line Hh Responsiveness: Shh increases the signal activator Gli 1 mRNA levels which is not attenuated with the addition of recombinant Hedgehog Inhibitory Protein 1 (Hip-1)

The effect of Hip-1 as a potential Hh signalling inhibitor was also assessed by real-time qRT-PCR. Shh treatment increased Gli 1 (constitutive Hh signalling activator) mRNA levels after 24 hrs. This effect was not attenuated with the addition of recombinant Hip-1. There was no significance between the Shh alone and Shh in the presence of Hip-1. Furthermore, Hip-1 alone increases Gli 1 levels (Figure 4.13).

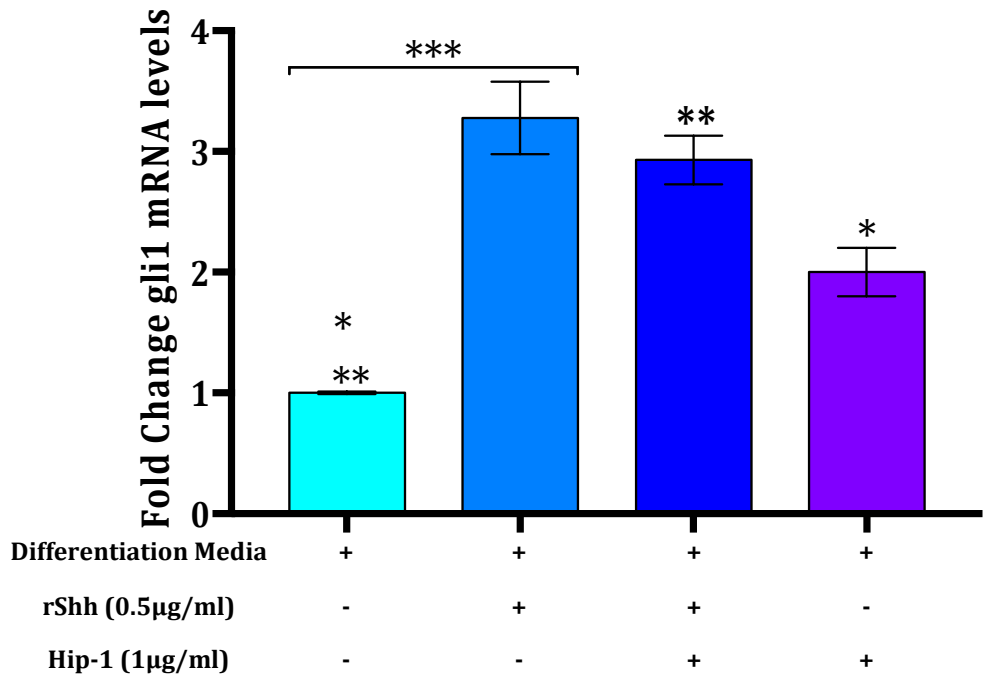

Figure 4.13: The effect of Shh on *Gli 1* (Hh signalling activator) mRNA levels in Sca1⁺ C3H cells in the absence or presence of Hip-1. qRT-PCR analysis of *Gli 1* mRNA levels. n = 3, one-way ANOVA statistical analysis result: *: p = 0.036, **: p = 0.01, ***: p ≤ 0.0002.

4.2.14 C3H/10T1/2 (C3H) Cell Line Hh Responsiveness: Shh increases the signal activator and repressor Gli 2 mRNA levels which is attenuated by the addition of Hedgehog Inhibitory Protein 1 (Hip-1)

The effect of Shh treatment on Gli 2 (Hh signalling activator and repressor) mRNA levels after 24 hrs was also assessed by real-time qRT-PCR. Shh increases Gli 2 mRNA levels, an effect significantly attenuated following treatment with Hedgehog Interacting Protein 1 (Hip-1) (Figure 4.14).

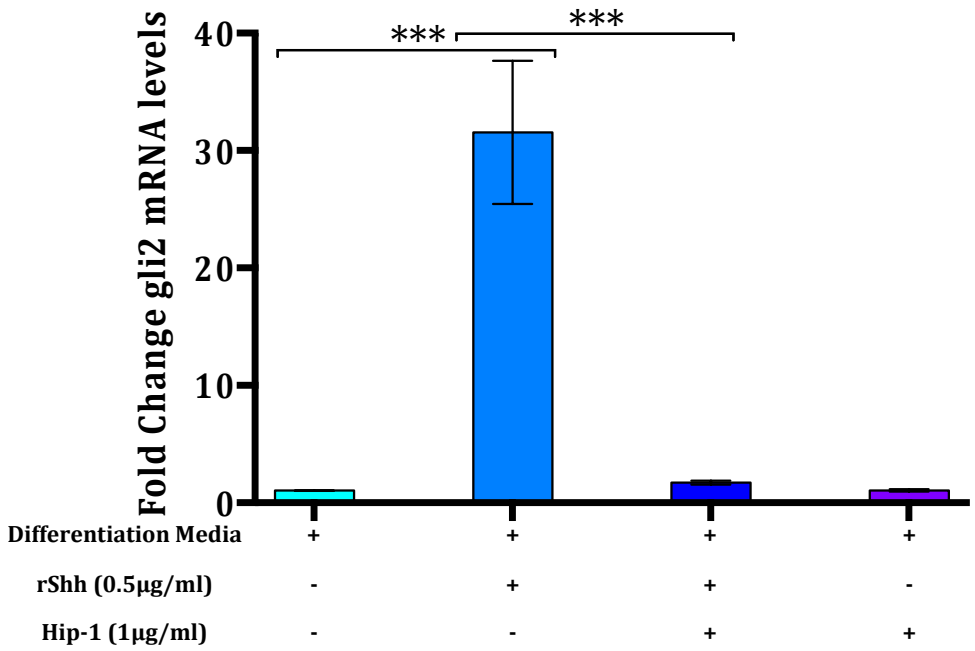

Figure 4.14: The effect of Shh on *Gli 1* (Hh signalling activator) mRNA levels in Sca1⁺ C3H cells in the absence or presence of Hip-1. qRT-PCR analysis of *Gli 2* mRNA levels. n = 3, one-way ANOVA statistical analysis result: ***: $p \leq 0.0005$.

4.2.15 C3H/10T1/2 (C3H) Cell Line Hh Responsiveness: Shh increases the signal activator Gli 1 mRNA levels which is attenuated with the addition of HPI-4

The effect of another smoothened inhibitor, HPI-4 on Shh-stimulated Hh target gene expression was also assessed by real-time qRT-PCR. Shh treatment increased Gli 1 (constitutive Hh signalling activator) mRNA levels after 24 hrs, an effect that is attenuated following the addition of HPI-4 (Figure 4.15).

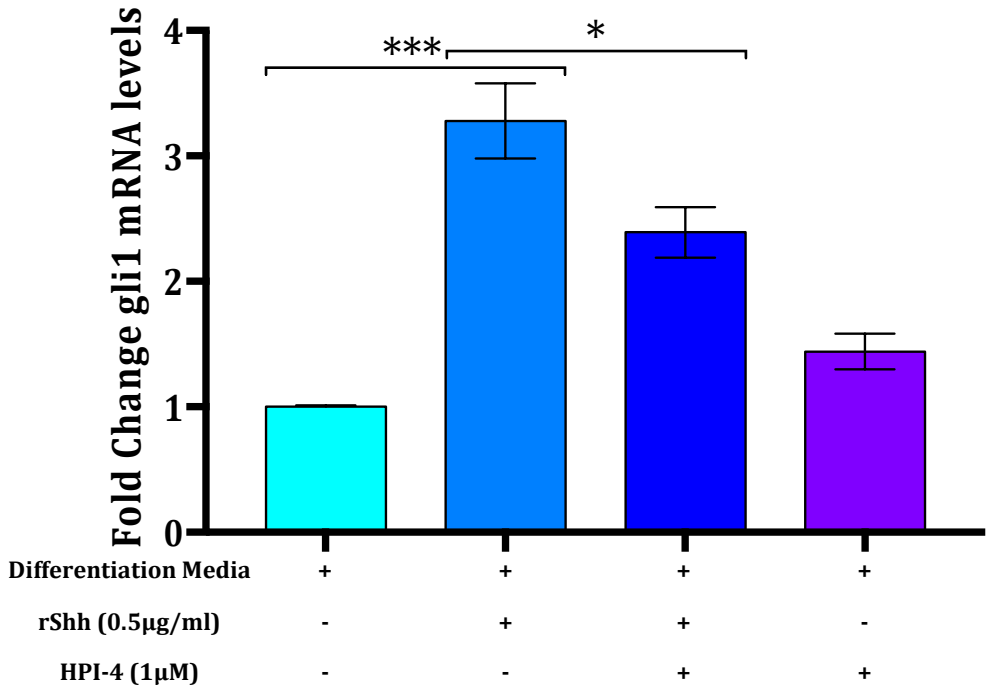

Figure 4.15: The effect of Shh on *Gli 1* (Hh signalling activator) mRNA levels in Sca1⁺ C3H cells in the absence or presence of HPI-4. qRT-PCR analysis of *Gli 1* mRNA levels. n = 3, *: $p \leq 0.04$, one-way ANOVA statistical analysis result: ***: $p \leq 0.0002$.

4.2.16 C3H/10T1/2 (C3H) Cell Line Hh Responsiveness: Shh increases the signal activator and repressor Gli 2 mRNA levels which is attenuated with the addition of HPI-4

The effect of Shh treatment on Gli 2 (Hh signalling activator and repressor) mRNA levels after 24 hrs was assessed by real-time qRT-PCR. Shh significantly increases Gli 2 mRNA levels, an effect that is significantly attenuated with the addition of HPI-4 (Figure 4.16).

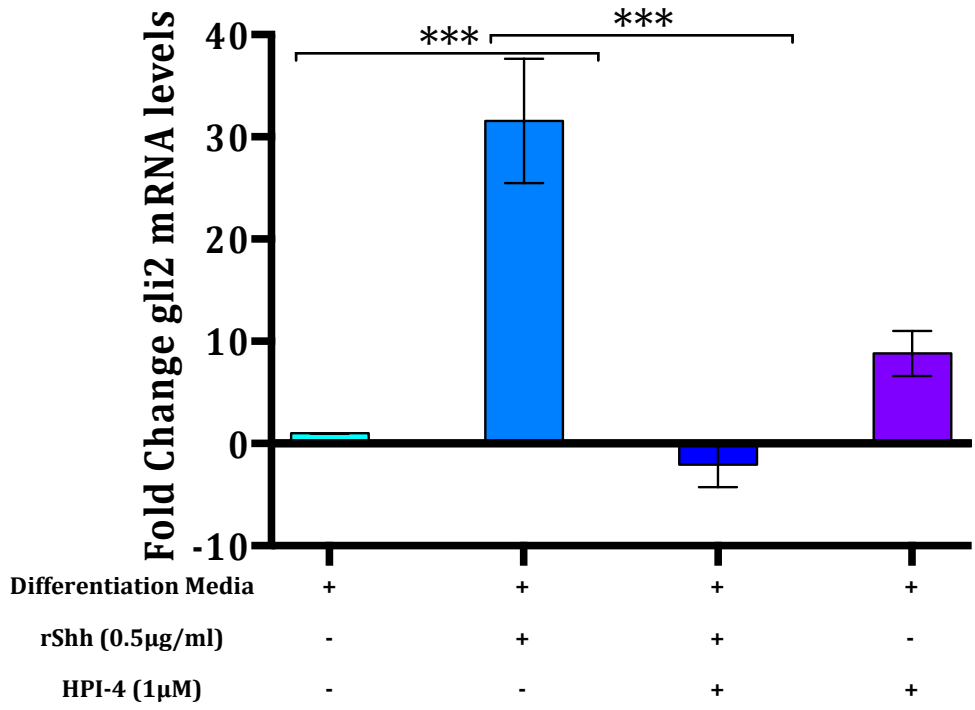

Figure 4.16: The effect of Shh on *Gli 2* (Hh signalling activator) mRNA levels in Sca1⁺ C3H cells in the absence or presence of HPI-4. qRT-PCR analysis of *Gli 2* mRNA levels. n = 3, one-way ANOVA statistical analysis result: ***: $p \leq 0.0005$.

4.2.17 Sca1⁺ mESC Self-Renewal: Sca1 Preservation

The effects of Shh on self-renewal of Sca1⁺ mESC was examined by the examining of the number of Sca1⁺ cell within a poulation by FACS. Flow cytometry analysis shows that there was a dramatic change in Sca1⁺ cells cultured in differentiation media, when comapred to maintenance medium (Figure 4.17.A). Following this discovery, the effect of FBS dependency on the number of Sca1⁺ cells expression was assessed. Graphical representation of the statistical data generated from flow cytometry shows that the routine FBS concentration (10 %) of embryonic stem cell approved FBS is criticial for Sca1 expression maintenance (Figure 4.17.B). The analysis also shows that non-approved embryonic stem cell FBS (differentiation media) at an identical concentration (10 %) dramatically changes the Sca1⁺ population (Figure 4.17.B).

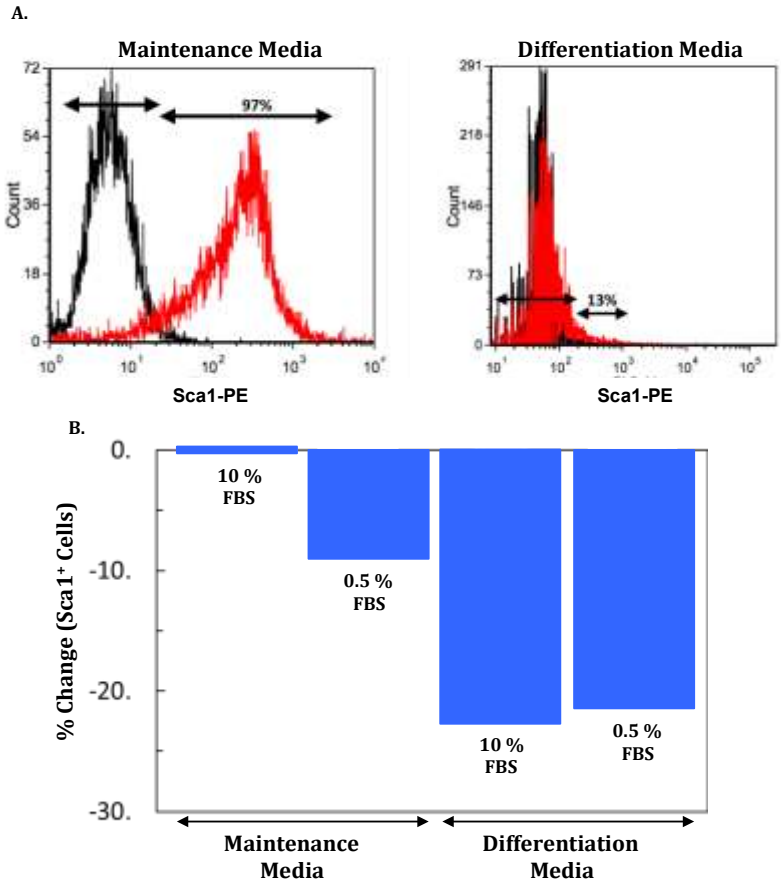

Figure 4.17: The Sca1 profile of Sca1⁺ ESC is dependent on the culture media. A: Representative Flow Cytometry analysis of Sca1⁺ ESC Sca1 profile following culture in stem cell maintenance media/differentiation medium (Black histogram is IgG-PE control, Red is Sca1-PE) n = 3, B: Graphical representation of Flow Cytometry analysis of Sca1⁺ ESC Sca1 profile data displayed in A.

The effect of low dose (75 ng/mL) Shh in differentiating medium in maintaining the number of Sca1⁺ cells and cell number after 48 hrs was subsequently investigated. Graphical representation of the flow cytometry results indicate that Shh changes the Sca1⁺ cell population and appears to induce Sca1 self-renewal (Figure 4.18).

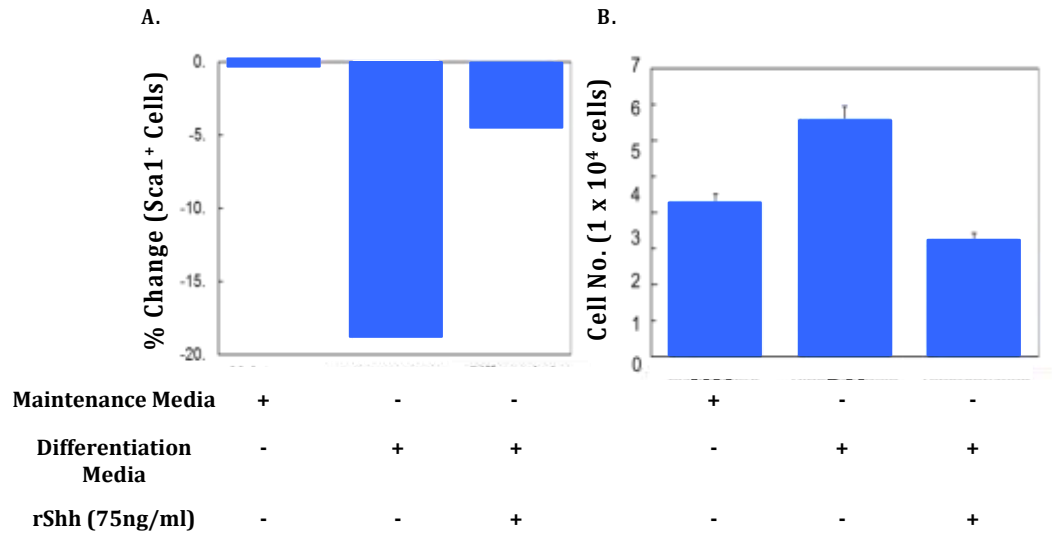

Figure 4.18: Shh treatment maintains Sca1 profile in Sca1⁺ ESC. A: Graphical representation of Flow Cytometry analysis of Sca1⁺ ESC Sca1 profile data after 48 hrs in stem cell maintenance media, differentiation medium and differentiation medium + 75 ng/mL Shh, B: Graphical representation of cell count analysis of Sca1⁺ ESC after 48 hrs in stem cell maintenance media, differentiation medium and differentiation medium + 75 ng/mL Shh n = 3.

As the initial preliminary analysis of Sca1 self-renewal used a low dose and short treatment time, an 8-day experiment using 500 ng/mL Shh was conducted. Treatment of cells with Shh promotes self-renewal (~ 15 % change in Sca1⁺ population expression) when Sca1⁺ mESC are subjected to myogenic differentiation stimuli for 8 days (Figure 4.19).

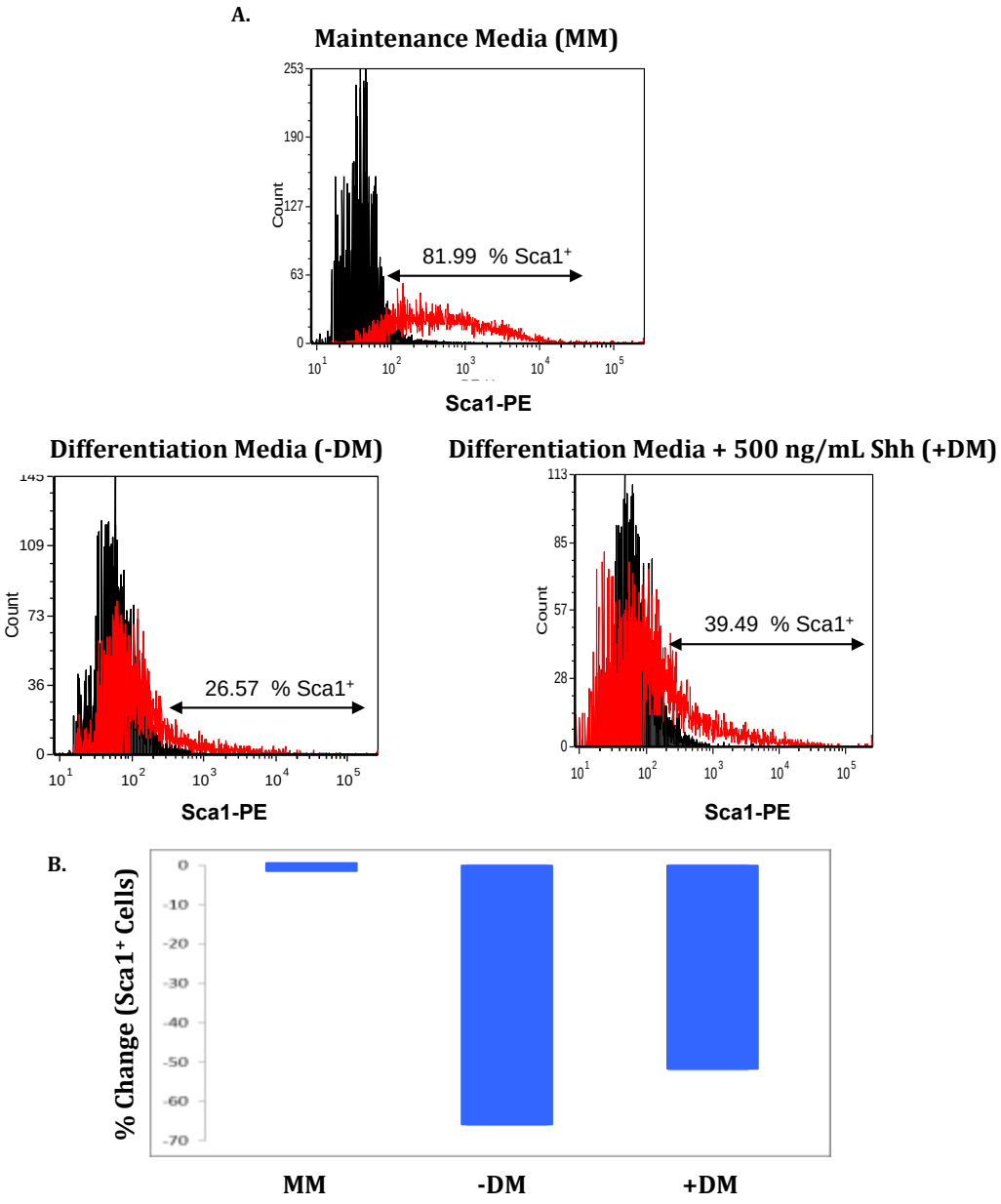

Figure 4.19: Shh treatment maintains Sca1 profile in Sca1⁺ ESC. A: Representative Flow Cytometry analysis of Sca1⁺ ESC Sca1 profile following culture in stem cell maintenance medium (MM), differentiation medium (-DM) and differentiation medium + 500 ng/mL Shh (+DM) for 8 days (Black histogram is IgG-PE control, Red is Sca1-PE) n = 3, B: Graphical representation of Flow Cytometry analysis of Sca1⁺ ESC Sca1 profile data displayed in A.

4.3 Discussion

The following section will discuss the results in the same manner as presented in the strategy outlined in section 4.1.2.

Shh-induced activation of Hh signalling in Sca1$^+$ stem cells

Our analysis shows that Sca1$^+$ cells respond to Shh treatment by activating Hh signalling. This was confirmed through the use of a Shh specific inhibitor cyclopamine, which when added to the medium consistently resulted in significant attenuation of Shh-induced Hh target gene expression. Our analysis of Sca1$^+$ APC shows they express Shh and it's receptor Patched 1 natively, which is interesting considering Passman et al., have previously shown Sca1$^+$ APC and Shh colocalization (Passman et al. 2008). It is also important to note that stem cell maintenance/"stemness" assessment by telomerase activity analysis *in vitro* shows that recombinant Shh has no effect on telomerase activity levels, suggesting that Hh signalling does not have a role in stem cell maintenance, at least for APCs. Moreover, the Hh signalling inhibitor cyclopamine completely prevents the differentiation media-associated decrease in telomerase activity. This indicates that activation of the Hh signalling pathway may not be involved in stem cell maintenance/ "stemness". Considering that the telomerase activity data suggested that Shh treatment of Sca1$^+$ APC does not induce stem cell niche maintenance, it is worth noting that Shh induced SMC differentiation as observed by SMC marker Cnn1 protein expression detected by immunocytochemistry (ICC), and increased *Cnn1* mRNA levels as detected by qRT-PCR; cyclopamine in both cases attenuates the Shh induced increase.

Interestingly, further analysis of the ICC images reveal that Shh increases the rate of proliferation (also reported by Li et al. 2010) which is again attenuated following cyclopamine treatment, confirming that Shh induces SMC differentiation through the Hh signalling pathway and inhibition by cyclopamine attenuates the response. It is important to note that Sca1$^+$ APC have SMC potential *in vitro* and *in vivo* (Li et al. 2000 and Hu et al. 2004). Notably, Hu et al. showed that Sca1$^+$ APC do not express the differentiating/differentiated SMC markers calponin 1 and smmhc (either protein or mRNA). However, Hu et al. showed that treatment with the known SMC inductive stimulus PDGF-BB resulted in marked expression of both these markers (including protein and mRNA). A relationship between

induction of SMC differentiation and Hh signalling *in vitro* has also been reported. Human fibroblasts and coronary artery SMC treated with PDGF-BB and TNF-α, two established compounds for the induction of SMC differentiation, stimulated significant Shh up-regulation and supernatant secretion (Daniel et al. 2013). Importantly, the Shh-specific inhibitor GDC-0449 blocked Shh signalling and SMC differentiation of both cell lines in a dose-dependent manner (Daniel et al. 2013). This is in agreement with our cyclopamine data. There were significant increases in Shh expression in neointimal and $Sca1^+$ perivascular stem cells during injury-induced vascular remodelling, and Shh-inhibition using GDC-0449 significantly reduces neointimal formation and $Sca1^+$ adventitial cell accumulation *in vivo* (Daniel et al. 2013). The observation that GDC-0449 results in the reduction of SMC induction and neointimal formation corroborates our evidence that the inhibition of Shh signalling results in the prevention of SMC induction and cellular proliferation. Since the evidence suggests that Shh-induced Hh activation results in proliferation and SMC induction rather than the promotion of stem cell maintenance, it is likely a secondary signalling pathway may be involved in the maintenance of the stem cell niche. This is a novel concept since it has been theorised that Shh is responsible for the maintenance of the $Sca1^+$ stem cell niche following the discovery of $Sca1^+$ APC and Shh colocalization by Passman et al., (Passman et al. 2008). Interestingly, the $Sca1^+$ C3H data that will be discussed in greater detail further on shows a contrasting result to the $Sca1^+$ APC. $Sca1^+$ C3H treatment with Shh induces a significant increase in telomerase activity (stem cell maintenance/"stemness"). However, it is possible that despite the fact that the $Sca1^+$ APC were cloned, Shh treatment may induce the two APC populations (a stem maintenance population and myogenic population), and considering the fact that telomerase activity is assessed by total protein, the dominant population (presumably of non-self renewing cells) may dilute the observable effect. There is also a chance that another unknown signalling system may be responsible for the maintenance of the $Sca1^+$ APC niche. The concept that there could be multiple cell fate signalling systems working within close proximity is worth considering. For example, the Notch

signalling system (involved in cell fate and previously described in section 1.6), which when activated in oligodendrocyte progenitor cells promotes stem cell renewal, is also activated during vascular remodelling (Park and Appel 2003 and Morrow et al. 2009). Morrow et al., provide evidence that Shh induces SMC Notch target gene expression and SMC proliferation (which can be attenuated using Notch inhibitors) *in vitro* (Morrow et al. 2009). Morrow et al., also show evidence of Notch up-regulation *in vivo*, however since their *in vitro* evidence suggests that Notch is involved in SMC proliferation, it is unlikely that Notch is involved in the maintenance of vascular stem cells (Morrow et al. 2009). It is important to note that Morrow et al., examined both their rat and human SMC for the SMC markers α-Actin, Calponin, Myosin and Smoothelin and noted that they were positive for α-Actin; however Calponin, SMMHC and Smoothelin expression was weak (Morrow et al. 2009). As previously mentioned in section 3.2.1, Calponin 1 is an early-differentiated SMC marker and SMMHC is a late-differentiated SMC marker. Also, Morrow et al., previous showed that SMC *in vitro* express key Hh signalling components (Shh, Patched 1, Smoothened and Gli 2) (Morrow et al. 2007). The paper also reported that Shh-treatment of SMC activated Hh signalling and induced SMC proliferation (as discussed in section 4.1), however, it only reported assessing SMC morphology and α-Actin status, neither of which are now considered as appropriate methods for the confirmation of differentiated SMC (Morrow et al. 2007). Nevertheless, these facts do not render either paper redundant, and it is possible that what Morrow et al., were working on may not have been a homogenous population of SMC, and may in fact have been de-differentiated SMCs and/or stem cell-derived SMC progeny.

The same can be said for the previously discussed Li et al., paper which demonstrated that Shh signalling is activated following vein graft injury (significantly high levels of key Shh signalling components in neointimal cells) and that the induction of Shh signalling in human vascular SMC promoted cell proliferation (Li et al. 2010). Li et al., did not make any attempt to characterize the explanted "SMC", therefore whether their SMC were in

fact de-differentiated SMC or a stem cell-derived progeny cell type remains inconclusive (Li et al. 2010). Considering this, it is important to re-evaluate their results which showed that cyclopamine and Gli 2-siRNA inhibition of Hh signalling in SMC dramatically reduced cell numbers, DNA replication and proliferative marker expression, and that Shh induced DNA replication and proliferative marker expression (Li et al. 2010). Considering that our study using SMC progenitor cells ($Sca1^+$ APC treated with Shh) also shows that Shh treatment induces proliferation, it is plausible that Li et al., may have been conducting their experiments on SMC progenitor cells rather than what they presumed to be differentiated SMC. It is crucial to point out that Morrow et al., and Li et al., are not the only papers that were written under the presumption of using differentiated SMC that may in fact have been SMC progenitor cells and/or their progeny. The work of Wang et al., Frontini et al., and many others should also be re-evaluated to consider the possibility that they were in fact de-differentiated SMC or a stem cell-derived progeny cell type (Yoshida et al. 2003; Mayr et al. 2005; Tang et al. 2010; Wang et al. 2010; Frontini et al. 2011; Hsu et al. 2012 and Zeng et al. 2016).

Our analysis of the model cell line $Sca1^+$ C3H also confirms that Shh induces Hh activation, a process that can be consistently attenuated using cyclopamine. Considering that C3H were a readily available and robust cell line, it was decided to compare the validated Hh inhibitors cyclopamine, HPI-4, HIP-1, a Shh mAb, and the unknown inhibitory activity of a Patched 1 mAb. Analysis of the Hh signalling target gene mRNA levels (*Gli 1, 2* and *3*) show that after 24 hours the Hh signalling activator Gli 1 mRNAs levels are increased with the addition of Shh in comparison to the medium alone control, confirming that Shh activates Hh signalling. The addition of the Hh signalling inhibitors cyclopamine and anti-Shh monoclonal antibody (anti-Shh mAb), and the potential inhibitor, an anti-Patched 1 monoclonal antibody (anti-PTCH 1 mAb) show significant attenuation of Hh activation. The validated Hh inhibitor HPI-4 showed incomplete attenuation (not as significant as the aforementioned monoclonal antibodies) and the validated inhibitor Hip-1 did not attenuate the response at all and appears to activate

Hh signalling instead of inhibiting it. Analysis of the Hh signalling activator and repressor Gli 2 mRNA levels showed that Shh increases Gli 2 mRNA levels, and is attenuated by the addition of cyclopamine, the anti-PTCH 1 mAb, the anti-Shh mAb, Hip-1 and HPI-4. Also, analysis of the Hh signalling repressor Gli 3 mRNA levels showed that Shh significantly reduces Gli 3 mRNA levels when compared to the medium alone, suggesting that Shh suppresses the repression of Hh signalling. This suppression of Gli 3 mRNA is attenuated by cyclopamine and the anti-Shh mAb, however is not attenuated by the anti-PTCH 1 mAb. Hip-1 and HPI-4 were not assessed for their potential to attenuate Gli 3 mRNA levels' as their *Gli 1* attenuation was not deemed sufficient for use as inhibitors. Therefore, the only viable inhibitors that provide sufficient Hh signalling attenuation are cyclopamine and the anti-Shh mAb. It is noteworthy that variability observed between the Hh signalling target gene expression analysis was a result of different seeding densities. Interestingly, Zacharias et al., also observed that C3H express Patched 1 and Gli 1 mRNA, and they also assessed the effect of Shh treatment with respect to SMC induction (Zacharias et al. 2011). Zacharias et al., show that Shh treatment induced a significant increase in α-actin (protein and mRNA) and Myocardin (smooth muscle master regulator/myogenic transcription factor) (mRNA) levels and a similar morphological shape as TGFβ1 treated cells (they concluded that these were signs of robust SMC differentiation) (Zacharias et al. 2011). However, as mentioned previously this is not an acceptable method for the confirmation of SMC differentiation, so while their observation that C3H express Hh signalling components natively can be taken into account (and corroborates with this study), their evidence that Shh induces SMC differentiation should not be taken at face value. Interestingly, as well as confirming that Shh induces Hh signalling, we analyzed the effect of Shh on the maintenance of $Sca1^+$ C3H "stemness". Hh responsiveness analysis strongly suggests that the culture of $Sca1^+$ C3H cells in stem cell maintenance medium is required for maintenance of their Sca1 positive profile, as this is lost when C3H cells are cultured in differentiation media. Shh modestly promotes Sca1 maintenance when cultured in differentiation medium yet significantly increases telomerase activity in

comparison to both the differentiation and maintenance medium controls. This highlights an inherent and significant difference between the Sca1$^+$ C3H model cell line and the Sca1$^+$ APC previously discussed. Interestingly, initial analysis of the Sca1$^+$ mESC model cell line shows a similarity between the Sca1$^+$ model cell lines. Maintenance of Sca1$^+$ mESC Sca1$^+$ profile also requires them to be cultured in stem cell maintenance media, as the Sca1 antigen expression changes if cultured in other medium types, and initial experiments show that Shh can promote minor Sca1 self-renewal when cells are subjected to differentiation media. While the Sca1$^+$ C3H model cell line analysis is by no means exclusive to the possibility that Shh strictly induces stem cell renewal and does not induce Sca1$^+$ C3H SMC differentiation, the difference in the telomerase results (a validated stem cell renewal assay) may indicate a subtle difference between the Sca1$^+$ C3H model cell line and the resident Sca1$^+$ APC.

4.4 Conclusion

Collectively, the data presented in this chapter confirms that Shh treatment of Sca1$^+$ cells (both resident and model) induces Hh activation, and that the Shh-induced effects can be attenuated using Shh-specific inhibitors *in vitro*. This compliments current literature showing that Shh-induces Hh activation *in vitro* and *in vivo,* despite the aforementioned issues with their presumptive use of differentiated SMC; in fact as previously mentioned, re-evaluation of literature may in fact confirm our observations (Morrow et al. 2007; Li et al. 2010 and Daniels et al. 2013). Importantly, our results also corroborate with the literature in that there is a strong association between Hh signalling and SMC differentiation *in vitro* and *in vivo* (Daniels et al. 2013). Additionally, it is imperative to note that Shh-inhibition has been confirmed to prevent SMC accumulation *in vitro* and *in vivo*, cementing Shh-inhibition as a serious contender for therapeutic use as a preventative therapeutic in the fight against vascular remodelling (and ultimately in-stent restenosis) (Morrow et al. 2007; Li et al. 2010 and Daniels et al. 2013).

Chapter 5

Hedgehog Control of Sca1^{+} Cell Renewal and Differentiation *In Vivo*

5.1 Introduction

5.1.1 Rationale

Animal Models Contribution to the Understanding and Therapy of Cardiovascular Disease

The elucidation of numerous pathologies including but not limited to Alzheimer's disease, cancer, stroke, schizophrenia, viral infections such as influenza and the topic of this research, cardiovascular disease, would not have been possible without the use of animal models (Götz and Ittner 2008; Klohs et al. 2014; Ruggeri et al. 2014; Casals et al. 2011; Jones et al. 2011; Thangavel and Bouvier 2014; Zaragoza et al. 2011; Grundtman 2012 and Tabas et al. 2015). The first published work on atherogenesis in an animal model was as early as 1908 by Ignatowski whose study was conducted on rabbits. Since then, other animal species such as mice, pigs and non-human primates have been investigated in the effort to unravel the complexities of atherosclerosis, each with their own advantages and limitations (reviewed by Grundtman et al., 2012). Technologies have also advanced from using naturally occurring animal models such as the hyperlipidemic rabbit model "WHHL" to genetically modified animal models such apolipoprotein (apo) E deleted mouse species "ApoE$^{-/-}$", and the recently developed transgenic "Rainbow" mice developed for cell-lineage tracing studies (Grundtman 2012 and Roy et al. 2014). It would be nearly 70 years after the first experiments on atherogenesis in 1908 that the first animal study would be reported using what would become the foundation for treatment of this disease using the gold standard percutaneous transluminal coronary angioplasty (PTCA) (Angioplasty 2015). Julio Palmaz advanced understanding of how to treat clinical atherosclerosis in 1978 when he designed the first bare metal stent. Palmaz design the stents to be deployed by a balloon during angioplasty, and support arterial walls preventing them from mechanical collapse, and between 1980 and 1985, Palmaz used dogs as a model to test the biocompatibility and conduct design optimization (Price 2013).

Cardiovascular Disease: Atherosclerotic Therapy Complications

However despite these advances, two complications were observed following stent implantation: thrombosis caused by endothelial injury and inflammation, and 30 % of patient cohorts would present with post-angioplasty in-stent restenosis (ISR) (Cox and Gotlieb 1986). Notably, while thrombosis has been successfully treated using the tissue plasminogen activator "Tenecteplase", advances in pharmacological treatments and mechanical devices over the last 3 decades have not fully overcome the complication of ISR and as such it's eradication remains a significant unmet clinical need. The rate of ISR for bare-metals is approximately 20% and current drug-eluting stents at roughly 10% (Sciahbasi et al. 2009 and Marx et al. 2011). Both animal models of ISR and human postmortem sections have been analyzed and assessed mechanistically to determine the etiology of the ISR process. Mechanistically, ISR is similar to wound healing with three phases documented; inflammatory, cellular proliferation and extracellular matrix remodelling (Marx et al. 2011). The exact nature of the cellular proliferative phase has remained inconclusive and there are two schools of thought that are divided on the subject.

Introduction to The Debate: Stem Cells Versus SMC

It is universally accepted that ISR is ultimately 'lumenal narrowing' due to inward vascular remodelling (intimal formation) due to a significant accumulation of predominantly vascular SMCs rather than plaque formation (Ward et al. 2000 and Nikolsky et al. 2003). The source of SMCs that contribute to intimal formation leading to inward vascular remodelling is a subject of controversy arising from the ongoing debate on the putative role of SMCs derived from either circulating bone marrow-derived hematopoietic stem cells and/or resident vascular stem cells or native mural cell derived "de-differentiated" SMC. Intimal formation was originally considered to be primarily composed of "de-differentiated" SMC; a concept which will be addressed in the next paragraph; nonetheless the last two decades have seen a significant amount of evidence supporting a putative role for resident

vascular stem cells (both adventitial and medial) in contributing to intimal formation (Li et al. 2000; Hu et al. 2004; Passman et al. 2008; Liang et al. 2011; Tang et al. 2012; Tiggges et al. 2013 and Potter et al. 2014).

Due to experimental advances over the past decade, the scientific community has witnessed a dramatic change in the definition and functional classification of SMC and progenitor cells. Current experimental evidence suggests that the SMC marker, Smooth-Muscle Myosin Heavy Chain (SMMHC or also denoted Mhy11) is the most reliable marker for determining a "differentiated" SMC phenotype (Stevens et al. 2008). The identification of SMMHC as a "differentiated" SMC marker has been central to the stem cell versus SMC "de-differentiation"/proliferation debate and interestingly, animal models designed to investigate the origin of intimal SMCs using this marker have produced conflicting results.

The Origins of the Stem Cell Debate

The putative role of stem cells in contributing to intimal formation was first proposed by Sata et al., in a seminal paper addressing the contribution of hematopoietic stem cells to vascular remodelling (Sata et al. 2002). It was the first paper to challenge the established and accepted theory of intimal formation being a proliferative de-differentiated SMC phenomenon. Sata et al., performed wire-induced injury of the femoral artery (considered to resemble angioplasty) on lethally irradiated wild-type mice 4 weeks after they had undergone bone marrow transplantation from Rosa26 ubiquitously expressing $LacZ^{+}$ mice (Sata et al. 2002). This design meant that any cells derived from bone marrow would express LacZ and immunofluorescence analysis showed that 63.0 ± 9.3 % of intimal formation cells and 45.9 ± 6.9 % of medial cells were bone marrow-derived (Sata et al. 2002). The paper sparked newfound interest in tackling the issue of intimal formation, since this advancement opened up a novel therapeutic target. However as other groups began to further investigate, the validity of bone marrow-derived

cells contributing to intimal formation became increasingly unlikely and was ultimately ruled out for the following reasons:

1. Bone marrow progenitor cells rarely produce SMC/ECs
2. Bone marrow cells accumulating in the intimal formations were in fact monocytes/macrophages which left the vicinity at later time points
3. Intimal size in irradiated and bone marrow transplanted mice was dose-dependently attenuated
4. Bone marrow contribution was injury type and severity dependent (with wire-induced injury causing anything from complete endothelial denudation to massive medial cell apoptosis.

(Tanaka et al. 2003; Sainz and Sata 2006 and Daniel at al. 2010)

Despite being ultimately undermined, the early results of Sata et al., challenged prevailing scientific theories and paved the way for the current debate of resident vascular stem cells versus SMC de-differentiation/proliferation of SMC (Sata et al. 2002; Hu et al. 2004; Sainz et al. 2006; Passman et al. 2008; Vliet et al. 2008; Daniel et al. 2010; Hoglund et al. 2010; Oyama et al. 2010; Nemenoff et al. 2011; Klein et al. 2011; Alexander and Owens 2012; Daniel et al. 2012; Tigges et al. 2012; Naito et al. 2012; Tang et al. 2012; Tang et al. 2013; Nguyen et al. 2013; Wong et al. 2013; Herring et al. 2014; Kabara et al. 2014; Gomez et al. 2015 and Leach et al. 2015).

Key Players in the Debate

The most noteworthy contributions to this debate are to follow, however it must be noted that each animal model described is unique and the authors do not always provide a full nomenclature in order to fully elucidate the genetic background of their models.

Oikawa et al. 2009

Oikawa et al., used unmodified Sprague Dawley rats to identify Nestin expression in vascular SMC. They demonstrated developmental Nestin expression in aortic medial SMC, and that this Nestin expression is abolished in adulthood. The group also demonstrated the re-appearance of $Nestin^+$ cells on the lumenal side (frontier) of an intimal formation and concluded that intimal $Nestin^+$ cells are not necessarily proliferating SMC and queried their derivation, suggesting a possible role for $Nestin^+$ cells in the progression of vascular remodelling (intimal formation) (Oikawa et al. 2009).

Nemenoff et al. 2011

Nemenoff et al., used a B6.FVB.–Tg(SMMHC-CreERT2)1Soff/J (tamoxifen inducible) transgenic mouse model background to track differentiated SMC progeny following injury and vascular remodelling. Using this model, all progeny derived from $SMMHC^+$ cells expressed LacZ. The study demonstrated the presence of adventitial and intimal $SMMHC^+$ cells in injured vessels. The group concluded that the migration of differentiated medial SMC are the main contributor to intimal formation, and suggest there is a previously unidentified role for SMC in the remodelling of the adventitia (Nemenoff et al. 2011) (for more details on this mouse model see The Jackson Laboratory 2016).

Tang et al. 2012

Tang et al., used SMMHC-Cre/LoxP-EGFP (non-inducible) mouse model to identify the role of multipotent vascular stem cells (MVSC) that are $Sox\ 10^+$, $Sox\ 17^+$ and $S100\beta^+$ in vascular remodelling. All SMMHC derived progeny cells expressed eGFP. The authors demonstrated that $SMMHC^-$ multipotent vascular stem cells (MVSC) can differentiate into neural and MSC-like cells and subsequently become SMC *in vitro*, and can become activated following injury *in vivo*. The authors concluded that MVSC (rather than SMC) become proliferative and differentiate into SMC during vascular remodelling and intima formation (Tang et al. 2012) (for more details on this mouse model see Xin et al. 2002).

Wan et al. 2012

Wan et al., used Nestin-Cre-EYFP (non-inducible) mouse model to identify the role of Nestin^{+} mesenchymal stem cells (MSC) in vascular remodelling. All Nestin^{+} progeny expressed eYFP. The authors demonstrated that TGF-β1 is essential for MSC participation in vascular remodelling, and intimal formation with frontier cells within the intima expressing both Nestin^{+} and Sca1^{+} and a large proportion of SMCs beneath these frontier cells expressing Nestin^{+} derived progeny. They concluded that MSC are a potential target in the prevention of intimal formation (Wan et al. 2012).

Herring et al. 2014

Herring et al., used Mhy11-CreERT2$^{+/-}$ on a C57BL6 background crossed with B6.129(Cg)-Gt(ROSA)26Sor$^{tm4(ACTB-tdTomato,-EGFP)Luo}$/J (tamoxifen inducible) lineage tracing mouse model to identify the role of SMC in vascular remodelling). This novel mouse model expressed tdTomato in progeny derived from SMMHC^{-} cells and eGFP in progeny derived from SMMHC^{+} cells. The group demonstrated SMMHC^{+} cells in the media and intimal formations and concluded that previously differentiated medial SMC contribute to the majority of intimal formations (Herring et al. 2012).

Yang et al. 2015

Yang et al., used *R26R^{+}; Mhy11-CreER^{+}* (tamoxifen inducible) transgenic mouse model to lineage trace and identify the fate of differentiated SMC in vascular remodelling. Progeny derived from SMMHC^{+} cells expressed LacZ. The authors demonstrated SMMHC^{+} cells in the media and intimal formation following injury. Interestingly, they also noted that in some intimal leisons where the underlying SMC were preserved, LacZ (SMMHC^{+} cells) were barely detected. They argued that this was not due to random loss of LacZ by stating that SMC remained lacZ homogenous after several generations of continuous passages or PDGF stimulation. They further suggested that age influences intimal cellular content because Herring et al., reported ~ 80 % of intimal cells in juvenile mice were derived from SMC and they reported < 30 % SMC derived cells contributed to intimal formations. The group

concluded that SMC physically migrate from the tunica media to contribute to the intimal formation (Herring et al. 2014 and Yang et al. 2015).

Sca1 Animal and Injury Model

In this context, we therefore utilised a Tg(Ly6a-EGFP)G5Dzk transgenic mouse model to monitor temporal expression of Sca1 in normal and arteriosclerotic vessels. This transgenic mouse strain, commercially available from The Jackson Laboratory, has been designed with an enhanced green fluorescent protein under the control of murine lymphocyte antigen 6 complex, locus A (Ly6a) promoter (The Jackson Laboratory 2016). The Ly6a promoter directs the expression of GFP in all functional repopulating adult stem cells (The Jackson Laboratory 2016). The GFP transgenes expression pattern corresponds to that of the protein of interest, Sca1, hence the animal model from here on in will be denoted as Sca1-eGFP (The Jackson Laboratory 2016). It is important to note that this animal model encodes for transient expression therefore lineage tracing information cannot be obtained from it.

Arteriosclerosis (including restenosis) and atherosclerosis, as well as other vasculopathies such as coronary intervention, venous graft restenosis and vascular rejection, are characterized by remodelling in vascular branches and bifurcations where blood flow is perturbed. The partial carotid ligation injury model mimics pathological low-flow-induced vascular remodelling hence was used in the study to assess the role of $Sca1^{+}$ cells in vascular remodelling (Redmond et al. 2013). For more information on the injury model see sections 1.3 and 2.9.

5.1.2 Strategy: Addressing Thesis Aim 3: Evaluate Hedgehog Control of Sca1⁺ Cell Renewal and Differentiation In Vivo

1. **Assessing Sca1⁺ cell response during vascular remodelling (partial ligation injury model)**

and

2. **Assessing Sca1⁺ cell response during vascular remodelling following treatment with cyclopamine (Hh inhibitor)**

To achieve these aims, Sca1-eGFP mice were split into the following categories (n=4):

- Untouched control
- Sham partial carotid ligation control
- 3 day post partial carotid ligation
- 7 day post partial carotid ligation
- 14 day post partial carotid ligation
- Vehicle treated partial carotid ligation control
- Cyclopamine treated partial carotid ligation

The surgical procedure and downstream analysis are detailed in section 2.9 however the following is a short summation of the analysis conducted:

<u>Sca1 Expression</u>

Whole mounted carotid and aortic tissue was assessed by fluorscent microscopy and imaged prior to sectioning. (Whole mounted aortas and an identified Sca1⁺ carotid associated nerve were additionally stained for the axonal marker Peripherin and vasculature markers SMMHC and eNOS).

Carotid sections were assessed by confocal microscopy for the presence of eGFP, images were taken with the same exposure settings for comparative purposes.

Tissue Morphology and Morphometric Analysis

Carotid sections were stained with H + E and Verhoeff's Van Gieson stains in order to differentiate between the vascular compartments (i.e adventitia, media, lumen and intimal formation) (section 2.10). Morphometric analysis was conducted in accordance with the method outlined by Tulis 2007.

3. Characterisation of vascular cell phenotypes during vascular remodelling

Carotid sections were probed by immunohistochemistry (section 2.4) for a variety of cell-type markers to initiate elucidation of vessel's cellular composition at time of tissue extraction. Sections were assessed by fluorescent microscopy and 10x/20x images taken at the same exposure settings for comparative purposes. The following markers were used in the cell-type identification process:

i. SMC identitification: SMC/pericyte marker α-Actin and differentiated SMC marker SMMHC
ii. EC identitification: eNOS
iii. Hh responsive cell identitification: Patched 1 and Gli 2
iv. MVSC cell identification (Glial cell marker): S100β
v. MVSC cell identification (Neural Stem cell markers): Sox 10 and Nestin
vi. MVSC cell identification (Endodermal and Hematopoietic Cell marker): Sox 17

4. Assessing for Sca1^{+} cells in human vessels

Lastly, the relevance of the mouse Sca1-eGFP marker to the human condition was assessed by probing a human healthy adult artery and human arteriosclerotic aorta for the presence of Sca1 by immunohistochemistry (section 2.4)

5.2 Results

5.2.1 Temporal Expression of Sca1-eGFP^{+} Cells Following Injury

Representative images of control (untouched and sham) and ligated carotid vessels (3, 7 and 14 day post ligation). Comparable Verhoeff's Van Gieson, H + E stained sections and confocal images show intimal formation initiation 7 day post ligation with full occlusion occurring 14 day post ligation (Figure 5.1). The confocal images were taken at identical imaging settings for Sca1-eGFP comparative purposes. A spike in Sca1-eGFP expression was observed in the adventitia and endothelia/lumenal boundary 3 day post ligation, continuing expression occurring in the intima 7 day post ligation and a dramatic drop in expression upon full occlusion 14 day post ligation (Figure 5.1).

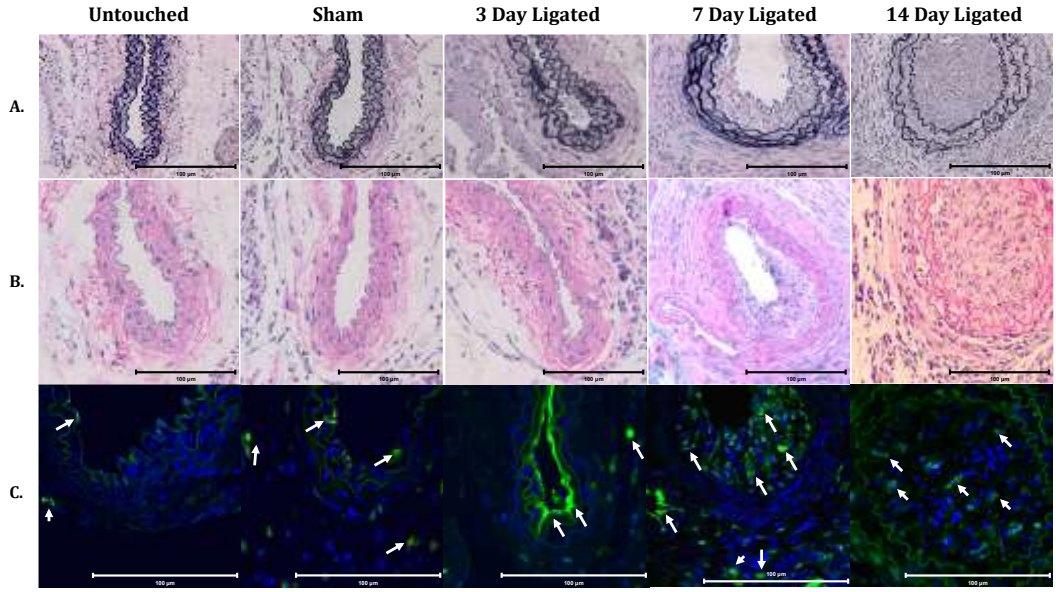

Figure 5.1: Temporal Expression of Sca1^{+} Cells Following Injury. A: Representative Verhoeff's Van Gieson stained brightfield images of untouched, sham and ligated vessels after 3, 7 and 14 day ($n \geq 15$), B: Corresponding representative H + E stained brightfield images of untouched, sham and ligated vessels after 3, 7 and 14 day ($n \geq 15$), C: Corresponding representative Sca1 confocal images of untouched, sham and ligated vessels after 3, 7 and 14 day ($n \geq 15$). Scale bars represent 100 microns.

5.2.2 Sca1-eGFP Expression in Vascular Layers

Sca1-eGFP expression was observed in the adventitia, media, lumenal boundary and intima of ligated vessels (Figure 5.2).

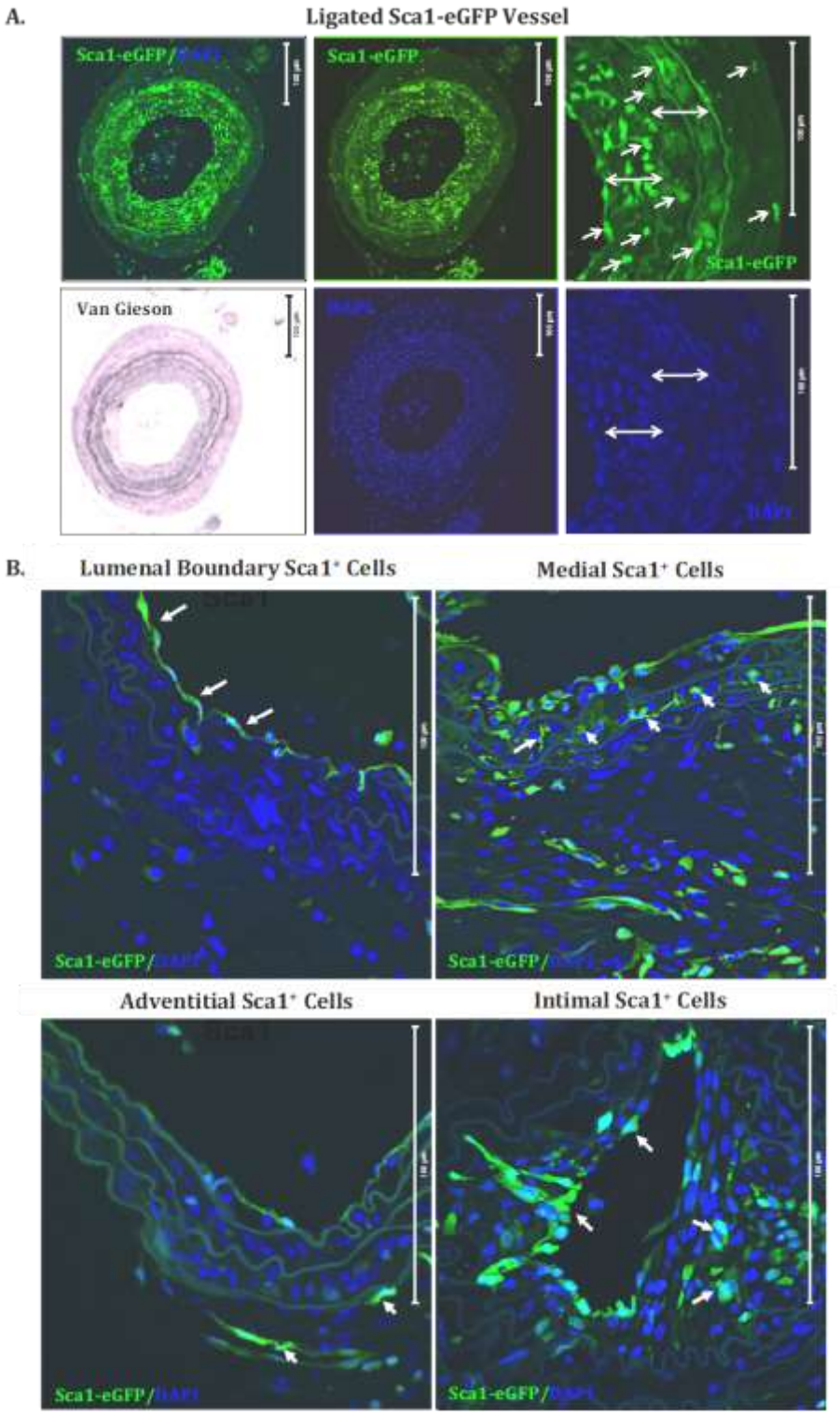

Figure 5.2: Sca1⁺ Cells Were Detected In The Adventitia, Media, Luminal Boundary And Intima. A: Representative Sca1 confocal and Verhoeff's Van Gieson images of a ligated vessel (n ≥ 15), B: Representative Sca1 confocal images of ligated vessels (n ≥ 15). Scale bars represent 100 microns.

5.2.3 14 Day Post Ligation: Sca1-eGFP Expression and Hh Inhibition with Cyclopamine Attenuates Intima Formation Following Injury

Cyclopamine attenuates intimal formation in 14 day post ligation treated vessels (Figure 5.3). As well as the attenuation of intimal formation, cyclopamine treated tissue does not appear to have as pronounced adventitial thickening, however it could be suggested that the medial volume remains unattenuated when compared with the 14 day ligated vehicle control (Figure 5.3). Notably, adventitial Sca1^{+} cells are detected in sham and cyclopamine treated vessels with attenuated remodelling but not in the vehicle control vessels where tissue remodelling is uninhibited (Figure 5.3). Sca1^{+} cells were detected in the intima of vehicle control vessels and lumenal Sca1^{+} cells in sham and cyclopamine treated attenuated vessels (Figure 5.3).

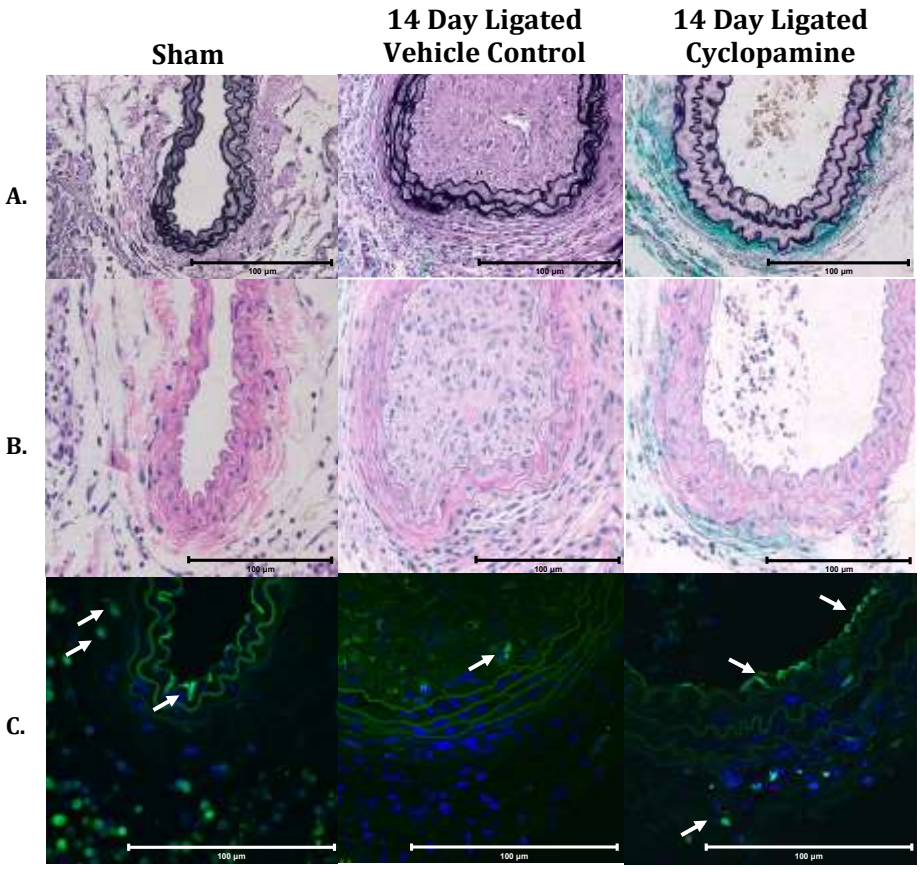

Figure 5.3: Sca1 Expression and Hh Inhibition Using Cyclopamine Attenuates Ligation-Induced Remodelling. A: Representative Verhoeff's Van Gieson stained brightfield images of sham and 14 day post ligation vehicle control/cyclopamine (n ≥ 15), B: Corresponding representative H + E stained brightfield images of sham and 14 day post ligation vehicle control/cyclopamine (n ≥ 15), C: Corresponding representative Sca1 confocal images of sham and 14 day post ligation vehicle control/cyclopamine (n ≥ 15). Scale bars represent 100 microns.

5.2.4 14 day Post Ligation Morphometric Analysis: Hh Inhibition with Cyclopamine Attenuates Ligation-Induced Intimal Formation

The cumulative morphometric data of carotid vessels shows that the ligation injury significantly increases the adventitial and medial compartments as well as stimulating intimal formation (Figure 5.4). The data also confirms that cyclopamine inhibits intima formation, with an additional tendency for reducing the adventitial compartment (Figure 5.4). The morphometric analysis also confirms the suspicion by visual assessment (discussed in section 5.3) that there is no significant difference between the medial volumes of the ligated cyclopamine treated versus ligated vehicle control vessels.

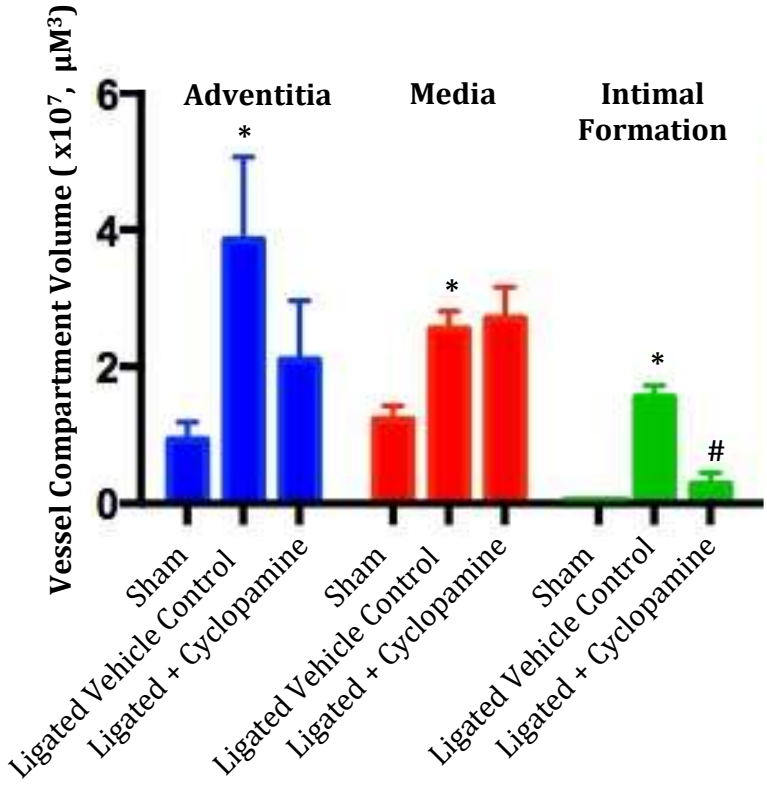

Figure 5.4: Hh Inhibition Using Cyclopamine Attenuates Ligation-Induced Arterial Remodelling. Partial carotid ligation/sham operation was performed on Sca1-eGFP mice treated with or without cyclopamine (10 mg/kg, IP every other day). Vessels were harvested 14 day post ligation, fixed, paraffin-embedded, sectioned and stained using Verhoeff's Van Gieson stain prior to morphological analysis. Data are given as mean ± SEM, 5 sections analyzed/animal, animals (n) ≥ 4, one-way ANOVA statistical analysis: * = $p < 0.05$ vs. sham, # = $p < 0.05$ vs. ligated control.

5.2.5 SMC Identification: Temporal Expression of Pericyte/SMC α- Actin and Differentiated SMC Marker SMMHC

To assess the SMC dynamic in injury-induced vascular remodelling, the pericyte/SMC marker α-Actin and differentiated SMC marker SMMHC were investigated by immunohistochemistry (IHC) analysis. As previously mentioned in Chapter 3 section 3.2.1, SMC lineage definition requires the presence of both α-Actin and SMMHC, however SMMHC is the critical marker for the identification of differentiated SMC as α-Actin is also a pericyte marker. It is also important to note that mature α-Actin and SMMHC are filamentous proteins. Images were taken at the same exposure length for comparative purposes. α-Actin IHC data confirms the presence of α-Actin exclusively in the media of untouched carotids, and medial expression does not change 7 and 14 day post ligation in the absence of intimal formation (remodelling) (Figures 5.5 and 5.6). However there is a reduction/loss of medial expression in sections of 14 day post ligation mice at points where intimal formation occurs, and intimal cells are observed to be highly α-Actin positive (Figure 5.5). The data also confirms medial and intimal expression of α-Actin (Figure 5.6). Detailed analysis of SMMHC shows the following (Figures 5.7 - 5.10):

- strong SMMHC expression is exclusive to the medial layer of untouched carotids
- an initial spike in adventitial and medial SMMHC expression 3 day post ligation with dramatic reduction in SMMHC observed in 7 and 14 day post ligation mice across the whole vessel including the media
- that this reduction in expression is continued into 14 day post ligation vessels, and the majority of intimal cells are in both partial and full intimal formation sections are negative for SMMHC

The study confirms that $SMMHC^{+}$ intimal cells at 7 or 14 day post ligation are not populous enough to define the tissue therefore the intimal cells cannot be considered as “differentiated” SMC (Figures 5.7 – 5.10).

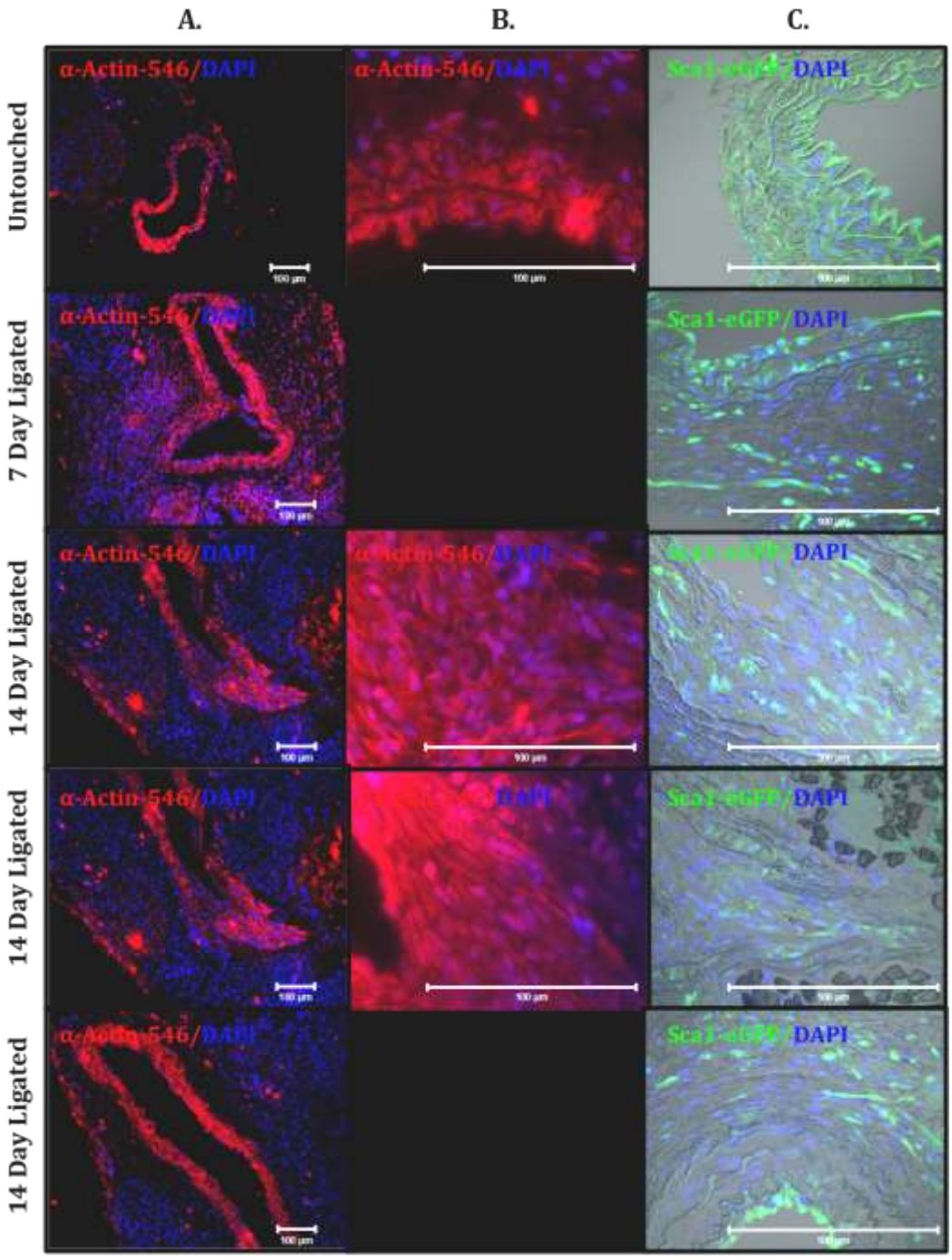

Figure 5.5: Sca1 and Pericyte/SMC Marker α-Actin Expression in Remodelling Vessels. A: Representative images of untouched, 7 day and 14 day post ligation vessels labelled with anti-α-Actin, B: Representative fluorescent images of untouched, 7 day and 14 day post ligation vessels labelled with anti-α-Actin, C: Corresponding confocal images of Sca1 untouched, 7 day and 14 day post ligation vessels, n ≥ 3, Scale bars represent 100 microns.

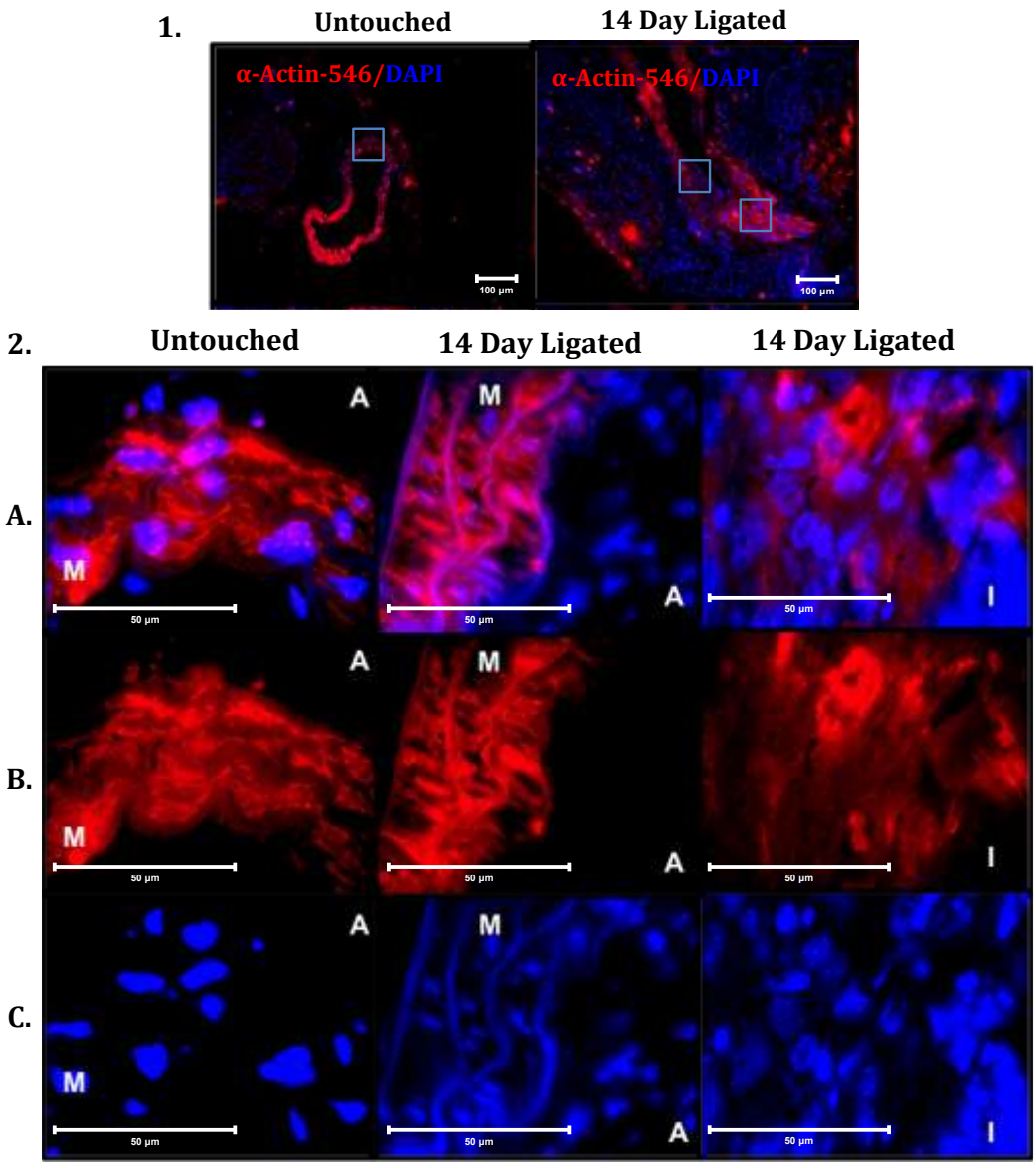

Figure 5.6: Pericyte/SMC Marker α-Actin Expression in Remodelling Vessels. 1: Low magnification representative image of untouched and 14 day post ligated vessels labelled with anti-α-Actin and nuclear stained with DAPI, 2. High magnification representative images of 1, 2A: Representative images of untouched and 14 day post ligation vessels labelled with anti-α-Actin and nuclear stained with DAPI (A = adventitia, M = media, I = intima), 2B: Corresponding images of untouched and 14 day post ligation vessels labelled with anti-α-Actin (A = adventitia, M = media, I = intima), 2C: Corresponding images of untouched and 14 day post ligation vessels labelled with nuclear stain DAPI (A = adventitia, M = media, I = intima), n ≥ 3, Scale bars represent 50 microns.

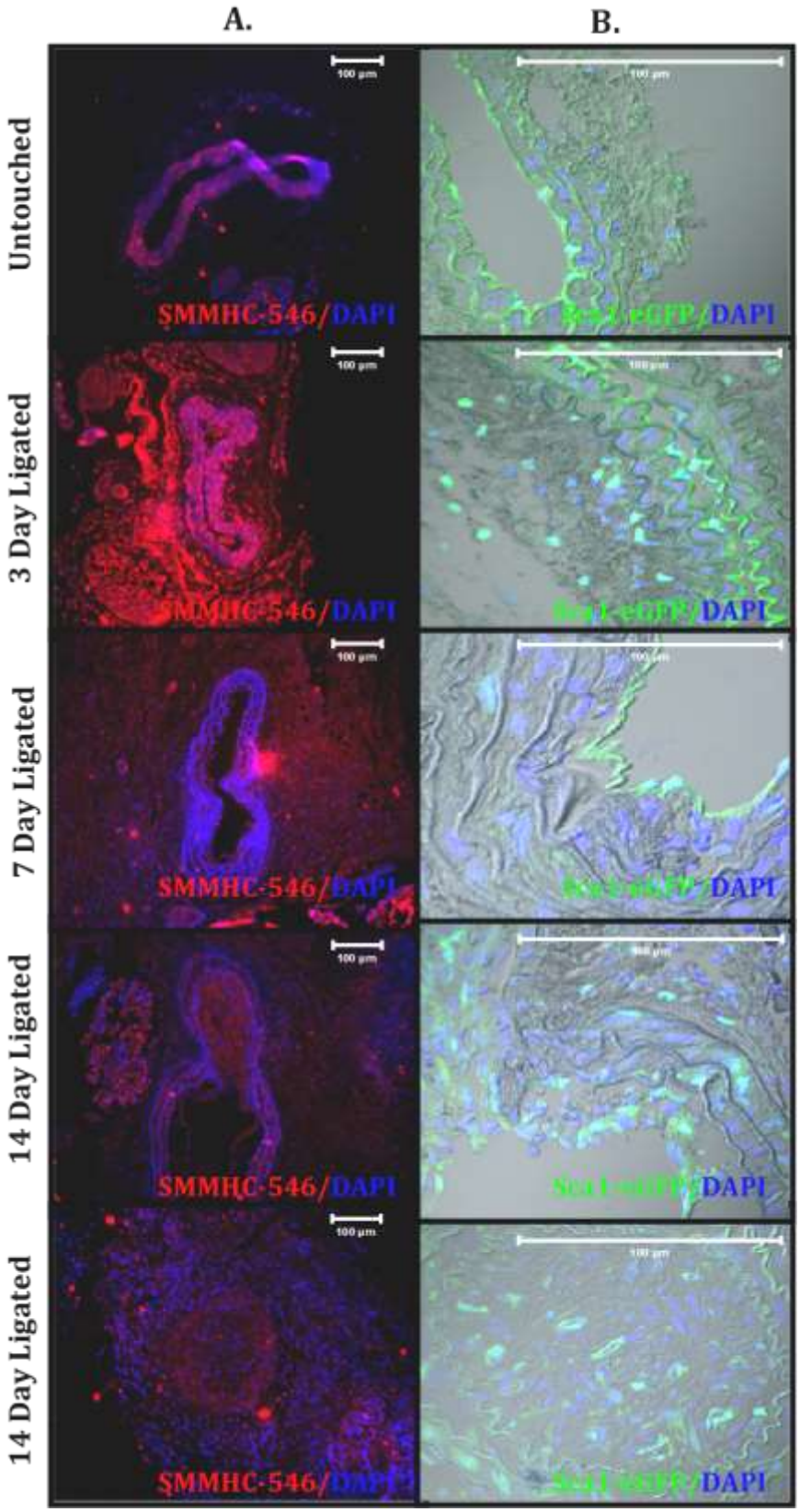

Figure 5.7: Temporal expression of Sca1 and SMMHC following carotid artery ligation. Representative (A) immunohistochemical images and (B) confocal images of untouched and ligated carotid arteries (3, 7 and 14 day post ligation) labelled with (A) anti-SMMHC and (B) Sca1, respectively, n ≥ 3, Scale bars represent 100 microns.

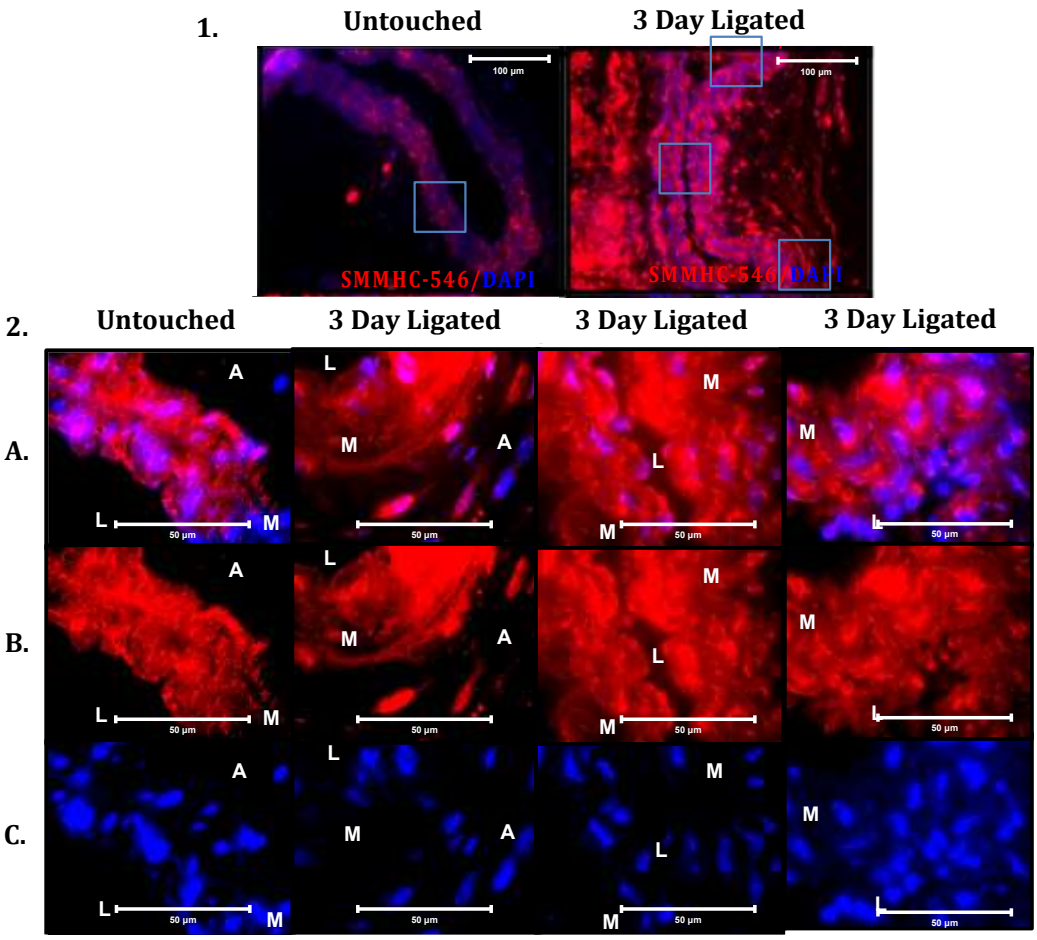

Figure 5.8: Differentiated SMC Marker SMMHC Expression in Remodelling Vessels (Untouched Vs. 3 Day Ligated). 1: Low magnification representative image of untouched and 3 day post ligated vessels labelled with anti-SMMHC and nuclear stained with DAPI, 2. High magnification representative images of 1, 2A: Representative images of untouched and 3 day post ligation vessels labelled with anti-SMMHC and nuclear stained with DAPI, 2B: Corresponding images of untouched and 3 day post ligation vessels labelled with anti-SMMHC, 2C: Corresponding images of untouched and 3 day post ligation vessels labelled with nuclear stain DAPI, n ≥ 3, Scale bars represent 50 microns.

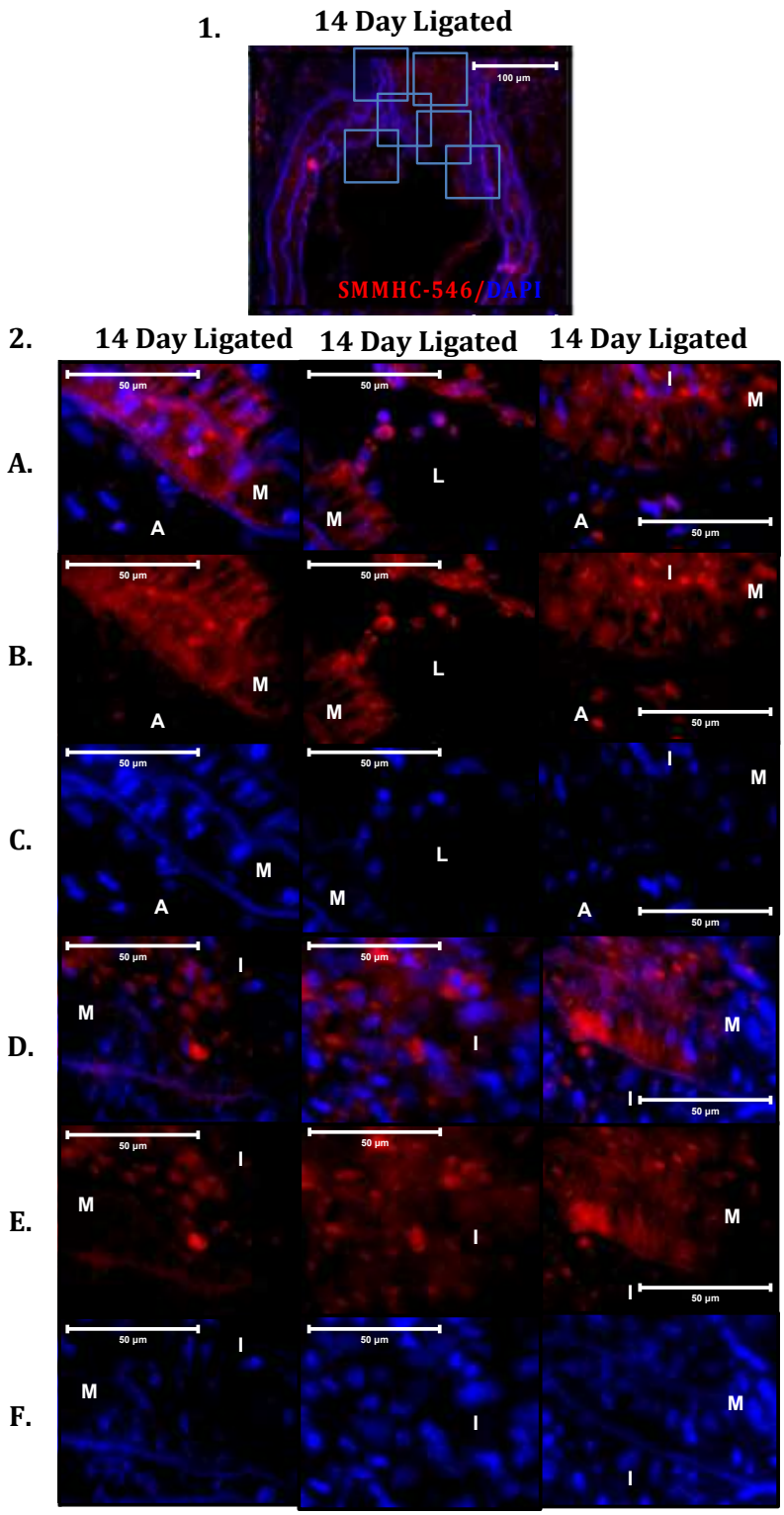

Figure 5.9: Differentiated SMC Marker SMMHC Expression in Remodelling Vessels (14 Day Ligated Partial Intimal Formation). 1: Low magnification representative image of untouched and 14 day post ligated partial intimal formation vessels labelled with anti-SMMHC and nuclear stained with DAPI, 2. High magnification representative images of 1, 2A + 2D: Representative images of 14 day post ligation vessels partial intimal formation labelled with anti-SMMHC and nuclear stained with DAPI, 2B + 2E: Corresponding images of 14 day post ligation partial intimal formation vessels labelled with anti-SMMHC, 2C + 2F: Corresponding images of 14 day post ligation partial intimal formation vessels labelled with nuclear stain DAPI, n ≥ 3, Scale bars represent 50 microns.

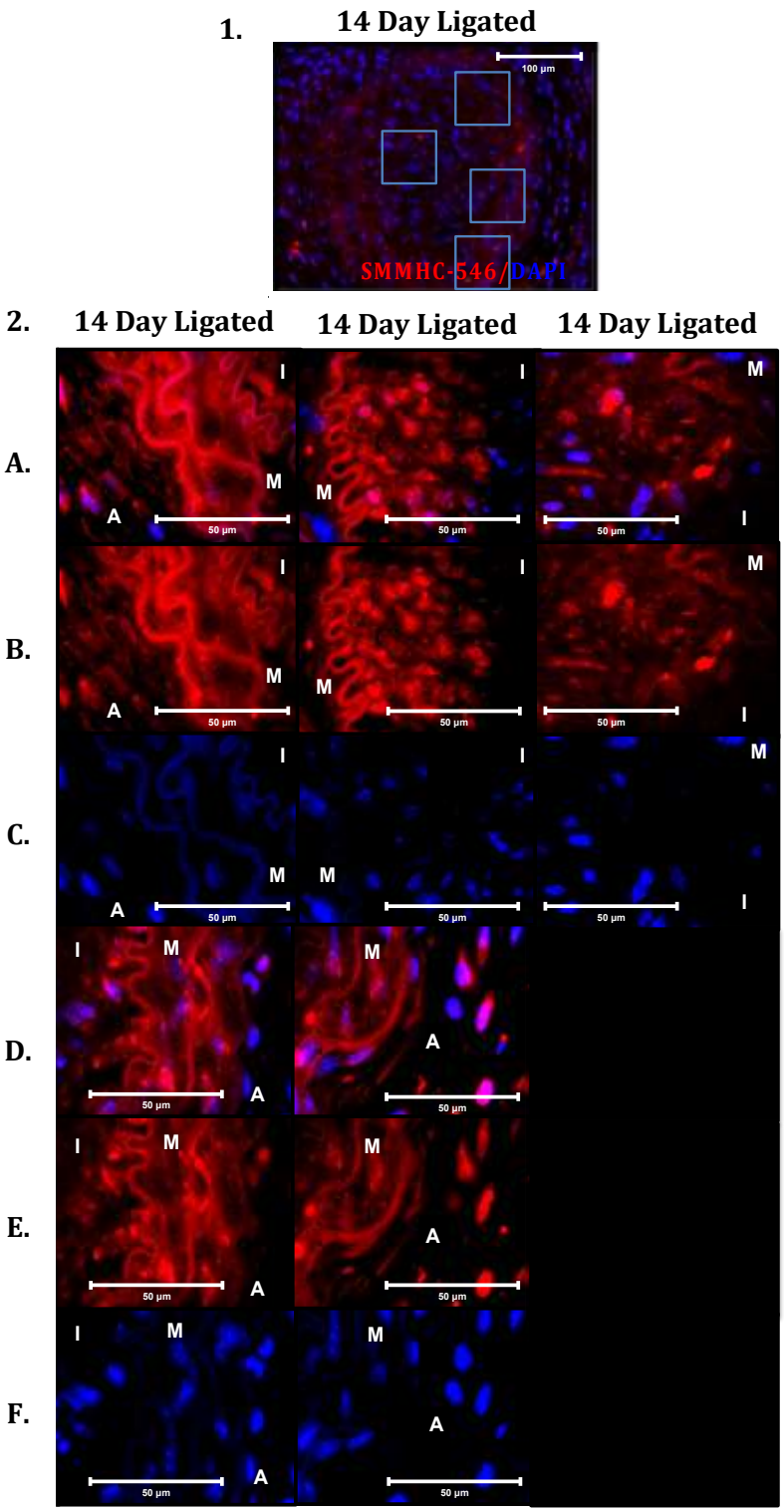

Figure 5.10: Differentiated SMC Marker SMMHC Expression in Remodelling Vessels (14 Day Ligated Full Intimal Formation). 1: Low magnification representative image of 14 day post ligated full intimal formation vessels labelled with anti-SMMHC and nuclear stained with DAPI, 2. High magnification representative images of 1, 2A: Representative images of 14 day post ligation full intimal formation vessels labelled with anti-SMMHC and nuclear stained with DAPI, 2B: Corresponding images of 14 day post ligation full intimal formation vessels labelled with anti-SMMHC, 2C: Corresponding images of 14 day post ligation full intimal formation vessels labelled with nuclear stain DAPI, n ≥ 3, Scale bars represent 50 microns.

5.2.6 Endothelial Identification: Expression of the Endothelial Marker eNOS

To address the issue of Sca1-eGFP expression on the lumenal/medial boundary 3 day post ligation, sections were investigated for the presence of the endothelial marker eNOS. The co-expression of eNOS and Sca1 suggests that endothelial cells may undergo endothelial-mesenchymal transition (EndMT) during the remodelling process (Figure 5.11).

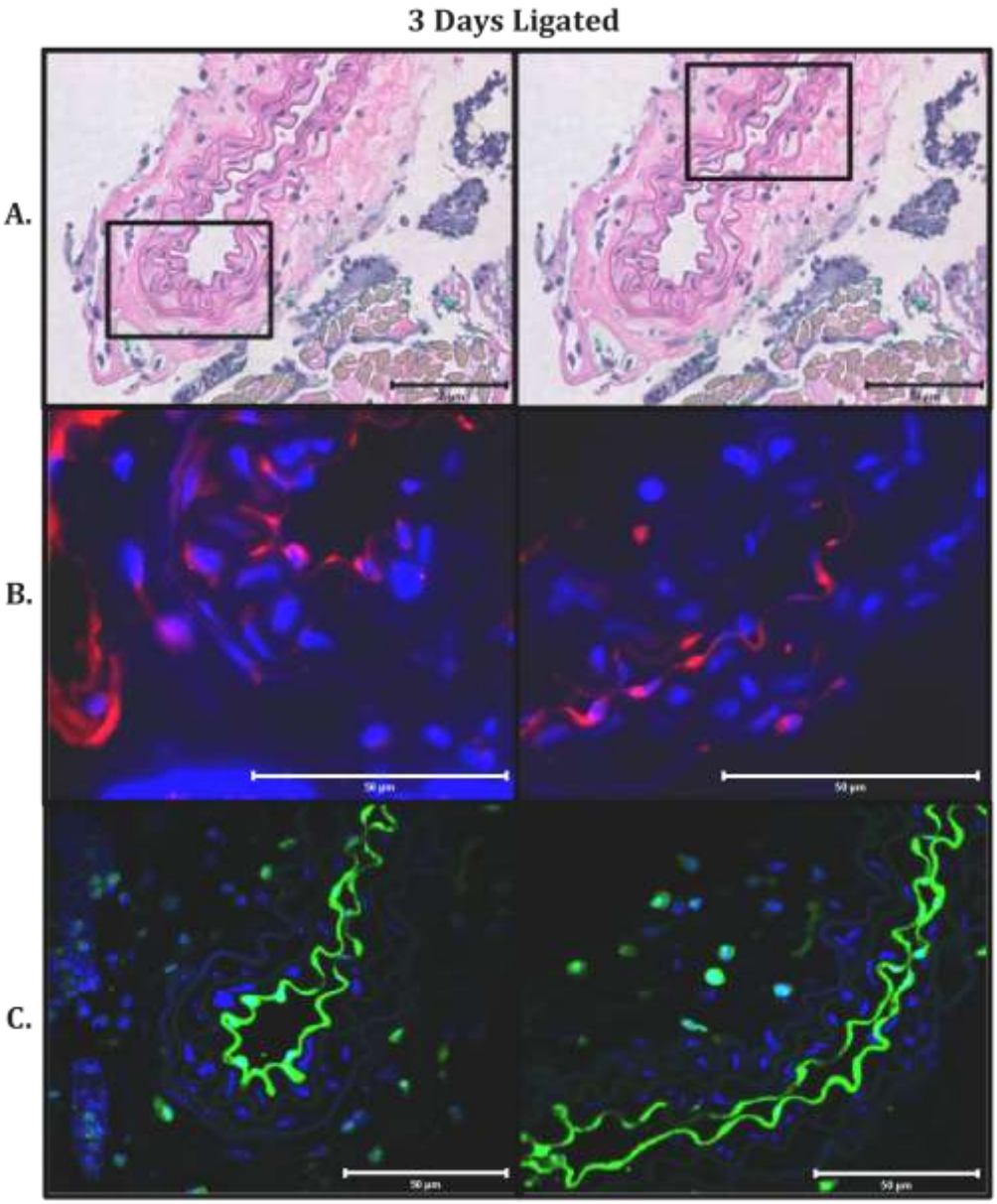

Figure 5.11: Endothelial Cell Marker eNOS Expression in Remodelling Vessels. A: Representative H + E stained brightfield images of 3 day post ligation vessels, B: Corresponding representative images of 3 day post ligation vessels labelled with anti-eNOS, C: Corresponding confocal images of Sca1 3 day post ligation vessels. n ≥ 3, Scale bars represent 50 microns.

5.2.7 Hh Responsive Cells Identification: Expression of the Patched 1 Receptor and Hh target gene and Hh signalling activator and repressor Gli2

The expression of the Hh signalling receptor Patched 1 and target gene Gli2 is critical to the theory of Hh signalling recapitulation instigating vascular remodelling. IHC data confirmed the presence of significant Patched 1 expression in the adventitia and media of 3 day post ligation vessels (Figure 5.12). It also indicates that Patched 1 expression is reduced in 7 day post ligated vessels however Patched 1 is highly expressed in all layers of 14 day post ligation vessels (adventitia, media and intima), suggesting that expression is dynamic (Figure 5.12). Further analysis confirms the presence of Patched 1 in the adventitia and media of 3 day post ligation vessels as well as the adventitia, media and intima of 14 day post ligation vessels, as observed at a higher magnification (Figure 5.13). In addition, Gli2 expression analysis 14 day post ligation shows limited Gli2 expression in sham controls, significant expression in ligated vessels (specificially intimal) and limited expression in cyclopamine treated ligated vessels (Figure 5.14). Additionally, Gli2 expression analysis 14 day post ligation shows the presence of $Sca1^{+}Gli2^{+}$ cells in the adventitia, media and neointima, and cyclopamine analysis shows EC boundary $Sca1^{+}Gli2^{+}$ expression (Figure 5.14). Both the Patched 1 and Gli2 analysis confirms that Hh signalling is recapitulated in remodelling vessels, and that this remodelling can be attenuated using a Hh specific inhibitor (cyclopamine). This confirms Patched 1 and Gli2 expression data by Morrow et al., and the potential for Hh signalling in injury-induced remodelling vessels (Morrow et al. 2009).

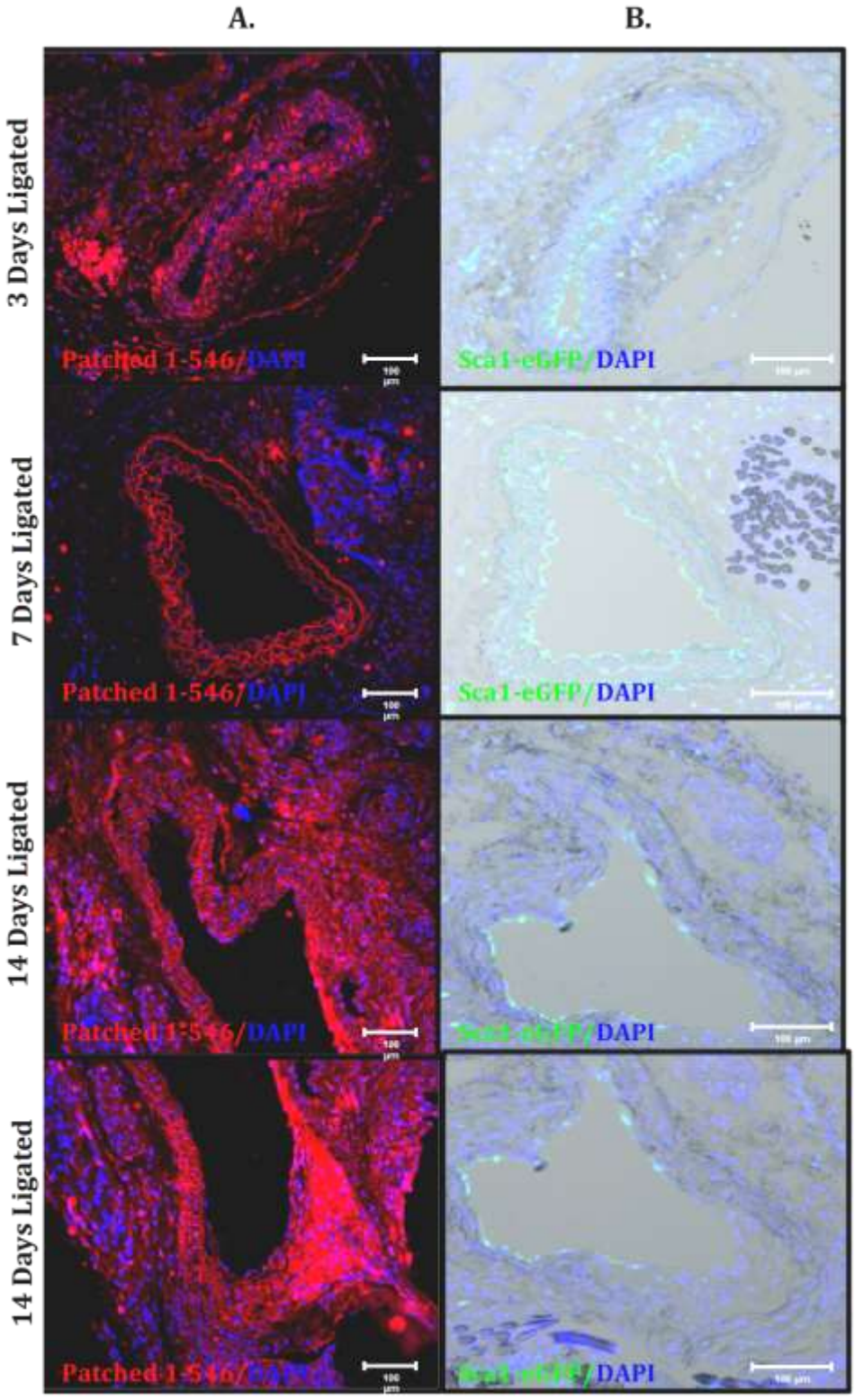

Figure 5.12: Sca1 and Hh Signalling Receptor Patched 1 Expression in Remodelling Vessels. A: Representative images of 3, 7 and 14 day post ligation vessels labelled with anti-Patched 1, B: Corresponding confocal images of Sca1 3, 7 and 14 day post ligation vessels. (N ≥ 3). Scale bars represent 100 microns.

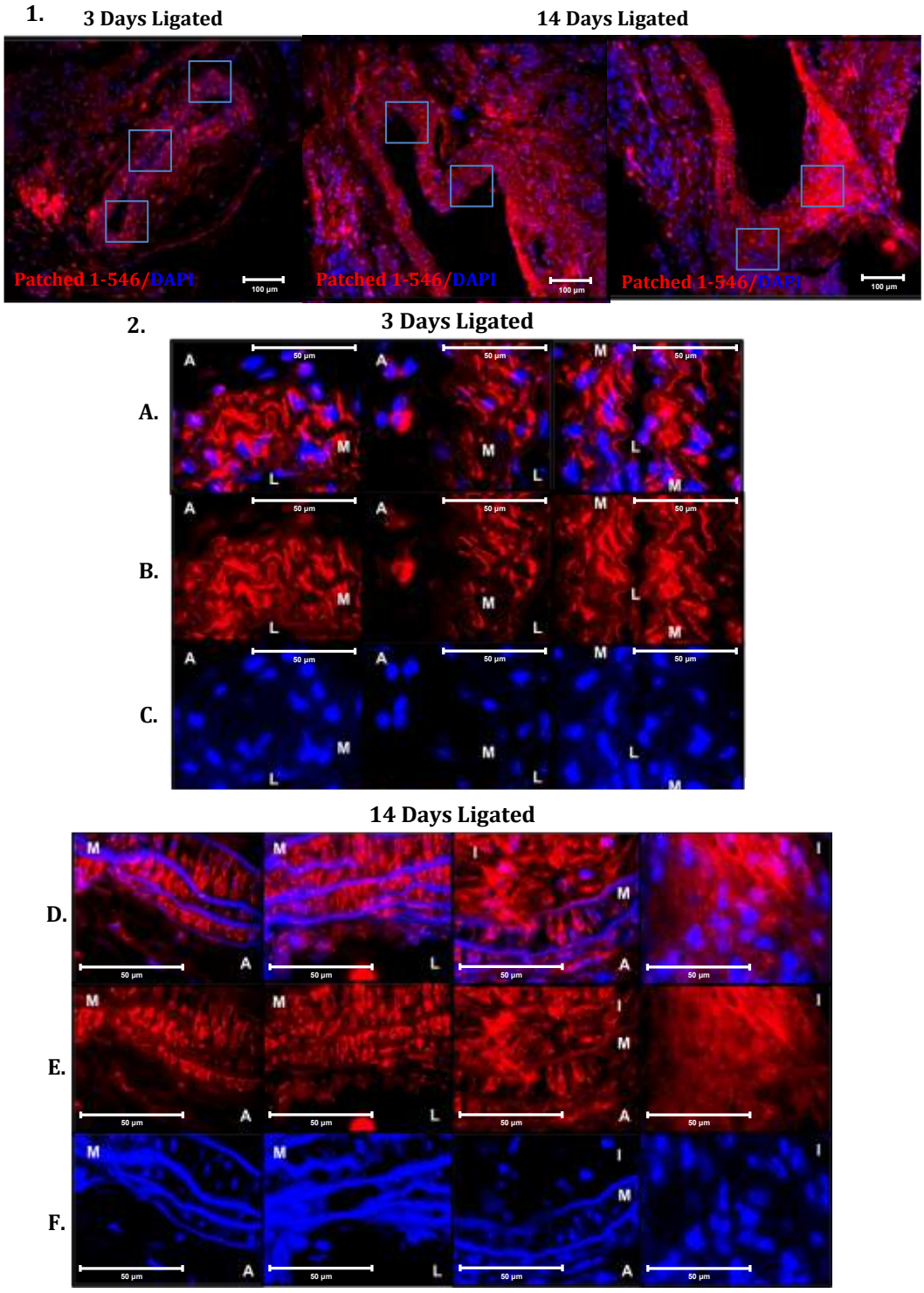

Figure 5.13: Hh Signalling Receptor Patched 1 Expression in Remodelling Vessels (3 Vs. 14 Day Ligated). 1: Low magnification representative images of 3 and 14 day post ligated vessels labelled with anti-Patched 1 and nuclear stained with DAPI, 2. High magnification representative images of 1, 2A + 2D: Representative images of 3 and 14 day post ligation vessels labelled with anti-Patched 1 and nuclear stained with DAPI, 2B + 2E: Corresponding images of 3 and 14 day post ligation vessels labelled with anti-Patched 1, 2C + 2F: Corresponding images of 3 and 14 day post ligation vessels labelled with nuclear stain DAPI, n ≥ 3, Scale bars represent 50 microns.

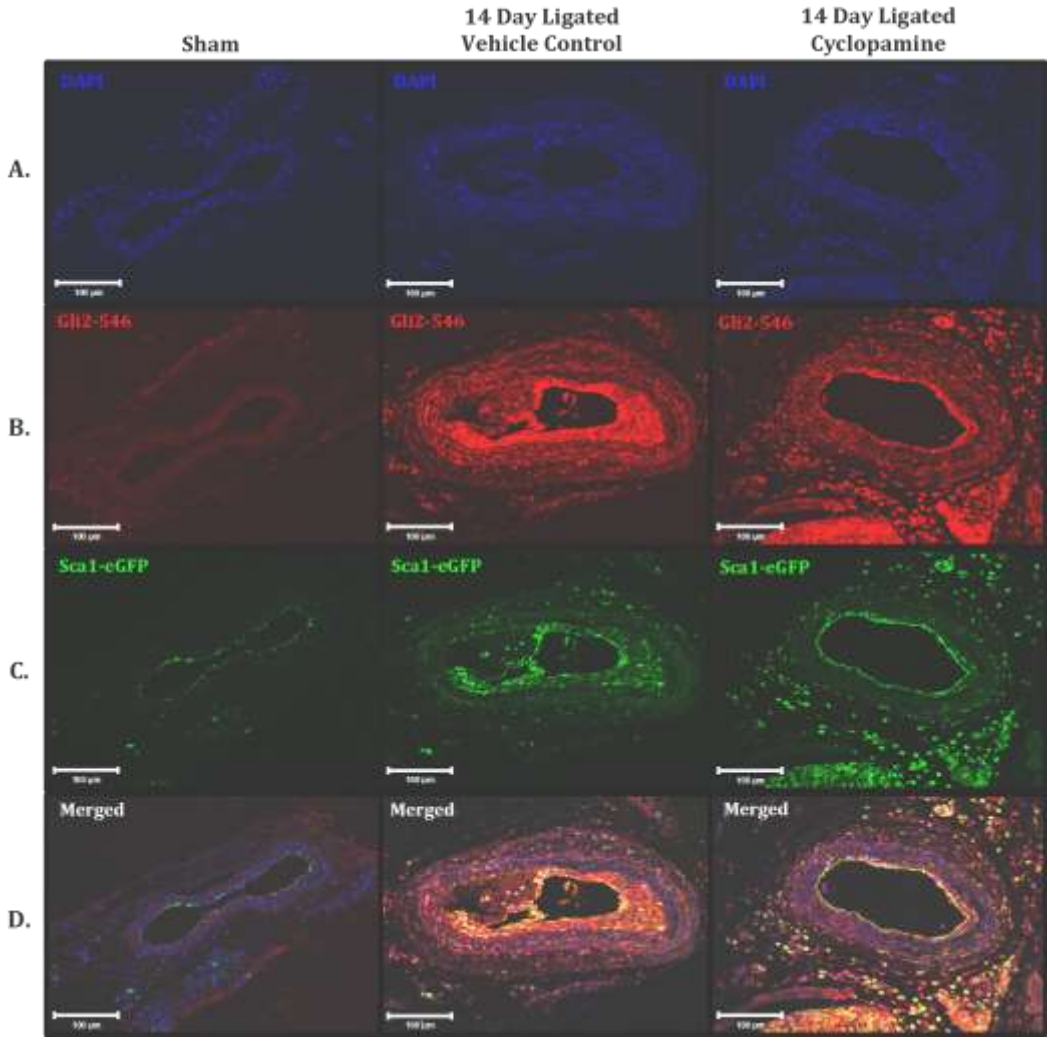

Figure 5.14: Hh Signalling Target Gene Gli2 Expression in Remodelling Vessels (Sham Vs. 14 Day Ligated Vehicle Control Vs. 14 Day Ligated Cyclopamine). A: Representative DAPI images of sham, 14 day ligated vehicle control and 14 day ligated cyclopamine, B: Corresponding representative Gli2 images of sham, 14 day ligated vehicle control and 14 day ligated cyclopamine, C: Corresponding representative Sca1 images of sham, 14 day ligated vehicle control and 14 day ligated cyclopamine, D: Corresponding representative merged images of sham, 14 day ligated vehicle control and 14 day ligated cyclopamine. (N ≥ 3). Scale bars represent 100 microns.

5.2.8 MVSC Identification: Expression of the Glial Cell Marker S100β

Carotids were assessed for the presence of the Glial cell marker S100β, and show little to no cells expressing S100β (Figures 5.16 and 5.17). Representative image analysis indicates the presence of a few adventitial S100β positive cells in untouched vessels and a discrete population of S100β^{+} intimal cells in 7 and possibly 14 day post ligation vessels (Figures 5.15 and 5.16). However, S100β positive cells are not populous enough to define the

tissue, therefore it is suggested that adventitial, medial and intimal cells cannot be defined as S100β⁺ in nature.

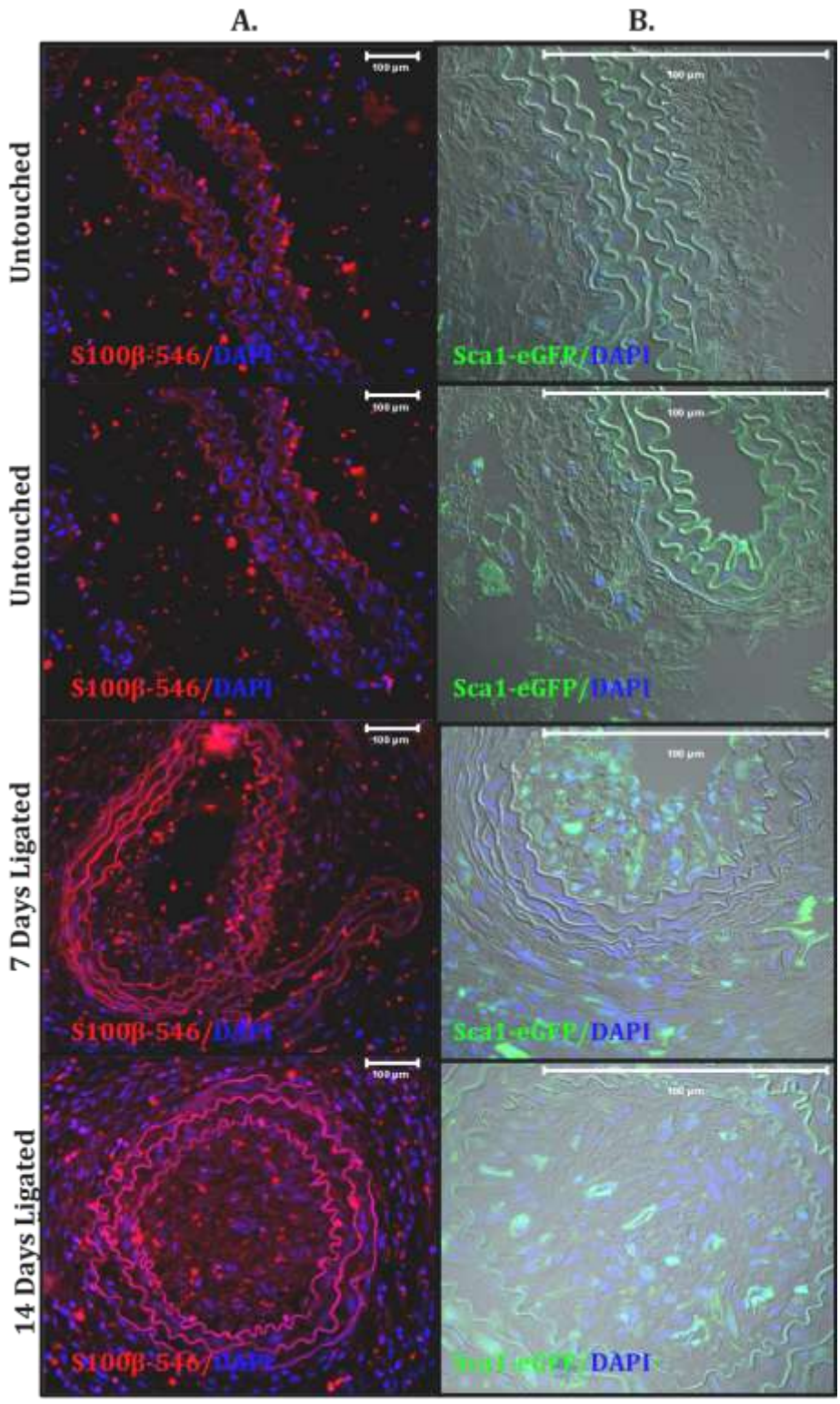

Figure 5.15: Glial Cell Marker S100β Expression in Remodelling Vessels. A: Representative images of untouched, 7 and 14 day post ligation vessels labelled with anti-S100β, B: Corresponding confocal images of Sca1 untouched, 7 and 14 day post ligation vessels., n ≥ 3, scale bars represent 100 microns.

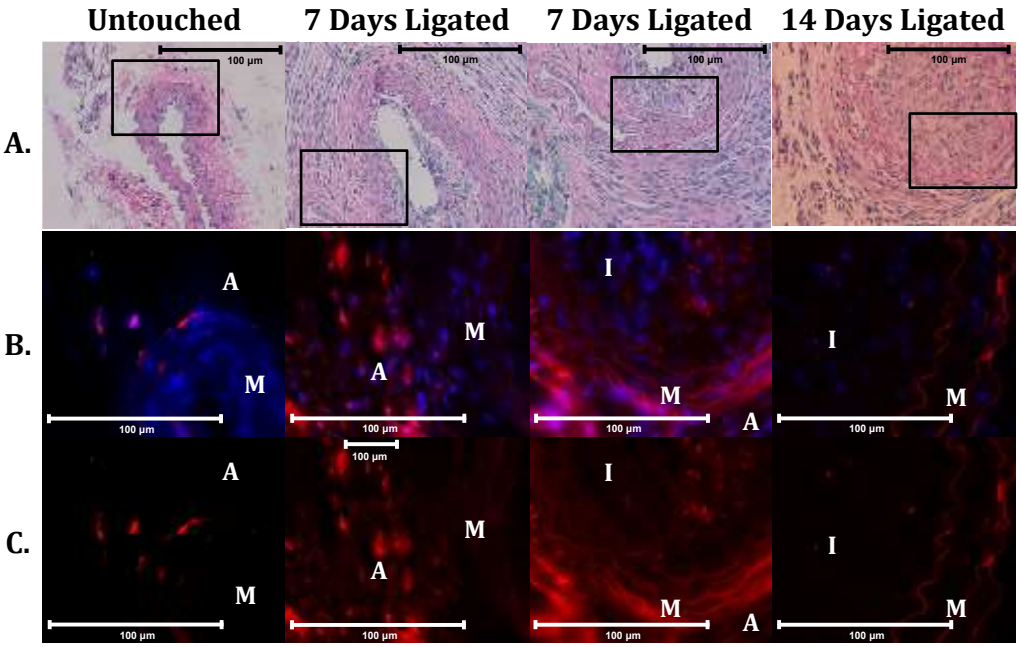

Figure 5.16: Glial Cell Marker S100β Expression in Remodelling Vessels. A: Representative H + E stained brightfield images of untouched, 7 and 14 day post ligation vessels, B: Corresponding images of untouched, 7 and 14 day post ligation vessels labelled with anti-S100β and nuclear stained with DAPI, C: Corresponding images of untouched, 7 and 14 day post ligation vessels labelled with anti-S100β, n ≥ 3, scale bars represent 100 microns.

5.2.9 MVSC Identification: Expression of the Neural Stem Cell Markers Sox 10 and Nestin.

Carotids were assessed for the presence of the Neural Stem Cell marker Sox 10 and show little to no cells expressing Sox 10 (Figures 5.17 and 5.18). Represenative image analysis indicates the presence of a couple of medial Sox 10^+ cells in untouched vessels and a few medial and intimal cells in 14 day post ligation vessels (Figures 5.17 and 5.18). However, Sox 10^+ cells are not populous enough to define the tissue therefore it is suggested that adventitial, medial and intimal cells cannot be defined as Sox 10^+ in nature. On the other hand Nestin analysis shows that Nestin is not expressed in untouched, 3 and 7 day post ligation vessels, however they appear in the media and intima 14 day post ligation (Figures 5.19 - 5.21). This suggests that a population of medial and intimal cells can be defined as Nestin$^+$ in nature.

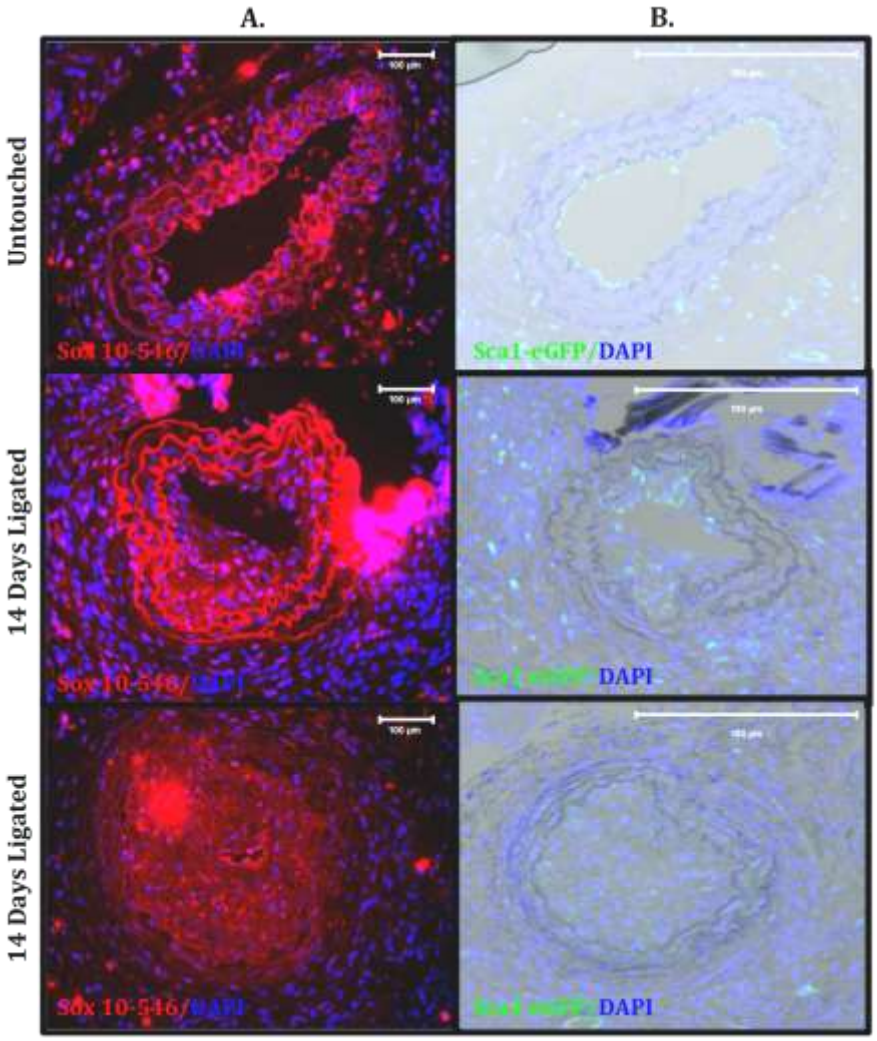

Figure 5.17: Neural Stem Cell Marker Sox 10 Expression in Remodelling Vessels. A: Representative images of untouched and 14 day post ligation vessels labelled with anti-Sox 10, B: Corresponding confocal images of Sca1 untouched and 14 day post ligation vessels, n ≥ 3, scale bars represent 100 microns.

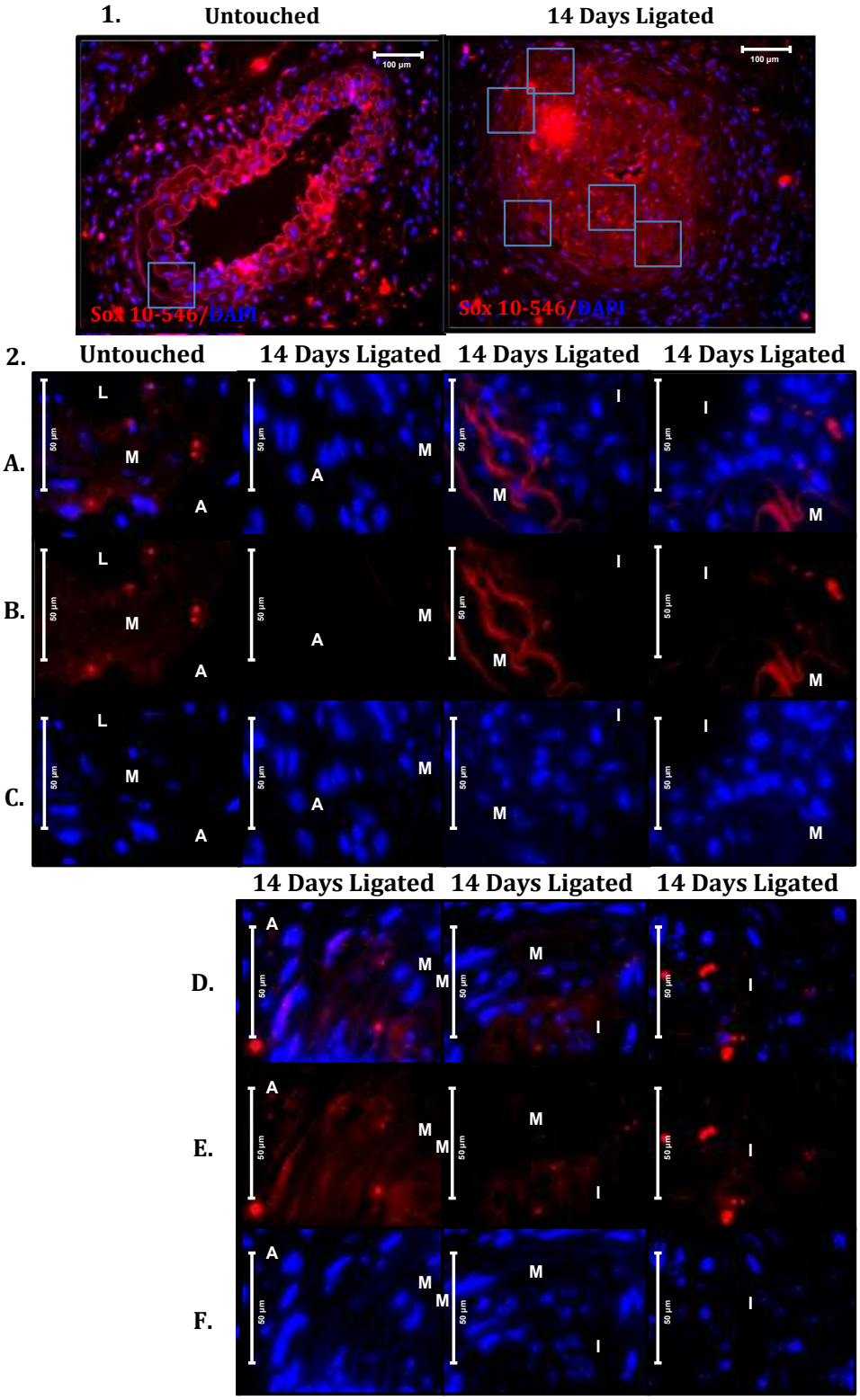

Figure 5.18: Neural Stem Cell Marker Sox 10 Expression in Remodelling Vessels. 1: Low magnification representative images of untouched and 14 day post ligated vessels labelled with anti-Sox 10 and nuclear stained with DAPI, 2. High magnification representative images of 1, 2A + 2D: Representative images of untouched and 14 day post ligation vessels labelled with anti-Sox 10 and nuclear stained with DAPI, 2B + 2E: Corresponding images of untouched and 14 day post ligation vessels labelled with anti-Sox 10, 2C + 2F: Corresponding images of untouched and 14 day post ligation vessels labelled with nuclear stain DAPI, n ≥ 3, scale bars represent 50 microns.

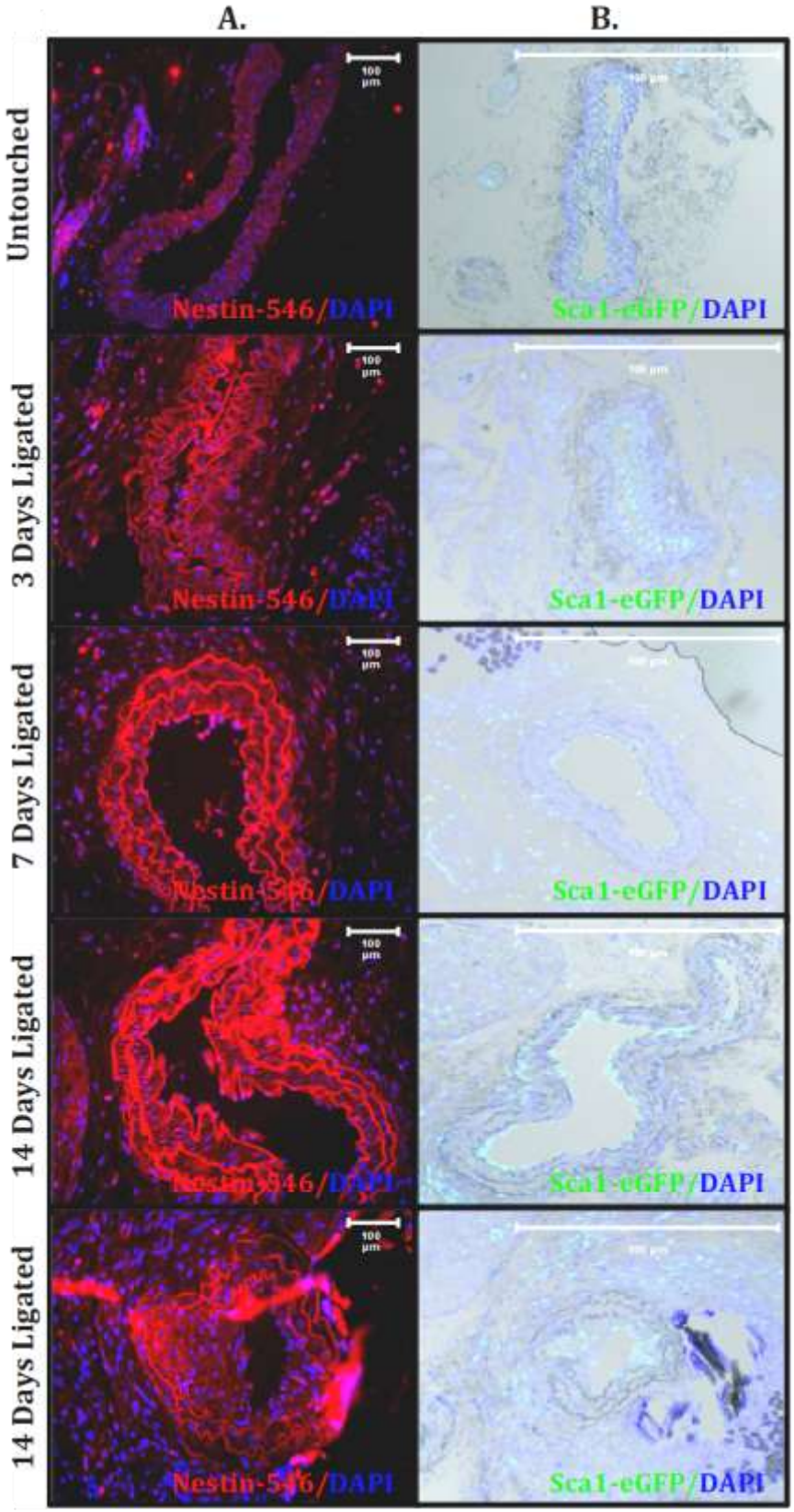

Figure 5.19: Neural Stem Cell Marker Nestin Expression in Remodelling Vessels. A: Representative images of untouched, 3, 7 and 14 day post ligation vessels labelled with anti-Nestin, B: Corresponding confocal images of Sca1 untouched, 3, 7 and 14 day post ligation vessels, n ≥ 3, scale bars represent 100 microns.

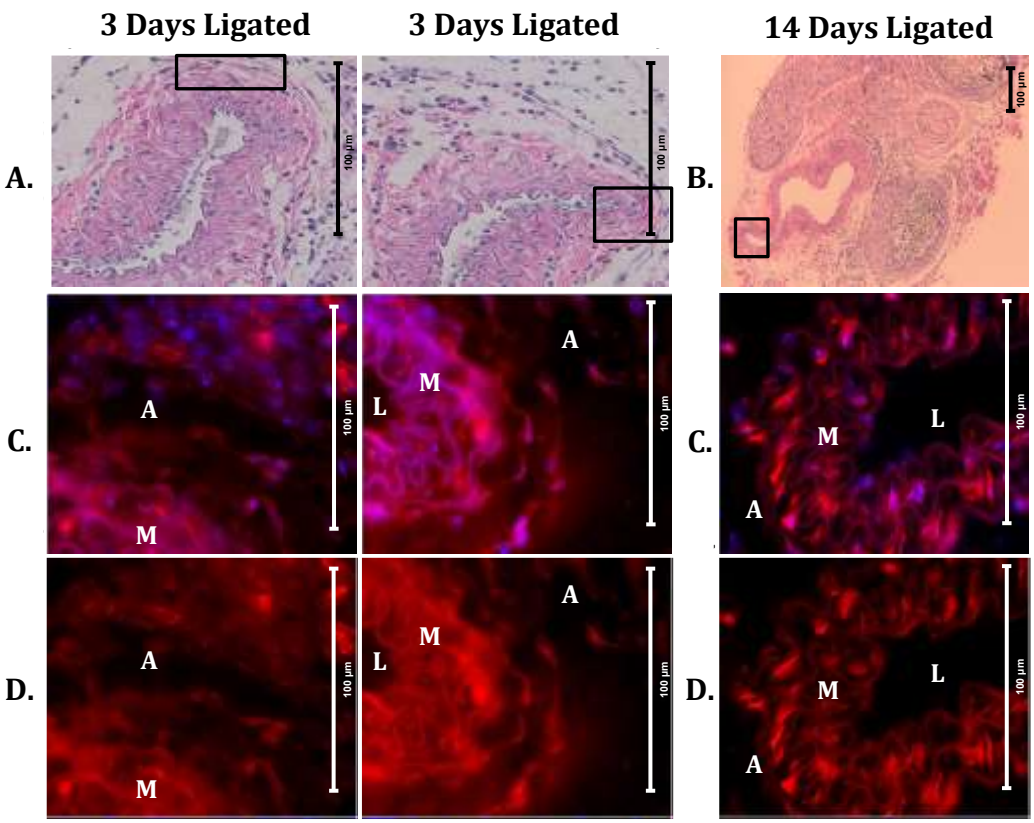

Figure 5.20: Neural Stem Cell Marker Nestin Expression in Remodelling Vessels (3 Day Vs. 14 Day Ligated). A: Representative H + E stained images of 3 day post ligation vessels, B: Representative H + E stained image of 14 day post ligation vessels, C: Representative images of 3 and 14 day post ligation vessels labelled with anti-Nestin and nuclear stained with DAPI, D: Representative images of 3 and 14 day post ligation vessels labelled with anti-Nestin, n ≥ 3, scale bars represent 100 microns.

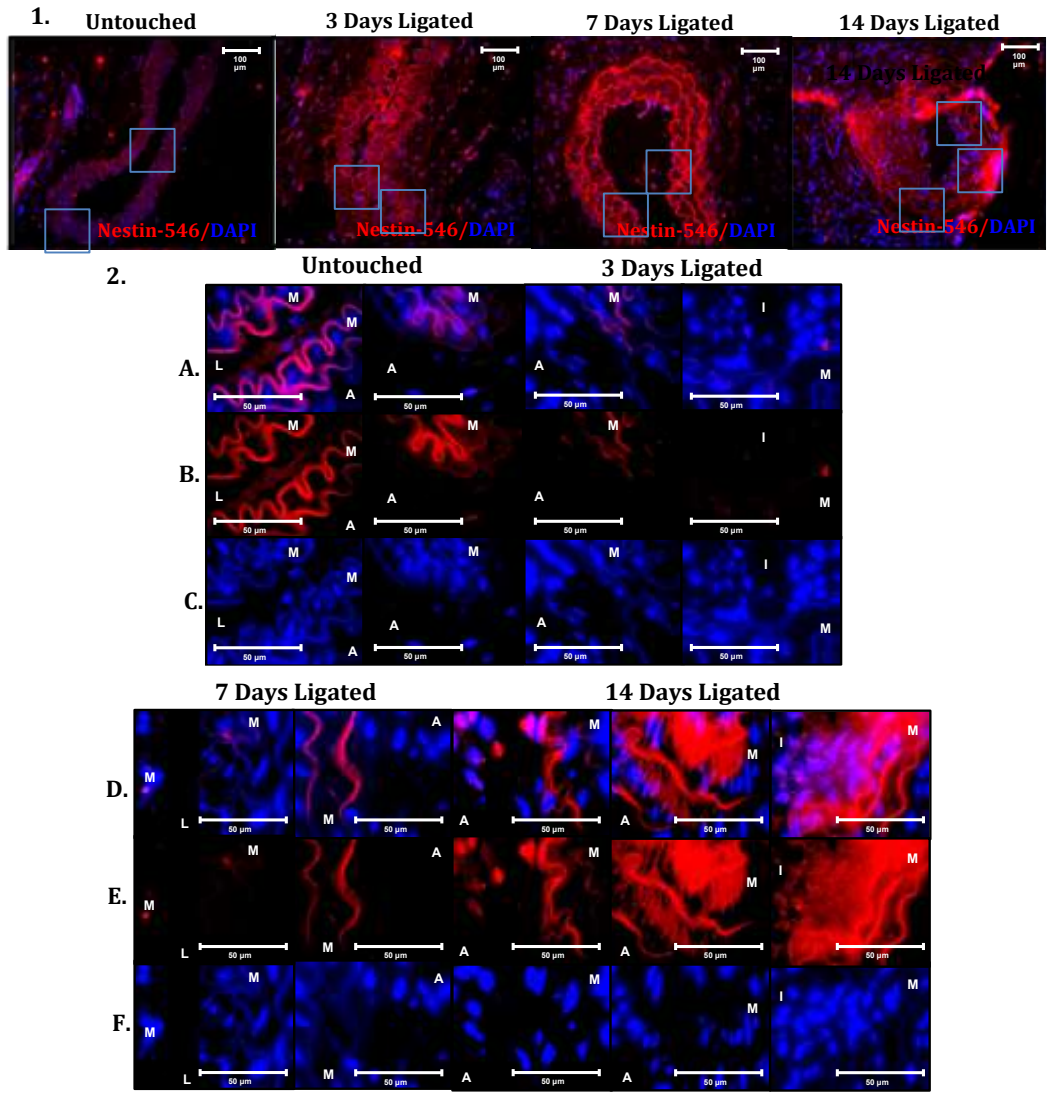

Figure 5.21: Neural Stem Cell Marker Nestin Expression in Remodelling Vessels. 1: Low magnification representative images of untouched, 3, 7 and 14 day post ligated vessels labelled with anti-Nestin and nuclear stained with DAPI, 2. High magnification representative images of 1, 2A + 2D: Representative images of untouched, 3, 7 and 14 day post ligation vessels labelled with anti-Nestin and nuclear stained with DAPI, 2B + 2E: Corresponding images of untouched, 3, 7 and 14 day post ligation vessels labelled with anti-Nestin, 2C + 2F: Corresponding images of untouched, 3, 7 and 14 day post ligation vessels labelled with nuclear stain DAPI, n ≥ 3, scale bars represent 50 microns.

5.2.10 MVSC Identification: Expression of the Endodermal and Hematopoietic Cell Marker Sox 17

Carotids were assessed for the presence of the Endodermal and Hematopoietic Cell marker Sox 17 and show little to no cells expressing Sox 17 (Figures 5.22 – 5.24). Representative image analysis indicates a lack of Sox 17^{+} cell in untouched, 7 and 14 day post ligation vessels (Figures 5.22 - 5.24). There seems to be a couple of Sox 17^{+} cells in the 14 day post ligated

vessels however they are a minority, therefore it is suggested that adventitial, medial and intimal cells cannot be defined as Sox 17^{+} in nature.

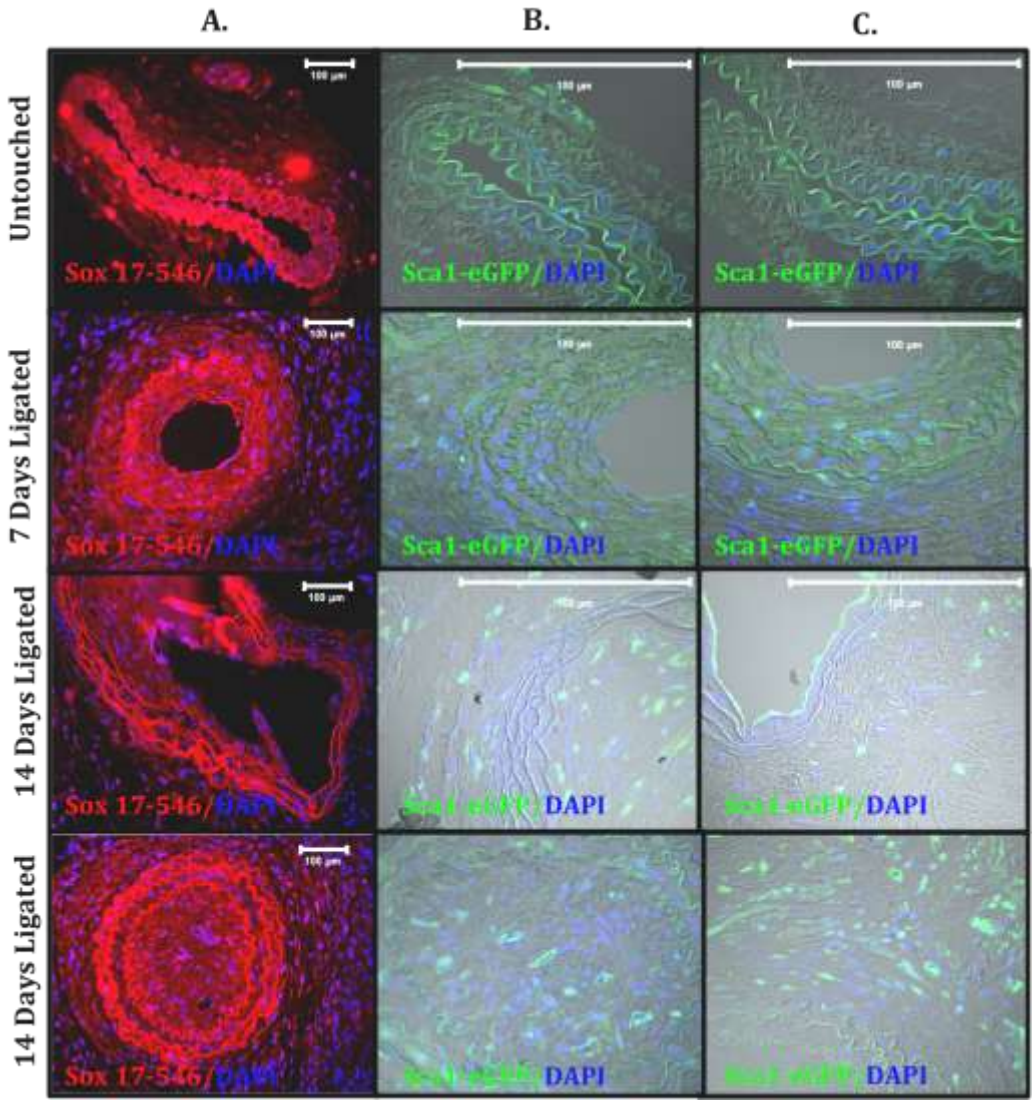

Figure 5.22: Endodermal and Hematopoietic Marker Sox 17 Expression in Remodelling Vessels. A: Representative images of untouched, 7 and 14 day post ligation vessels labelled with anti-Sox 17, B + C: Corresponding confocal images of Sca1 untouched, 7 and 14 day post ligation vessels. (N ≥ 3). Scale bars represent 100 microns.

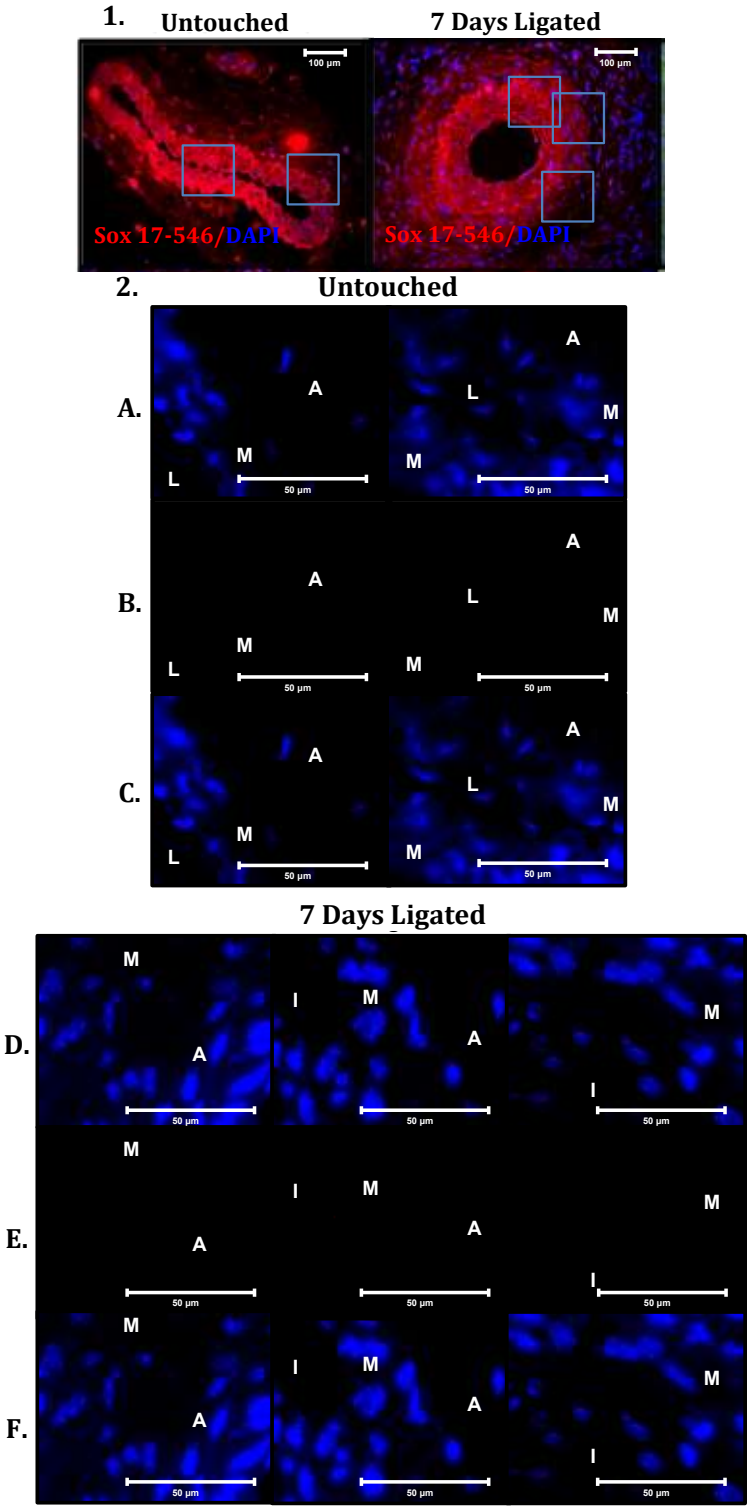

Figure 5.23: Endodermal and Hematopoietic Marker Sox 17 Expression in Remodelling Vessels (Untouched and 7 Day Ligated). 1: Low magnification representative images of untouched and 7 day post ligated vessels labelled with anti-Sox 17 and nuclear stained with DAPI, 2. High magnification representative images of 1, 2A + 2D: Representative images of untouched and 7 day post ligation vessels labelled with anti-Sox 17 and nuclear stained with DAPI, 2B + 2E: Corresponding images of untouched and 7 day post ligation vessels labelled with anti-Sox 17, 2C + 2F: Corresponding images of untouched and 7 day post ligation vessels labelled with nuclear stain DAPI, n ≥ 3, scale bars represent 50 microns.

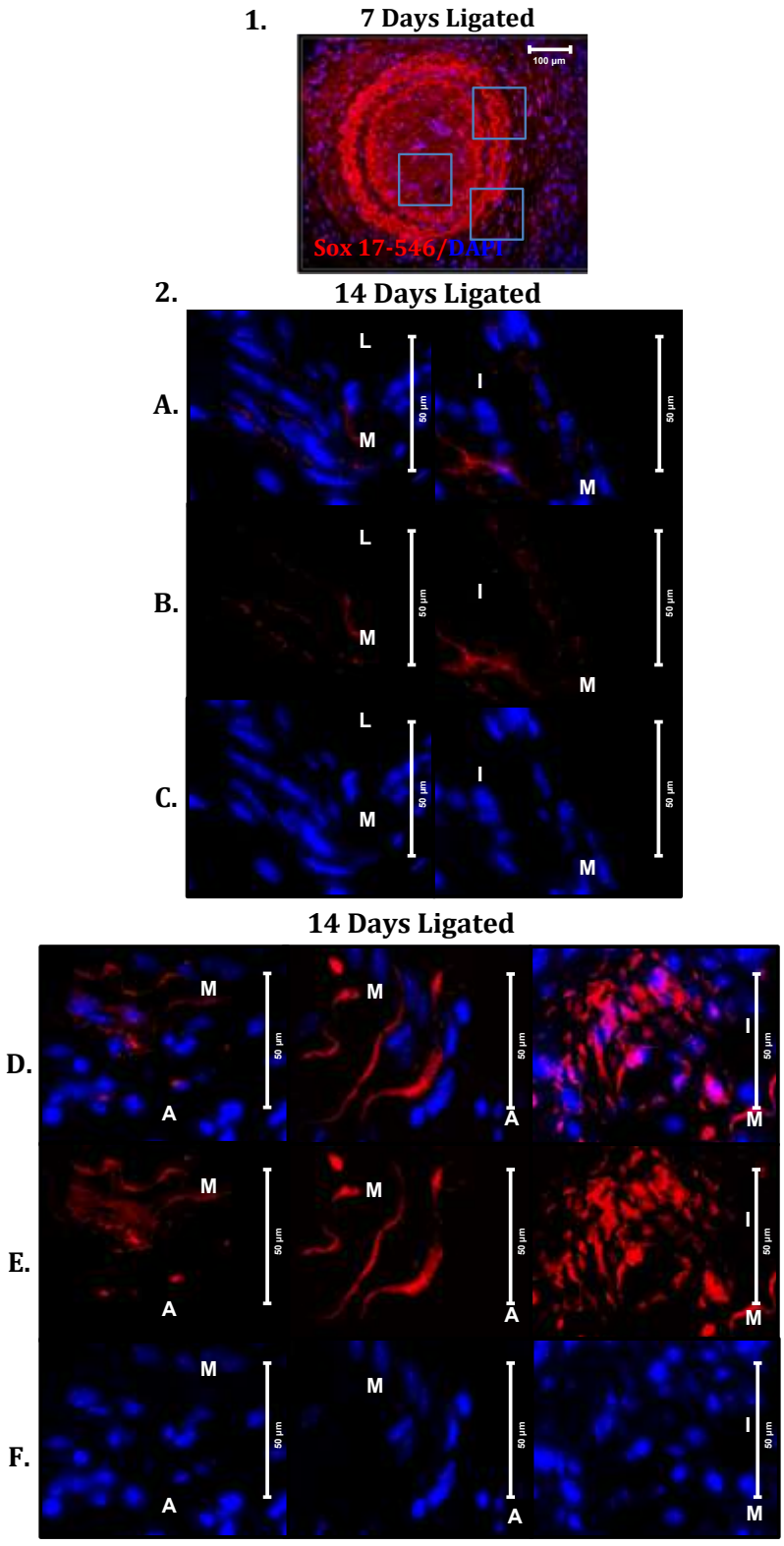

Figure 5.24: Endodermal and Hematopoietic Marker Sox 17 Expression in Remodelling Vessels (14 Day Ligated). 1: Low magnification representative images of 14 day post ligated vessels labelled with anti-Sox 17 and nuclear stained with DAPI, 2. High magnification representative images of 1, 2A + 2D: Representative images of 14 day post ligation vessels labelled with anti-Sox 17 and nuclear stained with DAPI, 2B + 2E: Corresponding images of 14 day post ligation vessels labelled with anti-Sox, 2C + 2F: Corresponding images of 14 day post ligation vessels labelled with nuclear stain, n ≥ 3, scale bars represent 50 microns.

5.2.11 Sca1 Expression in Whole Tissue

Considering that Sca1$^+$ cells are known to be enriched in the adventitia around the aortic root during development, whole mounted aortic sections were assessed for Sca1 enrichment (especially since cross sections suggest few adventitial cells/high power field (hpf)) (Passman et al. 2008). On examining the aorta, it was noticeable that Sca1$^+$ (eGFP) cells were enriched at the aortic arch, and dissipate distal to the ascending aorta and arch (Figures 5.25 and 5.27 – 5.29). Interestingly, Sca1 enrichment was also observed to be associated with aortic branches and carotid-associated nerves, hence the interest in neural circuits that may have Sca1 enrichment (Figures 5.25, 5.27 – 5.31). Therefore whole carotids, carotid associated nerve-like structures and aortas were mounted and assessed by fluorescent microscopy for the expression of Sca1-eGFP. The Thy-1-YFP mice described are B6.Cg-Tg(Thy1-YFP)16Jrs/J and axons in the motor and sensory nerves will express YFP. Analysis shows that the aortic Sca1$^+$ signatures observed are not neuronal (Figure 5.25.A). Sca1 expression assessment in a whole mounted carotid show Sca1-eGFP expression in discrete locations as well as carotid branches and small intricate networks surrounding the mounted vessel (Figure 5.26). Detailed Sca1-eGFP expression was observed along the length of an aorta (Figures 5.27 – 5.29). Sca1-eGFP expression in the aorta is similar to that of a carotid where Sca1-eGFP expression is observed in discrete locations as well as carotid branches and small intricate networks surrounding the mounted vessel. Representative images of the carotid associated nerve-like structures show Sca1-eGFP expression in what could be suggested as connective tissue, as well as in defined axon-like fibres within the structure (Figures 5.30 and 5.31).

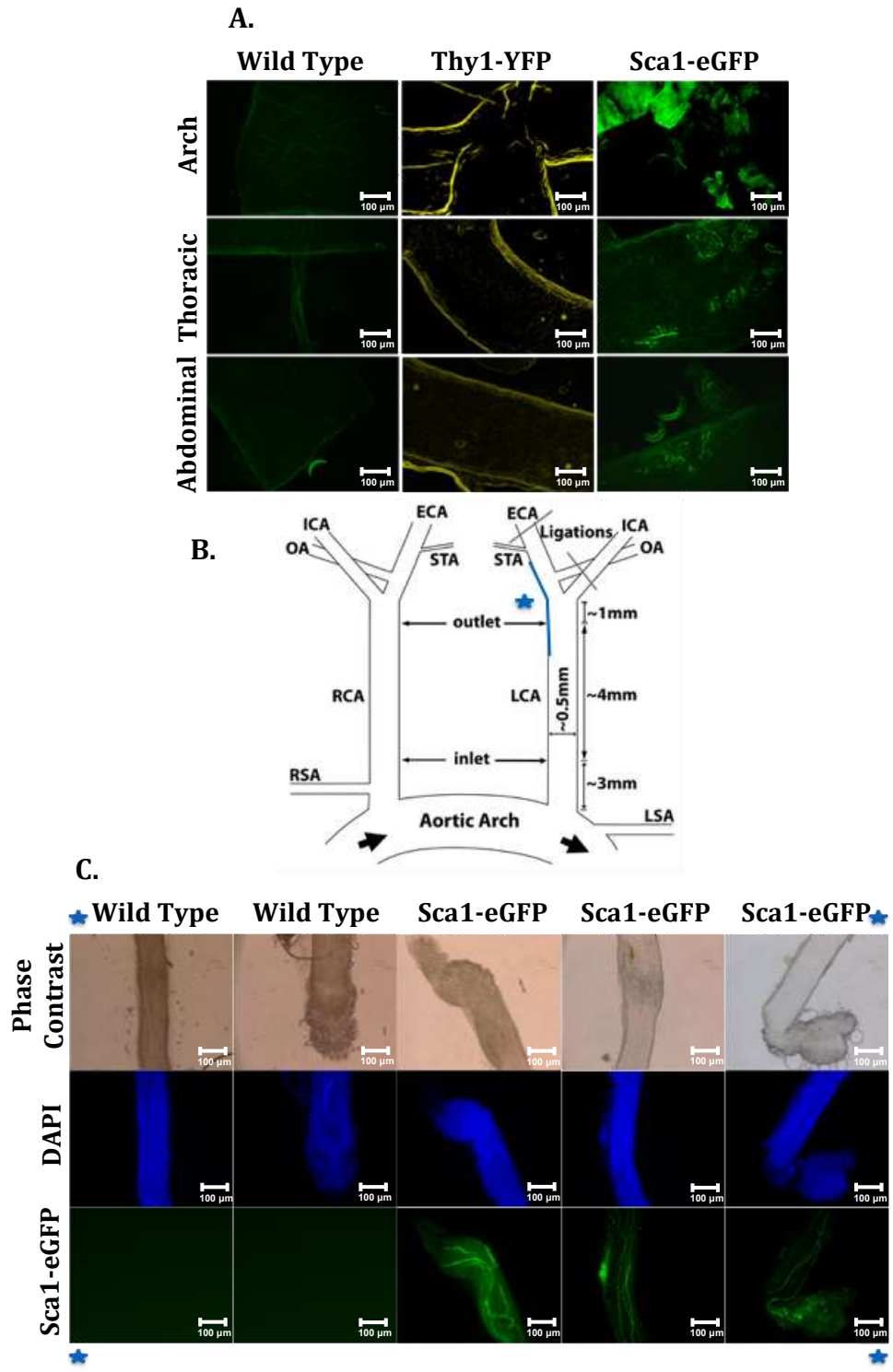

Figure 5.25: Aortic and Carotid-Associated Nerve Sca1 Expression. A: Representative images of whole mounted aortic arches, thoracic and abdominal regions of wild type, Thy1-YFP and Sca1-eGFP mice (N ≥ 3), B: Diagram of vascular network and ligation points (ECA: external carotid artery, ICA: internal carotid artery, STA: superficial temporal artery, OA: ophthalmic artery, RCA: right carotid artery, LCA: left carotid artery, RSA: right subclavian artery, LSA: left subclavian artery), C: Representative images of whole mounted carotid-associated nerve in wild type and Sca1-eGFP mice, n≥ 3, scale bars represent 100 microns.

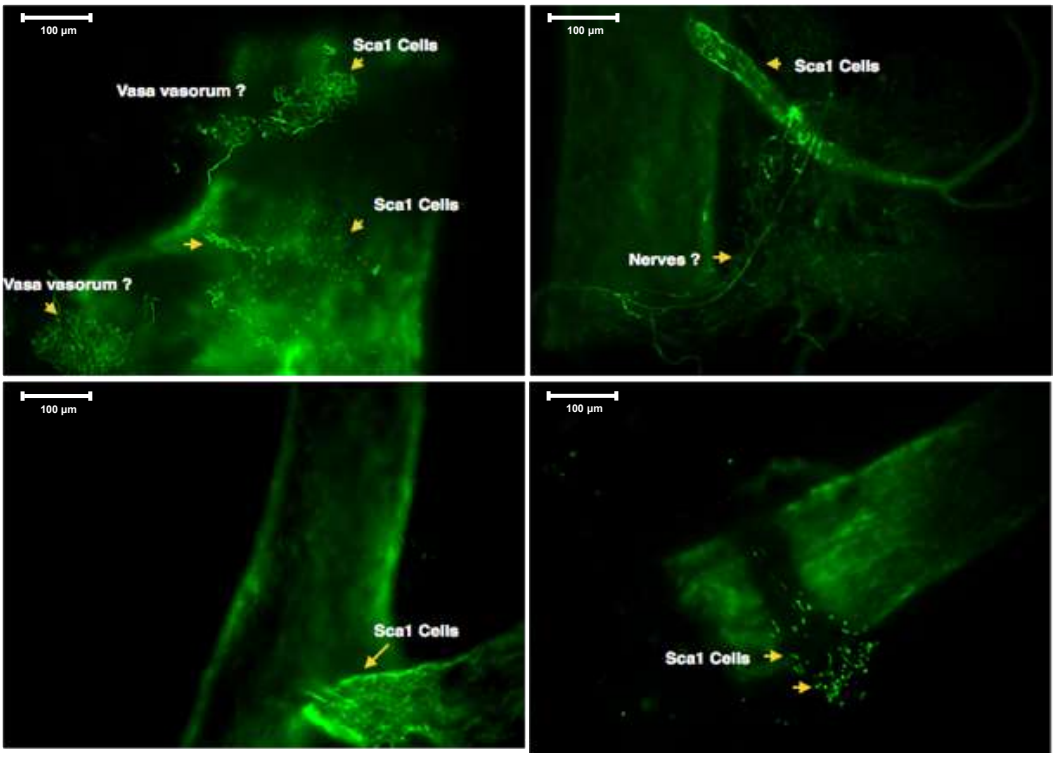

Figure 5.26: Whole Mount Carotid Sca1 Expression. Representative fluorescence images of whole mounted carotid arteries of Tg(Ly6a-EGFP)G5Dzk transgenic mice, n ≥ 20, scale bars represent 100 microns.

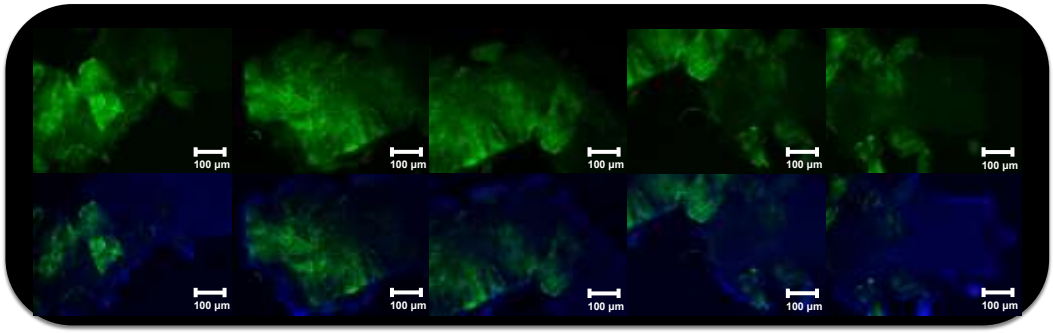

Figure 5.27: Whole Mount Aortic Arch Sca1 Expression. Representative fluorescence images of whole mounted aortic arch of Tg(Ly6a-EGFP)G5Dzk transgenic mice, n ≥ 20, scale bars represent 100 microns.

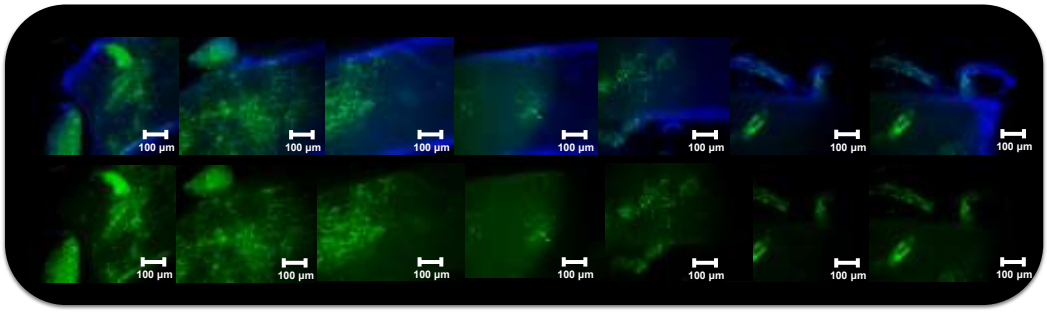

Figure 5.28: Whole Mount Thoracic Aorta Sca1 Expression. Representative fluorescence images of whole mounted aorta thoracic region of Tg(Ly6a-EGFP)G5Dzk transgenic mice, n ≥ 20, scale bars represent 100 microns.

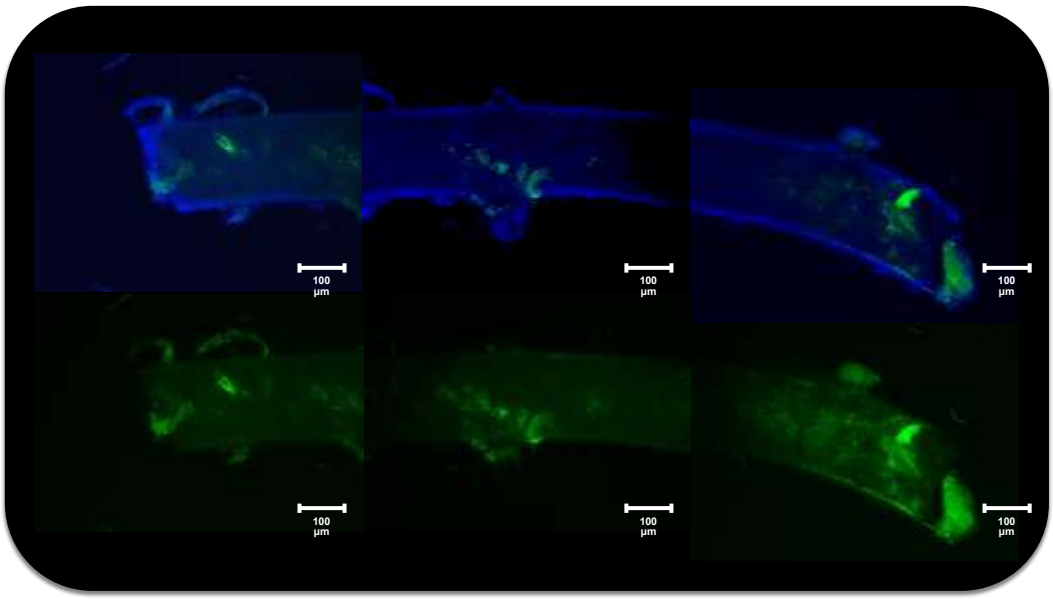

Figure 5.29: Whole Mount Abdominal Aorta Sca1 Expression. Representative fluorescence images of whole mounted aorta abdominal region of Tg(Ly6a-EGFP)G5Dzk transgenic mice, n ≥ 20, scale bars represent 100 microns.

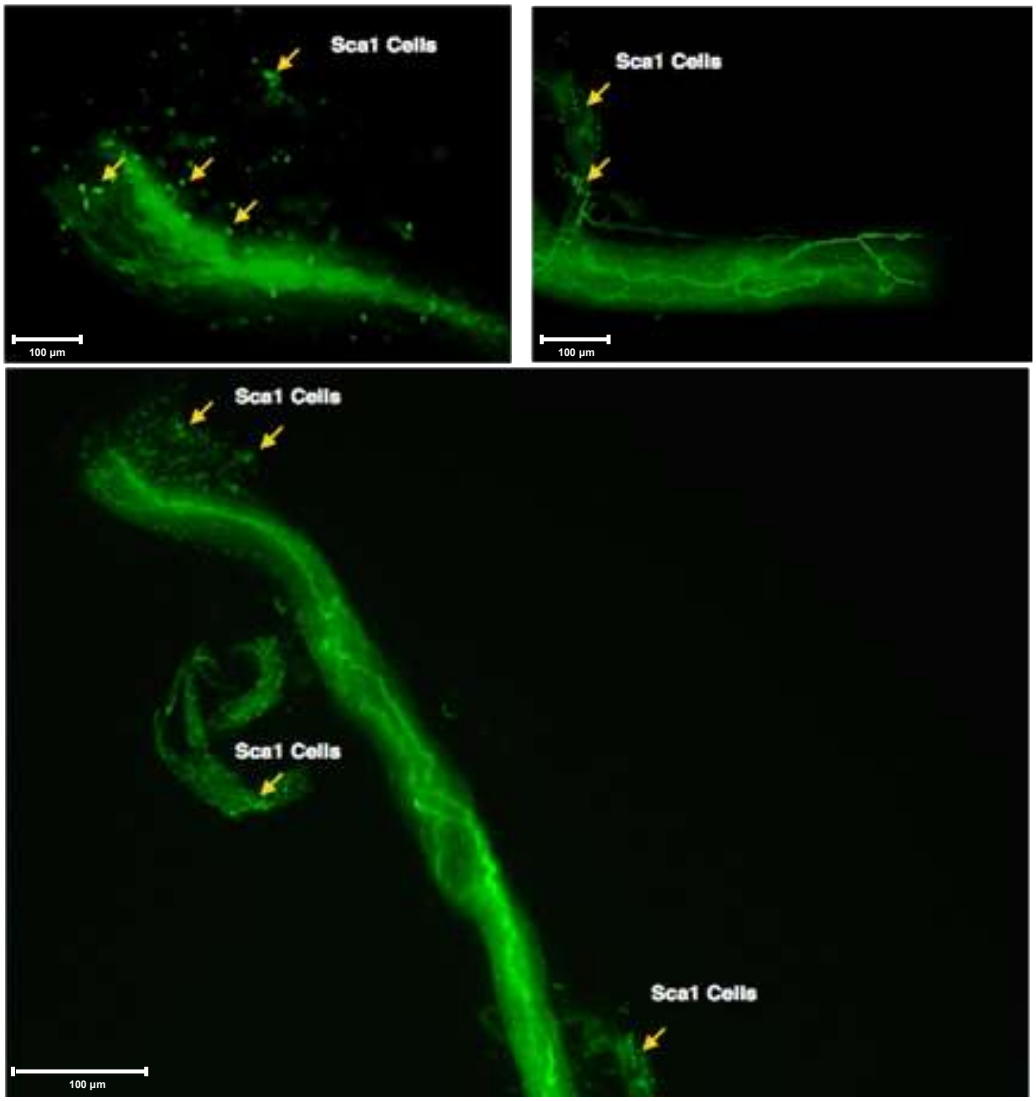

Figure 5.30: Whole Mount Left Carotid-Associated Nerve Sca1 Expression. Representative fluorescence images of whole mounted left carotid artery-associated nerve of Tg(Ly6a-EGFP)G5Dzk transgenic mice, n ≥ 15, scale bars represent 100 microns.

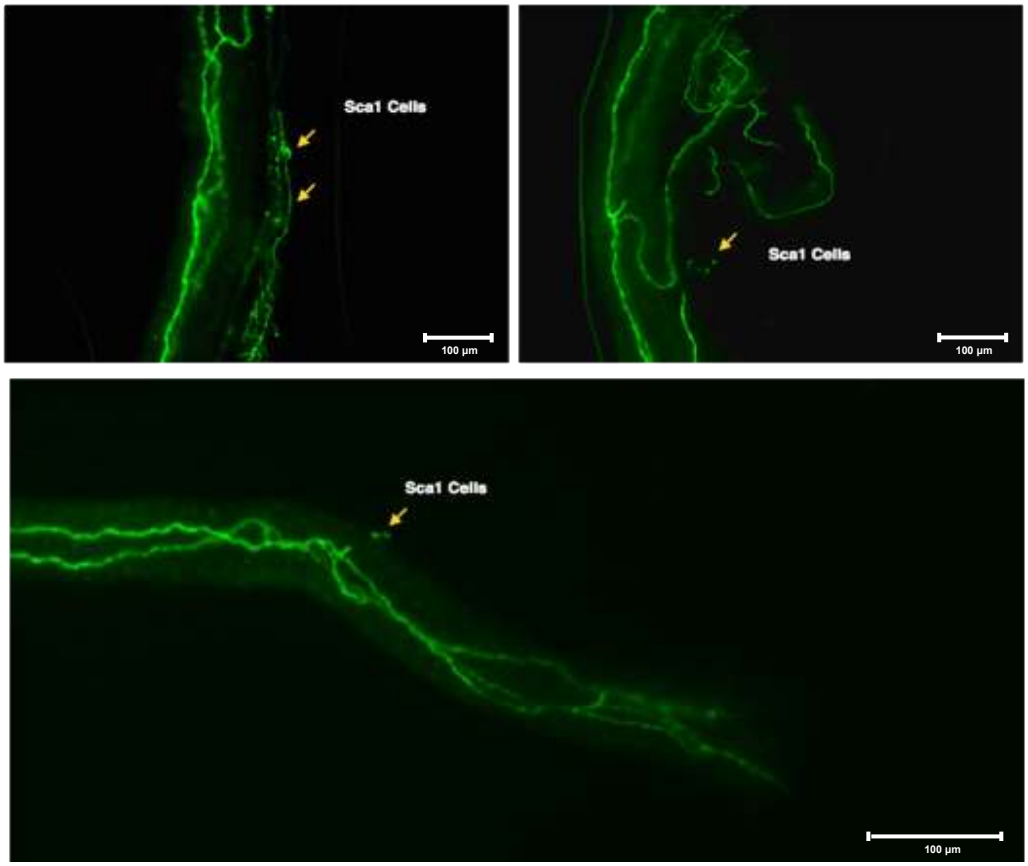

Figure 5.31: Whole Mount Right Carotid-Associated Nerve Sca1 Expression. Representative fluorescence images of whole mounted right carotid artery-associated nerve of Tg(Ly6a-EGFP)G5Dzk transgenic mice, n ≥ 15, scale bars represent 100 microns.

5.2.12 Axonal, Vascular Cell and Sca1 Expression in Whole Tissue

Following the observation of Sca1 populations identified by the whole mount fluorescent analysis, the axonal and vascular profile was investigated by probing for the axonal PNS and CNS marker Peripherin, the differentiated SMC marker SMMHC, and the endothelial marker eNOS. Firstly analysis shows that there are discrete neuronal signatures (Peripherin^{+}) observed on the surface of whole mounted aortas (Figure 5.32). Further analysis confirms that the suspected Sca1^{+} carotid-associated nerve like structure is a nerve (Figure 5.33). The Sca1^{+} structure within the nerve is the nerves vasculature (i.e the presence of SMMHC and eNOS in the nerve identifies a vessel within the nerve) (Figure 5.34).

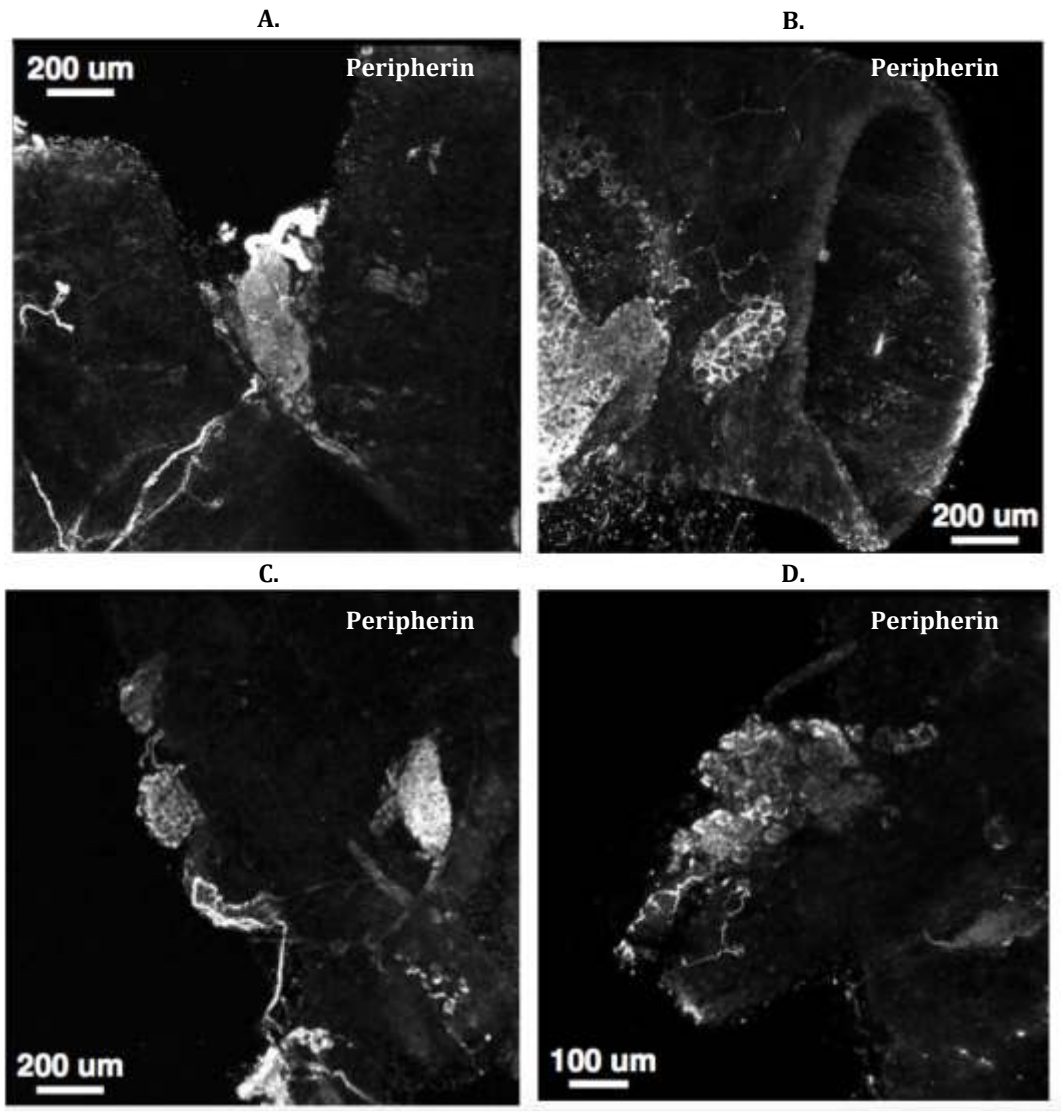

Figure 5.32: Whole Mount Aorta Peripherin Expression. A: Representative fluorescence images of whole mounted aortic arch (distal to heart and B) of Thy1-YFP mice labelled with anti-Peripherin, B: Representative fluorescence images of whole mounted aortic arch (laceration at point of contact with heart) of Thy1-YFP mice labelled with anti-Peripherin, C: Representative fluorescence images of whole mounted aorta (abdominal region – distal to A.) of Thy1-YFP mice labelled with anti-Peripherin, D: Representative fluorescence images of whole mounted aorta (abdominal region – distal to C.) of Thy1-YFP mice labelled with anti-Peripherin, $n \geq 3$.

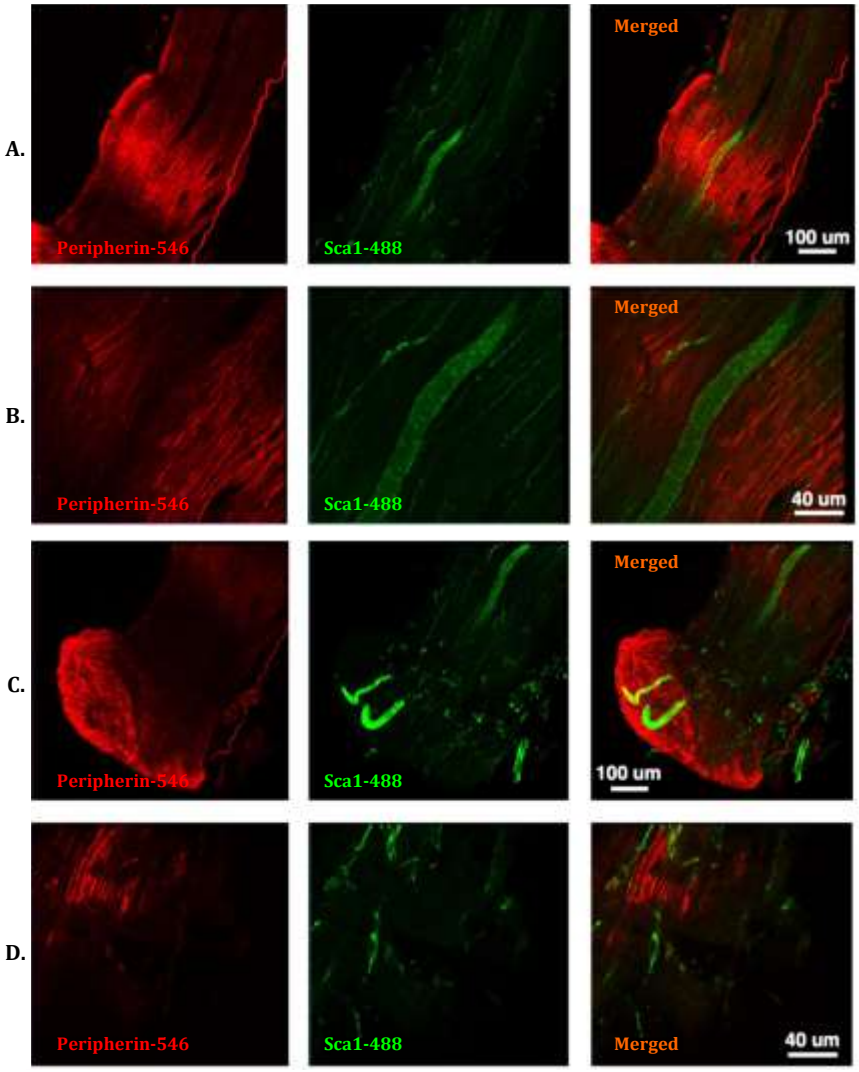

Figure 5.33: Whole Mount Carotid-Associated Nerve Expresses Sca1. A: Representative confocal images of whole mounted carotid-associated nerve labelled with Peripherin and Sca1 in Thy1-YFP mice, B: Representative confocal images of whole mounted carotid-associated nerve labelled with Peripherin and Sca1 in Thy1-YFP mice, C: Representative confocal images of whole mounted carotid-associated nerve surface labelled with Peripherin and Sca1 in Thy1-YFP mice, D: Representative confocal images of whole mounted carotid-associated nerve surface labelled with Peripherin and Sca1 in Thy1-YFP mice, $n \geq 3$.

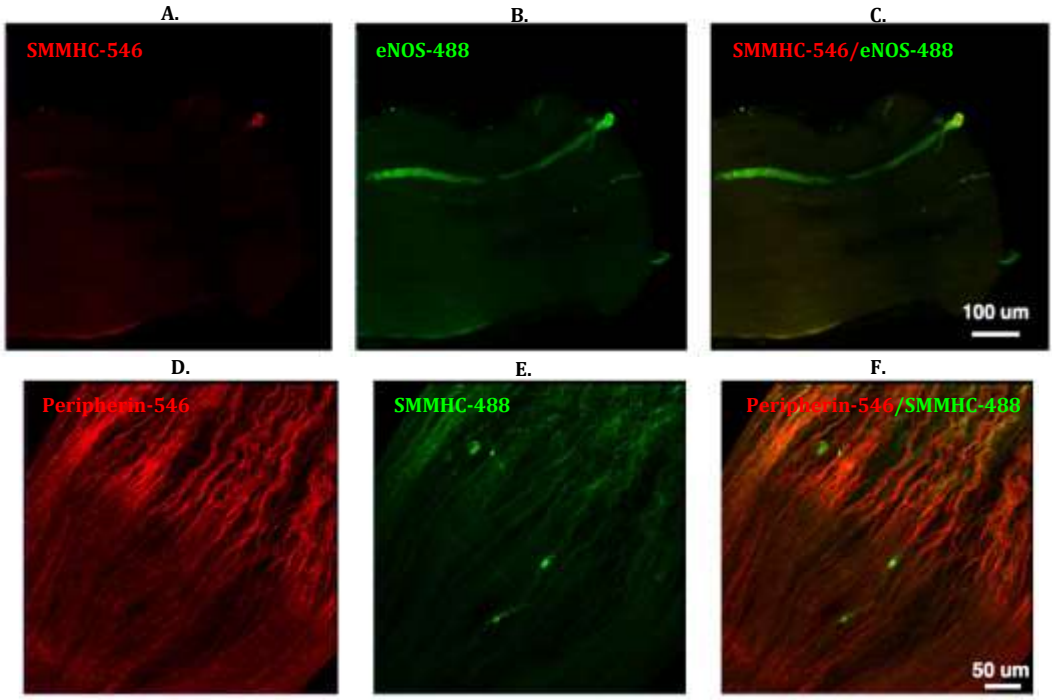

Figure 5.34: Whole Mount Carotid-Associated Nerve Expresses Endothelial (eNOS) and Differentiated SMC (SMMHC) Markers. A - C: Representative confocal images of whole mounted carotid-associated nerve labelled with SMMHC and eNOS in Thy1-YFP mice, D - F: Representative confocal images of whole mounted carotid-associated nerve labelled with Peripherin and SMMHC in Thy1-YFP mice, n ≥ 3.

5.2.13 Sca1 Expression in Humans

Human Sca1 expression is similar to that observed in mice, with Sca1 expression in the adventitial region of healthy human adult arteries and an increase in adventitial Sca1 expression in a human atherosclerotic aorta (Figure 5.35). Healthy versus atherosclerotic tissue in humans appears to have similar morphological trends to that observed in mice, with dramatic adventitial and medial thickening occurring in diseased tissue states. A significant increase in adventitial and medial expression of the pericyte marker α-Actin is also observed in human atherosclerotic tissue when compared to the healthy control artery.

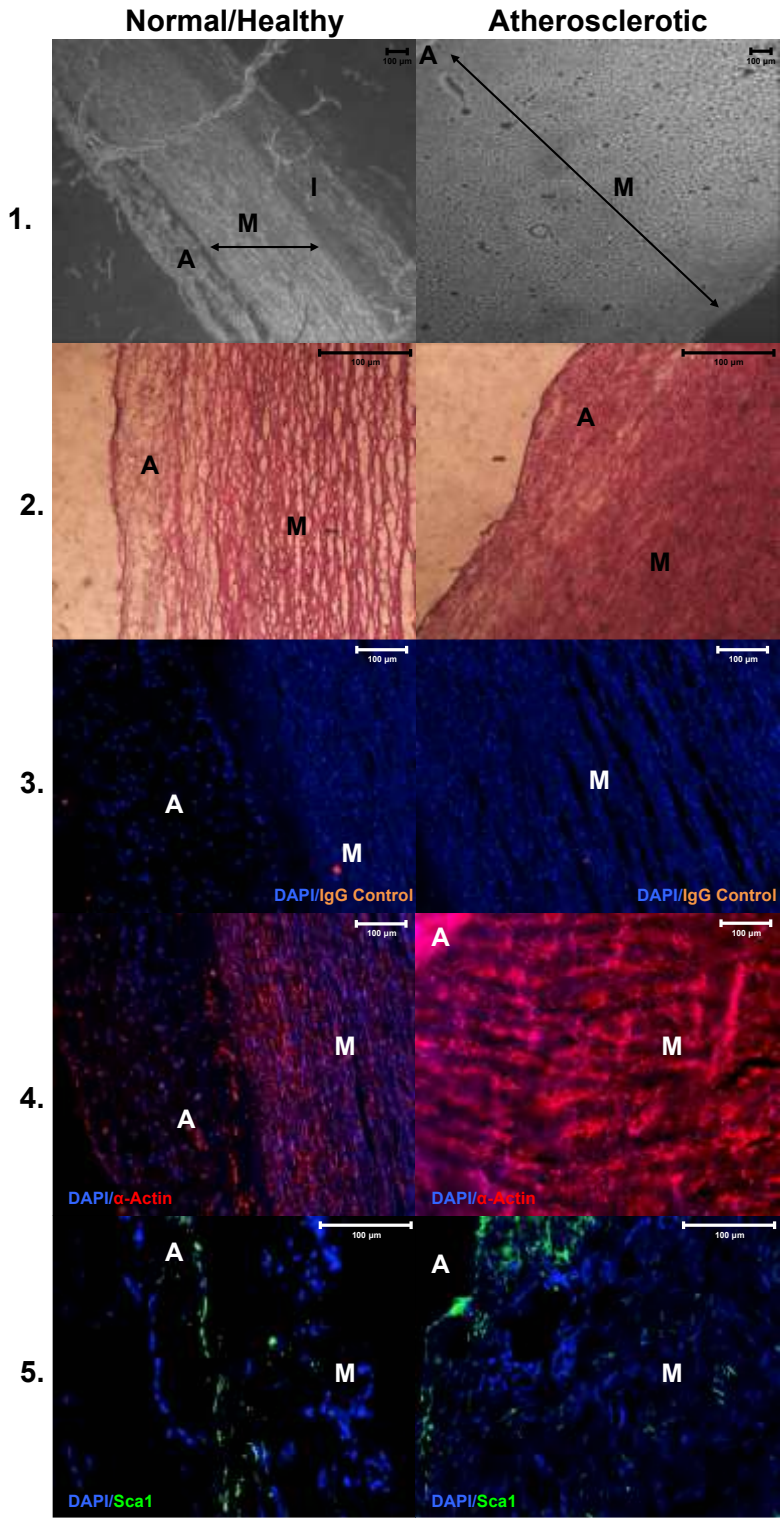

Figure 5.35: Sca1 Expression in Healthy and Atherosclerotic Human Aortas. 1: Representative phase contrast images of human adult healthy artery and human atherosclerotic aortic sections, 2: Representative H + E stained brightfield images of human adult healthy artery and human atherosclerotic aortic sections, 3: Representative IgG control (orange: 488 and 546) fluorescent images of human adult healthy artery and human atherosclerotic aortic sections, 4: Representative α-Actin fluorescent images of human adult healthy artery and human atherosclerotic aortic sections, 5: Representative Sca1 images of human adult healthy artery and human atherosclerotic aortic sections, n≥ 3, scale bars represent 100 microns.

5.3 Discussion

Sca1^{+} Cell Response during Vascular Remodelling

Analysis shows that during vascular remodelling, Sca1 expression is located primarily in the adventitia, medial/lumenal boundary (also reported by Tigges et al.,) and intimal formation, however Sca1^{+} medial cells have also been identified (Tigges et al. 2013). Sca1 expression is also dramatically increased 3 day after injury and continues until the vessel becomes occluded when Sca1 expression appears to diminish (Tigges et al., also report that Sca1 expression is rarely observed in neointimal cells 15 day post injury), indicating a role for Sca1^{+} cells during vascular remodelling (Tigges et al. 2013). Other groups have also shown evidence that Sca1^{+} cells are involved in the remodelling process both with respect to adventitial maintenance and vascular cell type expansion and differentiation, all of which collectively bolster the theory.

Evidence that Sca1^{+} cells expand and contribute to the accummulation of vSMC during vascular remodelling

Shikatani et al., used a c-Myb (transcription factor and stem cell regulator) deficient mouse model (*c-myb*$^{h/h}$) and found similar adventitial and medial thickening in *c-myb*$^{h/h}$ and *c-myb*^{WT} (control) mice 8 day post injury, however *c-myb*$^{h/h}$ mice had reduced remodelling in 14 and 28 day post injury, indicating that c-Myb activity is crucial to active remodelling long after the initial injury response has occurred (Shikatani et al. 2016). Shikatani et al., also assessed *c-myb*$^{h/h}$ and *c-myb*^{WT} mice for Sca1, and found increased adventitial Sca1^{+} cell levels in 14 and 28 day post injury *c-myb*^{WT} mice, and significantly reduced Sca1^{+} cell levels in 14 and 28 day post injury *c-myb*$^{h/h}$ mice, indicating that c-Myb is involved in Sca1^{+} cell expansion post injury (Shikatani et al. 2016). Importantly Shikatani et al., confirmed that > 99 % of all adventitial Sca1^{+} cells (carotid and aortic) were derived from the resident vessel and not recruited by circulatory cells, and that c-Myb regulates a specific Sca1^{+} APC (cKit^{+}CD34^{-}Flk1^{-}) during injury-induced vascular remodelling (Shikatani et al. 2016). Critically, Shikatani et al., *in vitro* analysis

shows that *c-myb*^{WT} Sca1^{+} APC can be differentiated into vSMC using TGFβ1 (significant upregulation of Calponin 1 and SMMHC) and interestingly, *c-myb*$^{h/h}$ Sca1^{+} APC do not, a process that is mirrored *in vivo* following analysis of endogenous vSMC gene expression, indicating that c-Myb is essential for Sca1^{+} APC differentiation to vSMC.

Additionally, it is important to note that Wan et al., also report Sca1^{+} cells as the contributory cell type in the development of intimal formation during vascular remodelling (Wan et al. 2012). Wan et al., show clear evidence that initial intimal cells are Sca1^{+} 7 day post injury, and that frontier cells during progressed vascular remodelling (intimal formation at 14 day post injury) are Sca1^{+} also (Wan et al. 2012).

<u>Evidence that Sca1^{+} cells expand and contribute to adventitial maintenance during vascular remodelling</u>

Interestingly, the previously mentioned Psaltis et al., (section 3.2) shows that during atherosclerosis, macrophage progenitor Sca1^{+}CD45^{+} APC levels are significantly increased, and are indicated to be the most actively proliferative cell type (proliferating APC account for 11.0 ± 1.0 % of adventitial cells during atherosclerosis, 63.7± 5.4 % of which are Sca1^{+}CD45^{+} APC). However, Psaltis et al., present data that suggests that Sca1^{+}CD45^{+} APC are heavily involved in the maintenance of the adventitia rather than leison formation and progression (Psaltis et al. 2014).

<u>Evidence of Sca1^{+} cell expansion, and the presence of multiple Sca1^{+} cell phenotypes/interactions during vascular remodelling</u>

Chen et al., report a significant increase in Sca1^{+} cells during vein graft arteriosclerosis development (Chen et al. 2013). Chen et al., also observed specific populations of

- Sca1^{+} APC co-localising with the platelet, blood leucocyte and EC marker CD31^{+} APC (Hu et al. examined and observed Sca1^{+}CD31^{+} APC however Chen et al. show co-localisation)

- APC expression of cardiac stem cell and mast marker c-Kit (CD117) (Hu et al. observe $Sca1^{+}c\text{-}Kit^{+}$ APC; Passman et al., report $Sca1^{+}c\text{-}Kit^{-}$; however Chen et al. did not assess Sca1c-Kit expression)
- APC expression of the diverse progenitor/stem cell marker CD34 (Hu et al. observed $Sca1^{+}CD34^{+}$ APC, however Chen et al., did not assess Sca1CD34 expression. Interestingly Torsney et al., observed adventitial and intimal $Sca1^{+}CD34^{+}$ cells in human atherosclerotic vessels)
- APC expression of the macrophage marker Mac-1 (accounted for ~ 12.6 % of total APC, as mentioned previously, Psaltis et al., also show that $Sca1^{+}CD45^{+}$ APC are a macrophage progenitor suggested to be heavily involved in adventitial maintenance following injury)

(Hu et al. 2004; Torsney et al. 2007; Passman et al. 2008; Chen et al. 2013 and Psaltis et al. 2014)

Interestingly Chen et al., postulate that due to their proximitiy, $CD31^{+}$ APC may have a role in the maintenance of the $Sca1^{+}$ APC population however this remains to be assessed (Chen et al. 2013). Considering the relatively high expression of the macrophage marker Mac-1, it would have been interesting if Chen et al., had examined for the regulatory immune (T- and B-) cell antigen receptor signalling molecule CD45, considering that Psaltis et al., report that $Sca1^{+}CD45^{+}$ APC are the origin of adventitial macrophages (Hu et al. 2004; Passman et al. 2008; Chen et al. 2013 and Psaltis et al. 2014).

<u>Evidence of APC (including $Sca1^{+}$ APC) migration</u>

Li et al., demonstrate using stably transduced $LacZ^{+}$ APC, that APC migrate into the neointima following balloon injury (Li et al. 2000). In addition, Hu et al., also demonstrate that isolated $Sca1^{+}$ APC (from ROSA26/$ApoE^{-/-}$ mice) transplanted into the adventitial side of vein graft injuries could migrate and account for approximately 21 % of all neointimal cells (Hu et al. 2004). Interestingly, Hu et al., discuss a contrasting report by de Leon et al., (who propose that resident fibroblasts do not migrate during carotid injury induced vascular remodelling) and suggest fibroblasts represent a different

population or stage in the differentiation process (de Leon et al. 2001 and Hu et al. 2004). Hu et al., based this theory on their comparison of $Sca1^+$ APC and later passage ($Sca1^-$) fibroblasts migratory ability (Hu et al. 2004). Rather intriguingly, Tigerstedt et al., present data on an aortic denudation injury where following injury, the aortas were removed, cultured and assessed for cellular influx, migration and neointimal cell maturation (Tigerstedt et al. 2009). They report a 4-fold increase in adventitial microvessels, a 5-fold increase in APC, followed by several 100-fold increase in neointimal cells 4 – 28 day post injury and extraction (Tigerstedt et al. 2009). Tigerstedt et al., also report an 8-fold increase in the frequncy of precursor cells compared with outgrowing cells (of which many displayed stem/undifferentiated profiles) 2 - 4 day post injury, and a 3.5-fold increase in cell migration and < 2-fold increase in cell migration 2 – 14 day post injury. Tigerstedt et al., conclude that adventitial activation is followed by precursor cell influx and the development of a neointima and suggest that cellular migration is responsible for neointimal formation to a greater degree than cellular proliferation. Taken together, the evidence presented by Li et al., Tigerstedt et al., and Hu et al., suggest that it is possible for APC (including $Sca1^+$ APC) to migrate in order to contribute to vascular remodelling (Li et al. 2000; Hu et al. 2004 and Tigerstedt et al. 2009).

Perivascular/Vasa Vasorum/Carotid Associated Nerve Sca1 Expression

Analysis of mounted whole tissue has brought light to some potential interesting phenomena. Analysis of whole mounted carotids and aorta suggests the presence of discrete $Sca1^+$ populations and intricate $Sca1^+$ vasa vasorum-like complexes on the external surface of the vessels, as well as an indication that vascular branches are rich in Sca1. While the concept that the vasa vasorum (adventitial microvessels) contain stem cells that may play a role in vascular remodelling is not novel, currently there is no specific phenotypic marker available in the literature due to the lack of appropriate methods to detect and isolate vasa vasorum cells (Kabara et al. 2014). Hence, the identification that the vasa vasorum highly expresses the stem cell antigen Sca1 could assist investigations. Interestingly, another group have

also identified perivscular $Sca1^{+}Gli1^{+}$ cells that they report to significantly contribute to vascular remodelling (discussed in detail in discussion chapter (chapter 6)) (Kramann et al. 2016 and Baker and Pe´ault 2016). Nevertheless, Kabara et al., show that capillary-derived pericyte cells (cPC) have both mesenchymal and neuronal stem cell like phenotypes, and the ability to reconstitute capilary like structures, indicating that cPC may contribute to vascular remodelling (Kabara et al. 2014). It is also noteworthy to consider the potential of vasa vasorum stem cell populations because adventitial neovascularization is observed in atherosclerotic plaque development, and neointimal formations also display the development of an immature vasa vasorum which is theorised to participate in delivery of immune cells, lipids and blood substrates involved in plaque growth and destabilisation (Langheinrich et al. 2006; Kawabe et al. 2014 and Kabara et al. 2014). Importantly, adventitial neovascularization is also observed following vascular injury (Kwon et al., were the first to show that adventitial neovascularization is proportional to the degree of injury-induced arterial stenosis) and accompanies APC proliferation and differention during vascular remodelling (Kwon et al. 1998 and Kabara et al. 2014). A previous report also presents data indicating that pulmonary APC cooperate with vasa vasorum EC in order to regulate vasa vasorum neovascularization (Davie et al. 2006). Neovascularization is considered to be induced by vascular remodelling associated ischemia (Kawabe et al. 2014). Additionally, nonhomogeneous adventitial pericyte cells (PCs) have been shown to contribute to vascular remodelling by participating in the restenotic response following arterial injury, and interestingly, studies indicate that PCs are also derived from various developmental origins and have the ability to transdifferentiate between germ layers (Campagnolo et al. 2010; Armulik et al. 2011; Corselli et al. 2012; Tigges et al. 2013 and Kabara et al. 2014). Others suggest that adventitial microvessels may act as a vascular niche in the maintenance of resident stem cell populations, and may also serve as a conduit for the circulation/migration of resident stem cells (Kawabe and Hasebe 2014). Additionally, the presence of Peripherin (the central nervous system and peripheral nervous system neuronal/axonal marker) on the

surface of whole mounted aortas highlights the complexity and the intricately connected nature of tissues and indicates the presence of perivascular nerves (Kabara et al. 2014 and Majesky 2015). All of this may support Majeskys' theory that the adventitia and periadventitial cells function in concert through interlinking microvessels, nerves and migratory cells to exert significant influence on vascular disease progression and regression (Majesky 2015). It is also interesting to note that the Hh signalling receptor and downstream target, Patched 1, is observed in both the perivascular space and adventitia (see figure 5.12), however the importance of this will be discussed in detail in the following section (Sca1$^+$ Cell Response during Vascular Remodelling following treatment with Cyclopamine).

Intriguingly, an unexpected and novel finding was the confirmation that whole mounted nerves, suggested to be the carotid sinus nerve due to its location, are enriched for Sca1$^+$-eGFP. This poses the interesting query into the purpose of the stem cell markers (Sca1) presence in a Peripherin$^+$ nerve bundle. The observation and functionality of discrete Sca1 cells on the external surface of the carotid sinus nerve should also be considered. Nevertheless, the data presented suggests that the Sca1$^+$ structures within the carotid sinus nerve lines the internal vasculature (due to defined eNOS staining), further linking endothelia and Sca1 expression (Sca1$^+$eNOS$^+$ cells were also observed in carotid lumenal analysis in section 5.2.6).

Sca1$^+$ Cell Response during Vascular Remodelling following treatment with Cyclopamine

Hh signalling inhibition by cyclopamine treatment attenuates the increase in adventitial volume, and adventitial Sca1$^+$ cells are observed in cyclopamine treated vessels with attenuated remodelling, and not in the vehicle control vessels where Sca1 expression appears to be expressed by intimal cells. This presence of adventitial Sca1$^+$ cells in attenuated Hh inhibited vessels and not in the vehicle control treated vessels indicates that Hh inhibition prevents adventitial Sca1$^+$ cell activation, and the presence of intimal Sca1$^+$ cells but not adventitial Sca1$^+$ cells in the vehicle control vessels indicates that

adventitial Sca1^{+} cells may migrate in concurance with other groups (see section above discussing APC migration) (Li et al. 2000; Hu et al. 2004 and Tigerstedt et al. 2009).

The results also confirm that Hh signalling inhibition using cyclopamine significantly attenuates intimal formation *in vivo*. This finding complements previous studies reported by Redmond et al., who used Patched 1 siRNA (to knockdown arterial Hh signalling following injury), to significantly attenuate vascular remodelling *in vivo* (Redmond et al. 2013). Immunohistochemical analysis was used to further investigate the link between Hh signalling/responsiveness and vascular remodelling. These results indicate that Hh signalling is dynamic in remodelling vessels; Patched1 is present in the adventitia and media of 3 day post injury vessels, decreased in the adventitia and media 7 day post injury, and significantly increased in the adventitia and media, as well as highly expressed in initmal cells 14 day post injury. Considering Patched 1 is both the receptor for Hh signalling, as well as a downstream target, it could be argued that Hh signalling is recapitulated during vascular remodelling and that Hh inhibition with cyclopamine attenuates intimal formation by reversing this global vascular recapitulation of Hh signalling. Analysis of Gli2 (another downstream Hh signalling target) further confirms the theory that Hh signalling is crucial during vascular remodelling. Immunohistochemistry analysis results show the absence of Gli2 expression in sham injured vessels and the presence of Gli2 expression in perivascular, adventitial, medial and intimal cells (significantly high levels were observed in intimal cells) in vehicle control treated injured vessels. Gli2 expression was also observed in the perivascular, adventitial, medial and intimal cells of cyclopamine treated injured vessels, however there is obvious and significant vascular remodelling attenuation. Importantly, previous studies have also produced reports with similar findings. Morrow et al., also observed significant increases in Patched 1 protein expression, as well as significant Patched 1 staining in intimal cells in 14 day post injury vessels (Morrow et al. 2009). Additionally, Redmond et al., observed an increase in Patched 1 and Gli2 mRNA levels following injury, both of which (as well as

observed vascular remodelling) were attenuated following Hh inhibition using Patched 1 siRNA treatment (Redmond et al. 2013). Additionally, a previously mentioned report provides substancial evidence of perivascular and adventitial Gli1^{+} progenitor cell contribution to vascular remodelling (see discussion chapter (chapter 6) for in depth discussion) (Kramann et al. 2016 and Baker and Péault 2016). Nevertheless, taken together these findings support the role of Hh responsive cells and their contribution to vascular remodelling.

Characterisation of Vascular Cell Phenotypes during Vascular Remodelling

For a summary of the vascular cell phenotypes observed please see table 5.1, however, immunohistochemistry results indicate that the majority of intimal cells at the time of tissue extraction are not differentiated SMC due to the absence of SMMHC; the same conclusion is reported by Tang et al., and interestingly Herring et al., present data identical to this thesis, showing a significant reduction in medial SMMHC expression 7 day post injury (Tang et al. 2012 and Herring et al. 2014). While Herring et al., and Nemenoff et al., provide evidence that intimal cells are derived from differentiated SMC, other groups like Tang et al., have also presented evidence that intimal cells are derived from resident vascular stem cells. Therefore in order to elucidate the reality, further analysis of the animal models is critical (and will be discussed in full in chapter 6). However, the following is a brief summary of the fundamental differences between the animal models used. The animal model used in this study utilised a non-inducible model where eGFP was expressed in real time following the transcription and translation of the stem cell *Sca1* gene, and Tang et al. used a non-inducible model where eGFP was expressed in real time following the transcription and translation of the SMC *SMMHC* gene (Tang et al. 2012). On the other hand, Nemenoff et al., Herring et al., and Yang et al., all used tamoxifen-inducible models for the purpose of lineage tracing (Nemenoff et al. 2011; Herring et al. 2014 and Yang et al. 2015). This fundamental difference is most likely the reason for the discrepancy observed and chapter 6 will discuss in greater detail the issues with lineage

tracing models that draws into question the validity of their conclusions. Nevertheless, interestingly, a novel observation is that the SMMHC marker is observed to peak 3 day after injury in the adventitia and media, however is dramatically reduced 7 and 14 day after injury. Notably, Herring et al., also assessed real time expression of SMMHC using an antibody, and similar to the findings observed in this thesis, there was strong SMMHC medial expression in uninjured control mice and a marked reduction of medial SMMHC expression in 7 day post injured mice (Herring et al. 2014). Also, it is important to reconsider at this point that Yang et al., also noted rare SMMHC^{+} intimal cells with preserved underlying SMC, and Tang et al., also observed only minimal SMMHC expression in 30 day post injury mice (Tang et al. 2012 and Yang et al. 2015). The pericyte/SMC marker α-Actin, found in the media of untouched vessels is observed in the media of non-remodelling sections of 7 and 14 day post injury vessels, however is notably lost in the media of remodelling vessels (denoted by intimal formation) and in such cases is observed in the intimal cells and not the corresponding media. The latter suggests the migration of pericyte/SMC from the media to intima, with an observed change occuring in the cells repopulating the media (medial cells are no longer α-Actin^{+}). Nemenoff et al., also report α-Actin in the media of minorly remodelling vessels 7 day post injury, and their data also suggests that a couple of intimal cells are α-Actin^{+} (Nemenoff et al. 2011). Klein et al., also report the presence of α-Actin^{+} cells primarily in the medial layer with single cells also staining α-Actin^{+} in the adventitia, both of which concur with the results presented in this thesis (Klein et al. 2011). Tang et al., also report medial α-Actin expression in control and injured vessels, importantly there is no observable intimal formation in the injured vessels and is therefore directly comparable with the results presented in this thesis (Tang et al. 2012). Wan et al., provides some of the clearest data on α-Actin expression in remodelling vessels, and their data also concurs with the results presented in this thesis (Wan et al 2012). Wan et al., present almost identical data to us showing that α-Actin expression is primarily in the media of control mice, however during development of a neointimal formation following injury (7 and 14 day post injury), α-Actin expression appears to dissipate in the media

and appear in intimal cells (Wan et al 2012). Interestingly, Wan et al. also show Sca1^{+}α-Actin^{+} intimal cells both as the frontier cells at initial intimal formation (7 day post injury) and progressed initimal formation (14 day post injury) (Wan et al 2012). Yang et al., also report α-Actin^{+} intimal cells in both carotid and femoral artery injured vessels however they do not show uninjured controls for comparison (Yang et al. 2015). Interestingly, a novel observation from this study was that lumenal boundary Sca1^{+} cells observed 3 day post injury are eNOS^{+}, suggesting a role for phenotypic switching of endothelial cells to a more stem cell state considering untouched endothelial cells are not Sca1^{+}. Other groups have also implicated resident EC as a potential causative force in disease, a concept which will be discussed in the following chapter (Medici et al. 2010; Piera-Velazquez et al. 2011; Kovacic et al. 2012; Cooley et al. 2014 and Sanchez-Duffhues et al. 2016). Glial, endodermal and hematopoietic marker positive cells do not appear to have a significant role in vascular remodelling due to the general absence of S100β and Sox 17 staining respectively. Tang et al., also show a relative absence of S100β expression in remodelling vessels, however this is contrary to the results presented in this thesis which shows significant S100β expression in uninjured control vessels (Tang et al. 2012). Analysis of the neural stem cell markers Sox 10 and Nestin show the vessels are negative for the presence of a neural stem cells marker until 14 day post injury when significant medial and intimal Nestin expression is activated. Tang et al., also show minimal Sox 10 staining in remodelling vessels (Tang et al. 2012). Interestingly Klein et al., report adventitial expression of the neural stem cell marker Nestin, and Wan et al., show evidence that Sca1^{+}Nestin^{+} cells are the frontier cell type at initial (7 day post injury) and advanced (14 day post injury) vascular remodelling phases (Klein et al. 2011 and Wan et al. 2012). The latter is also reported by Oikawa et al., (Oikawa et al. 2009). Analysis of data presented by Wan et al., also indicates the presence of medial Nestin^{+} cells however the majority of expression is concentrated to the frontier of the intimal formation (Wan et al. 2012).

Marker of Interest	Untouched/ Sham Vessel	3 Days Post Ligation Vessel	7 Days Post Ligation Vessel	14 Days Post Ligation Vessel
α- Actin	Adventitia: + Media: +++	Adventitia: not investigated (n.i) Media: n.i Intima: n.i	Adventitia: +++ Media: +++ Intima: +	Adventitia: + Media: no intima+++; intima + Intima: +++
SMMHC	Adventitia: - Media: ++	Adventitia: +++ Media: +++ Intima: +++	Adventitia: ++ Media: + Intima:+	Adventitia: + Media: + Intima: +
eNOS	Adventitia: n.i Media: n.i	Adventitia: + Media: + Intima: +++	Adventitia: n.i Media: n.i Intima: n.i	Adventitia: n.i Media: n.i Intima: n.i
Patched 1	Adventitia: n.i Media: n.i	Adventitia: +++ Media: +++ Intima: +++	Adventitia: ++ Media: + Intima: +	Adventitia: +++ Media: +++ Intima: +++
Gli 2	Adventitia: - Media: -	Adventitia: n.i Media: n.i Intima: n.i	Adventitia: n.i Media: n.i Intima: n.i	Adventitia: +++ Media: +++ Intima: +++
S100β	Adventitia: + Media: -	Adventitia: n.i Media: n.i Intima: n.i	Adventitia: + Media: - Intima: +	Adventitia: + Media: - Intima: +
Sox 10	Adventitia: + Media: +	Adventitia: n.i Media: n.i Intima: n.i	Adventitia: n.i Media: n.i Intima: n.i	Adventitia: - Media: + Intima: +
Nestin	Adventitia: - Media: -	Adventitia: - Media: - Intima: -	Adventitia: - Media: - Intima: -	Adventitia: Media: + Intima: +
Sox 17	Adventitia: - Media: -	Adventitia: n.i Media: n.i Intima: n.i	Adventitia: - Media: - Intima: -	Adventitia: - Media: - Intima: +

Table 5.1: Summary Analysis of Vascular Cell Phenotypes during Vascular Remodeling. +: a few positive cells, ++: majority of cells weakly stain positive, +++: majority of cells strongly stain positive.

Sca1$^+$ Cells in Human Vessels

Lastly, the identification of Sca1$^+$ adventitial cells in healthy human arteries, and an increase in adventitial Sca1$^+$ cells in atherosclerotic human tissue, suggests the presence of a similar stem cell population response to the murine injury model presented. Critically Torsney et al., examined human autopsies and also demonstrated the presence of Sca1$^+$ cells in the adventitia and neointima of human atherosclerotic plaques, and they suggest that Sca1$^+$ cells may be a source of EC and vSMC in atherosclerotic leisons (Torsney et al. 2007 and Kawabe and Hasebe 2014). This evidence previously published by Torsney et al., supports the finding presented in this thesis. However, it is important to note here that currently a human Sca1 ortholog remains to be identified. Despite this a number of potential human orthologs for the Ly6 family have been identified (Torsney et al. 2007). A deletion event of ~ 500 kb (9 genes including *sca1* and 5 other *ly6* genes) is considered to have been apart of the evolutionary process, and it is assumed that the roles of these proteins has been taken on by other Ly6 proteins or other glycosyl phosphatidylinositol-anchored cell surface proteins. Nevertheless, there are other human Ly6 family proteins (with diverse expression and functional charateristics) which are reminiscent of Sca1, and other glycosyl phosphatidylinositol proteins with functional similarities to Sca1 (Holmes and Stanford 2007). Therefore the Sca1 antibodies used in this study and in Torsney et al., may be identifying a human Ly6 protein that exhibits similar expression patterns to murine Sca1 (Torsney et al. 2007).

5.4 Conclusion

There is mounting evidence that supports the theory that adventitial cells contribute to vascular remodelling (Li et al. 2000; Sartore et al. 2001; Siow et al. 2003; Hu et al. 2004; Korshunov and Berk 2004; Torsney et al. 2005; Passman et al. 2008; Morrow et al. 2009 Klein et al. 2011 and Tigges et al. 2012). Currently this has been observed in the form of adventitial Sca1$^+$ cell expansion, differentiation, migration and presence in developing intimal formations in response to injury. Hh signalling also plays a critical role in vascular remodelling, with inhibition of the key Hh component, Patched 1,

establishing a potential therapy to combat vascular remodelling. It can also be suggested that intimal cells are not 'differentiated' vSMC due to the lack of differentiated vSMC marker (SMMHC) expression, a topic which will be discussed further in the coming chapter. However, there is significant evidence to suggest that a neural stem cell (Nestin^{+}) phenotype may be activated during the remodelling process. It is also crucial to note that Sca1^{+} cells have been reported in human physiology, and that Sca1^{+} cells have been identified in the adventitia and intima of atherosclerotic vessels, indicating that evidence gathered through murine models may provide invaluable information for the human condition.

Chapter 6

Discussion and Conclusion

6.1 Discussion

In order to provide structure to the discussion required, this chapter will address the two major themes at the heart of this thesis.

1. The involvement of Sca1$^+$ cells in neointimal formation
2. The role of Hh in contributing to Sca1$^+$ cell maintenance and differentiation underlying their contribution to neointimal formation

Therefore, the following discussion will be explicitly framed with these two themes in mind, and will critique the work conducted throughout this thesis as well relevant published literature.

1. The Involvement of Sca1$^+$ Cells in Neointimal Formation

The inherent nature of this theme is based on the complex and widely debated issue of the origins of the arteriosclerotic phenotype. Currently, there are two primary schools of thought that divide the cardiovascular community and they are the stem cell and the resident smooth muscle cell origin theories. The stem cell origins theory includes the putative role of circulating bone marrow-derived hematopoietic stem cells and/or resident vascular stem cells contribution to vascular remodelling. Importantly, Sca1$^+$ adventitial and bone marrow-derived stem cells have been observed, and shown to contribute to vascular pathology, however further studies have shown that bone marrow-derived progenitor contribution to arteriosclerotic vascular remodelling is increasingly unlikely (as detailed in section 5.1) (Tanaka et al. 2003; Hu et al. 2004; Sainz and Sata 2006 and Daniel at al. 2010 and Leszczynska et al. 2016). Therefore, Sca1$^+$ cells may be key during vascular remodelling, a phenomenon which will be discussed in the following paragraph.

Sca1 Expression is Increased During Vascular Remodelling

Sca1$^+$ cells have also been repeatedly shown to contribute to vascular remodelling (as detailed in section 5.3), a phenomenon which is supported by the *in vitro and in vivo* data presented in this thesis (Wan et al. 2012; Chen

et al. 2013; Psaltis et al. 2014 and Shikatani et al. 2016). While *in vitro* data discussed in section 4.3 confirms the previous observation that Sca1$^+$ APC can differentiate into SMC, *in vivo* analysis discussed in section 5.3 confirms that Sca1 expression is dramatically increased during vascular remodelling (Hu et al. 2004). Importantly, while this study cannot exclusively confirm that intimal cells are derived from adventitial Sca1$^+$ progenitor cells, this study does suggest that Sca1$^+$ cells are involved in the remodelling process. This conclusion is based on results discussed in sections 5.2 and 5.3. The following is a brief synopsis of the observations:

1. Adventitial Sca1 expression increases in 3 day post ligation tissue versus the untouched and sham controls.
2. The emergence of luminal Sca1$^+$ cells 3 day post ligation (compared to the untouched and sham controls).
3. The continued increased adventitial Sca1 expression in 7 day post ligation tissue versus the untouched and sham controls.
4. The emergence of intimal Sca1$^+$ cells in 7 day post ligation tissue.
5. The decline in Sca1 expression in 14 day post ligation tissue.
6. The absence of adventitial Sca1$^+$ cells in 14 day post-ligation vehicle control vessels and the presence of adventitial Sca1$^+$ cells in cyclopamine treated vessels (coupled with attenuated remodelling).

In addition to the general increased presence of Sca1$^+$ cells in remodelling vessels, the observation that luminal boundary cells highly expressed Sca1 3 day post injury presented unique evidence for the potential of endothelial cells (EC) phenotypically switching to a more stem-like cell type. The following paragraph will discuss this prospect in more detail.

The Presence of Sca1$^+$ EC: Potential for Endothelial Contribution

Intimal cells are positive for both the EC marker eNOS and Sca1 3 day post injury. This highlights the potential for EC contribution to intimal formation through endothelial transformation to a more stem like phenotype. Endothelial damage or disruption was not observed throughout the Sca1-eGFP mouse partial ligation injury study. A review of surgical injury and

remodelling techniques also notes the preservation of an intact endothelium in partial carotid ligation cases (Holt and Tulis 2013). Therefore, it could be suggested that the eNOS^{+} Sca1^{+} luminal cell is a resident EC and not a circulating endothelial progenitor cell. The theory of endothelial to stem cell transition has been previously implicated in human pathologies including fibrosis, cardiac failure, specific chronic vasculopathies, arterial and vein graft rejection and remodelling, pulmonary arterial hypertension and vascular remodelling, with each paper discussing the occurrence of an endothelial to mesenchymal/multipotent stem cell transition (Medici et al. 2010, Piera-Velazquez et al. 2011, Kovacic et al. 2012, Cooley et al. 2014 and Sanchez-Duffhues et al. 2016). It has also been highlighted that the endothelial to mesenchymal transition (EndMT) process is highly dynamic, with multiple steps resulting in a broad range of intermediate phenotypes (Sanchez-Duffhues et al. 2016). Arguably the complication of the existence of intermediate cell types means that the designation of specific cell type classification other than "stem cell/stem-like cell" is inaccurate.

Critique of Sca1 Analysis

Taken together, the *in vitro* and *in vivo* data confirms the involvement of Sca1^{+} cells in the vascular remodelling process. This being said, it is essential to note that the evidence presented in this thesis cannot directly elucidate the role of adventitial Sca1^{+} cell contribution to vascular remodelling as lineage tracing was not conducted, and only lineage tracing experiments are capable of deducing the exact role of the cell in question. Unfortunately, even at the time of writing this thesis, a Sca1 lineage trace animal model is not available, therefore it may be some time before a study can definitively determine if Sca1^{+} stem cells are the origin of vascular intimal cells. However, the significant presence of Sca1^{+} cells during vascular remodelling, combined with the Hh signalling element (which will be discussed further as part of the second theme) and *in vitro* work presented in this thesis showing Shh-induced Sca1^{+} APC differentiation to SMC validates the requirement to continue the investigation.

Other Considerations: Remodelling Induced Changes in Marker Expression - The Emergence of the Neural Stem Cell Marker Nestin

The most significant other stem cell marker observed in remodelling vessels is the emergence of the neural stem cell marker Nestin 14 day post injury. Our data concurs with previously published Nestin expression work, where Nestin is not expressed by the vessel until well into the remodelling process when it emerges in the media and intima (Oikawa et al. 2009 and Wan et al. 2012). The Pericyte/SMC marker α-Actin, which is strictly observed in the media of uninjured vessels is also observed in intimal cells and, as was discussed in section 5.2, not observed in the media adjacent to the intimal formation, but was found in medial compartments without intimal formation. This was suggested in section 5.2 as evidence of the possibility of α-Actin^{+} cells migrating into the intima. Our data also confirms previous evidence that the intima of remodelling vessels contains Sox 10, Sox 17 and S100β cells, however it is suggested that these cell markers are not individually abundant enough to completely define the intimal formation (Tang et al. 2012).

Scientific Advances That Have Changed The Playing Field

Apart from the discovery of stem cell markers in the vasculature, other scientific advances have also been employed in the elucidation of vascular remodelling and contribute to the stem cell versus resident smooth muscle origin debate.

<u>SMMHC: The Differentiated SMC Marker</u>

Due to experimental advances over the past decade, the scientific community has witnessed a dramatic change in the definition and functional classification of SMC and progenitor cells. Current experimental evidence suggests that the SMC marker, Smooth Muscle Myosin Heavy Chain (SMMHC, also denoted Mhy11) is the most reliable marker for determining a "differentiated" SMC phenotype (Stevens et al. 2008). The identification of SMMHC as a "differentiated" SMC marker has been central to the stem cell versus SMC "de-differentiation"/proliferation debate and interestingly,

animal models designed to investigate the origin of intimal SMCs using this marker have produced conflicting results.

Lineage Tracing: Cre Recombination Animal Models

The development of the Cre/Lox site-specific recombination system has transformed the genetic manipulation abilities of the scientific community. This intelligently designed method allows scientists to control gene activity from both a location and time perspective (i.e. location is the organ/cells where the gene of interest naturally expresses, and time is with respect to the fact that an inducer can be incorporated in order to control when the system is turned on) (Feil et al. 2009). The Cre/Lox system is complex and can be designed for many purposes (gene inversion, deletion and translocation) but its use as a tool for conducting lineage tracing (tamoxifen-induced Cre recombination) has been of significant importance (Sauer 1998).

Challenging the SMC Theory

SMMHC Lineage Tracing: Tamoxifen Induced Cre Recombination Animal Models

The "pulse-chase" lineage tracing experiments such as those using the tamoxifen inducible Cre recombinase models, poorly describe any verification of the use of an experimentally appropriate tamoxifen-dosing regimen. Unfortunately, this phenomenon is universal to the use of this technology and was originally highlighted as a potential cause of lineage tracing study discrepancies in pancreatic islet biology (Reinert et al. 2012). Reinert et al., emphasized the significant absence of consideration, and importance of appropriate experiment validation "not only for maximising the spatial extent of recombination in the target tissue but also by limiting the temporal extent of recombination" (Reinert et al. 2012). As previously discussed in section 5.1, the debate about vascular remodelling between the role of resident stem cell populations and "differentiated" SMC has included the use of tamoxifen-inducible Cre recombinase models, and unfortunately also lack sufficient evidence of appropriate experimental design validation.

The main aspects of experimental design and previously published work for consideration are described as follows:

- The use of differing Cre driver mice and reporter strains makes interpretation of conflicting results often difficult to reconcile, since varying models have incomparable specificity of Cre expression and efficiency of target gene induction (Reinert et al. 2012).
- The use of differing tamoxifen administration methods and doses (Reinert et al. 2012).
- The requirement for tamoxifen-induced recombination timeline analysis, crucial for "pulse-chase" experiments considering the consequences of a pulse phase unknowingly extending into the chase phase will result in newly generated cells being labelled, leading to misinterpretation of lineage tracing experimental results (Reinert et al. 2012).

Most importantly, Reinert et al., followed this discussion with a study that encompassed all of the above by designing a bioassay involving pancreatic islet transplantation of untreated tamoxifen-inducible β-cells into tamoxifen treated mice (Reinert et al. 2012). The recipient mice (*Pdx1^{PB}-CreER^{Tm}; R26R^{lacZ}*) were subcutaneously injected with either a "high" dose (3 x 8 mg tamoxifen/ vehicle control) or a "low" dose (3 x 1 mg tamoxifen/ vehicle control) (Reinert et al. 2012). The donor mice (also *Pdx1^{PB}-CreER^{Tm}; R26R^{lacZ}*) which had never previously been subjected to tamoxifen, had islet cells removed and transplanted into the tamoxifen treated recipients 48 hours, 1 week, 2 weeks and 4 weeks after tamoxifen treatment cessation. Experimental controls (*R26R^{lacZ}* and vehicle treated *Pdx1^{PB}-CreER^{Tm}; R26R^{lacZ}*) did not yield any β-gal, i.e. recombination did not occur in these mice; however significant β-gal levels (recombination) were observed even up to 4 weeks after termination of tamoxifen treatment in the high dose animals, and β-gal (recombination) was observed up to 1 week after termination of tamoxifen treatment in the low dose animals (Reinert et al. 2012). The study also examined the location of Cre in the *Pdx1^{PB}-CreER^{Tm}; R26R^{lacZ}* mice and

found that Cre localised in the cytoplasm 5 weeks after a single 8 mg dose of tamoxifen, however Cre was localised in the nucleus 5 weeks after the final dose of a 2 x 8 mg tamoxifen regime. The study concluded the following:

1. The longevity of tamoxifen's induction of recombination (pulse) period is dose dependent (Reinert et al. 2012).
2. Reporter allele recombination can occur weeks after the cessation of tamoxifen treatment (i.e. tissue levels remain sufficiently concentrated to continue inducing recombination long after treatment termination) (Reinert et al. 2012).

These insights are crucial to consider when analysing the tamoxifen-induced Cre recombinase models used in the assessment of the role of resident stem versus "differentiated" cells contribution to vascular remodelling. Considering the potential for tissue associated residual tamoxifen-induced recombination up to 4 weeks after tamoxifen treatment cessation, the tamoxifen-inducible lineage tracing experiments conducted by Nemenoff et al., Herring et al., and Yang et al., that concluded that differentiated SMC are the main contributor to vascular remodelling require review (Nemenoff et al. 2011, Herring et al. 2014 and Yang et al. 2015).

The following is a review of the animal models and tamoxifen dosing regimes associated with each lineage tracing experiment:

1. Nemenoff et al. 2011

Animal used B6.FVB.–Tg(SMMHC-CreERT2)1Soff/J . No mention of age used.

Tamoxifen treatment regime: 5 consecutive doses of 1 mg/mouse/day by intraperitoneal injection. Femoral artery wire-induced injury was conducted 1 weeks after the final tamoxifen treatment. Did not appear to use a vehicle control.

2. Herring et al. 2014

Animal used Mhy11-CreERT2$^{+/-}$ on a C57BL6 background crossed with B6.129(Cg)-Gt(ROSA)26Sor$^{tm4(ACTB-tdTomato,-EGFP)Luo}$/J. Used at 5-6 weeks old

Tamoxifen treatment regime: 5 consecutive doses of 1 mg/mouse/day by intraperitoneal injection. Carotid ligation injury was conducted 2 weeks after the final tamoxifen treatment. Used corn oil vehicle control.

3. Yang et al. 2015

Animal used *R26R^{+}; Mhy11-CreER^{+}*. Used at 6 and 11 weeks old

Tamoxifen treatment regime: 10 consecutive doses of 2.5 mg/mouse/day followed by 5 additional 2.5 mg every other day by intraperitoneal injection. Carotid ligation injury was conducted the next day. Did not appear to use a vehicle control only unmanipulated *R26R^{+}; Mhy11-CreER^{+}* mice.

Despite ultimately coming to the same conclusion, that SMC are the culprits of vascular remodelling, these three models importantly demonstrate some interesting anomalies:

Firstly Nemenoff et al., demonstrates adventitial SMMHC^{+} cells in injured vessels (Nemenoff et al. 2011). Secondly, Herring et al., show no such evidence of adventitial contribution and only report SMMHC^{+} cells in the media and intima (Herring et al. 2014). Thirdly, Yang et al., show no evidence of adventitial contribution, only report SMMHC^{+} cells in the media and intima (concurred with Herring et al.,), however they noted that in some intimal leisons where the underlying SMC were preserved, SMMHC^{+} cells were hardly detected (discussion in section 5.1), and suggest that age influences contribution as Herring et al., had used juvenile mice and reported ~80 % SMC contribution while they had used adult mice that indicated < 30 % of intimal cells were SMC derived (Herring et al. 2014 and Yang et al. 2015).

However even if these anomalies were disregarded, the fact that the mice are from non-comparable genetic backgrounds with the potential for different recombination efficiencies (Cre activity), and the non-comparable tamoxifen dosing regimens considering dosing concentrations varied and were given per mouse and not per weight; the fact that none of these models validated

the depletion of residual tissue tamoxifen levels in order to confirm completion of the pulse phase prior to the chase, casts doubt on their results and conclusion. Additionally, considering data shown in section 5.2. indicates real time adventitial and medial SMMHC expression 3 day after injury, and dramatic loss of real time adventitial and medial SMMHC expression by 7 day after injury, there is potential for experimental misinterpretation, if by any chance the pulse phase in these animal models continues to approximately the 3-day mark.

Intriguingly, a recent report using the SMMHC Tamoxifen-inducible model has suggested that differentiated SMC generate a subpopulation of $Sca1^+$ APC *in situ* (Majesky et al. 2016). The report shows phenotypically distinct subpopulations of APCs expressing SMC, hematopoietic stem-like and myeloid signatures, and the authors suggest that differentiated SMCs are the origin of these populations to varying degrees, with SMC-derived $Sca1^+$ APC exhibiting multipotency (SMC, resident macrophage and EC-like differentiation potential) (Majesky et al. 2016). The report also shows $Sca1^+$ APC expansion 3 day post injury (confirming our result) (Majesky et al. 2016). This is an interesting study that again highlights the importance of a validated tamoxifen dosing regimen (they use 1 mg/mouse/day followed by 10 day break prior to injury), however their observation that $SMMHC^+Sca1^+$ APC contribute to vascular remodelling may compliment our findings that $Sca1^+$ APC express SMMHC early on in the remodelling process (if residual tissue tamoxifen is present) (Majesky et al. 2016). The analysis of "SMC-derived" $Sca1^+$ APC also indicates that $SMMHC^+Sca1^+$ APC are a small subpopulation of $Sca1^+$ APC (8 % of total $Sca1^+$ APC are $SMMHC^+$) and that these $Sca1^+$ APC have SMC, EC-like and neovessel formation potential (Majesky et al. 2016).

<u>Additional Complication: Injury-Induced Apoptosis</u>

Another complication in the interpretation of tamoxifen-induced Cre recombination is the apoptotic phase that preludes proliferation associated with vascular injury. Vascular cell apoptosis is a prominent feature of

vascular remodelling, both during embryonic development (for example, regionalised SMC apoptosis occurs during human ductus arteriosus regression and closure) and postnatal pathologies (including atherosclerotic and restenotic lesions) (Bennett et al. 1995; Geng et al. 1995; Slomp et al. 1997; Mallat et al. 1997; Kolodgie et al. 1997; Bennett 1999; Walsh et al. 2000 and Walshe et al. 2011). This also holds true following vascular injury, where the vessels first major response is medial SMC apoptosis, which occurs both within hours of the injury and again at later time points (typically at lower frequencies), whether using the balloon, wire or ligation injury method (Walsh et al. 2000; Shoji et al. 2004 and Yu et al. 2011). Therefore 'marking'/tracing SMC may not be the best course of action considering the first significant fate change for 'marked' medial SMC may be apoptosis. With this in mind, it may be more prudent to track stem cells especially considering that when stem cells are 'marked' albeit constitutively (Nestin), they seem to be the source of a considerable amount of the neo-intimal SMCs. This comment is in reference to the Nestin-Cre-EYFP study previously mentioned, whereby all cells expressing and deriving from a Nestin-expressing cell were labelled with endogenous yellow fluorescent protein (EYFP). The results of which showed intimal cells were Nestin expressing/Nestin-expressing progeny, and interestingly, $Sca1^{+}$Nestin-expressing/Nestin-expressing progeny were observed at the intimal frontier, indicating a role for $Sca1^{+}$ neural stem cells during vascular remodelling. Additionally, our analysis also showed the emergence of $Nestin^{+}$ cells during vascular remodelling as previously described above and in section 5.2/5.3.

<u>Additional Complications: Smooth Muscle Myosin Heavy Chain (SMMHC) Isoform Ratios Determine Final Cell Length – May Be Involved in Post-Injury Stem Cell Remodelling; SMMHC SM1 Expression in the Adventitia Pre-Natally; Non-unique Nature of Myosin Re-Expression and Lack of Experimental SMMHC Isoform Distinction/Differentiation</u>

Considering the importance of SMMHC in tracing differentiated SMC progeny *in vivo*, the properties and role of SMMHC should be examined.

The myosin family of proteins, traditionally referred to as “the actin motor proteins”, are ATPases that hydrolyse ATP to undergo conformational changes, converting chemical energy into mechanical energy in order for myosin to traverse actin filaments (Lodish et al. 2000). However this 13-member family, while all functioning as motor proteins, contain myosins with other specific activities not involving actin (Lodish et al. 2000). One of these 13-members is myosin II, an abundant eukaryotic protein involved in muscle contraction and cytokinesis, and is known to be present in smooth muscle (Lodish et al. 2000 and Eddinger and Meer 2007). The most famous myosin II protein that exists in SMC, which is one of many, is transcribed from a single gene, *SMMHC,* and is translated via two alternate splice sites to produce one of four unique molecules (isoforms): SM1, SM2, SMA and SMB (DiSanto 2003 and Eddinger and Meer 2007). It is this *SMMHC* gene that is utilised in genetically modified animal models for the determination of SMCs contribution to vascular remodelling, including the previously mentioned (in section 5.1) (Nemenoff et al. 2011, Tang et al. 2012, Herring et al. 2014 and Yang et al. 2015).

SMC in normal healthy vascular media express the SMMHC isoforms SM1 and SM2, and therefore SMMHC is used as a marker for late stage SMC differentiation/maturation (Nagai et al. 1988, Negai et al. 1989 and Owens 1995). SMC SM1 expression is first detectable late in fetal development, and is more selectively expressed than SM2 during development, however both are expressed postnatally (Kuro-o et al. 1989, Aikawa et al. 1993 and Aikawa et al. 1998). Interestingly, data presented in Kuro-o et al., shows fetal aortic SM1 expression in the adventitia and media, however only medial SM1 and SM2 is detected in postnatal aortas (Kuro-o et al. 1989). However, they neglect to comment on the presence of adventitial SM1 expression, and unusually subsequent papers referencing the paper also refrain from commenting on the finding (Kuro-o et al. 1989). Nevertheless, the primary function of SM1 and SM2 has been linked with controlling cellular length, specifically, that the ratio of SM1/SM2 controls final cell length with

increased SM2 expression imparting the ability to establish a shorter final cell length (Meer and Eddinger 1997).

Considering that SM1/SM2 ratio is important to controlling the final length of a cell in the media, it could be suggested that the emergence of SMMHC expression in the adventitia, and the increased levels observed in the media 3 day post injury (section 5.2) could have a role in post-injury resident cell remodelling rather than being an indicator of the migration or proliferation of SMC. Some other considerations for the potential of temporal expression of SMMHC in resident adventitial progenitor cells, rather than the migration/proliferation of SMC are as follows:

- The re-expression of myosin isoforms following injury is not unique. Previous reports have showed transient and non-transient re-expression of skeletal muscle myosin isoforms during muscle regeneration; the myosin isoforms in question are initially expressed prenatally however are down regulated postnatally (Carraro et al. 1989 and Schiaffino et al. 2015).
- SMMHC transgenic animals and antibodies used in the assessment of SMMHC do not differentiate between SM1 and SM2. SM2, which has a shorter nonhelical tail, is considered to form less stable filaments than SM1, therefore it has been suggested that cells with higher SM2 levels could disassemble quickly without much internal resistance or reform (Meer and Eddinger 1997). Considering this, if the day-3 post-injury SMMHC expression observed in the adventitia in section 5.2 is adventitial progenitor cells temporally expressing SM2 as part of modulating cell length, then the ability to promptly reverse the process could be arguably advantageous.

<u>Reduction of "Differentiated" SMC Marker SMMHC Expression in Vascular Remodelling</u>

Considering all of the above it is also important to note that as already discussed in section 5.2, real time SMMHC expression in remodelling vessels is significantly reduced when compared with uninjured vessels. While a few

intimal cells express SMMHC, the majority of intimal cells cannot be defined as "differentiated" SMC. This observation has also been previously published (Tang et al. 2012).

Additional Consideration: Unlikely Feasibility of SMC migration

Poor cellular infiltration is a critical challenge to decellularised vascular tissue scaffold use, and arterial decellularisation studies have provided some insight into the difficult nature of internal vascular-layer cellular migration. Most recently, Sheridan et al., and Campbell et al., highlighted the difficulty of getting cultured SMCs to transverse and re-populate porcine arteries (Sheridan et al. 2011 and Campbell et al. 2012). Campbell et al., demonstrated that cultured SMCs can infiltrate a decellularised artery if cells are seeded at the adventitial and lateral (tissue is cut to expose the adventitia and media) edges, however could not infiltrate the vessel from the luminal side, which proved a barrier to cell infiltration irrespective of the duration of incubation (Campbell et al. 2012). Sheridan et al., demonstrated medial infiltration is possible following longitudal injection of cultured SMCs into the media of a decellularised artery (Sheridan et al. 2011).

Despite the admitted excessive cell seeding and culture times, whole vessel repopulation has yet to be achieved, however Sheridan et al., and Campbell et al., showed that cellular migration in the adventitia and media is possible, and also that SMC/EC migration into the vessel from the luminal side is highly unlikely (Sheridan et al. 2011 and Campbell et al. 2012).

SMC Theory Compromise

Despite the aforementioned confounding factors with the de-differentiation model, it may transpire that a population of SMC undergo 'de-differentiation' to a more stem cell/Sca1 progenitor phenotype. However, in order to come to this conclusion, the tamoxifen-induced Cre recombination queries shall have to be addressed and SMMHC should be seriously re-evaluated as the appropriate definitive marker for "SMC" (i.e. it is proven that resident vascular stem cells cannot transiently express SMMHC).

2. *The Role of Hh in Contributing to Sca1$^+$ Cell Maintenance and Differentiation Underlying their Contribution to Neointimal Formation*

This thesis and previous studies using murine models have shown that Hh signalling is recapitulated during vascular remodelling (Morrow et al. 2009 and Redmond et al. 2013). The following sections will detail what can be currently concluded on the role of Hh signalling in contributing to Sca1$^+$ cell maintenance and differentiation from both *in vitro* and *in vivo* experiments:

Confirmation of Hh Signalling Recapitulation During Vascular Remodelling *In Vivo*

Murine injury analysis (Gli 2 and Patched 1 IHC) has confirmed previous reports of Hh signalling recapitulation during vascular remodelling. Importantly, section 5.2 and 5.3 discuss the observation of Patched 1, the Hh signalling receptor activated by Shh, in the adventitia and media of remodelled vessels as early as 3 day post injury. The observation of further increased Patched 1 expression observed in the media and intimal cells 14 day into the remodelling process indicates that the Hh signalling pathway is activated (Patched 1 is a downstream target of the Hh signalling pathway), and increased Patched 1 mRNA and protein levels have been previously reported in remodelling vessels (Morrow et al. 2009 and Redmond et al. 2013). The significant attenuation of vascular remodelling by cyclopamine also confirms the extensive contribution of Hh signalling activation to the pathology of vessel remodelling.

Sca1$^+$ Hh Signalling Cells Contribute To The Neointimal Formation *In Vivo*

IHC results discussed in section 5.2 and 5.3 clearly show a significant population of neointimal Sca1$^+$Gli2$^+$ (Sca1 Hh responding) cells emerging during vascular remodelling. While it is important to note that not every neointimal cell is Sca1$^+$, the majority, if not all, of the neoinitmal cells express the Hh signalling target Gli 2. It is also interesting to note that Sca1$^+$Gli2$^+$ (Sca1 Hh responding) cells are present at the EC boundary of cyclopamine

treated vessels where significant remodelling attenuation is observed. Additionally, during vascular remodelling, $Sca1^{+}Gli2^{+}$ (Sca1 Hh responding) cells are also present in the adventitia and medial layers indicating that $Sca1^{+}Gli2^{+}$ (Sca1 Hh responding) cells are not unique to the neointima. These findings somewhat complement a previous study that observed significant increases in Shh expression in neointimal and $Sca1^{+}$ perivascular stem cells during injury-induced vascular remodelling (Daniel et al. 2013). The latter study also used a Shh-inhibitor (GDC-0449) and observed a significant reduction in neointimal formation and $Sca1^{+}$ adventitial cell accumulation *in vivo* (Daniel et al. 2013). This observation that Hh inhibition results in the reduction of neointimal formation corroborates our evidence.

Additionally, a recent publication reports the presence of adventitial and perivascular $Sca1^{+}Gli1^{+}$ cells, and while adventitial $Gli1^{+}$ cells have a tri-lineage differentiation capacity *in vitro* (osteoblast, adipocyte and chondrocyte potential), crucially, $Sca1^{+}Gli1^{+}$ cells have the potential to differentiate into SMC *in vitro* (Kramann et al. 2016). Interestingly, a Gli1 Cre Tamoxifen-inducible mouse model was used to assess $Gli1^{+}$ cells contribution to vascular remodelling, however unlike previous Tamoxifen-inducible studies, it is reported that the protocol used was designed to eliminate the possibility of post injury recombination (Kramann et al. 2016). With this in mind, the report shows significant $Gli1^{+}$ cell present in the media and intimal formation post injury (wire-induced), and that > 50 % of intimal cells are $Gli1^{+}$ progenitor cell-derived (Kramann et al. 2016). It is also worth noting that the report indicates that $Gli1^{+}$ cells migrate into the media and intimal formation during the development of both arteriosclerotic and atherosclerotic disease, that the majority of $Gli1^{+}$ cells are also $Sca1^{+}$ following single cell analysis, and that pre-injury genetic ablation of $Gli1^{+}$ cells significantly attenuates vascular remodelling (Kramann et al. 2016). Most importantly, the report also shows evidence of human adventitial $Gli1^{+}$ cells, and the presence of Shh in the adventitia, media and intimal formation strongly suggests that Hh signalling is involved in $Gli1^{+}$ cell expansion, especially considering that *in vitro* activation of Hh signalling results in $Gli1^{+}$ cell proliferation and differentiation (Kramann et al. 2016). Therefore, there

is strong evidence that adventitial Hh signalling (Gli1$^+$) cells/Sca1$^+$ Hh-responsive cells are significant contributors to vascular remodelling, which confirms data and observations reported in this thesis (Kramann et al. 2016 and Baker and Péault 2016).

Shh-Induced Hh Signalling Activation Primarily Induces Sca1$^+$ APC Differentiation *In Vitro*

Firstly, the work presented in this thesis confirms that exposure of Sca1$^+$ cells (both APC and C3H) to Shh *in vitro* initiates Hh signalling activation, a process that can be reliably attenuated using the Hh inhibitor cyclopmaine. Crucially, *in vitro* exposure of Sca1$^+$ APC to Shh appears to primarily result in differentiation to SMC rather than maintain Sca1$^+$ stem cell self-renewal. Nevertheless, it must be noted that the telomerase assay used for the quantification of "stemness" is based on total protein of an entire population of cells, and cannot detect self-renewal on a single cell basis. Therefore, just because there is no significant evidence of the population undergoing stem cell maintenance, does not mean that there are sub-populations within the Shh treated Sca1$^+$ APC, some of which may maintain their stemness while the majority of the population appear to be differentiating. Interestingly in this respect, preventing Hh signalling through the use of cyclopamine significantly increases "stemness", which could also suggest that Hh signalling activation with Shh does not initiate probable population maintenance. Additionally, Shh increases proliferation (also reported by Li et al. 2010), therefore this should also be taken into consideration when contemplating the telomerase assay result.

Previously, other reports have also shown that Sca1$^+$ APC have SMC potential however this is the first report to show that Sca1$^+$ APC can be differentiated into SMC using Shh (the Hh signalling activation ligand shown to co-localise with Sca1$^+$ APC, and this thesis shows that Sca1$^+$ cells also express both Shh and its receptor Patched 1) (Li et al. 2000; Hu et al. 2004 and Passman et al. 2008).

Additional Comment: Evaluation of *In Vitro* Model Cell Lines

Interestingly, papers describing the use of Sca1$^+$ ESC and Sca1$^+$ C3H as models for resident vascular cells and vascular remodelling do not include thorough characterisation analysis prior to manipulation (Korshunov and Berk 2003, Korshunov and Berk 2004, Yin et al. 2005, Xiao et al. 2006, Xiao et al. 2007, Xie et al. 2011 and Guo et al. 2013). The characterisation of C3H and Sca1$^+$ ESC prior to manipulation (chapters 4 and 5 respectively), was designed to be the foundation of the evaluation of these cell lines as models for Sca1$^+$ APC. Unfortunately, their appropriateness with respect to modelling Sca1$^+$ APC has yet to be resolved. However, the following details are the most important considerations and findings throughout their evaluation.

Of both the Sca1$^+$ ESC and C3H model cell lines, the least is known on the appropriateness of Sca1$^+$ ESC as a model cell line for Sca1$^+$ APC. Sca1$^+$ ESC culture was challenging from the start with a differentiation protocol that resulted in Sca1 expression leaving the cell line fragile, and Sca1 expression easily lost. It took a considerable amount of time and continuous culture before the Sca1$^+$ ESC cell line was stable enough for experimentation and even then it required frequent Sca1 re-purification and obtaining high enough Sca1$^+$ cells prior to experimentation was impractical. Unfortunately, at the time of conducting these experiments, a cloning procedure had yet to be established, therefore as a result the Sca1$^+$ ESC experimented on were not cloned. Considering the issues associated with Sca1$^+$ ESC, the second model cell line, C3H, were procured and characterised. Unlike the ESC, the C3H were natively high expressers of Sca1. Also unlike the Sca1$^+$ ESC, prior to manipulation, Sca1$^+$ C3H expressed the pericyte/SMC marker α-actin, the early SMC marker Calponin 1, the differentiated SMC marker SMMHC, and the glial cell marker S100β.

However, Sca1$^+$ C3H were still considered a viable option since the SMC markers were expressed along with stem cell markers, and SMC marker expression levels could be increased using a differentiation protocol. While the Sca1$^+$ C3H provided a valuable cell line for the investigation of Hh

signalling inhibitors, the extent of Sca1$^+$ C3H similarity to Sca1$^+$ APC remains inconclusive. While Shh treatment of Sca1$^+$ C3H clearly activates Hh signalling and increases telomerase activity ("stem cell maintenance"), Shh treatment of Sca1$^+$ APC does not increase telomerase activity but instead appears to primarily initiate proliferation and differentiation towards a SMC profile. Therefore, while the data currently suggests that Sca1$^+$ C3H are not an accurate model for Sca1$^+$ APC, the Sca1$^+$ C3H cell line has proved an invaluable tool for protocol optimisation due to its robust nature. However, it is also possible that there may be different Sca1$^+$ cell populations within the adventitia, one that mimics the C3H cells and the other the APC clone.

6.2 Future Directions

Despite technological and scientific advances to date, the debate between the contributions of SMC versus resident stem cells in vascular remodelling still rages on. While the field is inching towards the latter (considering the mounting evidence (including this thesis) to support the theory that resident stem cells have a role in disease progression), further smart and validated experiments will be crucial to resolving the matter. In fact, validating the tamoxifen experiments alone (as previously described in this chapter) will have a substantial impact on their validity. Additionally, further work with culturing different cloned populations of resident vascular stem cells may also assist in elucidating the variety of stem cell identities within a vessel and their respective differentiation/maintenance potentials. Interestingly, this thesis highlights another potentially crucial contender as a significant contributor to vascular remodelling, EC. As previously described, eNOS$^+$ Sca1$^+$ cells were observed at the lumenal boundary during the early phase of vascular remodelling, suggesting that EC have the potential to activate and phenotypically switch to become stem cell-like. Considering that this Sca1$^+$ EC is the frontier cell prior to the emergence of neointimal cells, it is possible that neointimal cells may be derived from a population of Sca1$^+$ EC.

In order to continue attempting to elucidate what cells are responsible for vascular remodelling, the following experiments should be considered.

Recommendations for Future Experiments That May Contribute Significantly to the Debate

While the generation of a validated tamoxifen-inducible Sca1 transgenic animal would shed light on the exact extent of $Sca1^+$ cell contribution to vascular remodelling, considering the multiple possible sources of $Sca1^+$ cells, the tamoxifen-inducible model would not be able to elucidate the exact $Sca1^+$ source (i.e. $Sca1^+$ APC, $Sca1^+$ EC, $Sca1^+$ BMP or $Sca1^+$ SMC). Therefore, if it were possible to make a validated dual marker lineage-tracing model, with different inducible systems, it may be possible to deduce the exact origin and extent of a single $Sca1^+$ cell source. For example, in order to investigate the possibility of $Sca1^+eNOS^+$ EC contributing to vascular remodelling, carotid ligation (which does not compromise EC) could be conducted on the following theoretical double transgenic mouse:

Tamoxifen-inducible Cre Sca1-eGFP – Tetracycline-inducible CRISPR-Cas eNOS-eRFP

For ease of description this transgenic can be broken into two parts:

1. Tamoxifen-inducible Cre Sca1-eGFP
2. Tetracycline-inducible CRISPR-Cas eNOS-eRFP

1. Tamoxifen-inducible Cre Sca1-eGFP

In this case, the previously described classical tamoxifen-inducible Cre Sca1-eGFP system would be employed, where $CreER^{T2}$ is under the control of Sca1 and the reporter (eGFP) is disrupted. Therefore, in the absence of tamoxifen, $CreER^{T2}$ would be inactive resulting in no change to the reporter (i.e. still disrupted), however, in the presence of tamoxifen, $CreER^{T2}$ would undergo a conformational change into an active form resulting in excision of the reporter disruption, therefore all progeny deriving from a $Sca1^+$ cell would be labelled with eGFP.

2. Tetracycline-inducible CRISPR-Cas eNOS-eRFP

Now, considering that the active CreER^{T2} of the Sca1 system would not be able to differentiate between the Sca1 disrupted reporter, and an eNOS disrupted reporter, a different system would have to be used. Therefore, if this same theory is applied to a Tetracycline-inducible CRISPR-Cas eNOS eRFP system, in that in the absence of tetracycline, CRISPR would be inactive resulting in no change to the reporter (i.e. still disrupted), however, in the presence of tetracycline, CRISPR would activate Cas signalling resulting in excision of the reporter disruption, therefore all progeny deriving from a eNOS^{+} cell would be labelled with eRFP.

Therefore, it would be possible if both of these transgenics were crossed to produce a double marker lineage-tracing transgenic, and track a double marked cell type, for example in this case a Sca1^{+}eNOS^{+}cell. Nevertheless, this is currently a pipe dream considering that a tamoxifen-inducible Sca1 transgenic mouse has yet to be reliably developed. Therefore, in the meantime some other recommendations would be to:

- Investigate the extent of Sca1^{+} APC vascular differentiation: Long-term analysis of different cloned Sca1^{+} APC following exposure to Shh will indicate whether Sca1^{+} APC can be differentiated into SMMHC^{+} SMC and/or whether they differentiate into a variety of progenitors and differentiated SMC
- Investigate Sca1^{+} APC multipotency: Determine whether Sca1^{+} APC can differentiate into other cell types following exposure to Shh. Other cell types indicated in vascular remodelling include inflammatory cells and EC
- Conduct EC transition studies and obtain cloned Sca1^{+} EC cell lines in order to investigate the potential of Sca1^{+} EC contribution to vascular remodelling

6.3 Thesis Conclusions

While this thesis has focused primarily on the pathology of ISR, it is important to note that the animal work conducted in this thesis mimics symmetrical vascular remodelling/arteriosclerosis; a phenomenon that

additionally encompasses natural vascular aging (including medial thickening and calcification) and transplant arteriosclerosis. Therefore, the evidence presented for the contribution of a (Hh responsive) resident stem cell to vascular remodelling has potential beyond the singular application of ISR. It is also important to note, that isolated Sca1$^+$ APC have the potential to be examined under a plethora of conditions *in vitro*, including assessing their response to lipids and other circulating factors observed in atherosclerotic vessels. Therefore, opening up the potential for investigating Sca1$^+$ APC contribution/response during asymmetrical vascular remodelling (atherosclerosis).

This thesis can be split into two main categories; hence will be concluded as such:

1. The contribution of Sca1$^+$ cells to the pathology of vascular remodelling
2. The role of Hh in contributing to Sca1$^+$ cell maintenance and differentiation underlying their contribution to vascular remodelling

Sca1$^+$ Cells Contribute to the Pathology That Emerges During Vascular Remodelling

This thesis provides additional evidence to support the theory that Sca1$^+$ resident stem cells play a key role in the vasculopathy that emerges during vascular remodelling. However unfortunately, current scientific technology falls short of deciphering the exact origin of the Sca1$^+$ cells that emerge during vascular remodelling, therefore all possible sources must be considered. The evidence in both this thesis and literature suggests the most likely sources of Sca1$^+$ cells contributing to vascular remodelling are:

1. Adventitial (considering *in vivo* analysis demonstrating adventitial expansion, increased adventitial Sca1 presence, and the presence of the Hh signalling activation ligand Shh, combined with *in vitro* analysis indicating Shh-induction of SMC differentiation of Sca1$^+$ APC) (Passman et al. 2008) (Figure 6.1)

2. Endothelial (considering *in vivo* evidence of luminal $Sca1^{+}eNOS^{+}$ cells and *in vitro* evidence of endothelial transitioning into mesenchymal stem cells) (Medici et al. 2010; Piera-Velazquez et al. 2011; Kovacic et al. 2012; Cooley et al. 2014 and Sanchez-Duffhues et al. 2016) (Figure 6.1)

There is also the possibility that $Sca1^{+}$ cells contributing to vascular remodelling originate from:

1. Bone marrow progenitors (BMP) (however previous *in vitro* and *in vivo* experiments show that BMP contribution is dependent on the extent of the injury, BMP leave the site of injury after a period of time and, BMP rarely produce SMC/EC (Tanaka et al. 2003; Sainz and Sata 2006 and Daniel at al. 2010) (Figure 6.1)
2. De-differentiating SMC (however the tamoxifen experiments would need to validate their tamoxifen dosing regime and confirm the absence of lingering/residual tissue-associated tamoxifen induced recombination, as well as confirm the inability of adventitial SMMHC expression)

Lastly, there is also the possibility of a combinatory effect rather than a single $Sca1^{+}$ cell source resulting in vascular remodelling and ultimately occlusive neointimal formation.

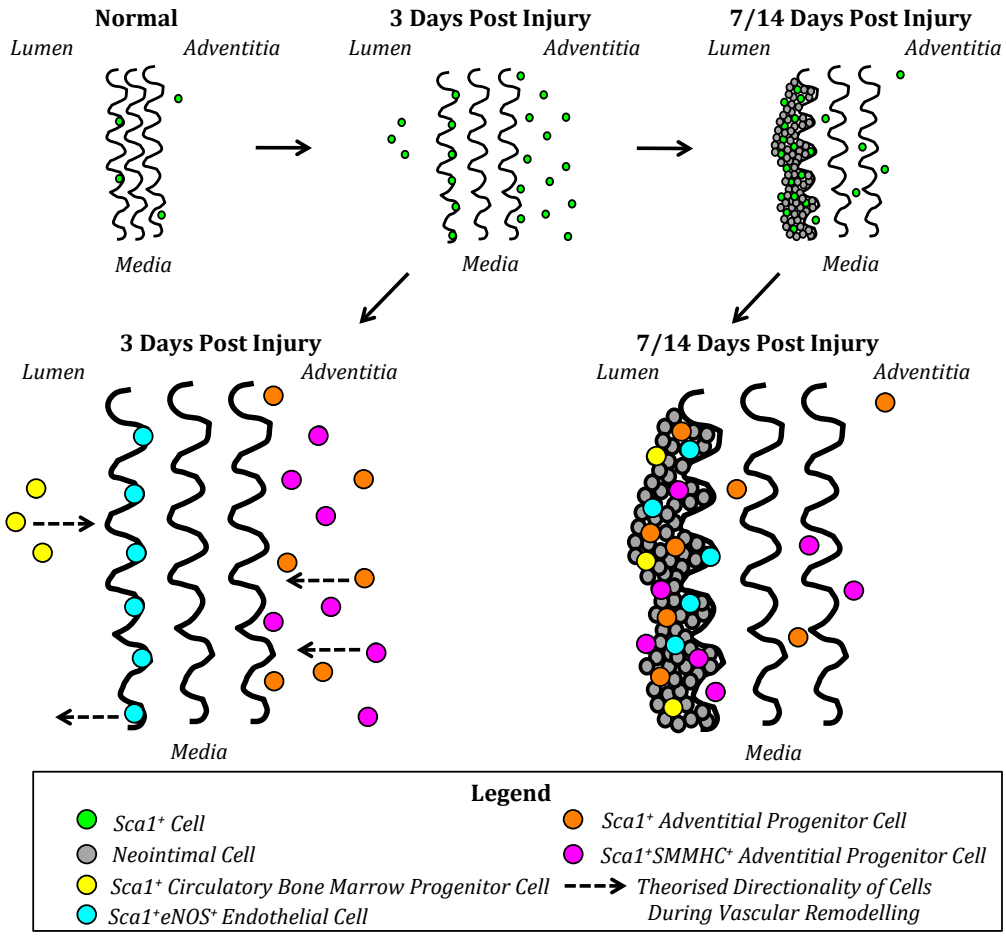

Figure 6.1: Theorised Sca1⁺ Cell Involvement in Neointimal Formation. Normal healthy vessels display a limited number of adventitial and luminal boundary Sca1⁺ cells. A significant increase in the presence of Sca1⁺ cells (adventitial, luminal boundary and circulating Sca1⁺ cells) occurs 3 day following vascular injury. Progressed vascular remodelling shows a marked presence of Sca1⁺ cells in the neointima, with a few Sca1⁺ cells found in the medial and adventitial layers. Sca1⁺ cells present during early vascular remodelling (3 day post injury) can be broken into four categories: 1: Sca1⁺ Circulatory Bone Marrow Progenitor Cells, 2: Sca1⁺eNOS⁺ Endothelial Cells, 3: Sca1⁺ Adventitial Progenitor Cells and 4: Sca1⁺SMMHC⁺ Adventitial Progenitor Cells. These four cell types may proliferate and differentiate into neointimal cells and be the Sca1⁺ cells present in neointimal formations. This figure does not illustrate the theory that some medial Sca1⁺ cell observed in progressed vascular remodelling (7/14 day post injury) may be de-differentiated SMC, however this is also something that must be considered.

Hh Responsive Sca1⁺ Cells Contribute to Vascular Remodelling

Hh signalling is recapitulated during vascular remodelling, and a significant portion of *in vivo* neointimal cells are Sca1⁺ Hh responding cells. Importantly, the number of Sca1⁺ cells was dramatically increased during vessel remodelling *in vivo*, concomitant with increased Patched 1 expression, and

inhibition of Hh signalling with cyclopamine attenuates adventitial thickening and intimal formation *in vivo*, concomitant with a reduction in the number of $Sca1^+$ cells. Additionally, *in vitro* analysis strongly indicates that Shh (Hh signalling activation) induces cellular proliferation, with the majority of cells appearing to differentiate towards SMC rather than self-renew.

Bibliography

Abcam 2016. *Introduction to Flow Cytometry* [Online]. Available from: http://www.abcam.com/protocols/introduction-to-flow-cytometry [Accessed 30 August 2016].

Abcam 2016. *Troubleshooting and using controls in IHC and ICC* [Online]. Available from: http://www.abcam.com/protocols/troubleshooting-and-using-controls-in-ihc-and-icc [Accessed 15 August 2016].

Adams, G.J., Simoni, D.M., Bordelon, C.B., Vick, G.W., Kimball, K/T., Insull, W., Morrisett, J.D. 2002. Bilateral Symmetry of Human Carotid Artery Atherosclerosis. *Stroke*, 33(11), pp.2575–2580.

A.D.A.M 2015. *Introduction* [Online]. http://www.adamimages.com/Illustration/SearchResult/1/stent [Accessed 20 January 2015].

Agathocleous, M., Locker, M., Harris, W.A., Perron, M. 2007. A general role of hedgehog in the regulation of proliferation. *Cell Cycle*, 6(2), pp.156–159.

Ahn, S. and Joyner, A.L. 2005. In vivo analysis of quiescent adult neural stem cells responding to Sonic hedgehog. *Nature*, 437(7060), pp.894–7.

Aikawa, M., Sivam, P.N., Kuro-o, M., Kimura, K., Nakahara, K., Takewaki, S., Ueda, M., Yamaguchi, H., Yazaki, Y., Nagai, R. Human smooth muscle myosin heavy chain isoforms as molecular markers for vascular development and atherosclerosis. *Circ Res*. 1993;73:1000 –1012.

Aikawa, M., Rabkin, E., Voglic, S.J., Shing, H., Nagai, R., Schoen, F.J., Libby, P. 1998. Muscle Cells Expressing Smooth Muscle Myosin Heavy. *Circulation research*, 83, pp.1015–1026.

Al-Wadei, M.H., Banerjee, J., Al-Wadei, H.A.N., Schuller, H.M. 2016. Nicotine induces self-renewal of pancreatic cancer stem cells via neurotransmitter-driven activation of sonic hedgehog signalling. *European Journal of Cancer*, 52, pp.188–196.

Alexander, M.R. and Owens, G.K., 2012. Epigenetic control of smooth muscle cell differentiation and phenotypic switching in vascular development and disease. *Annual review of physiology*, 74(January), pp.13–40.

Almada, A.E. and Wagers, A.J., 2016. Molecular circuitry of stem cell fate in

skeletal muscle regeneration, ageing and disease. *Nature*, 17(5), pp.267–279.

American Heart Association 2014. *Atherosclerosis* [Online]. Available from: http://www.heart.org/HEARTORG/Conditions/Cholesterol/WhyCholesterolMatters/Atherosclerosis_UCM_305564_Article.jsp/ [Accessed 05 May 2016].

Andersson, J., Libby, P. and Hansson, G.K., 2010. Adaptive immunity and atherosclerosis. *Clinical immunology*, 134(1), pp.33–46.

Angert, D., Berretta, R.M., Kubo, H., Zhang, H., Chen, X., Wang, W., Ogorek, B., Barbe, M., Houser, S.R. 2012. Repair of the Injured Adult Heart Involves New Myocytes Potentially Derived From Resident Cardiac Stem Cells. *Circulation Research*, 108(10), pp.1226–1237.

Angioplasty 2015. *History Centre* [Online]. Available from: http://www.ptca.org/nv/history.html [Accessed 25 May 2015].

Argenti, B., Gallo, R., Di Marcotullio, L., Ferretti, E., Napolitano, M., Canterini, S., De Smaele, E., Greco, A., Fiorenza, M. T., Maroder, M., Screpanti, I., Alesse, E., Gulion, A. 2005. Hedgehog antagonist REN(KCTD11) regulates proliferation and apoptosis of developing granule cell progenitors. *Neurosci*. 25, 8338-8346.

Armulik, A., Genove, G. and Betsholtz, C., 2011. Pericytes: Developmental, Physiological, and Pathological Perspectives, Problems, and Promises. *Developmental Cell*, 21(2), pp.193–215.

Atkinson, S. and Armstrong, L., 2008. Epigenetics in embryonic stem cells: Regulation of pluripotency and differentiation. *Cell and Tissue Research*, 331(1), pp.23–29.

Ayata, C., 2010. CADASIL: Experimental insights from animal models. *Stroke*, 41(10 SUPPL. 1), pp.129–135.

Bae, W.-J., Auh, Q.-S., Lim, H.-C., Kim, G.-T., Kim, H.-S., Kim, E.-C. 2016. Sonic Hedgehog Promotes Cementoblastic Differentiation via Activating the BMP Pathways. *Calcified Tissue International*, 99(4), pp.396–407.

Bai, C.B. and Joyner, A.L., 2001. Gli1 can rescue the in vivo function of Gli2. *Development*, 5172, pp.5161–5172.

Baker, C.S.R. and Gupta, S., 2001. Chemokines: The link between inflammation,

restenosis and atherosclerosis? *International Journal of Cardiology*, 80(2-3), pp.107–108.

Baker, A.H. and Pe´ault, B. 2016. A Gli(1)ttering Role for Perivascular Stem Cells in Blood Vessel Remodeling. *Cell Stem Cell.* 19, pp.563-565.

Ballard, V.L.T. and Edelberg, J.M., 2008. Stem cells for cardiovascular repair — The challenges of the aging heart. *Journal of Molecular and Cellular Cardiology*, 45(4), pp.582–592.

Barile, L., Messina, E., Giacomello, A., Marban, E. 2007. Endogenous Cardiac Stem Cells. *Progress in Cardiovascular Diseases*, 50(1), pp.31–48.

Barker, N., 2013. Adult intestinal stem cells : critical drivers of epithelial homeostasis and regeneration. *Nature*, 15(1), pp.19–33.

Barker, N., Wetering, M. Van De and Clevers, H., 2008. The intestinal stem cell. *Gene and Development*, 22, pp.1856–1864.

Bautch, V.L., 2011. Stem cells and the vasculature. *Nature medicine*, 17(11), pp.1437–43.

Beachy, P.A., Hymowitz, S.G., Lazarus, R.A., Leahy, D.J., Siebold, C. 2012. Interactions between Hedgehog proteins and their binding partners come into view. *Gene and Development*, 24, pp.2001–2012.

Beltrami, A.P., Barlucchi, L., Torella, D., Baker, M., Limana, F. Chimenti, S., Kasahara,H., Rota, M., Musso, E., Urbanek, K., Leri, A, Kajstura, J., Nadal-Ginard, B., Anversa, P. 2003. Adult Cardiac Stem Cells Are Multipotent and Support Myocardial Regeneration. *Cell*, 114, pp.763–776.

Benetos, G., Toutouzas, K., Drakopoulou, M., Tolis, E., Masoura, C., Nikolaou, C., Tsekoura, D., Tsiamis, E., Grassos, H., Siores, E., Stephanadis, C., Tousoulis, D. 2015. Bilateral Symmetry of Local Inflammatory Activation in Human Carotid Atherosclerotic Plaques. *Cardiology*, 56, pp.118–124.

Bennett, M.R., 1999. Apoptosis of vascular smooth muscle cells in vascular remodelling and atherosclerotic plaque rupture. *Cardiovascular Research*, 41, pp.361–368.

Bennett, M.R., Evan, G. and Schwartz, S.M., 1995. Apoptosis of Human Vascular Smooth Muscle Cells Derived from Normal Vessels and Coronary Atherosclerotic Plaques. *The American Society for Clincial Investigatio,* 65 pp.2266-2274.

Bernstein, H.S. and Ling, V., 2016. Stem Cell Antigen - 1 in Skeletal Muscle Function. *PLOS Currents Muscular Dystrophy*, pp.1–28.

Bhagirath, K.M., Lester, S.J., Humphries, J., Hentz, J.G., Hurst, R.T. 2012. Carotid intima-media thickness measurements are not affected by the ultrasound frequency. *Echocardiography*, 29(3), pp.354–357.

Bijlsma, M.F., Peppelenbosch, M.P. and Spek, C.A., 2006. Hedgehog morphogen in cardiovascular disease. *Circulation*, 114(18), pp.1985–91.

Blanpain, C. and Simons, B.D., 2013. Unravelling stem cell dynamics by lineage tracing. *Nature reviews. Molecular cell biology*, 14(8), pp.489–502.

Boland, M.J., Nazor, K.L. and Loring, J.F., 2014. Epigenetic regulation of pluripotency and differentiation. *Circulation Research,* 115(2), pp.311–324.

Bradfute, S.B., Graubert, T.A. and Goodell, M.A., 2005. Roles of Sca-1 in hematopoietic stem/progenitor cell function. *Experimental Hematology*, 33(7), pp.836–843.

Briscoe, J. and Thérond, P.P., 2013a. The mechanisms of Hedgehog signalling and its roles in development and disease. *Nature reviews. Molecular cell biology*, 14(7), pp.416–29.

Briscoe, J. and Thérond, P.P., 2013b. The mechanisms of Hedgehog signalling and its roles in development and disease. *Nature reviews. Molecular cell biology*, 429, pp.416–429.

Brittan, M., Wright, N.A. and Wright, N.A., 2002. Gastrointestinal stem cells. *Journal of Pathology*, (197), pp.492–509.

Brunelli, S., Tagliafico, E., De Angelis, F.G., Tonlorenzi, R., Baesso, S., Ferrari, S., Niinobe, M., Yoshikawa, K., Schwartz, R.J., Bozzoni, I., Ferrari, S., Cossu, G. 2004. Msx2 and necdin combined activities are required for smooth muscle differention in mesoangioblast stem cells. *Circulation Research*, 94(12), pp.1571–1578.

Buckley, S.M., Aranda-Orgilles, B., Strikoudis, A., Apostolou, E., Loiziu, E., Moran-Crusio, K., Farnsworth, C.L., Koller, A.A., Dasgupta, R., Silva, J.C., Stadtfeld, M., Hochedlinger, K., Chen, E.I., Aifantis, I. 2012. Regulation of pluripotency and cellular reprogramming by the ubiquitin-proteasome system. *Cell Stem Cell*, 11(6), pp.783–798.

Burke, Z.D., Thowfeequ, S., Peran, M., Tosh, D. 2007. Stem cells in the adult

pancreas and liver. *The Biochemical journal*, 404, pp.169–178.

Campagnolo, P., Cesselli, D., Al Haj Zen, A., Beltrami, A.P., Krankel, N., Katare, R., Angelini, G., Emanueli, C., Madeddu, P. 2010. Human adult vena saphena contains perivascular progenitor cells endowed with clonogenic and proangiogenic potential. *Circulation*, 121: 1735–1745. 38.

Campbell, E.M., Cahill, P.A. and C. Lally. Investigation of a small-diameter decellularised artery as a potential scaffold for vascular tissue engineering; Biomechanical evaluation and preliminary cell seeding. *Journal of the Mechanical Behavior of Biomedical Materials*, 2012; 14:130-142

Carraro U, Dalla Libera L, Catani C. 1983. Myosin light and heavy chains in muscle regenerating in absence of the nerve: transient appearance of the embryonic light chain. *Exp Neurol.,* Jan;79(1):106-17

Casals, J.B., Pieri, N.C.G., Feitosa, M.L.T., Ercolin, A.C.M., Roballo, K.C.S., Barreto, R.S.N. Bressan, F.F., Martins, D.S., Miglino,M.A., Ambrosio, C.E. 2011. The use of animal models for stroke research: A review. *Comparative Medicine*, 61(4), pp.305–313.

Catravas, Callow, Ryna. 1999. *Vascular Endothelium: Mechanisms of Cell Signaling. Endothelial cell matric interactions* pg 179 – 183. IOS Press.

Cell Signaling Technologies 2014. *Hedgehog Signaling Pathway* [Online]. Available from: https://www.cellsignal.com/contents/science-pathway-research-stem-cell-markers/hedgehog-signaling-pathway/pathways-hedgehog [Accessed 18 February 2015].

Chen, J.K., Taipale, J., Cooper, M.K., Beachy, P.A. 2002. Inhibition of Hedgehog signaling by direct binding of cyclopamine to Smoothened. *Genes and Development*, 16(21), pp.2743–2748.

Chen, Y., Wong, M.M., Campagnolo, P., Simpson, R., Winkler, B., Margariti, A., Hu, Y., Xu, Q. 2013. Adventitial stem cells in vein grafts display multilineage potential that contributes to neointimal formation. *Arteriosclerosis, Thrombosis, and Vascular Biology*, 33(8), pp.1844–1851.

Cheung, C., Bernardo, A.S., Trotter, M.W.B., Pedersen, R.A. 2012. Generation of human vascular smooth muscle subtypes provides insight into

embryological origin-dependent disease susceptibility. *Nature biotechnology*, 30(2), pp.165–173.

Choudhry, Z., Rikani, A.A., Choudhry, A.M., Tariq, S., Zakaria, F., Asghar, M.W., Sarfraz, M.K., Haider, K., Shafiq, A.A. 2014. Sonic hedgehog signalling pathway : a complex network. *Annals of Neuroscience*, 21(1), pp.19–22.

Clempus, R.E., Sorescu, D., Dikalova, A.E., Pounkova, L., Jo, P., Sorescu, G.P., Lassegue, B., Griendling, K.K. 2007. Nox4 is required for maintenance of the differentiated vascular smooth muscle cell phenotype. *Arteriosclerosis, Thrombosis, and Vascular Biology*, 27(1), pp.42–48.

Clevers, H. 2013. Review The Intestinal Crypt , A Prototype Stem Cell Compartment. *Cell*, 154(2), pp.274–284.

Clowes, Reidy, and Clowes. Mechanisms of stenosis after arterial injury, *Laboratory Investigation*, vol.49, no. 2, pp. 208–215, 1983. (A)

Clowes, Reidy, and Clowes, Kinetics of cel- lular proliferation after arterial injury. I. Smoothmuscle growth in the absence of endothelium, *Laboratory Investigation*, vol.49, no. 3, pp. 327–333, 1983. (B)

Cohen, M.M. 2010. Hedgehog signaling update. *American journal of medical genetics*., 152A(8), pp.1875–914.

Cooley, B.C., Nevado, J., Mellad, J., Yang, D., St. Hilaire, C., Negro, A., Fang, F., Chen, G., San, H., Walts, A.D., Schwartzbeck, R.L., Taylor, B., Lanzer, J.D., Wragg, A., Elagha, A., Beltran, L.E., Berry, C., Feil, R., Virmani, R., Ladich, E., Kovacic, J.C., Boehm, M. 2014. TGF-β Signaling Mediates Endothelial-to-Mesenchymal Transition (EndMT) During Vein Graft Remodeling. *Science Translational Medicine*, 6(227), pp.227ra34–227ra34.

Corselli M, Chen CW, Sun B, Soloman, Y., Rubin, J.P., Peault, B. 2012. The tunica adventitia of human arteries and veins as a source of mesenchymal stem cells. *Stem Cells Dev*,21:1299–1308. 39.

Cox, J.L. and Gotlieb, A.I., 1986. Restenosis following percutaneous transluminal angioplasty: Clinical, physiologic and pathological features. *Canadian Medical Association Journal*, 134(10), pp.1129–1132.

Dahmann, C., Oates, A.C. and Brand, M. 2011. Boundary formation and maintenance in tissue development. *Nature reviews. Genetics*, 12(1), pp.43–55.

Daniel, J.M., Bielenberg, W., Stieger, P., Weinert, S., Tillmanns, H., and Sedding, D.G. 2010. Time-course analysis on the differentiation of bone marrow-derived progenitor cells into smooth muscle cells during neointima formation. *Arterioscler Thromb Vasc Biol* 30, 1890–1896.

Daniel, J.M., Dutzmann, J., Bielenberg, W., Widmer-Teske, R., Gunduz, D., Hamm, C.W., Sedding, D.G. 2012. Inhibition of STAT3 signaling prevents vascular smooth muscle cell proliferation and neointima formation. *Basic research in cardiology*, 107(3), p.261.

Daniel, J.M., Dutzmann, J., Koch, A., Bauersachs, J., Sedding, D.G. 2013. Inhibition of Sonic Hedgehog signaling impedes perivascular stem cell signaling and prevents neointimal lesion formation. *European Heart*, pp.115–116.

Davie, N.J., Gerasimovskaya, E.V., Hofmeister, S.E., Richman, A.P., Jones, P.L., Reeves, J.T., Stenmark, K.R. 2006. Pulmonary Artery Adventitial Fibroblasts Cooperate with Vasa Vasorum Endothelial Cells to Regulate Vasa Vasorum Neovascularization. *The American Journal of Pathology*, 168(6), pp.1793–1807.

Davignon, J. and Ganz, P., 2004. Role of endothelial dysfunction in atherosclerosis. *Circulation*, 109(23 Suppl 1), pp.III27–32.

Debakey, M.E., 2000. Patterns of Atherosclerosis : Effect of Risk Factors on Recurrence and Survival — Analysis of 11 , 890 Cases With More Than 25-Year Follow-Up. *American Journal of Cardiology* , 85, pp.1045–1053.

De Leon, H., Ollerenshaw, J.D., Griendling, K.K., and Wilcox, J.N. 2001. Adventitial cells do not con- tribute to neointimal mass after balloon angio- plasty of the rat common carotid artery. *Circulation*. 104:1591–1593.

Desai, V.D., Hsia, H.C. and Schwarzbauer, J.E., 2014. Reversible modulation of myofibroblast differentiation in adipose-derived mesenchymal stem cells. *PLoS ONE*, 9(1).

Doe, C.Q., 2008. Neural stem cells: balancing self-renewal with differentiation. *Development*, 135(9), pp.1575–1587.

Doi, H., Iso, T., Shiba, Y., Sato, H., Yamazaki, M., Oyama, Y., Akiyama, H., Tanaka, T., Tomita, T., Arai, M., Takahashi, M., Ikeda, U., Kurabayashi, M. 2009. Notch signaling regulates the differentiation of bone marrow-derived cells into smooth muscle-like cells during arterial lesion formation. *Biochemical and*

biophysical research communications, 381(4), pp.654–9.

Douarin, N.M.L.E. and Nantes, U. De, 1975. Mesenchymal derivatives of the neural crest : analysis of chimaeric quail and chick embryos. *Journal of Embryology and Experimental Morphology*, 34, pp.125–154.

Drüeke, T.B. and London, G.M., 1997. Atherosclerosis and arteriosclerosis in chronic renal failure. *Kidney International*, 51, pp.1678–1695.

Dutta, P., Courties, G., Wei, Y., Leuschner, F., Gorbatov, R., Robbins, C.S., Iwamoto, Y., Thompson, B., Carlson, A.L., Heidt, T., Majmudar, M.D., Lasitschka, F., Etzrodt, M., Waterman, P., Waring, M.T., Chicoine, A.T., Van der Laan, A.M., Niessen, H.W.M., Piek, J.J., Rubin, B.B., Butany, J., Stone, J.R., Katus, H.A., Murphy, S.A., Morrow, D., Sabatine, M.S., Vinegoni, C., Moskowitz, M.A., Pittet, M.J., Libby, P., Lin, C.P., Swirski, F.K., Weissleder, R., Nahrendorf, M. 2012. Myocardial infarction accelerates atherosclerosis. *Nature*, 487(7407), pp.325–329.

Dyer, L.A. and Kirby, M.L., 2009. Sonic hedgehog maintains proliferation in secondary heart field progenitors and is required for normal arterial pole formation. *Developmental Biology*, 330(2), pp.305–317.

Echelard, Y., Epstein, D.J., St-Jacques, B., Shen, L., Mohler, J., McMahon, J.A., and McMahon, A.P. 1993. Sonic hedgehog, a member of a family of putative signaling molecules, is implicated in the regulation of CNS polarity. *Cell,* 75, 1417–1430.

Eddinger, T.J. and Meer, D.P., 2007. Myosin II isoforms in smooth muscle: heterogeneity and function. American journal of physiology. *Cell physiology,* 293(May 2007), pp.C493–C508.

Ellis P, Fagan B.M, Magness S.T, Hutton S, Taranova, Hayashi S, McMahon A, Pevny L. Sox2, a persistent marker for multipotential neural stem cells derived from embryonic stem cells, the embryo or the adult. *Dev Neurosci.* 2004;26:148-165.

Ellison, G.M., Vicinanza, C., Smith, A.J., Aquila, I., Leone, A., Waring, C.D., Agosti, V., Henning, B.J., Stirparo, G.G., Papait, R., Scarfo, M., Viglietto, G., Condorelli, G., Indolfi, C., Ottolenghi, S., Torella, D. 2013. Adult c-kit pos Cardiac Stem Cells Are Necessary and Sufficient for Functional Cardiac Regeneration and Repair. *Cell*, (154), pp.827–842.

Epting, C.L., López, J.e., Shen, X., Liu, L., Bristow, J., Bernstein, H.S. 2004. Stem cell antigen-1 is necessary for cell-cycle withdrawal and myoblast differentiation in C2C12 cells. *Journal of cell science*, 117(Pt 25), pp.6185–95.

Faggin, E., Puato, M., Zardo, L., Franch, R., Millino, C., Sarinella, F., Pauletto, P., Sartore, S., Chiavegato, A. 1999. Smooth Muscle-Specific SM22 Protein Is Expressed in the Adventitial Cells of Balloon-Injured Rabbit Carotid Artery. *Atherosclerosis, Thrombosis and Vascular Biology,* 19, pp.1393-1404.

Falkenstein, K.N. and Vokes, S. a, 2014. Transcriptional regulation of graded Hedgehog signaling. *Seminars in cell & developmental biology*, 33, pp.73–80.

Farrington, S.M., Belaoussoff, M. and Baron, M.H., 1997. Winged-Helix, Hedgehog and Bmp genes are differentially expressed in distinct cell layers of the murine yolk sac. *Mechanisms of Development*, 62(2), pp.197–211.

Favaro, R., Valotta, M., Ferri, A.L.M., Latorre, E., Mariani, J., Giachino, C., Lancini, C., Tosetti, V., Ottolenghi, S., Taylor, V., Nicolis, S.K. 2009. Hippocampal development and neural stem cell maintenance require Sox2-dependent regulation of Shh. *Nature neuroscience*, 12(10), pp.1248–1256.

Feil, S., Valtcheva, N. and Feil, R., 2009. Inducible Cre Mice. *Methods in Molecular Biology*, 530, pp.15-27.

Fink, T. , Lund, P., Pilgaard, L., Rasmussen, J., Duroux, M., Zachar, V. 2008. Instability of standard PCR reference genes in adipose-derived stem cells during propagation, differentiation and hypoxic exposure. *BMC Molecular Biology*, 9(1), p.98.

Firestone, A.J., Weinger, J.S., Maldonado, M., Barlan, K., Lance, D. 2012. Small-molecule inhibitors of the AAA+ ATPase motor cytoplasmic dynein. *Nature*, 484(7392), pp.125–129.

Fischer, A., Schumacher, N., Maier, M., Sendtner, M., Gessler, M. 2004. The Notch target genes Hey1 and Hey2 are required for embryonic vascular development.. *Genes and Development*, pp.901–911.

Franco, R.S., 2012. Measurement of Red Cell Lifespan and Aging. *Transfusion Medicine and Hemotherapy*, (39), pp.302–307.

Friedman S.G. 2005. *A History of Vascular Surgery*. 2nd Ed. Wiley-Blackwell

Frontini, M.J., Nong, Z., Gros, R., Drangova, M., O'Neil, C., Rahman, M.N., Akawi, O.,

Yin, H., Ellis, C.G., Pickering, J.G. 2011. Fibroblast growth factor 9 delivery during angiogenesis produces durable, vasoresponsive microvessels wrapped by smooth muscle cells. *Nature biotechnology*, 29(5), pp.421–427.

Fu, X., Wang, H., Hu, P. 2015. Stem cell activation in skeletal muscle regeneration. *Cellular and Molecular Life Sciences*, (72), pp.1663–1677.

Gadson, P.F., Dalton, M.L., Patterson, E., Svoboda, D.D., Hutchinson, L., Schram, D., Rosenquist, T.H. 1997. Differential Response of Mesoderm- and Neural Crest-Derived Smooth Muscle to TGF- b 1 : Regulation of c-myb and a 1 (I) Procollagen Genes. *Experimental Cell Research*, 180(230), pp.169–180.

Garcia, C.M., Kwon, G.P. and Beebe, D.C., 2008. Alpha smooth muscle actin is constitutively expressed in lens epithelial cells in several species. *Experimental Eye Research*, 83(4), pp.999–1001.

Geng, Y.J. and Libby, P., 1995. Evidence for apoptosis in advanced human atheroma. Colocalization with interleukin-1 beta-converting enzyme. *The American journal of pathology,* 147(2), pp.251–66.

Gilbert, S.F. 2000. *Developmental Biology*.6th Ed. Sunderland: Sinauer Associates.

Gomez, D., Swiatlowska, P. and Owens, G.K., 2015. Epigenetic Control of Smooth Muscle Cell Identity and Lineage Memory. *Arteriosclerosis, Thrombosis, and Vascular Biology*, 35(12), pp.2508–2516.

Götz, J. and Ittner, L., 2008. Animal models of Alzheimer's disease and frontotemporal dementia. *Nature Reviews Neuroscience*, 9(7), pp.532–544.

Grundtman, C., 2012. Animal models of atherosclerosis. *Inflammation and Atherosclerosis*, 9783709103(5), pp.133–169.

Hahn, H., Wicking, C., Zaphiropoulos, P.G., Gailani, M.R., Shanley, S., Chidambaram, A., Vorechovsky, I., Holmberg, E., Unden, A.B., Gillies, S., Negus, K., Smyth, I., Pressman, C., Leffell, D.J., Gerrard, B., Goldstein, A.M., Dean, M., Toftgard, R., Chenevix-trench, G., Wainwright, B., Bale, A.E. 1996. Mutations of the Human Homolog of Drosophila patched in the Nevoid Basal Cell Carcinoma Syndrome. *Cell*, 85, pp.841–851.

Haimovici and Maier. Fate of Aortic Homografts in Canine AtherosclerosisIII. Study of Fresh Abdominal and Thoracic Aortic Implants Into Thoracic Aorta: Role of Tissue Susceptibility in Atherogenesis. *Arch Surg*., 89(6):961-969.

Haimovici and Maier. Experimental canine atherosclerosis in autogenous abdominal aortic grafts implanted into the jugular vein. *Atherosclerosis*. 1971;13(3):375-384.

Haines, N. and Heuvel, M. Van Den, 2000. A Directed Mutagenesis Screen in Drosophila melanogaster Reveals New Mutants That Influence hedgehog Signaling. *Genetics*, 156, pp.1777 – 1785.

Hammond, C.L. and Schulte-Merker, S., 2009. Two populations of endochondral osteoblasts with differential sensitivity to Hedgehog signalling. *Development*, 136(23), pp.3991–4000.

Handin, R.I, Lux, S.E, Stossel, T.P. 2003. *Blood: Principles and Practices of Hematology*. 2nd Ed. U.S.A. Lippincott Williams and Wilkins.

Hashimoto D, Chow A, Noizat C, Teo P, Beasley MB, Leboeuf M, Becker CD, See P, Price J, Lucas D, Greter M, Mortha A, Boyer SW, Forsberg EC, Tanaka M, van Rooijen N, García-Sastre A, Stanley ER, Ginhoux F, Frenette PS, Merad M. 2013. Tissue-resident macrophages self- maintain locally throughout adult life with minimal contribution from cir- culating monocytes. *Immunity*, 38:792–804. 13.

Heiden, K.B., Williamson AJ, Doscas ME, Ye J, Wang Y, Liu D, Xing M, Prinz RA, Xu X. 2014. The sonic hedgehog signaling pathway maintains the cancer stem cell self-renewal of anaplastic thyroid cancer by inducing snail expression. *The Journal of clinical endocrinology and metabolism*, 99(11), pp.E2178–87.

Herring, B.P., Hoggatt AM, Burlak C, Offermanns S. 2014. Previously differentiated medial vascular smooth muscle cells contribute to neointima formation following vascular injury. *Vascular cell*, 6(1), p.21.

High, FA, Lu MM, Pear WS, Loomes KM, Kaestner KH, Epstein JA. 2008. Endothelial expression of the Notch ligand Jagged1 is required for vascular smooth muscle development. *Proceedings of the National Academy of Sciences of the United States of America*, 105(6), pp.1955–9.

Hinz, B., Celetta, G., Tomasek, J.J., Gabbiani, G., Chaponnier, C. 2001. Alpha-Smooth Muscle Actin Expression Upregulates Fibroblast Contractile Activity. *Molecular Biology of the Cell*, 12(9), pp.2730–2741.

Hirschi, K.K., Rohovsky, S.A. and D'Amore, P.A., 1998. PDGF, TGF-beta1, and heterotypic cell-cell interactions mediate endothelial cell-induced

recruitment of 10T1/2 cells and their differentiation to a smooth muscle fate. *Journal of Cell Biology*, 141(3), pp.805–814.

Hoglund, V.J., Dong, X.R. and Majesky, M.W., 2010. Neointima formation: a local affair. *Arteriosclerosis, thrombosis, and vascular biology*, 30(10), pp.1877–9.

Holmes, C. and Stanford, W.L., 2007. Concise review: stem cell antigen-1: expression, function, and enigma. *Stem cells,* 25(6), pp.1339–47.

Holt, A.W. and Tulis, D.A., 2013. Experimental Rat and Mouse Carotid Artery Surgery: Injury and Remodeling Studies. *ISRN Minimally Invasive Surgery*, 10.

Holtz, A.M. Peterson KA, Nishi Y, Morin S, Song JY, Charron F, McMahon AP, Allen BL. 2013. Essential role for ligand-dependent feedback antagonism of vertebrate hedgehog signaling by PTCH1, PTCH2 and HHIP1 during neural patterning. *Development*, 140(16), pp.3423–34.

Hruban, R.H, Beschorner WE, Baumgartner WA, Augustine SM, Ren H, Reitz BA, Hutchins GM. 1990. Accelerated arteriosclerosis in heart transplant recipients is associated with a T-lymphocyte-mediated endothelialitis. *The American journal of pathology*, 137(4), pp.871–882.

Hu, Y., Zhang Z, Torsney E, Afzal AR, Davison F, Metzler B, Xu Q. 2004. Abundant progenitor cells in the adventitia contribute to atherosclerosis of vein grafts in ApoE-deficient mice. *Journal of Clinical Investigation*, 113(9).

Hu, Y. and Xu, Q., 2011. Adventitial biology: differentiation and function. *Arteriosclerosis, thrombosis, and vascular biology*, 31(7), pp.1523–9.

Huangfu, D., Liu A, Rakeman AS, Murcia NS, Niswander L, Anderson KV. 2003. Hedgehog signalling in the mouse requires intraflagellar transport proteins. *Nature*, 426(November), pp.83–87.

Hui, C.-C. and Angers, S., 2011. Gli proteins in development and disease. *Annual review of cell and developmental biology*, 27, pp.513–37.

Imhof, B.A. and Aurrand-lions, M., 2004. Adhesion Mechanisms Regulating The Migration of Monocytes. *Nature Reviews Immunology*, 4(June), pp.432–444.

Ishikawa, H. and Marshall, W.F., 2011. Ciliogenesis: building the cell's antenna. Nature reviews. *Molecular cell biology*, 12(4), pp.222–34.

Irish Heart Foundation 2014. *Facts on Heart Disease and Stroke* [Online]. Available from:

https://www.irishheart.ie/iopen24/facts-heart-disease-stroke-t-7_18.html [Accessed 18 May 2015].

Iso, T., Hamamori, Y. and Kedes, L., 2003. Notch signaling in vascular development. *Arteriosclerosis, thrombosis, and vascular biology*, 23(4), pp.543–53. (A)

Iso, T., Kedes, L. and Hamamori, Y., 2003. HES and HERP families: Multiple effectors of the Notch signaling pathway. *Journal of Cellular Physiology*, 194(3), pp.237–255. (B)

Ito, C.Y., Li CY, Bernstein A, Dick JE, Stanford WL. 2003. Hematopoietic stem cell and progenitor defects in Sca-1 / Ly-6A – null mice. *Blood*, 101(2), pp.517–523.

Jain, M.K., Layne MD, Watanabe M, Chin MT, Feinberg MW, Sibinga NE, Hsieh CM, Yet SF, Stemple DL, Lee ME. 1998. In vitro system for differentiating pluripotent neural crest cells into smooth muscle cells. *Journal of Biological Chemistry*, 273(11), pp.5993–5996.

Jenkins SJ, Ruckerl D, Cook PC, Jones LH, Finkelman FD, van Rooijen N, MacDonald AS, Allen JE. Local macrophage proliferation, rather than recruitment from the blood, is a signature of TH2 inflammation. *Science*. 2011;332:1284–1288.

Jia, Y., Wu D, Zhang R, Shuang W, Sun J, Hao H, An Q, Liu Q. 2014. Bone marrow-derived mesenchymal stem cells expressing the Shh transgene promotes functional recovery after spinal cord injury in rats. *Neuroscience Letters*, 573, pp.46–51.

Jiang, X., Rowitch, D. and Soriano, P., 2000. Fate of the mammalian cardiac neural crest. *Development*, 1616, pp.1607–1616.

Johnson, R.L., Rothman AL, Xie J, Goodrich LV, Bare JW, Bonifas JM, Quinn AG, Myers RM, Cox DR, Epstein EH Jr, Scott MP. 1996. Human Homolog of patched , a Candidate Gene for the Basal Cell Nevus Syndrome. *American Association for the Advancement of Science*, 272(5268), pp.1668–1671.

Jones, C., Watson, D. and Fone, K., 2011. Animal models of schizophrenia. *British Journal of Pharmacology*, 164(4), pp.1162–1194.

Joutel A, Corpechot C, Ducros A, Vahedi K, Chabriat H, Mouton P, Alamowitch S, Domenga V, Cecillion M, Marechal E, Maciazek J, Vayssiere C, Cruaud C,

Cabanis EA, Ruchoux MM, Weissenbach J, Bach JF, Bousser MG, Tournier-Lasserve E. Notch3 mutations in CADASIL, a hereditary adult-onset condition causing stroke and dementia. *Nature*. 1996;383:707–710.

Kabara, M., Kawabe J, Matsuki M, Hira Y, Minoshima A, Shimamura K, Yamauchi A, Aonuma T, Nishimura M, Saito Y, Takehara N, Hasebe N. 2014. Immortalized multipotent pericytes derived from the vasa vasorum in the injured vasculature. A cellular tool for studies of vascular remodeling and regeneration. *Laboratory investigation; a journal of technical methods and pathology,* 94(12), pp.1340–54.

Kafadar, K.A.,□□ 2010. Sca1 expression is required for efficient remodeling of the extracellular matric during skeletal muscle regeneration. *Biomedical Research*, 326(1), pp.47–59.

Kappler, R., Bauer R, Calzada-Wack J, Rosemann M, Hemmerlein B, Hahn H. 2004. Profiling the molecular difference between Patched- and p53-dependent rhabdomyosarcoma. *Oncogene*, 23(54), pp.8785–95.

Kawabe, J.I. and Hasebe, N., 2014. Role of the vasa vasorum and vascular resident stem cells in atherosclerosis. *BioMed Research International*, 2014, 701571.

Kereiakes, D.J., Kuntz RE, Mauri L, Krucoff MW. 2005. Surrogates, substudies, and real clinical end points in trials of drug-eluting stents. *Journal of the American College of Cardiology*, 45(8), pp.1206–12.

Klein, D., Philip, W., Veronika, K., Holger, J., Heinz, G.J., and Süleyman E.2011. Vascular wall-resident CD44+ multipotent stem cells give rise to pericytes and smooth muscle cells and contribute to new vessel maturation. *PloS one*, 6(5), p.e20540.

Klohs, J., Rudin M, Shimshek DR, Beckmann N. 2014. Imaging of cerebrovascular pathology in animal models of Alzheimer's disease. *Frontiers in Aging Neuroscience*, pp.1–30.

Kockx, M 1995. *Spontaneous Induced Intima Formation in Blood Vessels*.1st Ed. Berlin: Springer- Verlag.

Kondo M, Weissman IL, Akashi K. Identification of clonogenic common lymphoid progenitors in mouse bone marrow. *Cell* 1997;91:661–672. 27

Kolodgie, F.D., Narula, J., Guillo, P., Virmani, R. 1999. Apoptosis in human atherosclerotic plaques. *Apoptosis : an international journal on programmed cell death*, 4, pp.5–10.

Korshunov, V.A and Berk, B.C. 2003. Flow-induced vascular remodeling in the mouse: a model for carotid intima-media thickening. *Arteriosclerosis*, thrombosis, and vascular biology, 23(12), pp.2185–91.

Korshunov, V.A and Berk, B.C. 2004. Strain-dependent vascular remodeling: the "Glagov phenomenon" is genetically determined. *Circulation*, 110(2), pp.220–6.

Kos, C.H., 2004. Cre/loxP system for generating tissue-specific knockout mouse models. *Nutrition reviews*, 62(6 Pt 1), pp.243–246.

Kovacic, J.C., Mercader N, Torres M, Boehm M, Fuster V. 2012. Epithelial-to-mesenchymal and endothelial-to-mesenchymal transition from cardiovascular development to disease. *Circulation*, 125(14), pp.1795–1808.

Kramann, R., Goettsch, C., Wongboonsin, J., Iwata, H., Schneider, R.K., Kuppe, C., Kaesler, N., Chang-Panesso, M., Machado, F.G., Gratwohl, S., Madhurima, K., Hutcheson, J.D., Jain, S., Aikawa, E., Humphreys, B.D. 2016. Adventitial MSC-like Cells Are Progenitors of Vascular Smooth Muscle Cells and Drive Vascular Calcification in Chronic Kidney Disease. *Cell Stem Cell*. 19 (5), pp. 628-642.

Kubo, Y., 1991. Comparison of initial stages of muscle differentiation in rat and mouse myoblastic and mouse mesodermal stem cell lines. *The Journal of physiology*, 442, pp.743–59.

Kuro-o M, Nagai R, Tsuchimochi H, Katoh H, Yazaki Y, Ohkubo A, Takaku F. Developmentally regulated expression of vascular smooth muscle myosin heavy chain isoforms. *J Biol Chem*. 1989;264:18272–18275.

Kwon, H.M., Sangiorgi G, Ritman EL, Lerman A, McKenna C, Virmani R, Edwards WD, Holmes DR, Schwartz RS. 1998. Adventitial vasa vasorum in balloon-injured coronary arteries: Visualization and quantitation by a microscopic three-dimensional computed tomography technique. *Journal of the American College of Cardiology*, 32(7), pp.2072–2079.

Lacolley, P., Regnault V, Nicoletti A, Li Z, Michel JB. 2012. The vascular smooth muscle cell in arterial pathology: A cell that can take on multiple roles. *Cardiovascular Research*, 95(2), pp.194–204.

Langheinrich, A.C., Michniewicz A, Sedding DG, Walker G, Beighley PE, Rau WS, Bohle RM, Ritman EL. 2006. Correlation of vasa vasorum neovascularization and plaque progression in aortas of apolipoprotein E-/-/low-density lipoprotein-/- double knockout mice. *Arteriosclerosis, Thrombosis, and Vascular Biology*, 26(2), pp.347–352.

Larrivee, B., Freitas C, Suchting S, Brunet I, Eichmann A. 2009. Guidance of vascular development: Lessons from the nervous system. *Circulation Research*, 104(4), pp.428–441.

Lawson, N.D., Vogel, A.M. and Weinstein, B.M., 2002. sonic hedgehog and vascular endothelial growth factor act upstream of the Notch pathway during arterial endothelial differentiation. *Developmental cell*, 3(1), pp.127–36.

Leach, D.F., Nagarkatti, M., Nagarkatti, P., Cui, T. 2015. Functional states of resident vascular stem cells and vascular remodeling. *Frontiers in Biology*, 10(5), pp.387–397.

Leclair, R.J., Durmus T, Wang Q, Pyagay P, Terzic A, Lindner V. 2007. Cthrc1 Is a Novel Inhibitor of Transforming Growth Factor- β Signaling and Neointimal Lesion Formation. *Circulation Research*, 1, pp.826–833.

Leite, C.F., Almeida TR, Lopes CS, Dias da Silva VJ. 2015. Multipotent stem cells of the heart — do they have therapeutic promise ? *Frontiers in Physiology*, 6(May), pp.1–17.

Leri, A., Rota, M., Hosoda, T., Goichberg, P., Anversa, P. 2014. Cardiac stem cell niches. *Stem Cell Research*, 13(3), pp.631–646.

Leroux-Berger, M., Queguiner I, Maciel TT, Ho A, Relaix F, Kempf H. 2011. Pathologic calcification of adult vascular smooth muscle cells differs on their crest or mesodermal embryonic origin. *Journal of bone and mineral research : the official journal of the American Society for Bone and Mineral Research,* 26(7), pp.1543–53.

Leszczynska, A., O'Doherty, A., Farrell, E., Pindjakova, J., O'Brien, F.J., O'Brien, T., Barry F., Murphy, M. 2016. Differentiation of Vascular Stem Cells

Contributes to Ectopic Calcification of Atherosclerotic Plaque. *Stem Cells*, 34(4), pp.913–923.

Li, F., Duman-Scheel M, Yang D, Du W, Zhang J, Zhao C, Qin L, Xin S. 2010. Sonic hedgehog signaling induces vascular smooth muscle cell proliferation via induction of the G1 cyclin-retinoblastoma axis. *Arteriosclerosis, thrombosis, and vascular biology,* 30(9), pp.1787–94.

Li, G., Chen SJ, Oparil S, Chen YF, Thompson JA. 2000. Direct In Vivo Evidence Demonstrating Neointimal Migration of Adventitial Fibroblasts After Balloon Injury of rat carotid arteries. *Circulation*, (101), pp.1362 – 1365.

Li, J., Xiong J, Yang B, Zhou Q, Wu Y, Luo H, Zhou H, Liu N, Li Y, Song Z, Zheng Q. 2015. Endothelial cell apoptosis induces TGF-β signaling-dependent host endothelial-mesenchymal transition to promote transplant arteriosclerosis. *American Journal of Transplantation*, 15(12), pp.3095–3111.

Liang, S.X., Khachigian LM, Ahmadi Z, Yang M, Liu S, Chong BH. 2011. In vitro and in vivo proliferation, differentiation and migration of cardiac endothelial progenitor cells (SCA1+/CD31+ side-population cells). *Journal of thrombosis and haemostasis :* JTH, 9(8), pp.1628–37.

Lifescience 2015. *Genotyping using the LightCycler 480 System* [Online]. Available from: https://lifescience.roche.com/shop/products/genotyping-using-the-lightcycler-480-system [Accessed 30 August 2016]

V. Lindner, J. Fingerle, and M. A. Reidy, "Mousemodel of arte- rial injury," *Circulation Research*, vol.73, no.5,pp. 792–796, 1993.

Liu, L. and Shi, G.P., 2012. CD31: Beyond a marker for endothelial cells. *Cardiovascular Research*, 94(1), pp.3–5.

Liu, S., 2006. Hedgehog Signaling and Bmi-1 Regulate Self-renewal of Normal and Malignant Human Mammary Stem Cells. *Cancer Research*, 66(12), pp.6063–6071.

Liu, Y., Deng B, Zhao Y, Xie S, Nie R. 2013. Differentiated markers in undifferentiated cells: expression of smooth muscle contractile proteins in multipotent bone marrow mesenchymal stem cells. *Development, growth & differentiation*, 55(5), pp.591–605.

Lodish H, Berk A, Sipursky SL, Matsudaira P, Baltimore D, Darnell. 2000. *Molecular Cell Biology*. 4th ed. New York: W.H. Freeman.

Lu, X., Dunn, J., Dickinson, A.M., Gillespie, J.I., and Baudouin, S. Smooth Muscle Alpha Actin Expression in Endothelial Cells Derived from CD34+ Human Cord Blood Cells. *Stem Cells and Development*. November 2004, 13(5): 521-527.

Lunyak, V. V. and Rosenfeld, M.G., 2008. Epigenetic regulation of stem cell fate. *Human Molecular Genetics*, 17(R1), pp.28–36.

Lüscher, T.F., Steffel J, Eberli FR, Joner M, Nakazawa G, Tanner FC, Virmani R. 2007. Drug-eluting stent and coronary thrombosis: biological mechanisms and clinical implications. *Circulation*, 115(8), pp.1051–8.

Ma, C., Zhou Y, Beachy PA, Moses K.1993. The segment polarity gene hedgehog is required for progression of the morphogenetic furrow in the developing Drosophila eye. *Cell*, 75(5), pp.927–938.

Majesky, M.W., Horita, H., Ostriker, A., Lu, S., Regan, J.N., Bagchi, A., Dong, X.R., Poczobutt, J., Nemenoff, R.A., Weiser-Evans, M.C.M. 2016. Differentiated Smooth Muscle Cells Generate a Subpopulation of Resident Vascular Progenitor Cells in the Adventitia Regulated by KLF4. *Circulation Research,* 119 (11), pp. 1 - 51.

Majesky, M.W., 2015. Adventitia and perivascular cells. *Arteriosclerosis, Thrombosis, and Vascular Biology,* 35(8), pp.e31–e35.

Majesky, M.W., Lindner, V., Twardzik, D.R., Schwartz, S.M and Reidy, M.A. 1991. Production of transforming growth factor beta 1 during repair of arterial injury. *The Journal of clinical investigation*, 88(3), pp.904–10.

Majesky, M.W., Dong, X.R., Hoglund, V., Mahoney, W.M., Daum, G. 2011. The adventitia: a dynamic interface containing resident progenitor cells. *Arteriosclerosis, thrombosis, and vascular biology*, 31(7), pp.1530–9.

Majesky, M.W., Dong, X.R. and Hoglund, V.J., 2011. Parsing aortic aneurysms: more surprises. *Circulation research*, 108(5), pp.528–30.

Manabe, I. anf Owens, G.K., 2001. Recruitment of serum response factor and hyperacetylation of histones at smooth muscle-specific regulatory regions during differentiation of a novel P19-derived in vitro smooth muscle differentiation system. *Circulation research*, 88(11), pp.1127–1134.

Marasani, A.R., Anakonti, R. and Rudrapati, D., 2010. Hedgehog signaling pathway. *Annals of Biological Research*, 1(4), pp.73–84.

Martínez, C., Cornejo, V.H., Lois, P., Ellis, T., Solis, N.P., Wainwright, B.J. 2013. Proliferation of Murine Midbrain Neural Stem Cells Depends upon an Endogenous Sonic Hedgehog (Shh) Source. *PLoS ONE*, 8(6), pp.1–11.

Martinez, N.J. and Gregory, R.I., 2010. MicroRNA gene regulatory pathways in the establishment and maintenance of ESC identity. *Cell Stem Cell*, 7(1), pp.31–35.

Marx, S.O., Totary-Jain, H. and Marks, A. R., 2011. Vascular Smooth Muscle Cell Proliferation in Restenosis. *Circulation: Cardiovascular Interventions*, 4(1), pp.104–111.

Mallat Z, Ohan J, Leseche G, Tedugi A. Colocalization of CPP-32 with apoptotic cells in human atherosclerotic plaques. *Circulation*. 1997;96: 424–428.

Matova, E.E. and Vihert, A.M., 1976. Atherosclerosis and hypertension. *Bulletin of the World Health Organisation*, 53, pp.539–546.

Mayr, U., Mayr M, Yin X, Begum S, Tarelli E, Wait R, Xu Q. 2005. Proteomic dataset of mouse aortic smooth muscle cells. *Proteomics*, 5(17), pp.4546–57.

McGrath, J.C., Deighan C, Briones AM, Shafaroudi MM, McBride M, Adler J, Arribas SM, Vila E, Daly CJ. 2005. New aspects of vascular remodelling: the involvement of all vascular cell types. *Experimental physiology*, 90(4), pp.469–75.

MDPulp 2015. *Suturing techniques* [Online]. Available from: http://www.mdpulp.com/2015/11/suturing-techniques-md-pulp/suturing-techniques-md-pulp-2/ [Accessed 30 May 2016].

Medici, D., Shore, E.M., Lounev, V.Y., Kaplan, F.S., Kalluri, R. 2010. Conversion of vascular endothelial cells into multipotent stem-like cells. *Nature medicine*, 16(12), pp.1400–1406.

Medvedev, S.P., Shevchenko, A.I. and Zakian, S.M., 2010. Molecular basis of Mammalian embryonic stem cell pluripotency and self-renewal. *Acta Naturae*, 2(3), pp.30–46.

Meloche, S. and Pouysségur, J., 2007. The ERK1/2 mitogen-activated protein kinase pathway as a master regulator of the G1- to S-phase transition. *Oncogene*, 26(22), pp.3227–39.

Michel, J.B., Thaunat O, Houard X, Meilhac O, Caligiuri G, Nicoletti A. 2007. Topological determinants and consequences of adventitial responses to arterial wall injury. *Arteriosclerosis, Thrombosis, and Vascular Biology*, 27(6), pp.1259–1268.

Michos, E.D., Nasir K, Braunstein JB, Rumberger JA, Budoff MJ, Post WS, Blumenthal RS. 2006. Framingham risk equation underestimates subclinical atherosclerosis risk in asymptomatic women. *Atherosclerosis*, 184(1), pp.201–206.

Mitchell, R.N. and Libby, P., 2007. Vascular remodeling in transplant vasculopathy. *Circulation Research*, 100(7), pp.967–978.

Moldovan, N.I., Anghelina M, Varadharaj S, Butt OI, Wang T, Yang F, Moldovan L, Zweier JL. 2014. Reoxygenation-derived toxic reactive oxygen/nitrogen species modulate the contribution of bone marrow progenitor cells to remodeling after myocardial infarction. *Journal of the American Heart Association*, 3(1), pp.1–16.

Molinari, F., Pattichis CS, Zeng G, Saba L, Acharya UR, Sanfilippo R, Nicolaides A, Suri JS. 2012. Completely automated multiresolution edge snapper-A new technique for an accurate carotid ultrasound IMT measurement: Clinical validation and benchmarking on a multi-institutional database. *IEEE Transactions on Image Processing*, 21(3), pp.1211–1222.

Molinari, F., Zeng, G. and Suri, J.S., 2010. A state of the art review on intima-media thickness (IMT) measurement and wall segmentation techniques for carotid ultrasound. *Computer Methods and Programs in Biomedicine*, 100(3), pp.201–221.

Morrow, D., Sweeney C, Birney YA, Guha S, Collins N, Cummins PM, Murphy R, Walls D, Redmond EM, Cahill PA. 2007. Biomechanical regulation of hedgehog signaling in vascular smooth muscle cells in vitro and in vivo. *American journal of physiology. Cell physiology,* 292(1), pp.C488–96.

Morrow, D., Guha S, Sweeney C, Birney Y, Walshe T, O'Brien C, Walls D, Redmond EM, Cahill PA. 2008. Notch and vascular smooth muscle cell phenotype. *Circulation research*, 103(12), pp.1370–82.

Morrow, D., Cullen JP, Liu W, Guha S, Sweeney C, Birney YA, Collins N, Walls D, Redmond EM, Cahill PA. 2009. Sonic hedgehog induces notch target gene

expression in vascular smooth muscle cells via VEGF-A. *Arteriosclerosis, Thrombosis, and Vascular Biology,* 29(7), pp.1112–1118.

Murdoch, J. and Copp, A., 2010. The relationship between Sonic hedgehog signalling , cilia and neural tube defects. *Birth Defects Research*, 88(8), pp.633–652.

Nadal-Ginard, B., Ellison, G.M. and Torella, D., 2014. The cardiac stem cell compartment is indispensable for myocardial cell homeostasis , repair and regeneration in the adult. *Stem Cell Research*, 13(3), pp.615–630.

Nagai R, Larson DT, Periasamy M. Characterization of a mammalian smooth muscle myosin heavy chain cDNA clone and its expression in various smooth muscle types. *Proc Natl Acad Sci U S A*. 1988;85:1047–1051.

Nagai R, Kuro-o M, Babij P, Periasamy M. Identification of two types of smooth muscle myosin heavy chain isoforms by cDNA cloning and immunoblot analysis. *J Biol Chem*. 1989;264:9734–9737.

Naito, H., Kidoya H, Sakimoto S, Wakabayashi T, Takakura N. 2012. Identification and characterization of a resident vascular stem/progenitor cell population in preexisting blood vessels. *The EMBO journal,* 31(4), pp.842–55.

Nakagawa, O., McFadden DG, Nakagawa M, Yanagisawa H, Hu T, Srivastava D, Olson EN. 2000. Members of the HRT family of basic helix-loop-helix proteins act as transcriptional repressors downstream of Notch signaling. *Proceedings of the National Academy of Sciences of the United States of America*, 97(25), pp.13655–60.

Nakamura, M., Kubo M, Yanai K, Mikami Y, Ikebe M, Nagai S, Yamaguchi K, Tanaka M, Katano M. 2007. Anti-patched-1 antibodies suppress hedgehog signaling pathway and pancreatic cancer proliferation. *Anticancer Research*, 27(6 A), pp.3743–3747.

Nakamura, T., Colbert, M.C. and Robbins, J., 2006. Neural crest cells retain multipotential characteristics in the developing valves and label the cardiac conduction system. *Circulation research*, 98(12), pp.1547–54.

National Institutes of Health 2009. *The Adult Stem Cell - National Institutes of Health* [Online]. Available from: http://stemcells.nih.gov/info/scireport/pages/chapter4.aspx [Accessed 18 July 2016].

National Institutes of Health 2015. *Stem Cell Basics: Introduction – National Institutes of Health* [Online]. Available from: http://stemcells.nih.gov/info/basics/pages/basics1.aspx [Accessed 18 July 2016].

National Centre for Biotechnology Information 2016a. *Ly6a lymphocyte antigen 6 complex, locus A [Mus musculus (house mouse)]* [Online]. Available from: http://www.ncbi.nlm.nih.gov/gene/110454 [Accessed 09 July 2016].

National Centre for Biotechnology Information 2016b. *Acta2 actin, alpha 2, smooth muscle, aorta [Mus musculus (house mouse)]*[Online]. Available from: http://www.ncbi.nlm.nih.gov/gene/11475 [Accessed 09 July 2016].

National Centre for Biotechnology Information 2016c. *CNN1 calponin 1 [Homo sapiens (human)]* [Online]. Available from: http://www.ncbi.nlm.nih.gov/gene/1264 [Accessed 09 July 2016].

National Centre for Biotechnology Information 2016d. *MYH11 myosin heavy chain 11 [Homo sapiens (human)]* [Online]. Available from: http://www.ncbi.nlm.nih.gov/gene/4629 [Accessed 09 July 2016].

National Centre for Biotechnology Information 2016e. *SOX10 SRY-box 10 [Homo sapiens (human)]* [Online]. Available from: http://www.ncbi.nlm.nih.gov/gene/6663 [Accessed 09 July 2016].

National Centre for Biotechnology Information 2016f. *SOX17 SRY-box 17 [Homo sapiens (human)]* [Online]. Available from: http://www.ncbi.nlm.nih.gov/gene/64321 [Accessed 09 July 2016].

National Centre for Biotechnology Information 2016g. *S100B S100 calcium binding protein B [Homo sapiens (human)]* [Online]. Available from: http://www.ncbi.nlm.nih.gov/gene/6285 [Accessed 09 July 2016].

National Centre for Biotechnology Information 2016h. *NES nestin [Homo sapiens (human)]* [Online]. Available from: http://www.ncbi.nlm.nih.gov/gene/10763 [Accessed 09 July 2016].

National Centre for Biotechnology Information 2016i. *PAX6 paired box 6 [Homo sapiens (human)]* [Online]. Available from: http://www.ncbi.nlm.nih.gov/gene/5080 [Accessed 09 July 2016].

National Centre for Biotechnology Information 2016j. *PAX1 paired box 1 [Homo sapiens (human)]* [Online]. Available from:

http://www.ncbi.nlm.nih.gov/gene/5075 [Accessed 09 July 2016].
National Centre for Biotechnology Information 2016k. *KIT KIT proto-oncogene receptor tyrosine kinase [Homo sapiens (human)]* [Online]. Available from: http://www.ncbi.nlm.nih.gov/gene/3815 [Accessed 15 July 2016].
National Centre for Biotechnology Information 2016l. *PDGFRB platelete derived growth factor receptor beta [Homo sapiens (human)]* [Online]. Available from: http://www.ncbi.nlm.nih.gov/gene/5159 [Accessed 23 July 2016].
National Centre for Biotechnology Information 2016m. *PTPRC protein tyrosine phosphatase, receptor type C [Homo sapiens (human)]* [Online]. Available from: http://www.ncbi.nlm.nih.gov/gene/5788 [Accessed 23 July 2016].
National Centre for Biotechnology Information 2016n. *CD68 CD68 molecule [Homo sapiens (human)]* [Online]. Available from: http://www.ncbi.nlm.nih.gov/gene/968 [Accessed 23 July 2016].
National Centre for Biotechnology Information 2016o. *THY1 Thy-1 cell surface antigen [Homo sapiens (human)]* [Online]. Available from: http://www.ncbi.nlm.nih.gov/gene/7070 [Accessed 24 July 2016].
National Centre for Biotechnology Information 2016p. *CD44 CD44 molecule (Indian blood group) [Homo sapiens (human)]* [Online]. Available from: http://www.ncbi.nlm.nih.gov/gene/960 [Accessed 24 July 2016].
National Centre for Biotechnology Information 2016q. *SOX2 SRY-box 2 [Homo sapiens (human)]* [Online]. Available from: http://www.ncbi.nlm.nih.gov/gene/6657 [Accessed 24 July 2016].
Nemenoff, R., Horita, H., Ostriker, A.C., Furgeson, S.B., Simpson, P.A., VanPutten, V., Crossno, J., Offermanns, S., Weiser-Evans, M.C.M. 2011. SDF-1α induction in mature smooth muscle cells by inactivation of PTEN is a critical mediator of exacerbated injury-induced neointima formation. *Arteriosclerosis, thrombosis, and vascular biology*, 31(6), pp.1300–8.
Nguyen, A.T., Gomez, D., Bell, R.D., Campbell, J.H., Clowes, A.W., Gabbiani, G., Giachelli, C.M., Parmacek, M.S., Raines, E.W., Rusch, N.J., Speer, M.Y., Sturek, M., Thyberg, J., Towler, D.A Weiser-Evans, M.C., Yan, C., Miano, J.M,, Owens, G.K. 2013. Smooth muscle cell plasticity: fact or fiction? *Circulation research*,

112(1), pp.17–22. 2013].

Nickenig, G. and Sinning, J.M., 2009. Response to drug-eluting stents do we need drugs to recompense drug elution? *Journal of the American College of Cardiology*, 54(24), pp.2330–2.

Nikol, S., Isner JM, Pickering JG, Kearney M, Leclerc G, Weir L. 1992. Expression of transforming growth factor-beta 1 is increased in human vascular restenosis lesions. *The Journal of clinical investigation*, 90(4), pp.1582–92.

Nikolsky, E., Gruberg L, Pechersky S, Kapeliovich M, Grenadier E, Amikam S, Boulos M, Suleiman M, Markiewicz W, Beyar R. 2003. Stent deployment failure: reasons, implications, and short- and long-term outcomes. *Catheterization and cardiovascular interventions : official journal of the Society for Cardiac Angiography & Interventions*, 59(3), pp.324–8.

Ocbinaac, R., 2009.Is a cilia-associated Mouse Kif7 / Costal2 that protein Sonic hedgehog regulates signaling. *PNAS*, 106(32), pp.13377–13382.

Oikawa, H., Hayashi K, Maesawa C, Masuda T, Sobue K. 2009. Expression profiles of nestin in vascular smooth muscle cells in vivo and in vitro. E*xperimental Cell Research*, 316(6), pp.940–950.

Orlandi, A. and Bennett, M., 2010. Progenitor cell-derived smooth muscle cells in vascular disease. *Biochemical pharmacology*, 79(12), pp.1706–13.

Owens GK. Regulation of differentiation of vascular smooth muscle cells. *Physiol Rev*. 1995;75:487–517.

Owens, G.K., Kumar, M.S. and Wamhoff, B.R., 2004. Molecular regulation of vascular smooth muscle cell differentiation in development and disease. *Physiological reviews,* 84, pp.767–801.

Oyama, N., Takeshita K, Liu PY, Satoh M, Oyama N, Mukai Y, Chin MT, Krebs L, Kotlikoff MI, Radtke F, Gridley T, Liao JK. 2010. Smooth Muscle Notch1 Mediates Neointimal Formation Following Vascular Injury. *Circulation*, 119(20), pp.2686–2692.

Pansky, B. 1982. *Review of Medical Embryology*.1st Ed. U.S.A.: Macmillan

Pardali, E., Goumans, M.J. and Dijke, P., 2010. Signaling by members of the TGF-β family in vascular morphogenesis and disease. *Trends in Cell Biology*, 20(9), pp.556–567.

Park, H.-C. and Appel, B., 2003. Delta-Notch signaling regulates oligodendrocyte specification. *Development*, 130(16), pp.3747–3755.

Passman, J.N., Dong, X.R., Wu, S-P., Maguire, C.T., Hogan, K.A., Bautch, L. and Majesky, M. 2008. A sonic hedgehog signaling domain in the arterial adventitia supports resident Sca1+ smooth muscle progenitor cells. *Proceedings of the National Academy of Sciences of the United States of America,* 105(27), pp.9349–54.

Paulick, M.G. and Bertozzi, C.R., 2008. The glycosylphosphatidylinositol anchor: A complex membrane-anchoring structure for proteins. *Biochemistry*, 47(27), pp.6991–7000.

Pfaltzgraff, E.R., Shelton EL, Galindo CL, Nelms BL, Hooper CW, Poole SD, Labosky PA, Bader DM, Reese J. 2015. Embryonic domains of the aorta derived from diverse origins exhibit distinct properties that converge into a common phenotype in the adult. *Journal of molecular cell cardiology,* 69, pp.88–96.

Piera-Velazquez, S., Li, Z. and Jimenez, S.A., 2011. Role of endothelial-mesenchymal transition (EndoMT) in the pathogenesis of fibrotic disorders. *American Journal of Pathology*, 179(3), pp.1074–1080.

Pinney, D.F. and Emerson, C.P., 1989. 10T1/2 cells: An in vitro model for molecular genetic analysis of mesodermal determination and differentiation. *Environmental Health Perspectives*, 80(4), pp.221–227.

Pires-daSilva, A. and Sommer, R.J., 2003. The evolution of signalling pathways in animal development. Nature reviews. *Genetics*, 4(1), pp.39–49.

Plissonnier D, Nochy D, Poncet P, Mandet C, Hinglais N, Bariety J, Michael JB. 1995. Sequential immunological targeting of chronic experimental arterial allograft. *Transplantation*;60:414–424.

Plissonnier D, Henaff M, Poncet P, Paris E, Tron F, Thuillez C, Michael JB. 2000. Involvement of antibody-dependent apoptosis in graft rejection. *Transplantation*;69: 2601–2608. 2.

Potter, C.M.F., Lao KH, Zeng L, Xu Q. 2014. Role of biomechanical forces in stem cell vascular lineage differentiation. *Arteriosclerosis, Thrombosis, and Vascular Biology,* 34(10), pp.2184–2190.

Prasad, M.S., Sauka-Spengler, T. and LaBonne, C., 2012. Induction of the neural crest state: Control of stem cell attributes by gene regulatory, post-

transcriptional and epigenetic interactions. *Developmental Biology*, 366(1), pp.10–21.

Price 2013. *Coronary Stenting: A Companion to Topol's Textbook of Interventional Cardiology.* 1st Ed. Philidelphia: Elsevier Health Science.

Psaltis, P.J., Puranik AS, Spoon DB, Chue CD, Hoffman SJ, Witt TA, Delacroix S, Kleppe LS, Mueske CS, Pan S, Gulati R, Simari RD. 2014. Characterization of a resident population of adventitial macrophage progenitor cells in postnatal vasculature. *Circulation Research*, 115(3), pp.364–375.

Qi, Y.-X., Jiang, J., Jiang, X.-H., Wang, X.-D., Ji, S.-Y., Han, Y., Long, D.-K., Shen, B.-R., Yan, Z.-Q., Chien, S., Jiang, Z.-L. 2011. PDGF-BB and TGF-{beta}1 on cross-talk between endothelial and smooth muscle cells in vascular remodeling induced by low shear stress. *Proceedings of the National Academy of Sciences of the United States of America*, 108(5), pp.1908–13.

Ramos, T., Sánchez-Abarca LI, Muntión S, Preciado S, Puig N, López-Ruano G, Hernández-Hernández Á, Redondo A, Ortega R, Rodríguez C, Sánchez-Guijo F, del Cañizo C. 2016. MSC surface markers (CD44, CD73, and CD90) can identify human MSC-derived extracellular vesicles by conventional flow cytometry. *Cell Communication and Signaling*, 14(1), p.2.

Ray, A. Tamsma JT, Hovens MM, op 't Roodt J, Huisman MV. 2010. Accuracy of carotid plaque detection and intima-media thickness measurement with ultrasonography in routine clinical practice. *European Journal of Internal Medicine*, 21(1), pp.35–39.

Redmond, E.M., Hamm K, Cullen JP, Hatch E, Cahill PA, Morrow D. 2013. Inhibition of patched-1 prevents injury-induced neointimal hyperplasia. *Arteriosclerosis, thrombosis, and vascular biology*, 33(8), pp.1960–4.

Redmond, E.M., Guha S, Walls D, Cahill PA. 2011. Investigational Notch and Hedgehog inhibitors--therapies for cardiovascular disease. *Expert opinion on investigational drugs*, 20(12), pp.1649–64.

Reinert, R.B., Kantz, J., Misfeldt, A.A., Poffenberger, G., Gannon, M., Brissova, M., Powers, A.C. 2012. Tamoxifen-induced cre-loxp recombination is prolonged in pancreatic islets of adult mice. *PLoS ONE*, 7(3).

Rensen, S.S.M., Doevendans, P.A.F.M. and van Eys, G.J.J.M., 2007. Regulation and characteristics of vascular smooth muscle cell phenotypic diversity.

Netherlands heart journal : monthly journal of the Netherlands Society of Cardiology and the Netherlands Heart Foundation, 15(3), pp.100–8.

Rimkus, T., Carpenter RL, Qasem S, Chan M, Lo HW. 2016. Targeting the Sonic Hedgehog Signaling Pathway: Review of Smoothened and GLI Inhibitors. *Cancers*, 8(2), p.22.

Roessler, E. and Muenke, M., 2003. How a Hedgehog might see holoprosencephaly. Human *Molecular Genetics*, 12(90001), pp.R15–R25.

Romanyukha, A.A. and Yashin, A.I., 2003. Age related changes in population of peripheral T cells : towards a model of immunosenescence. *Mechamisms of Ageing and Development*, 124, pp.433–443.

Roy, E., Neufeld Z, Livet J, Khosrotehrani K. 2014. Concise review: Understanding clonal dynamics in homeostasis and injury through multicolor lineage tracing. *Stem Cells*, 32(12), pp.3046–3054.

Ruggeri, B.A., Camp, F. and Miknyoczki, S., 2014. Animal models of disease: Pre-clinical animal models of cancer and their applications and utility in drug discovery. *Biochemical Pharmacology*, 87(1), pp.150–161.

Sahara, M., Sata M, Morita T, Nakamura K, Hirata Y, Nagai R. 2007. Diverse contribution of bone marrow-derived cells to vascular remodeling associated with pulmonary arterial hypertension and arterial neointimal formation. *Circulation*, 115(4), pp.509–517.

Sainz, J., Al Haj Zen A, Caligiuri G, Demerens C, Urbain D, Lemitre M, Lafont A. 2006. Isolation of "side population" progenitor cells from healthy arteries of adult mice. *Arteriosclerosis, thrombosis, and vascular biology*, 26(2), pp.281–6.

Sainz, J. and Sata, M., 2006. Maintenance of vascular homeostasis by bone marrow-derived cells. *Arteriosclerosis, Thrombosis, and Vascular Biology*, 26(6), pp.1196–1197.

Sakata, Y., Xiang F, Chen Z, Kiriyama Y, Kamei CN, Simon DI, Chin MT. 2004. Transcription factor CHF1/Hey2 regulates neointimal formation in vivo and vascular smooth muscle proliferation and migration in vitro. *Arteriosclerosis, thrombosis, and vascular biology*, 24(11), pp.2069–74.

Sanchez-Duffhues, G., Orlova, V.and Ten Dijke, P., 2016. In Brief: Endothelial-to-mesenchymal transition. *Journal of Pathology*, 238(3), pp.378–380.

Sartore, S., Chiavegato A, Faggin E, Franch R, Puato M, Ausoni S, Pauletto P. 2001. Contribution of Adventitial Fibroblasts to Neointima Formation and Vascular Remodeling: From Innocent Bystander to Active Participant. *Circulation Research*, 89(12), pp.1111–1121.

Sasamura and Itoh. 2011. Hypertension and arteriosclerosis. *Nihon Rinsho*, 69(1), p 125-130.

Sata, M., 2003. Circulating vascular progenitor cells contribute to vascular repair, remodeling, and lesion formation. *Trends in Cardiovascular Medicine*, 13(6), pp.249–253.

Sata, M., Saiura A, Kunisato A, Tojo A, Okada S, Tokuhisa T, Hirai H, Makuuchi M, Hirata Y, Nagai R. 2002. Hematopoietic stem cells differentiate into vascular cells that participate in the pathogenesis of atherosclerosis. *Nat Med*, 8(4), pp.403–409.

Sauer, B., 1998. Inducible gene targeting in mice using the Cre/lox system. *Methods*, 14(4), pp.381–92.

Schiaffino, S., Rossi AC, Smerdu V, Leinwand LA, Reggiani C. 2015. Developmental myosins: expression patterns and functional significance. *Skeletal muscle*, 5, p.22.

Schlendorf, K.H., Nasir, K. and Blumenthal, R.S., 2009. Limitations of the Framingham risk score are now much clearer. *Preventive Medicine*, 48(2), pp.115–116.

Schulz C, Gomez Perdiguero E, Chorro L, Szabo-Rogers H, Cagnard N, Kierdorf K, Prinz M, Wu B, Jacobsen SE, Pollard JW, Frampton J, Liu KJ, Geissmann F. 2012. A lineage of myeloid cells independent of Myb and hematopoietic stem cells. *Science*, 336:86–90.

Schwartz, deBois, O'Brien. 1995. The Intima: Soil for Atherosclerosis and Restenosis. *Circ Res.* 1995;77:445-465

Sciahbasi, A., Patrizi, R., Madonna, M., Summaria, F., Scioli, R., Carlino, G., Lioy, E. 2009. Successful thrombolysis in patients with subacute and late stent thrombosis. *The Canadian journal of cardiology*, 25(6), pp.e213–4.

Shemin, D. and Rittenberg, D., 1946. The Life Span Of The Human Red Blood Cell. *Journal of Biological Chemistry*, (166), pp.627 – 636.

Sheridan, W.S., Duffy, G.P. and Murphy, B.P., 2011. Mechanical characterisation of

a customised decellularized scaffold for vascular tissue engineering. *Journal of the Mechanical Behavior of Biomedical Materials*, pp.58–70.

Shi Y, O'Brien JE, Fard A, Mannion JD, Wang D, Zalewski A. 1996. Adventitial myofibroblasts contribute to neointimal formation in injured porcine coronary arteries. *Circulation*, 94:1655–1664. 15.

Shi Y, O'Brien JE Jr, Mannion JD, Morrison RC, Chung W, Fard A, Zalewski A. 1997. Remodeling of autologous saphenous vein grafts: the role of perivascular myofibroblasts. *Circulation*, 95:2684–2693. 16.

Shi, X. and Garry, D.J., 2006. Muscle stem cells in development , regeneration , and disease. *Genes and Development*, (20), pp.1692–1708.

Shikatani, E.A, Chandy M, Besla R, Li CC, Momen A, El-Mounayri O, Robbins CS, Husain M. 2016. c-Myb Regulates Proliferation and Differentiation of Adventitial Sca1 $^{+}$ Vascular Smooth Muscle Cell Progenitors by Transactivation of Myocardin. *Arteriosclerosis, Thrombosis, and Vascular Biology*, 36(7), pp.1367–1376.

Shoji, M., Koba, S., Kobayashi,Y. 2014. Roles of Bone-Marrow-Derived Cells and Inflammatory Cytokines in Neointimal Hyperplasia after Vascular Injury. *BioMedical Research International*, 2014, pp.1–8.

Shoji, M., Sata M, Fukuda D, Tanaka K, Sato T, Iso Y, Shibata M, Suzuki H, Koba S, Geshi E, Katagiri T. 2004. Temporal and spatial characterization of cellular constituents during neointimal hyperplasia after vascular injury: Potential contribution of bone-marrow-derived progenitors to arterial remodeling. *Cardiovascular Pathology*, 13(6), pp.306–312.

Sidney, L.E., Branch, M.J., Dunphy, S.E., Dua, H.S., Hopkinson, A. 2014. Concise review: Evidence for CD34 as a common marker for diverse progenitors. *Stem Cells*, 32(6), pp.1380–1389.

Sigma 2014. *Embryonic Stem Cell Differentiation* [Online] . Available from: http-//www.sigmaaldrich.com/life-science/stem-cell-biology.html. [Accessed 10 May 2014].

Simard, T., Hibbert B, Ramirez FD, Froeschl M, Chen YX, O'Brien ER.2014. The evolution of coronary stents: a brief review. *The Canadian journal of cardiology*, 30(1), pp.35–45.

Siow, R.C.M., Mallawaarachchi, C.M. and Weissberg, P.L., 2003. Migration of

adventitial myofibroblasts following vascular balloon injury : insights from in vivo gene transfer to rat carotid arteries. *Cardiovascular Research*, 59, pp.212–221.

Skvortsov, D.A. , Zvereva, M.E., Shpanchenko, O.V., Dontsova, O.A. 2011. Assays for detection of telomerase activity. *Acta naturae*, 3(1), pp.48–68.

Slomp J, Gittenberger-de Groot AC, Glukhova MA, van Musteren C, Kockx MM, Schwarz SM, Koteliansky VE. 1997. Differentiation, dedifferen- tiation, and apoptosis of smooth muscle cells during the development of the human ductus arteriosus. *Arterioscler Thromb Vasc Biol.*,17: 1003–1009.

Spence JR, Madhavan M, Ewing JD, Jones DK, Lehman BM, Del Rio-Tsonis K. 2004. The hedge- hog pathway is a modulator of retina regeneration. *Development*, 131:4607-21. 22.

Sprague, A.H. and Khalil, R.A., 2010. Inflammatory Cytokines in Vascular Dysfunction and Vascular Disease. *Biochem Pharmacol.*, 78(6), pp.539–552.

Spangrude GJ, Klein J, Heimfeld S, Aihara Y, Weissman IL. 1989. Two monoclonal antibodies identify thymic-repopulating cells in mouse bone marrow. *J Immunol*, 142:425–430. 28

Stenmark, K.R., Davie N, Frid M, Gerasimovskaya E, Das M. 2006. Role of the adventitia in pulmonary vascular remodeling. *Physiology*, 21, pp.134–45.

Stern, R.H., 2014. Problems With modified framingham risk score. *Canadian Journal of Cardiology*, 30(2), p.248.

Steven Hsu, Julia S.Chu, Fanqing F.Chen, Aijun Wang, S.L., 2012. Effects of Fluid Shear Stress on a Distinct Population of Vascular Smooth Muscle Cells. *Cell Mol Bioeng.*, 4(4), pp.627–636.

Stevens, T., Pha, S., Frid, M.G., Alvarez, D., Herzog, E., Stenmark, K.R. 2008. Lung vascular cell heterogeneity: endothelium, smooth muscle, and fibroblasts. *Proceedings of the American Thoracic Society*, 5(7), pp.783–91.

Suwanabol, P.A., Kent, K.C. and Liu, B., 2011. TGFbeta and restenosis revisited: A smad link. *Journal of Surgical Research*, 167(2), pp.287–297.

Tabas, I., Garcia-Cardena, G. and Owens, G.K., 2015. Recent insights into the cellular biology of atherosclerosis. *Journal of Cell Biology*, 209(1), pp.13–22.

Tanaka, K. , Sata M, Hirata Y, Nagai R. 2003. Diverse Contribution of Bone Marrow Cells to Neointimal Hyperplasia After Mechanical Vascular Injuries. Circulation Research, 93(8), pp.783–790.

Tang, Y., Urs S, Boucher J, Bernaiche T, Venkatesh D, Spicer DB, Vary CP, Liaw L. 2010. Notch and transforming growth factor-beta (TGFbeta) signaling pathways cooperatively regulate vascular smooth muscle cell differentiation. The Journal of biological chemistry, 285(23), pp.17556–63.

Tang, Z., Wang, A., Yuan, F., Yan, Z., Liu, B., Chu, J.S., Helms, J.A., Li, S. 2012. Differentiation of multipotent vascular stem cells contributes to vascular diseases. *Nature communications*, 3, p.875.

Tang, Z., Wang A, Wang D, Li S. 2013. Smooth muscle cells: to be or not to be? Response to Nguyen et Al. Circulation research, 112(1), pp.23–6.

Tanous, D., Benson, L.N. and Horlick, E.M., 2009. Coarctation of the aorta: evaluation and management. *Current opinion in cardiology*, 24(6), pp.509–15.

Tay, Y.M.-S., Tam WL, Ang YS, Gaughwin PM, Yang H, Wang W, Liu R, George J, Ng HH, Perera RJ, Lufkin T, Rigoutsos I, Thomson AM, Lim B. 2008. MicroRNA-134 modulates the differentiation of mouse embryonic stem cells, where it causes post-transcriptional attenuation of Nanog and LRH1. Stem cells, 26(1), pp.17–29.

Tedesco, F.S., Dellavalle, A., Diaz-Manera, J., Messina, G., Cossu, G. 2010. Review series Repairing skeletal muscle : regenerative potential of skeletal muscle stem cells. *The Journal of Clinical Investigation*, 120(1), pp.11–19.

Teperino, R., Aberger F, Esterbauer H, Riobo N, Pospisilik JA. 2014. Canonical and non-canonical Hedgehog signalling and the control of metabolism. Seminars in cell & developmental biology, 33, pp.81–92.

Thangavel, R.R. and Bouvier, N.M., 2014. Animal models for influenza virus pathogenesis, transmission, and immunology. *Journal of Immunological Methods*, 410, pp.60–79.

The Jackson Laboratory 2016. *B6.FVB.–Tg(SMMHC-CreERT2)1Soff/J* [Online]. Available from: https://www.jax.org/strain/019079 [Accessed 05 June 2016].

Tigerstedt, N.M., Savolainen-Peltonen H, Lehti S, Hayry P. 2009. Vascular Cell Kinetics in Response to Intimal Injury ex vivo. Journal of Vascular Research, 47(1), pp.35–44.

Tigges, U., Komatsu, M. and Stallcup, W.B., 2013. Adventitial Pericyte Progenitor/Mesenchymal Stem Cells Participate in the Restenotic Response to Arterial Injury. *Journal of Vascular Research*, 50(2), pp.134–144.

Topouzis, S. and Majesky, M.W., 1996. Smooth Muscle Lineage Diversity in the Chick Embryo Two Types of Aortic Smooth Muscle Cell Differ in Growth and Receptor-Mediated Transcriptional Responses to Transforming Growth Factor- b. *Dev Biol*, 445(0229), pp.430–445.

Torella, D., Ellison GM, Nadal-Ginard B, Indolfi C. 2005. Cardiac Stem and Progenitor Cell Biology for Regenerative Medicine. Trends in Cardiovascular Medicine, 15(6), pp.229–236.

Torsney, E., Hu, Y. and Xu, Q., 2005. Adventitial progenitor cells contribute to arteriosclerosis. Trends in Cardiovascular Medicine, 15(2), pp.64–68.

Torsney E, Mandal K, Halliday A, Jahangiri M and Xu Q. 2007. Characterisation of progenitor cells in human atherosclerotic vessels. *Atherosclerosis* 191, 259–264.

Tulis, D.A. 2007. Histological and morphometric analysis for rat carotid ballon injury midel. *Methods in molecular medicine*. 139, pp.31-66

Uchida, S., De Gaspari P, Kostin S, Jenniches K, Kilic A, Izumiya Y, Shiojima I, Grosse Kreymborg K, Renz H, Walsh K, Braun T. 2013. Sca1-Derived Cells Are a Source of Myocardial Renewal in the Murine Adult Heart. Stem Cell Reports, 1, pp.397–410.

Van de Rijn M, Heimfeld S, Spangrude GJ Weissman IL. Mouse hematopoietic stem-cell antigen Sca-1 is a member of the Ly-6 antigen family. Proc Natl Acad SciUSA 1989;86:4634–4638. 7

Van der Loo B, Martin JF. The adventitia, endothelium and atherosclerosis. *Int J Microcirc Clin Exp*. 1997;17:280–288.

van Vliet, P., Roccio, M., Smits, A.M., van Oorschot, A.A.M., Metz, C.H.G., van Veen, T.A.B., Sluijter, J.P.G, Doevendans, P.A., Goumans, M.-J. 2008. Progenitor cells isolated from the human heart : a potential cell source for regenerative therapy. *Neth Heart J*, 16(5), pp.163–169.

Vanhoutte, P.M., 2009. Endothelial Dysfunction - The first step towards coronoary arteriosclerosis -. *Circulation Journal*, 73, pp.595–601.

Varjosalo, M. and Taipale, J., 2008. Hedgehog : functions and mechanisms. *Genes and Development*, 22, pp.2454–2472.

Vernay, A. and Cosson, P., 2013. Immunofluorescence labeling of cell surface antigens in Dictyostelium. *BMC Research Notes,* 6(1), p.317.

Villavicencio, E.H., Walterhouse, D.O. and Iannaccone, P.M., 2000. The sonic hedgehog-patched-gli pathway in human development and disease. *American journal of human genetics*, 67(5), pp.1047–54.

Vyas, N., Goswami D, Manonmani A, Sharma P, Ranganath HA, VijayRaghavan K, Shashidhara LS, Sowdhamini R, Mayor S. 2008. Nanoscale Organization of Hedgehog Is Essential for Long-Range Signaling. Cell, 133(7), pp.1214–1227.

Walsh, K., Smith, R.C. and Kim, H., 2000. Vascular Cell Apoptosis in Remodeling, Restenosis and Plaque Rupture. *Circulation research*, (87), pp.184–188.

Walshe, T.E., Connell P, Cryan L, Ferguson G, Gardiner T, Morrow D, Redmond EM, O'Brien C, Cahill PA. 2011. Microvascular retinal endothelial and pericyte cell apoptosis in vitro: role of hedgehog and Notch signaling. Investigative ophthalmology & visual science, 52(7), pp.4472–83.

Wan, M., Li C, Zhen G, Jiao K, He W, Jia X, Wang W, Shi C, Xing Q, Chen YF, Jan De Beur S, Yu B, Cao X. 2012. Injury-activated transforming growth factor β controls mobilization of mesenchymal stem cells for tissue remodeling. Stem Cells, 30(11), pp.2498–2511.

Wang, G., Zhang, Z., Xu, Z, Yin, H., Bai, L., Ma, M., DeCoster, M.A., Qian, G., Wu, G. 2010. Activation of the sonic hedgehog signaling controls human pulmonary arterial smooth muscle cell proliferation in response to hypoxia. *Biochim Biophys Acta*, 1803(12), pp.1359–1367.

Wang, G., Jacquet L, Karamariti E, Xu Q. 2015. Origin and differentiation of vascular smooth muscle cells. The Journal of Physiology, 593(14), pp.3013–3030.

Wang, W., Prince CZ, Hu X, Pollman MJ. 2003. HRT1 modulates vascular smooth muscle cell proliferation and apoptosis. Biochemical and Biophysical Research Communications, 308(3), pp.596–601.

Wang, X., Hu Q, Nakamura Y, Lee J, Zhang G, From AH, Zhang J. 2006. The role of the sca-1+/CD31- cardiac progenitor cell population in postinfarction left ventricular remodeling. Stem cells (Dayton, Ohio), 24(7), pp.1779–88.

Ward, M.R., Pasterkamp, G., Yeung, A.C., Borst, C. 2000. Arterial Remodeling - Mechanisms and Clinical Implications. *Circulation Journal*, 102, pp.1186–1191.

Warzecha J[1], Göttig S, Brüning C, Lindhorst E, Arabmothlagh M, Kurth A. 2006. Sonic hedgehog protein promotes proliferation and chondrogenic differentiation of bone marrow-derived mesenchymal stem cells in vitro. *Journal of Orthopedic Science.* 5:491-496

Wasteson, P., Johansson, B.R., Jukkola, T., Breuer, S., Akyurek, L.M., Partanen, J., Lindahl, P. 2008. Developmental origin of smooth muscle cells in the descending aorta in mice. *Development*, 135(10), pp.1823–32.

Wechsler-Reya, R. J. and Scott, M. P. 1999. Control of neuronal precursor proliferation in the cerebellum by Sonic Hedgehog. *Neuron* 22, 103-114.

Westphal, D., Dewson G, Czabotar PE, Kluck RM. 2010. Molecular biology of Bax and Bak activation and action. Biochimica et Biophysica Acta - Molecular Cell Research, 1813(4), pp.521–531.

Weyrich, A.S., Prescott, S.M. and Zimmerman, G.A., 2002. Platelets, endothelial cells, inflammatory chemokines, and restenosis: Complex signaling in the vascular play book. *Circulation*, 106(12), pp.1433–1435.

Wiechman, K., Walch, H. and Seiler, A., 2011. Identification of Valid Endogenous References for Monitoring Gene Expression Changes in Human Multipotent Mesenchymal Stromal Cells using RealTime ready Assays. *Lifescience Roche*, (6).

Wilson, C.W. and Chuang, P.-T., 2010. Mechanism and evolution of cytosolic Hedgehog signal transduction. *Development*, 137(13), pp.2079–94.

Wilson, C.W. and Stainier, D.Y.R., 2010. Vertebrate Hedgehog signaling: cilia rule. *BMC biology*, 8, p.102.

Wong, M.M., Winkler B, Karamariti E, Wang X, Yu B, Simpson R, Chen T, Margariti A, Xu Q. 2013. Sirolimus Stimulates Vascular Stem/Progenitor Cell Migration and Differentiation Into Smooth Muscle Cells via Epidermal Growth Factor

Receptor/Extracellular Signal-Regulated Kinase/β-Catenin Signaling Pathway. Arteriosclerosis, thrombosis, and vascular biology, 33(10), pp.2397–406.

Woyda, W. C., Berkas, E. M. & Ferguson, D. J. 1960. The atherosclerosis of aortic and pulmonary artery exchange autografts. *Surg. Forum* 11, pg. 174–176.

Wynne, B.M., Chiao, C.-W. and Webb, R.C., 2009. Vascular Smooth Muscle Cell Signaling Mechanisms for Contraction to Angiotensin II and Endothelin-1. *J Am Soc Hypertens,* 3(2), pp.84–95.

Xiang, W. et al., Jiang T, Guo F, Gong C, Yang K, Wu Y, Huang X, Cheng W, Xu K. 2014. Hedgehog pathway inhibitor-4 suppresses malignant properties of chondrosarcoma cells by disturbing tumor ciliogenesis. *Oncology Reports*, 32(4), pp.1622–1630.

Xiao, Q., Luo Z, Pepe AE, Margariti A, Zeng L, Xu Q. 2009. Embryonic stem cell differentiation into smooth muscle cells is mediated by Nox4-produced H 2 O 2. American journal of physiology. *Cell physiology,* 296(November 2008), pp.711–723.

Xiao, Q., Zeng L, Zhang Z, Margariti A, Ali ZA, Channon KM, Xu Q, Hu Y. 2006. Sca-1+ progenitors derived from embryonic stem cells differentiate into endothelial cells capable of vascular repair after arterial injury. *Arteriosclerosis, thrombosis, and vascular biology*, 26(10), pp.2244–51.

Xiao, Q., Zeng L, Zhang Z, Hu Y, Xu Q. 2007. Stem cell-derived Sca-1+ progenitors differentiate into smooth muscle cells, which is mediated by collagen IV-integrin alpha1/beta1/alphav and PDGF receptor pathways. American journal of physiology. Cell physiology, 292(1), pp.C342–52.

Xie, C., Ritchie RP, Huang H, Zhang J, Chen YE. 2011. Smooth muscle cell differentiation in vitro: Models and underlying molecular mechanisms. Arteriosclerosis, Thrombosis, and Vascular Biology, 31(7), pp.1485–1494.

Xie, C.-Q., Huang, H., Wei, S., Song, L.-S., Zhang, J., Ritchie, P., Chen, L., Zhang, M., Chen, Y.E. 2009. A comparison of murine smooth muscle cells generated from embryonic versus induced pluripotent stem cells. *Stem Cells Dev*, 18(5), pp.741–8.

Xu, Q., 2004. Mouse models of arteriosclerosis: from arterial injuries to vascular grafts. *The American journal of pathology*, 165(1), pp.1–10.

Yamashita, J., Itoh H, Hirashima M, Ogawa M, Nishikawa S, Yurugi T, Naito M, Nakao K, Nishikawa S. 2000. Flk1-positive cells derived from embryonic stem cells serve as vascular progenitors. *Nature*, 408(6808), pp.92–96.

Yang, P., Hong MS, Fu C, Schmit BM, Su Y, Berceli SA, Jiang Z. 2015. Preexisting smooth muscle cells contribute to neointimal cell repopulation at an incidence varying widely among individual lesions. Surgery, 159(2), pp.602–612.

Yen, T. and Wright, N.A., 2006. The Gastrointestinal Tract Stem Cell Niche. Stem cell reviews, 00, pp.203–212.

Yoshida, T., Sinha S, Dandré F, Wamhoff BR, Hoofnagle MH, Kremer BE, Wang DZ, Olson EN, Owens GK. 2003. Myocardin is a key regulator of CArG-dependent transcription of multiple smooth muscle marker genes. Circulation Research, 92(8), pp.856–864.

Yu, H., Clarke MC, Figg N, Littlewood TD, Bennett MR. 2011. Smooth muscle cell apoptosis promotes vessel remodeling and repair via activation of cell migration, proliferation, and collagen synthesis. Arteriosclerosis, Thrombosis, and Vascular Biology, 31(11), pp.2402–2409.

Yu, J., Carroll, T.J. and Mcmahon, A.P., 2002. Sonic hedgehog regulates proliferation and differentiation of mesenchymal cells in the mouse metanephric kidney. *Development*, 5312, pp.5301–5312.

Yuan, H., Upadhyay, G., Yin, Y., Kopelovich, L., Glazer, R.I. 2012. Stem cell antigen-1 deficiency enhances the chemopreventive effect of peroxisome proliferator-activated receptorg activation. *Cancer Prevention Research*, 5(1), pp.51–60.

Zacharias, W.J., Madison BB, Kretovich KE, Walton KD, Richards N, Udager AM, Li X, Gumucio DL. 2011. Hedgehog signaling controls homeostasis of adult intestinal smooth muscle. Developmental Biology, 355(1), pp.152–162.

Zalewski, A., and Shi, Y. 1997. Vascular myofibro- blasts. Lessons from coronary repair and remodel- ing. *Arterioscler. Thromb. Vasc*. Biol. 17:417–422. 18.

Zaragoza, C., Gomez-Guerrero, C., Martin-Ventura, J. Blanco-Colio, L., Lavin, B., Mallavia, B., Tarin, C., Mas, S., Ortiz, A., Egido, J. 2011. Animal models of cardiovascular diseases. *J Biomed Biotechnol*, 2011, p.497841.

Zeng, Q., Wei B, Zhao Y, Wang X, Fu Q, Liu H, Li F. 2016. Shh mediates PDGF-induced contractile-to-synthetic phenotypic modulation in vascular smooth muscle cells through regulation of KLF4. Experimental Cell Research, 345(1), pp.82–92.

Zhang, D., Zhao, T., Ang, H.S., Chong, P., Saiki, R., Igarashi, K., Yang, H., Vardy, L.A. 2012. AMD1 is essential for ESC self-renewal and is translationally down-regulated on differentiation to neural precursor cells. *Genes and Development*, 26(5), pp.461–473.

Zhao, E., Xu H, Wang L, Kryczek I, Wu K, Hu Y, Wang G, Zou W. 2012. Bone marrow and the control of immunity. Cellular and Molecular Immunology, (July 2011), pp.11–19.

Zhou, H., Bian ZY, Zong J, Deng W, Yan L, Shen DF, Guo H, Dai J, Yuan Y, Zhang R, Lin YF, Hu X, Li H, Tang QZ. 2012. Stem Cell Antigen 1 Protects Against Cardiac Hypertrophy and Fibrosis After Pressure Overload. Hypertension, (60), pp.802–809.

Zhou, J., Hu, G. and Wang, X., 2010. Repression of smooth muscle differentiation by a novel high mobility group box-containing protein, HMG2L1. *The Journal of biological chemistry*, 285(30), pp.23177–85.

Zon, L.I., 2001. Self-renewal versus differentiation, a job for the mighty morphogens. *Nature Immunology*, 2(2).